THE UNIVERSITY
of EDINBURGH

EXTRACELLULAR MATRIX MODULATES EXOSOME SECRETION IN MACROPHAGES IN FIBROTIC LUNGS THROUGH THE AUTOPHAGY PATHWAY

FENG LI

Presented for the degree of Doctor of Philosophy

The University of Edinburgh

2017

Declaration of authorship

I hereby declare that the thesis presented has been composed only by me under the supervision of my supervisors. The work contained within this thesis has been performed wholly by me except in certain circumstances, for which the contributors and level of contribution are clearly indicated and acknowledged.

I also declare that the work presented herein has not been submitted for any other degree or professional qualification.

FENG LI

TO BOTH OF MY PARENTS,

MY SISTER, JIN,

MY WIFE, WEN-YING,

AND THE SPECIAL ONES.

“Whoever has will be given more….”

(Matthew 13:12a, NIV, the Holy Bible)

Acknowledgements

The completion of the thesis would not have been possible without the help and support of my supervisors Dr. Nik Hirani, Professor Adriano Rossi and Professor William MacNee. It has been a long journey but Nik always offered his tremendous help in many ways especially in the most difficult times in his own life to which I will be always grateful. For Adriano, I am grateful for his advice and continuous input all through the years and especially on big occasions which are the milestones marking my journey towards the completion of my study. Many thanks to Bill for providing me with the amazing people to work with in the ELEGI lab and all the inspirations and encouragement whenever I went to him. It is my privilege to work with the three of them; they have been the most optimistic people with endless enthusiasm that I have known and a huge resource of knowledge. Lastly, I do appreciate the advice and support from my co-supervisor, Prof. Nanshan Zhong in China who established the GMU-UoE PhD project and taking me as his PhD student for this program. It is indeed my privilege being Prf. Zhong's student and the first student of the program. So I thank them again for all their guidance, suggestions, help and support in many ways.

I would like to give my thanks to many other colleagues and friends who helped me with my studies in CIR and QMRI. Prof. Sarah Howie, who helped me in the very first days of this study and continued her help and advice until the very end of my work. I am very grateful that she is such a nice person who would support me whenever I knocked on her door. Dr. John Marwick who was a post-doc researcher with Nik and showed me the "modern" western blotting which was the main technique throughout my autophagy study. I am also thankful for his advice and opinions whenever he was around and also for his technical support. Dr. Alison MacKinnon is such a nice and knowledgeable person that helped me in the last part of my exosome study, especially on the exosome flow cytometry project. I would also like to thank Prof. Ian Drainsfield for his advice and generosity in supplying me with the antibodies. It was a great time working with Ross Mills and Dr. Lisa Nicol who were the Hirani Group even though we were physically in two labs. Many thanks go to Ms. Pauline McFarlane for her excellent work on the clinical side.

I would like to give my thanks to Dr. Ailiang Zhang, who works in Prof. John Savill's lab. She is such an amazing person to me and she had spent a lot of time helping me set up the flow cytometry and offered me in-depth discussions which could bring the projects forward. In fact, she helped me when I started the autophagy project with advice on many techniques. I would like to give special thanks to Miss Rong-ling Wang who was doing her masters in QMRI and now is starting her own PhD. I received great help from her with the last few experiments to complete the exosome study as there were so many samples to handle. With her gifted talents and a very open mind, she helped me with a few graphs on depicting and summarizing my studies. Through the interactive and enlightening discussions with Rong-ling, I figured out a few puzzles and had overcome a few barriers and draw the studies to a finish before I could have further discussions with my supervisors. Her contribution comes even beyond her time in Edinburgh and her input is invaluable and to which I am truly grateful.

I am very much appreciated the time and discussion I had with Dr. Chara Charsou and Dr. Kanchan Phadwal who were doing their own autophagy projects in CIR. I would also like to give thanks to Fiona Rossi, Shonna Johnston, and Will Ramsey in the flow lab for setting up the flow analysis and their endless patience in solving the problems. I also appreciate the help from Shona for the training with the confocal and fluorescent microscopy. There are many others that helped me with the exosomes projects with the skills and equipment of exosome purification, antibodies, labelling kit and the NTA analysis, from both CVS and CIR. They are particularly Dr. Wilna Oosthuyzen, Dr. Emma Morrison, and especially Dr. Boris Betz, Dr. John Pound and Maggie Paterson. Many thanks to Steve Mitchell in the King's Buildings who helped me with the electron microscopy work which was a technique that really opened my eyes to such a beautiful, invisible world.

I would like to give my thanks to the folks in the HoD lab especially from Prof. Whyte's and Dr. Walmsley's group. These are the lovely friends and colleagues I made in the last part of my study when ELEGI re-settled. They are Dr. Allison Harris, Dr. Patricia Coelho, Joe Wilson, Dr. Eilise Ryne, Dr. Tracy Plant, Dr. Emily Watts, Dr. Becky Dickinson and Dr. Fiona Murphy. It was a great time to work together with Donald Davison's group again in the last two years when ELEGI moved in, many thanks to

Brian, Emily, Annie who has retired, Bing-Jie, Holly, Lisa, Tina and Lauren. I would like to extend my thanks to folks from the previous lab, Dr. Albert Andreas, June-Allison Stroud, Sharon Moncur, and Dr. Gareth Tomlins.

I would especially give my thanks to people whom I worked with in the ELEGI Colt Laboratories, they are the best people to work with in the office and have fun when taking a night out. I would like to thank both past and present members of the ELEGI Professor Ken Donaldson, Dr. Ellen Drost, Dr. Jenifer Raftis, Dr. Anja Schinwald, Jen McLeish, Dr. Roberto Rabinovich, Dr. Santiago Giavedoni, Dr. Gourab Choudhury, Dr. Ramzi Lakhdar and Leandro Mantoani. The CIR, in general, is a great place to work. Thanks to all people on Level 2, especially the blood donors, the phlebotomists and the friendly people who had helped me on many occasions, especially to the support team. I also owe a big thank you to Karen Colvin, Lyndsey Woolrych, Dr. Paul Fitch in CIR and Carol Wilson in the postgraduate office for their help with administrative issues.

Personally, I would like to give my sincere thanks to a few friends that helped me in my stay in Edinburgh. Without their support, I would not be able to complete the work. Special thanks go to Dr. Jeff Hodgson who is such an invaluable friend in Edinburgh and helped me with proof-reading of my chapters and the final thesis. Also Jeff's lovely wife, Dr. Helen Palmer who always welcomed me home with tasty soups and cakes. I would like to thank Kirsty Forsyth who is a close friend that I would talk about almost everything with. Thanks to Roy and Helena Barker who I knew as neighbours and welcomed me into their family. I am grateful for the support from Jean McIntyre, Norma and Charles Beckham, Kate Jackson, Eddie and Jean Monroe, Darrel, Gail, Rev. Mike Taylor and many others in Northfield Church. Also, I am grateful to a few Chinese folks who are great friends I made while I am in Edinburgh, especially Dr. Cong-shan Zhang, Dr. Kai-ming Yin and Dr. Zhuan Li and their families. Especially, I would also like to give thanks to Dr. Tracey Bradshaw, Nik's partner, leader of asthma clinical and research in RIE, for being such a good friend and also for her contribution of encouragement, advice and proof-reading of my thesis. It is my privilege to know Nik's family and I felt very special of being introduced as part of his family.

I would like to give my utmost thanks to my family whom I am indebted to, especially my mum and dad for their support throughout the years. Sincere thanks to my younger

sister Jin for such a surpportive and caring sister. I would like to give thanks to my wife, Dr. Wen-ying Zhang for her support, trust, and faith in me and our relationship, it was a long journey for both of us. I also want to give thanks to all other family members, especially to my uncle and my cousin who supported me since the very beginning of my study.

Finally, I would like to thank the China Scholarship Council/ University of Edinburgh Scholarship and the UCB-CIR funding for supporting my study at the University of Edinburgh.

Abstract

Lung fibrosis is characterised by increased deposition of fibrotic extracellular matrix (ECM) in the lung interstitium causing lung dysfunction. Idiopathic pulmonary fibrosis (IPF) is the most common form of fibrotic interstitial lung diseases. It is believed that the disruption of alveolar homoeostasis and abnormal wound healing drives the lung fibrosis process and leads to a dysregulated chronic fibrotic condition. The macrophage is a key effector cell in normal wound healing and fibrosis.

Autophagy is an important mechanism for the maintenance of cellular homoeostasis, however, its role in macrophages and lung fibrosis is largely unknown. ECM has been proposed as an active functional component that regulates cell biology and it can modulate the autophagy process. Modulation of autophagy affects the secretion of exosomes which are mediators of cell-cell communication. Thus, it is hypothesised in this thesis that fibrotic ECM modulates the autophagy pathway in alveolar macrophages (AM) and subsequently affects exosome secretion in the fibrotic lung.

In this thesis, I investigated the effect of ECM on macrophage autophagy and the subsequent effect on exosome biology using *in vitro* models and clinical samples. It was shown that collagen-I, the most common type of increased ECM in IPF, upregulated the basal autophagy pathway in macrophages in that it increased the formation and facilitated the degradation of autophagosomes. It was also shown that there is a blockage of the autophagy pathway and lysosomal dysfunction in AM from the fibrotic lungs (fibrotic AM). ECM derived from IPF lung fibroblasts did not block the autophagy pathway, but it increased both the basal and rapamycin-induced autophagy in macrophages. Modulation of the autophagy pathway in macrophages affected exosome secretion *in vitro* and fibrotic AM released fewer exosomes *ex vivo*. BAL fluid exosome levels were significantly lower in fibrotic ILD and low baseline exosome levels in BAL fluid may be associated with progressed IPF. BAL fluid exosomes expressed classic exosome markers but their origin remained unclear because they did not express the typical surface markers of specific cell types.

To summarise, this study suggests the normal homeostatic process of autophagy and exosome biosynthesis in AM is subverted in the fibrotic lungs. Fibrotic ECM may

exacerbate the impairment of autophagy in the setting of dysfunctional lysosomes which affects exosome secretion and compromises cellular communication and signalling. Thus, normalising the autophagy pathway and restoring the cellular communication via alveolar exosomes may have a role in normal lung healing and gain therapeutic benefit for patients with lung fibrosis.

Lay abstract

Lung fibrosis is scarring in the lungs and idiopathic pulmonary fibrosis (IPF) is the most common form of serious lung fibrosis. The cause of IPF is unknown. Scar tissue, called extra-cellular matrix (ECM) affects normal lung function and may affect the behaviour of the surrounding cells. The macrophage is an important type of immune cell. The specific macrophages that live in the lung air sacs are named alveolar macrophages (AMs). Functional macrophages are essential for the normal tissue repair and maintaining cell fitness.

Autophagy ("self-eating") is an important process that removes cell waste and keeps cells functional and healthy. ECM has biological roles and it regulates many processes including autophagy. Autophagy affects the production of exosomes which are small vesicles produced by cells. Exosomes contain biological information which can be passed on to other cells. Thus, it is hypothesised that ECM can change the exosome production in AMs by affecting "self-eating", thereby affecting the normal reparative mechanisms and worsens fibrosis.

During this PhD study, the interplay among ECM, "self-eating" and exosome production in different macrophages was investigated. It was shown that collagen-I, the most common ECM in IPF, increased basal "self-eating" in macrophages. In AMs that were obtained from patients with lung fibrosis, "self-eating" was blocked and dysfunctional. In these fibrotic AMs, the waste degradation units of "self-eating", called lysosomes, were also dysfunctional. ECM is mainly produced by cells termed as fibroblasts. ECM was generated from cultured fibroblasts obtained from patients with fibrotic or non-fibrotic lung diseases. The fibrotic ECM increased basal and stimulated "self-eating" response in macrophages when compared to the non-fibrotic ECM, but neither ECM blocked "self-eating" in macrophages. Changes in "self-eating" affected the exosome production in macrophages. Exosome levels in the lung fluid acquired from patients with lung fibrosis were lower than those without fibrosis. It was shown that exosomes in the lung fluid contain specific proteins, but the precise source of the exosomes is uncertain.

To summarise, these studies showed that both “self-eating” and exosome production are impaired in macrophages in fibrotic lungs. When lysosomes are not functional, fibrotic ECM may worsen the damage to macrophages by stimulating basal “self-eating”. Damage to “self-eating” may reduce exosome production and impairs communication between macrophages. Thus, normalising “self-eating” process and restoring lung exosome signals may help the repair of the lung and may be beneficial for patients with lung fibrosis.

Contents

Table of Figures

Abbreviations

AIP	Acute interstitial pneumonia
ALI	Acute lung injury
alpha-SMA	Alpha-smooth muscle actin
AM	Alveolar macrophages
Arg 1	Arginase 1
ATG	Autophagy-related
ATS	American thoracic society
BAL	Bronchoalveolar lavage
BCA	Bicinchoninic acid
BD	Beckton Dickenson
CCN1	CYR61/CTGF/NOV family 1
CMFPBS	Ca^{2+}/Mg^{2+}-free PBS
CO_2	Carbon dioxide
COPD	Chronic obstructive pulmonary diseases
CS	Cigarette smoke
CTGF	Connective tissue growth factor
CXR	Chest radiography
DAPI	4',6-diamidino-2-phenylindole
DFDP-1	Double FYVE domain containing protein 1
DIP	Desquamative interstitial pneumonia
DMEM	Dulbecco's modified eagle medium
DNA	Deoxyribonucleic acid
DNase	Deoxyribonuclease
dsDNA	Double stranded DNA
EBSS	Earle's balanced salt solution
ECM	Extracellular matrix
EDTA	Ethylenediaminetetraacetic acid
EMT	Epithelial-mesenchymal transition
EP	Eosinophilic pneumonia
ER	Endoplasmic reticulum
ERS	European respiratory society
ESCRT	Endosomal sorting complex required for transport
EVs	Extracellular vesicle
FACS	Fluorescence-activated cell sorting
FAK	Focal adhesion kinase
FAs	Focal adhesions
FBS	Foetal bovine serum
FcR	Fc receptor
FF	Fibroblastic foci
FITC	Fluorescein isothiocyanate

FVC	Forced vital capacity
GAG	Glycosaminoglycan
GERD	Gastroesophageal reflux disease
GM-CSF	Granulocyte-macrophage colony-stimulating factor
GMs	Gaucher macrophages
HBSS	Hank's balanced salt solution
HHV	Human herpes viruses
HLA-DR	Human leucocyte antigen - antigen D Related
HP	Hypersensitivity pneumonitis
HRCT	High-resolution computed tomography
HRP	Horseradish peroxidase
HSC	Hepatic stellate cells
IFN-γ	Interferon-γ
IgG	Immunogloblin G
IHC	Immunohistochemistry
IIP	Idiopathic interstitial pneumonia
IL	Interleukin
ILD	Interstitial lung disease
IM	Interstitial macrophages
IMDM	Iscove's modified dulbecco's media
IPF	Idiopathic pulmonary fibrosis
ISEV	International Society for Extracellular Vesicles
LAMP	Lysosome-associated membrane proteins
LC3	Microtubule-associated protein light chain 3
LOX	Lysyl oxidase
LPS	Lipopolysaccharides
LSDs	Lysosome storage disorders
MCB	Membranous cytoplasmic bodies
M-CSF	Macrophage colony-stimulating factor
MDC	Monodansylcadaverine
MDM	Monocyte-derived macrophages
MES	4-morpholineethane sulfonic acid
MFL	Mean fluorescence
Mfge8	Milk fat globule epidermal growth factor
MGC	Multinucleated giant cells
MHC	Major histocompatibility complex,
MMP	Matrix metalloproteases
mRNA	Messenger RNA
Mtb	Mycobacterium tuberculosis
mTOR	Mammalian target of rapamycin
MUC5B	Mucin 5B gene
MVB	Multivesicular bodies

MVE	Multivesicular endosomes
NBR1	Neighbor of BRCA1
NDP52	Nuclear dot protein 52
NH_4OH	Ammonium hydroxide
NSIP	Nonspecific interstitial pneumonia
NTA	Nanoparticle tracking analysis
O_2	Oxygen
PAMs	Pathogen associated molecular patterns
PAP	Pulmonary alveolar proteinosis
PBMC	Peripheral blood mononuclear cells
PBS	Phosphate-buffered saline
PDGF	Platelet-derived growth factor
PE	Phosphatidylethanolamine
pen/strep	Penicillin and streptomycin
PFA	Paraformaldehyde
PKC	Protein-kinase-C
PMA	Phorbol 12-myristate 13-acetate
PMSF	phenylmethylsulfonyl fluoride
PrP	Prion protein
RBC	Red blood cells
RBILD	Respiratory bronchiolitis interstitial lung disease
RILD	Rheumatic interstitial lung disease
RIPA	Radioimmunoprecipitation assay
RNA	Ribonucleic acid
ROS	Reactive oxygen species
RPMI-1640	Roswell park memorial institute-1640
S1P	Sphingosine 1-phosphate
S1PL	Sphingosine 1-phosphate lyase
SEM	Scanning electron microscope
SDS-PAGE	sodium dodecyl sulfate polyacrylamide gel electrophoresis
SPC	Surfactant proteins C
SQSTM1	Sequestosome 1
TC	Tissue culture
TEM	Transmission electron microscope
TFP	Trifluoperazine
TfR-1	Transferrin-iron-transferrin receptor-1
TGF-β	Transforming growth factor β
TIMPs	Tissue inhibitors of metalloproteinase
TLR	Toll-like receptor
TSG101	Tumour susceptibility gene 101
UIP	Usual interstitial pneumonia
ULK1	Uncoordinated 51-like kinase-1

V-ATPase	Vacuolar-type H^+ -ATPase
VC	Vital capacity

Chapter 1 Introduction

1.1 Idiopathic pulmonary fibrosis (IPF): scarring in the lung

Idiopathic pulmonary fibrosis (IPF) is a type of chronic and progressive interstitial lung disease (ILD) that is characterised by irreversible fibrosis and an unknown aetiology [1]. ILD is an umbrella medical term that covers more than 200 parenchymal lung conditions [1]. Lung fibrosis is associated with excessive deposition of collagen-I rich extracellular matrix proteins within the interstitial space and the alveolar space of the lung [2-4].

1.1.1 Function and structure of the lung

The primary function of the lung is gas exchange which occurs at the functional unit called alveolar sacs. These functional units are the terminal parts of the respiratory tree. Gas exchange in the lungs includes the elimination of waste gases, mainly carbon dioxide (CO_2), and in exchange, the diffusion of oxygen (O_2) from the air to the bloodstream which is transported to the whole body.

For this simple but fundamental purpose, the lung has a delicate structure that comprises a range of unique and specialised cell types: 1) pulmonary epithelial cells are the major cells that form the respiratory airways; 2) under the alveolar epithelial lining lies the basement membrane; 3) next to the basement membrane, there is the pulmonary blood vessel which consists of endothelial cells, smooth muscle cells, and adventitial fibroblast components, which again is also surrounded by the basement membrane; 4) in the lung interstitium, there are supportive extracellular matrix structures which are mainly produced by lung fibroblasts, and are separated from the alveolar sacs and blood vessels by the basement membrane; 5) in the alveolar space, there are residential alveolar macrophages. In the case of inflammation, other leucocytes such as lymphocytes, neutrophils, eosinophils, and monocytes will migrate into the alveolar space. The lung and its constituent cells are responsive to the injury and stimuli that are caused by the inhalation of foreign material and pathogens [5-7].

1.1.2 Clinical feature of idiopathic pulmonary fibrosis: rapid decline

Idiopathic pulmonary fibrosis makes up more than half of the ILD cases in clinical practice, making it the most common type of ILD [8].The prevalence of ILD is approximately 23 in 100,000 in Europe [9] and 43 in 100,000 in the United States [10]. The estimated incidence of IPF is dependent on geographical regions, ranging from 3 to 9 cases each year worldwide [11]. In the UK, the incidence of IPF is about 7 in 100,000 and the incidence continues to rise [12]. IPF is more common in men than women and it is more often found in people over 60 years of age [13]. The median survival time of IPF patients is 3 years which is a much worse prognosis compared with many malignancies [14].

1.1.3 Risk factors and demographics of IPF

Lung fibrosis is a dysregulated wound healing process that results in scarring of the lungs [15, 16]. There are many risk factors that contribute to the fibrotic lung injury and healing process which include inhaled exposures (e.g. air pollution and smoking), viral infections, gastrointestinal comorbidities (e.g. gastroesophageal reflux disease/ GERD), ageing, and genetic factors [17].

Smoking has been a recognised risk factor in both sporadic and familial IPF [18, 19]. Tobacco history is strongly linked with IPF and may be associated with disease progression [20, 21].

Several lines of evidence have suggested a link between environmental and occupational exposures with IPF [13]. A variety of dust and particles have been strongly related to the diagnosis of IPF [18, 22], which include metal dust [18, 22-24], wood dust [18, 25], silica [18], livestock and farming [18, 22, 26].

The chronic exposure and inhalation of viruses have been linked with IPF but the role of infection in IPF is still unclear [13]. Different types of viruses have been studied in IPF which include cytomegalovirus [27], Epstein-Barr virus [27], hepatitis C virus [28], human herpes viruses (HHV)-7 and HHV-8 [27].

A strong association of GERD with IPF has been demonstrated in a few studies, and the microaspiration of gastric contents has been proposed as the mechanism [10, 29, 30]. GERD is a very common comorbidity with IPF patients. Several studies have shown that 67 - 88% of IPF patients may have distal oesophageal reflux and 33 - 71% may have proximal oesophageal reflux [31]. Chronic microaspiration occurs when the weakened lower oesophageal sphincter allows the gastric fluid, includes gastric acid and bile, to travel up into the oesophagus and then enter the airways. Repeated lung epithelium injury via the chronic microaspiration of gastric fluid may lead to granulomatous pneumonitis, dysregulated wound healing, and eventually lung fibrosis [31].

Familial IPF was previously thought to be account for less than 5% of total IPF [32, 33], but recent studies suggest it may be underestimated [34, 35]. The potential mutations that are associated with familial IPF include surfactant proteins C (SPC) [36, 37], SP2A [38], and telomerase-related genes [39-41]. These were not commonly found in sporadic IPF.

The identification of a common polymorphism in the promoter of mucin 5B gene (MUC5B) in both familial and sporadic IPF in 2011 led to the discovery of other single nucleotide polymorphisms in sporadic IPF [42, 43]. Since then, more than 10 other loci have been found in association with IPF, and taking all the cases together they may represent more than 1/3 of the genetic risk for IPF [44]. More importantly, some gene polymorphisms have been associated with specific outcomes in IPF patients. For example, MUC5B polymorphism is not associated with interstitial pneumonia in systemic sclerosis [45], but TOLLIP and TLR3 polymorphism are associated with disease progression and early mortality [46, 47]. Even though it is not recommended to carry out genetic testing routinely with either familial or sporadic IPF, it is clearly suggested the outcome of IPF is associated with genetic factors and might affect the management of IPF patients in the future.

1.1.4 Diagnosis of idiopathic pulmonary fibrosis: multidisciplinary teamwork

IPF can be diagnosed based on the symptoms, physical examination and high-resolution computed tomography (HRCT) [13, 48, 49]. BAL fluid assessment offers

complimentary data for the exclusion of other similar conditions [50]. A multi-disciplinary team meeting is advised to categorise them into different stages of the disease [13].

By definition, IPF means interstitial lung diseases (ILD) with an unknown cause. Thus to be diagnosed with IPF, one has to rule out other possible causes of lung fibrosis, such as occupational or environmental exposures, toxic drugs, radiation and underlying connective tissue disease. [13, 51].

A detailed history and physical examination are necessary for the diagnosis of IPF. Dyspnoea is the main complaint when patients come to the clinic. Developing from breathless to dyspnoea could take more than a year and chronic dyspnoea has recently been associated with poor prognosis [52]. Smoking history, family history, use of certain medications and exposure to risk factors should also be included. Patient age may also be helpful in making the diagnosis as IPF most commonly presents in patients aged over 60 [13]. Patients with other ILD are often present at a younger age, most commonly in their 50s, and the majority of sarcoidosis present even younger, aged between 25 to 40 years [53]. Pulmonary examination often observes the classic bilateral fine-end inspiratory crepitations. In addition, extrapulmonary findings such as finger clubbing (occurs in more than 50% IPF), pulmonary hypertension (e.g., loud second heart sound), and peripheral oedema [53] may be apparent.

Chest radiography (CXR) and HRCT are important radiological tools to diagnose IPF and monitor the disease [53, 54]. The typical CXR features of IPF are reticulations and reduced lung volumes. It is a simple but important method to help distinguish IPF from other lung conditions, such as lung malignancy, pulmonary oedema and infection. HRCT is a powerful tool and now used routinely to diagnose IPF. The main feature of IPF on HRCT is honeycombing, which is the cystic dilation of distal bronchioles secondary to the fibrotic destruction of adjacent airspaces. When honeycombing is present with a basal predominance together with septal thickening, this is indicative of the underlying pathology being usual interstitial pneumonia (UIP). However, there are UIP-similar patterns which can occur with drug exposure, environmental factors and in association with collagen vascular diseases [55]. UIP-similar patterns on HRCT can be very difficult to be distinguished from the UIP-IPF pattern. Therefore, other evidence,

such as clinical presentation, physical examination, and lung function testing are necessary to secure the diagnosis. In some cases, bronchoscopy or even surgical biopsy (for the histology evidence of UIP) may be required to confirm the diagnosis [13, 51].

Instillation of saline solution into the alveolar space was first performed by Stitt in 1927 [56]. Later, it was used as a tool for the treatment of septic lung disease and pulmonary alveolar proteinosis by lavage of the distal airways [57, 58]. Bronchial lavage with a flexible bronchoscope for research purposes was first introduced by Reynolds and Newball in 1974 [59]. The technique of saline lavage of a defined portion of the lung became known as bronchoalveolar lavage (BAL) [60-62].

BAL is a well-tolerated and useful tool for the diagnosis of ILD and IPF when used in conjunction with clinical observations and HRCT imaging [13, 50]. The gross appearance of the BAL fluid can be informative of certain lung conditions, such as pulmonary haemorrhage (pink coloured fluid) or pulmonary alveolar proteinosis (PAP, cloudy and milky fluid). BAL cell differential count provides helpful information. Normally the differential cell count of healthy human adults consists of macrophages as the main cells (>85%), variable lymphocytes (<15%) and small numbers of granulocytes with neutrophils (<3%) and eosinophils (<1%) [48, 60, 62]. Increased red blood cells (RBCs) in cytocentrifuge preparations also suggests pulmonary haemorrhage. An increase in neutrophils indicates infection and inflammation. Greater than 10% of eosinophils is uncommon in ILD and more than 25% of eosinophils indicates eosinophilic pneumonia (EP) or other eosinophilic lung disorders [63, 64]. For IPF diagnosis, BAL is useful in excluding other causes of ILD. Furthermore, it may offer information that relates to the disease severity and progression. In Dr. Hirani's group, we have shown that $CD74^{+}$ macrophages may be associated with disease progression in IPF [65]. Others have also shown that increased number of lymphocytes may indicate a better prognosis [66-68], whereas increased eosinophils may be linked to a severe condition with a worse outcome [68, 69]. In addition to the cell population and phenotypes, the levels of cytokines, growth factors and mediators in the BAL fluid can also be relevant to the disease and are candidates for research, drug development and potential treatments [70] [71].

Disease progression is critical in the management of patients and can be life-threatening. Lung function is important in monitoring disease progression and it should be regularly measured once IPF is diagnosed. There is robust evidence that a 10% or greater reduction in forced vital capacity (FVC) within 6 – 12 month is associated with an increased risk of death and therefore accepted as a marker of progression [13]. A decline in FVC is the FDA approved primary end-point for Phase 3 clinical trial in IPF and this reiterates the importance of FVC decline as a measure of disease progression [72]. CXR and HRCT can confirm the severity of the lung fibrosis and also contribute to monitoring the disease during its natural course after diagnosis [13].

Following the clinical examinations and investigations, a dedicated multidisciplinary team should discuss, confirm and categorise the case. This team should include respiratory physicians (lung fibrosis specialist), thoracic radiologists, pathologists, and specialist nurses [13]. The aims of the meeting are 1) to confirm the diagnosis and the stage of the disease, and 2) to establish a future management plan for the patient. Management options may include available clinical trials. Some cases, however, may be too complex to reach a management plan or sometimes even a defined diagnosis.

1.1.5 Current strategy of working with lung fibrosis and ILD

Lung fibrosis was first known as the Hamman-Rich Syndrome following the presentation of four cases of pulmonary diseases at John's Hopkins Hospital in the 1940s [73]. Hamman-Rich syndrome is now classified as acute interstitial pneumonia (AIP) rather than the IPF type usual interstitial pneumonia (UIP). The classification of ILD only began in the 1960s, when Dr. Liebow and his group proposed five histopathologic subgroups of chronic idiopathic interstitial pneumonia (IIP) which included UIP [74]. In 1964, Dr. Scadding in the United Kingdom proposed the term "fibrosing alveolitis", to which "cryptogenic" was added to describe what is now termed IPF [75]. More than three decades after the Liebow classification, in 1998 Drs Katzenstein and Myers suggested an update to the classification of IIPs and four other histologically distinct forms of IIP were presented with UIP, which were: desquamative interstitial pneumonia (DIP), respiratory bronchiolitis interstitial lung disease (RBILD), acute interstitial pneumonia (AIP, Hamman–Rich disease) and nonspecific interstitial pneumonia (NSIP) [76]. By 2002, the American Thoracic Society and European

Respiratory Society (ATS/ ERS) published a consensus classification of IIPs which added clinical and radiographic features to the Katzenstein/ Myers classification [77]. The ATS/ERS 2002 guideline, which was revised in 2011, and later in 2013 and 2015, is now the standard workbook in diagnosing and classifying IIPs in practice [13, 54, 78].

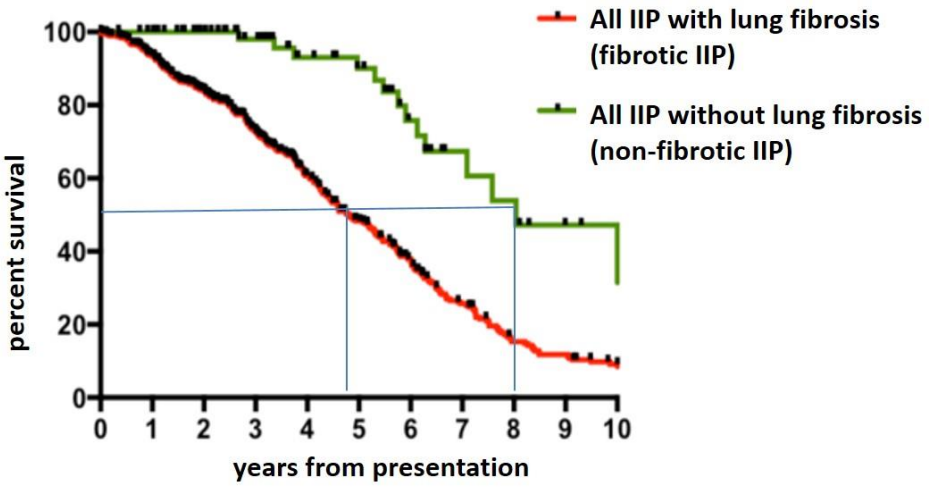

Figure 1-1 Survival in idiopathic interstitial pneumonia.

Idiopathic interstitial pneumonia (IIP) with fibrosis (which includes IPF) has lower survival rate than IIP without fibrosis (graphed by Dr. Nik Hirani, University of Edinburgh). Survival rate of Edinburgh cohort (2007-2016) stratified according to HRCT on the presence of lung parenchymal fibrosis. Patients with fibrosis (n=565) had a median survival of 4.8 years compared to 8 years for those without fibrosis (n=77), hazard ratio (HR) 3.9, 95% confidence interval (CI) 2.9-5.3, *p=0.0001*, unadjusted for baseline variables.

The classification of ILD is currently achieved by a multidisciplinary approach which is recommended by the ATS/ERS. The classification of ILD is largely based on the aetiology of fibrosis and the histopathological findings. In fact, the majority of ILD conditions can be characterised by the different level of inflammation and the degrees of fibrosis [79]. For example, sarcoidosis is primarily inflammatory, however, IPF in nature is predominating fibrotic with a lack of inflammation [79-81]. On the other hand, a few conditions are characterised by the filling of certain cells or materials in the alveolar airspace such as desquamative interstitial pneumonitis (with macrophages) and alveolar proteinosis (with granular proteinaceous material). There are also some cases that remain unclassifiable in ILD even following the multidisciplinary discussion.

However, these unclassifiable diseases appear to have a better prognosis when compared to IPF but may be worse than non-IPF ILD [82]. It has been shown that IPF has a much poorer prognosis than non-IPF ILD [82, 83]. Even without a definite diagnosis of a specific ILD, the clinician can identify 'fibrotic' versus 'non-fibrotic' disease based on HRCT and/or biopsy, thus can monitor the lung function to identify 'progressive' cases from 'non-progressive' cases. In patients that die of interstitial pneumonia, most die of progressive lung fibrosis. The presence of fibrosis on HRCT at presentation has been shown to be associated with a poor prognosis in the Edinburgh cohort (Fig 1.1). Thus, a simple method is to group patients based on the presence of fibrosis on HRCT scan which is more relevant to prognosis.

1.1.6 Limited treatments for ILD and IPF

Currently, there are limited treatments for many ILD conditions [53]. In IPF, the aim is to stabilise the condition and slow down disease progression [13, 54]. Other ILD are self-limiting and potentially reversible, such as sarcoidosis and respiratory bronchiolitis associated interstitial lung disease. In patients with chronic hypersensitivity pneumonitis or non-specific interstitial pneumonia, regardless of the strategy of immunosuppression treatment, some of the cases can progress to severe fibrosis. In unclassifiable ILD, a working diagnosis should be reached for the treatment and management of the disease [82, 84]. Treatment plans should also include supportive therapies which include pulmonary rehabilitation, symptomatic relief (for example, cough and anxiety), and supplementary oxygen [13, 54].

Pirfenidone is the first licensed treatment for IPF and has been currently approved by the National Institute for Health and Care Excellence in the UK in 2013 [85]. Later in 2016, the use of Nintedanib was also approved [86]. NICE recommends the use of both drugs in patients with a forced vital capacity of 50-80% predicted. Randomised controlled trials have shown that neither drugs reverse the established fibrosis but both can slow the decline in lung function and modestly reduce mortality [54]. They have similar side effects mainly gastrointestinal (diarrhoea, nausea, and dyspepsia) together with fatigue and in the case of pirfenidone, photosensitivity [87]. According to NICE guidelines, the treatment should be discontinued if lung function declines by 10% or more from baseline in a year. There are other drugs that are currently in phase 2a trials

(TD139) and phase 2b trials (simtuzimab and lebrikizumab) [88]. Certain patients may benefit from enrolment into drug trials for emerging new treatment options, which may slow down the inexorable declining rate of lung function. The future of clinical treatment for IPF is more promising.

Previous treatments for IPF patients have been shown to be ineffective or even harmful. These include corticosteroids, cyclophosphamide, triple therapy (prednisolone, azathioprine and N-acetylcysteine), or N-acetylcysteine alone [89, 90]. Interestingly, a recent study was suggested that some patients may be more responsive to treatment with N-acetylcysteine when associated with certain genetic polymorphisms [91].

The availability of lung transplantation is limited in IPF patients but remains the only treatment with proven benefit for carefully selected subjects [92]. In total, IPF represents about 23% of total lung transplants worldwide [93]. There are many factors to be considered for lung transplantation, the predominant factor being the rapid decline in lung function which shortens the life expectancy of the patient [94]. Age of the patient is a challenge for the success of lung transplantation, and 65 years of age is suggested as the upper age limit although successful cases have been performed on patients over this limit [95]. About half of patients with IPF receive bilateral lung transplants and one in six patients dies before the donor organ is available [53]. In IPF patients, the unadjusted three-month mortality after lung transplantation is 15%. The five-year survival is 60% for patients who survive one year post-surgery [93]. In successful cases, the mobility and general physical activity of the patients are greatly improved.

1.1.7 IPF: challenges and opportunities

The rapid decline in lung function and unpredictable clinical course are the major challenges of IPF management [14]. Lack of the biomarkers has prevented researchers from understanding the disease and the development of new therapies [14, 96].

To date, early diagnosis of IPF has not been possible due to the lack of diagnostic tools [96]. However, early diagnosis is essential for the accurate diagnosis and appropriate management which may affect prognosis. Early diagnosis may also help monitor disease progression and create opportunities for new therapies. For nearly half of patients, the mean time to referral to a specialist from the onset of dyspnoea is more

than 18 months [97]. It is suggested that half of the patients have already got the late stage of disease at the time of diagnosis [97]. A late diagnosis is related to a poorer prognosis and these patients may have limited treatment options and be ineligible for clinical trials with newly developed medications [97, 98].

The natural course of IPF can be very rapid and disease progression is a poor prognostic marker [14]. Besides the very limited and effective treatments, there is currently no marker that can accurately predict the prognosis of IPF [13]. A few candidates markers of disease progression, such as cytokines and inflammatory factors have been elevated, and more recently, genetic and epigenetic significance, transcriptional and post-transcriptional mechanisms, and metabolic factors have also been studied [96]. However, there is no evidence that the any of these have a better correlation to disease progression. It is now believed that in IPF there are different subgroups with a specific signature that are associated with the vulnerability, development, progression, treatment, and prognosis of the disease. It is the aim of clinicians and researchers to identify such groups of patients and develop personalised care strategies to further develop the management of IPF. The breakthrough will be the identification of disease-relevant biomarkers and early diagnosis of IPF.

1.2 IPF pathogenesis and extracellular matrix (ECM) biology

In the last few decades, there has been progress in the definition and diagnosis of IPF, [13, 51, 54, 77, 78]. However, there has been limited progress towards understanding the fundamental pathogenic mechanisms in usual interstitial pneumonia (UIP) which is the pathological feature of IPF. Current understanding of UIP has been focused on recurrent epithelial injury and aberrant epithelial/ fibroblastic communication. Inflammation, which was hypothesised as the initiating event in lung fibrosis, is now not regarded as the primary driver of UIP, although the evidence for the absence of inflammation is limited. Nevertheless, inflammation is an essential component of the wound healing process with important roles in the regulation of tissue fibrosis and its resolution [99-102].

1.2.1 Epithelial injury and abnormal wound healing in IPF

Normal wound healing can be divided into three steps that include: initial injury, initiation and resolution of inflammation, and finally tissue repair. In lung fibrosis, especially UIP, the normal wound healing is disrupted. The aberrant wound healing and on-going injury result in excessive deposition of ECM in the lungs [16, 80, 103].

The “fibroblastic focus” is a well-recognised morphological lesion of UIP that is the subepithelial accumulation of (myo)fibroblasts [104-106]. Fibroblastic foci are prominent in UIP but can be seen in other fibrotic lung diseases such as chronic hypersensitivity pneumonitis (HP), non-specific interstitial pneumonia (NSIP) and rheumatic interstitial lung disease (RILD) [107-109]. Fibroblast foci represent the classic alveolar epithelial cell injury response that leads to fibrosis [110] and they are identified as the areas of active fibrosis [111, 112]. Fibroblastic foci are observed in the interstitium and are lined by alveolar epithelium [3, 113]. In advanced fibrosis, fibroblasts can migrate through the damaged epithelial barriers into the alveolar space and continue to proliferate and produce ECM in the alveolar space [80].

It is proposed that there are at least three potential origins of the fibroblast foci 1) activation of interstitial lung fibroblasts by pro-fibrotic growth factors; 2) type-II epithelial cells undergoing epithelial-mesenchymal transition (EMT); and 3) fibrocytes,

circulating bone marrow-derived progenitor cells [114]. ECM components are dominant in the fibroblastic foci, including pro-collagen type I, tenascin-C and the glycosaminoglycan (GAG) versican [105, 115-118]. In relation to the development of fibrosis, fibroblastic foci have been categorised into three stages based on the expression of GAGs and collagen [119-121]. Fibroblastic foci also have been correlated with poor prognosis in IPF, however, there is conflicting evidence for this initial finding and the relationship needs to be further investigated [102, 122-124].

There are a number of cell types and pathways implicated in this complicated process of lung fibrosis. Cells present different roles during the three stages of fibrosis: initiation (early stage), development (inflammation stage), and repair or fibrosis (later stage).

In the early stage, the initial injury causes damage and dysfunction in the lung epithelium cells which leads to apoptosis or EMT. It is documented that type II alveolar epithelial cell injury is an important early feature in the pathogenesis of pulmonary fibrosis [80]. Important events in this early stage include activation and increase of transforming growth factor β (TGF-β), the release of different chemokines, the increase of oxidative stress and the accumulation of endoplasmic reticulum (ER) stress [100, 125, 126]. It has been reported that TGF- β promoted the EMT of normal peripheral lung epithelial cells *in vitro* [127].

The initiation of inflammation is triggered by epithelial cell death. Epithelial injury leads to the recruitment of local lung macrophages and the infiltration of inflammatory cells such as neutrophils, lymphocytes, and monocytes from the blood vessels. The presence of inflammatory cells on the site of injury triggers a cascade of inflammatory events and creates a profibrotic microenvironment by releasing cytokines and chemokine in response to the injury.

In the later stage, the important events in the remodelling of lung fibrosis include the activation of fibroblasts, myofibroblast differentiation, EMT and fibrocyte recruitment [128, 129]. The pathological changes in fibrocyte in the lungs may promote mesenchymal cell activation and leads to progressive fibrosis [130, 131]. Excessive deposition of ECM is initiated in the lungs if the normal tissue repair was disturbed and

an abnormal amount of matrix was produced or the nature of matrix changed to a fibrillar type with increased stiffness [132].

In summary, currently, the dysregulated fibrosis process is thought to be triggered by the epithelial injury, continued with or without inflammation and resulting in the activation of (myo)fibroblasts. The excessive deposition of ECM resulted in the structural changes and eventually leads to respiratory failure.

1.2.2 Role of inflammation in IPF

As described above, currently, it is thought that epithelium injury and aberrant wound healing are the primary driving forces of UIP. The role of inflammation in UIP is not fully established. In fact, there is no study in serial lung biopsies of human IPF or good animal models of UIP that can address the question. It is clear that inflammation plays a critical role in other forms of lung fibrosis such as chronic HP and NSIP. The evidence for inflammation in UIP includes the observation of increased inflammatory cells, such as neutrophils and eosinophils, in the alveolar lavage fluids in IPF patients [133]. Some studies show a correlation with BAL inflammatory cells and prognosis [134]. However, in stable IPF, histologic findings in tissue showed very mild inflammation and disproportionate fibrosis. This pathologic pattern is not much changed from the early phase of the disease (i.e. mild disease) to the late stage (i.e. severe disease), which is against the on-going chronic inflammation theory. More importantly in clinical trials, subjects were not responsive to immunosuppressive treatments and this may even be harmful in IPF [89]. It may be that inflammation in UIP is an outcome of the injury and tissue repair rather than the driving force of the progressive fibrosis process [101, 102].

Regardless, inflammation is inevitably present within the epithelial injury/remodelling theory. Epithelial injury recruits inflammatory cells and exaggerates the inflammation response which is an essential part of the normal wound healing process. The inflammatory cells, especially macrophages, are responsible for the clear up of the apoptotic cells and debris to limit the spread of inflammation. In the repair stage, inflammatory cells release pro-fibrotic mediators, such as cytokines and growth factors, to enhance the tissue repair and wound healing [135]. These mediators enhance the activation, proliferation, and differentiation of fibroblasts to myofibroblasts thus

promoting the deposition and accumulation of ECM. Dysregulation of the normal tissue repair leads to the disturbance of cellular homoeostasis which favours chronic abnormal tissue repair, scarring in the lungs, alveolar destruction, and respiratory failure.

In all, epithelial injury and cell death are regarded as the major events in UIP, the on-going inflammation response in chronic wound healing process may be secondary to this process but the pro-fibrotic inflammatory mediators released by immune cells are likely to be important for the regulation and modification of normal wound healing.

1.2.3 Macrophages are essential for tissue repair

Macrophages are found in almost all tissues and organs and they are essential for the normal wound healing [15, 136]. Macrophages are key regulators of the recruitment, proliferation, and activation of fibroblast which are the key steps of tissue fibrosis [137]. Macrophages are found in sites of wound healing and they regulate the normal wound healing process by the synthesis and secretion of chemokines and cytokines [135].

Animal studies have shown that the depletion of macrophages results in retarded tissue repair and failure of wound healing [138-140]. The depletion of macrophages in a lung-specific TGF-β1 transgenic mouse model led to the attenuation of fibrosis. These studies suggested the importance of the monocyte/ macrophage lineage cells in the TGF-β driven lung fibrosis [141].

Studies have demonstrated that macrophages have complex and specific functions in wound healing. It has been shown that some macrophages clearly promote the fibrosis process, while other macrophages may facilitate the resolution and/or reversal of tissue fibrosis [137, 142]. More interestingly, macrophages have shown different functions at different stages of the wound healing process. A study in a mouse model of liver fibrosis demonstrated different roles of macrophages in different phases of the fibrosis process [143]. It was reported that if macrophages were depleted during the early inflammatory phase of a fibrotic response, the fibrosis was reduced and the differentiation to myofibroblasts was also decreased. However, if macrophages were depleted during the late remodelling phase, the fibrosis persisted. This study confirmed that macrophages could play distinct roles in different phases of the fibrosis process. Later, in a skin model

of tissue repair, macrophages were also shown to have different roles at different stages of the normal wound healing process [144].

1.2.4 Macrophages and lung fibrosis

The macrophage is a key regulatory cell of the normal wound healing process and is at the centre of inflammation regulation in the lung and in the alveolar space. In general, there are two types of macrophages in the lungs: alveolar macrophages (AM) that live in the airways and the interstitial macrophages (IM) that are resident in the parenchymal tissues [145, 146].

The number of AM increases in the terminal airways and they are the most common cell type in the BAL fluid from the healthy human lungs [147]. In normal lungs, AM reside in surfactant rich alveolar lining fluid at the interface of air and the alveolar epithelial barrier [148, 149]. AM are in contact with alveolar epithelial cells via small pseudopodia [148]. They interact with each other by releasing many mediators, cytokines and growth factors in biological and pathological conditions.

Upon the epithelium injury, AM are amongst the first group of cells to respond to the damage, by producing pro-inflammatory cytokines and trigger a cascade of inflammation response. Studies have shown that cytokines and chemokines that are related to activated macrophages may have a pro-fibrotic role in the pathogenesis of lung fibrosis [150-152]. Upon activation, AM can release mediators that regulate the growth and the phenotype of epithelial cells [153]. When the epithelial cells are injured or the epithelial barrier is compromised, the AM are exposed to the cells and structures that lie underneath the epithelial lining [153]. In lung fibrosis, the on-going injury and repair of lung epithelial cells increase the exposure of AM to the excessive ECM and ECM components in the alveolar space repeatedly. ECM and its components are regarded as biologically functional mediators that regulate many processes which affect cell proliferation, migration, activation and cytokine production [154]. They also influence the fibrosis process by affecting the cellular behaviour of the effector cells such as fibroblasts and macrophages in the lungs [155, 156].

In IPF, the number of AM is greatly increased, and they also exhibited a distinct “wound-healing” phenotype (alternative activated) [151, 157]. Alternatively activated

macrophages produce pro-fibrotic mediators, such as TGF-β and platelet-derived growth factor (PDGF), that promote the proliferation and activation of collagen-secreting human fibroblasts [158]. AM isolated from human fibrotic lung tissues can produce pro-fibrotic cytokines such as IL-13 [159], interleukin-1β and TNF-α [160]. On the other hand, macrophages can also inhibit tissue fibrosis by promoting (myo)fibroblast apoptosis and promoting inflammation resolution [137]. Macrophages also showed the ability to digest and engulf ECM components [161]. They can also induce the production of matrix metalloproteases (MMPs) in different cell types for the degradation of collagens [137].

Macrophages are a heterogeneous population of cells that are derived from peripheral blood monocytes. However, studies also suggested that the original AM may have different origins and have distinct roles than the newly differentiated macrophages from blood [162]. In general, once AM are activated they can adopt a spectrum of activation states, but can be broadly dived to two populations: pro-inflammatory (classically activated, M1) macrophages and pro-resolution (alternatively activated, M2) macrophages [163-165]. It has been well-established that the dominant phenotype of AM in lung fibrosis is broadly towards the M2 spectrum of macrophages. More importantly, it is believed that M2 macrophages are important regulators of the development and progression of the fibrosis process [166-168]**.** Macrophages are polarised to M1 or M2 phenotypes in response to cytokines in the microenvironment. It has been well-recognised that IFN-γ and LPS trigger the classic activation (M1) whereas IL-4 and IL-13 lead to the alternative activation (M2). IL-4 and IL-13 mediated alternative activation has been shown both *in vitro* and *in vivo* [169, 170]. Arginase 1 (Arg 1) and macrophage mannose receptor 1 (CD206) are commonly used markers for M2 activation [171, 172].

1.2.5 ECM production and degradation

In normal lungs, ECM is a constitutive compartment of the human body and it is a highly organised network of proteins where other lung cells are resident. ECM not only provides structural support but more recently has been shown to be a bio-active material that is involved in cell adhesion, differentiation, migration and proliferation [114, 173, 174]. The quantity of ECM is highly dynamic and it is dependent on its production and

degradation, and the dysregulation of either process can lead to fibrotic pathologies [175, 176].

ECM is mainly produced by (myo)fibroblasts, but other cells such as epithelial cells can also contribute to ECM production [177]. Once stimulated, collagen mRNA transcripts will first be increased and then the collagen propeptides will be synthesised [178]. Post-translational modification is an important step before the formation of the triple helix collagen structure in the endoplasmic reticulum. The modifications include hydroxylation and glycosylation of collagen residues and the formation of disulfide bond. The triple helix structure will be processed in the Golgi apparatus and then secreted out of the cells [178]. Mature monomeric collagen molecules are produced after further modification by other peptidases. The monomeric collagen molecules are used to compose microfibril which interdigitates with other microfibrils to form a collagen fibril [179]. The collagen fibrils then formed collagen fibre by extensive cross-linking and right-handed supertwist [180]. The recognition and binding of ECM with its ligands is depended on the structure and orientation of the collagen fibril. Integrins are the primary binding sites of collagen [181] other binding sites include metalloproteinases [182], fibronectin [183], proteoglycans [184], and von Willebrand factor [185]. Some of these sites are not accessible for the ligand recognition as they are buried within the microfibrillar structure [186, 187].

Collagen degradation is mainly through the production and activation of extracellular matrix metalloproteinases (MMPs). However, collagen can be recognised and internalised by macrophages and fibroblasts for intracellular degradation through lysosomes. Impaired matrix degradation at least is recognised as part of mechanisms leading to persistent lung fibrosis together with the activation of (myo)fibroblasts with increased matrix production [178]. Of note, the intact fibrillar collagen can only be degraded by certain MMPs including MMP-1, MMP-8, MMP-13, MMP-14, MMP-16, and MMP-18 [182]. Fragments of cleaved collagen can be further degraded by gelatinases (MMP-2 and MMP-9) or cathepsin K or lose their triple-helical structure spontaneously [114, 188].

MMPs are a family of zinc enzymes that perform matrix-degrading functions. In the lungs, MMPs are secreted by many cells including AM, neutrophils, and lung epithelial

cells [189]. They are released in an inactivated latent form which is then activated extracellularly by the proteolytic process. There are at least 24 well-defined MMPs and they are divided into subgroups according to the specific ECM proteins they degrade [190]. The changes of MMPs and the tissue inhibitors of metalloproteinase (TIMPs) are the co-factors that modulate the local ECM microenvironment in biological and pathological conditions [191].

The internalised collagen in macrophages and fibroblasts was first observed by electron microscope [192, 193]. Four different mechanisms have been reported as independent means of internalisation of collagens [114]. Collagen can be recognised by specific receptors, especially through α2β1 integrin, before internalisation [194]. Collagen can also be internalised by endocytosis which is mediated by the transmembrane mannose receptors uPARAP/Endo180 on fibroblast [195] and mannose receptor/CD206 on macrophages [196]. Mfge8, an extracellular glycoprotein can also mediate the internalisation of collagens as a bridging molecule in macrophages [161]. And lastly, collagen can be taken up non-selectively through a form of endocytosis termed macropinocytosis [197]. Interestingly, collagen internalisation can be modulated by cytokines, for example, TGF-β can promote collagen uptake [198] whereas TNF-α and IL-1α inhibit this process [199]. The engulfed collagen has been shown to be directed to lysosomes for degradation [192].

1.2.6 ECM in the fibrotic tissue

The composition of ECM in fibrotic tissue is different from normal tissue. The excessive deposition of collagen in UIP [200] has been characterised as the continuous deposition of type-I collagen rich matrix in the lung interstitium [2, 3]. However, the composition of ECM changes at different stages of the disease [201, 202]. Collagen type-I, III and IV may be associated with early stage of lung fibrosis [203]. At the later stage of UIP, type-I collagen was found increased and type-IV collagen was found decreased [204]. In the areas of established (end-stage) fibrosis, there was almost exclusively type I collagen [205]. The increased stiffness of the alveolar spaces prevents normal gas exchange and destroys the alveolar structure which leads to respiratory failure and consequently cardiac compromise [206, 207].

Besides the composition of fibrotic ECM, many other properties should be considered, including the stiffness [208], the organisation and orientation (e.g. cross-linking) [175] and the post-translational modifications of ECM [175, 209]. Together with other physical/mechanical changes, they all contribute to the functional properties of ECM.

The elasticity/ stiffness of ECM is important for cell biology which is largely depended on the ratio of elastin and collagens [210, 211]. With increased ECM stiffness, fibroblasts increased proliferation, became resistant to apoptosis and enhanced collagen production [208].

In addition, the orientation of the ECM components may also affect the efficiency of their degradation through collagenases. The orientation of collagen in the skin scar tissue is more parallel orientated relative to the epithelial surface than normal skin [212].

Excessive activation of cross-linking enzymes such as lysyl oxidase (LOX) promotes the interaction between hydroxylysine and collagen that can enhance the matrix stabilisation and prevent it from degradation [213].

1.2.7 ECM is bioactive matter in the body

ECM modulates cell behaviour through biomechanical and biochemical signals [173]. The changes ECM components during fibrosis are now regarded as a pathogenic factor that contributes to the establishment of fibrosis. Fibrotic ECM causes the perpetuation of tissue inflammation, promotes fibroproliferation, and triggers aberrant differentiation of cells which all lead to continuous fibrosis [154].

ECM in fibrotic tissue interacts with major effector cells of fibrosis. Fibrotic ECM with increased stiffness enhances the proliferation and differentiation of fibroblast. The phenotype of normal fibroblasts is altered to pro-fibrotic in matrices with increased stiffness [202]. The modification and the re-organisation of ECM can also change the nature of ECM to be resistant to degradation enzymes thus enhances ECM accumulation [178]. *In vitro*, IPF fibroblast-derived ECM can change the gene expression profile of the fibroblast and forms a positive feedback loop of fibrosis that maintains the pro-fibrotic environment [155]. ECM also plays an important role in determining innate cell function in inflammation [156]. The interaction between macrophages and ECM affects

the inflammation effector functions of macrophages [214]. ECM may also have instructive roles on fundamental cellular homeostatic processes. Recently, it was found modulating the autophagy pathway [215]. ECM increases basal autophagy in epithelial cells through adhesion molecules [216] and the detachment from ECM also induces autophagy as a surviving signal [217]. Many of the ECM components have been shown to modulate the autophagy pathway [215]. ECM may also affect many signalling pathways that are associated with autophagy such as the redox signalling and reactive oxygen species (ROS) production [154].

ECM also interacts with growth factors thus modulating lung fibrosis. ECM proteins can activate the latent form of TGF-β which is a key mediator in lung fibrosis and promote ECM production and deposition in the lungs [218]. Connective tissue growth factor (CTGF) is another important mediator of lung fibrosis which can be induced by TGF-β and is highly expressed on activated fibroblasts [219, 220]. CTGF interacts with ECM components and enhances the expression of TIMPs, thus inhibiting the matrix degradation and promotes tissue fibrosis [221].

1.3 Autophagy: key mechanism for cellular homoeostasis

Cellular homoeostasis provides cells with the critical conditions to survive and to perform their functions. The disruption and loss of homoeostasis have pathological consequences [175, 222]. Autophagy is one of the important, fundamental and constitutive mechanisms that control and regulate cellular homoeostasis [223, 224].

1.3.1 A brief history of autophagy: a cellular constitutive mechanism for homoeostasis

The discovery of the lysosome by C de Duve in the 1950s led to the observation of autophagy in 1963. Autophagy is described as a "self-eating" (derived from Greek) process as the cell captures part of its own cytoplasmic material to form autophagosomes (termed as macroautophagy) and then deliver it to lysosomes for degradation [225].

The formation of an autophagosome starts with a structure named as "isolation membrane" which is formed around the cellular waste. The isolation membrane elongates, encloses the waste and seals up as a double-membrane autophagosome which is then directed to a lysosome for degradation. The understanding of this process progressed in the 1990s when starvation-induced autophagy was observed in yeast, which consequently led to the discovery of autophagy-related genes (ATG) and their products [226]. The ATG homologues have since been identified and extensively studied by other researchers in many organisms, and remarkable progress has been made in its role in human health and diseases [226]. The highlight of autophagy research was when Yoshinori Ohsumi was awarded the Nobel Prize of 2016 (in Physiology or Medicine) for his contribution to understanding the fundamental mechanisms of the autophagy process [227, 228].

In the last two decades, research in autophagy rapidly progressed towards the understanding of its molecular mechanisms and broader role in its involvement in human health and disease [223, 229].

1.3.2 The regulation of autophagy: step by step

Macroautophagy (autophagy) can be divided into five steps: initiation of the isolation membrane/ phagophore; membrane elongation; formation of autophagosomes (maturation); fusion with lysosomes; and lastly the degradation and release of the products back to the cytoplasm [230]. The discovery of autophagy-related genes and proteins had promoted the research and understanding of the autophagy process [226].

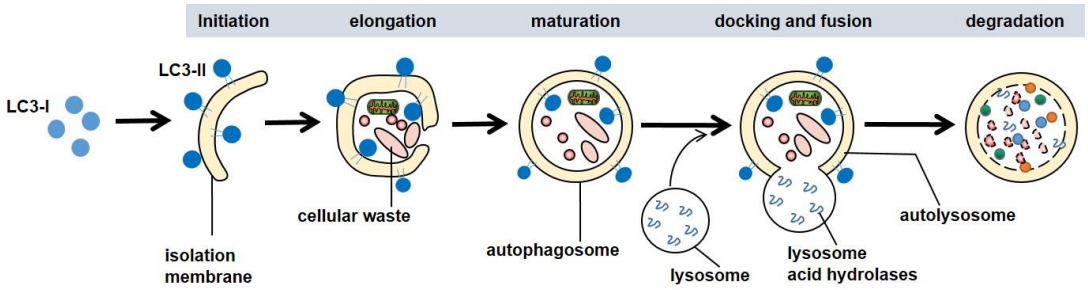

Figure 1-2 The autophagy-lysosome pathway step by step.

Macroautophagy (autophagy) includes five steps: initiation of the isolation membrane; membrane elongation; formation of autophagosomes (maturation); fusing with lysosomes; and the degradation and release of the products back to the cytoplasm.

The first step of autophagy is the initiation of the isolation membrane. The endoplasmic reticulum (ER) is proposed as the major resource of the autophagosome membrane, but there is evidence that mitochondrial membranes, Golgi apparatus, recycling endosomes, and the plasma membrane may also contribute to this structure [231]. The autophagosome formation process involves many proteins, among which double FYVE domain containing protein 1 (DFDP-1), Atg-14L, uncoordinated 51-like kinase-1 (ULK1) complex, Atg5, and Atg9/Atg16L are key regulators [231].

Once the cup-shaped isolation membrane is closed up to form an autophagosome, it is directed to a lysosome. The outer membrane of a matured autophagosomes eventually fuses with a lysosome to form a single membrane structure (autolysosomes). The exact mechanisms for autophagosome-lysosome fusion are under investigation, but it is known that small GTPases, especially Rab7, and lysosome-associated membrane proteins (e.g., LAMP-1 and LAMP-2) are heavily involved and functionally relevant [232-234]. With the lysosomal enzymes such as hydrolases, the autophagosome cargo will be degraded which begins once the lysosomal enzymes are activated by acidification of the cytosol pH values through the proton pump on the lysosome surface

[235]. Autophagy is completed by releasing the degraded products back to the cytoplasm and the free amino acid, nucleotide, glucose, and fatty acid are then recycled through anabolic pathways [236].

In mammalian cells, microtubule-associated protein light chain 3 (LC3), the mammalian homologue of yeast ATG8, is recognised as the primary autophagy marker [237]. After synthesis, nascent LC3 is cleaved by ATG-4 to produce the cytosolic form (LC3-I). LC3-I is converted to LC3-II after conjugation with phosphatidylethanolamine (PE) by ATG-7 and ATG-3 [238, 239]. LC3-II is the only protein found to be present on both the inner and outer membrane of autophagosomes in mammalian cells [237, 240]. LC3-II on inner autophagosomes membrane is degraded with the cargo and LC3-II on the outer autophagosome membrane is recycled by ATG4B [241].

The upper stream of the autophagy pathway is controlled by two distinct signalling complexes: Tor-Atg13-Atg1 [242, 243] and Beclin 1 (Atg6)-Atg14-hVPS34 [244-247]. The deprivation of amino acid, inhibition of the mammalian target of rapamycin (mTOR), hypoxia, ER stress, immune mediators [248], and cellular receptors such as pattern recognition receptors [249, 250] and Fc receptor [251] can trigger the autophagy process through these two mechanisms.

1.3.3 Autophagy pathway: the experimental measurements

It is estimated that in every hour around 1%–1.5% of cellular proteins are recycled through basal autophagy in the liver [252]. Autophagy is a rapid process and an autophagy cycle takes about 7-9 minutes in yeast [253]. The formation of autophagosomes takes approximately 4-5 minutes in yeast and 5-10 minutes in mammals [252-254].

Autophagy occurs under resting conditions (basal autophagy) and in response to cellular stress (induced autophagy). Basal autophagy is regarded as an important ‘quality control’ mechanism for cellular homoeostasis [255]. Induction of autophagy occurs through mTOR-dependent and -independent pathways. The most frequently used methods of autophagy induction *in vitro* are starvation and rapamycin treatment, both

of which act by inhibiting the mTOR [256]. *In vitro,* activated functional autophagy returns to basal status rapidly if the autophagy stimulus is removed [257-260].

Autophagy can be non-selective and selective processes depending on the involvement of specific adaptor proteins [255, 261]. Selective autophagy targets specific dysfunctional protein aggregates (aggrephagy), damaged cellular organelles (mitochondria and mitophagy), foreign pathogens (xenophagy) and excessive lipids (lipophagy). The most extensively studied adaptor for selective autophagy is p62. However, other adaptor proteins (e.g., NDP52 and NBR1) have also been proposed as adaptor proteins for selective autophagy [261, 262].

The experimental measurement of the autophagy pathway is largely dependent on measuring the expression of the autophagy-related proteins of which LC3-II is the only specific autophagy marker in mammals [263]. The measurement and interpretation of LC3 expression, usually by western blotting, can be complicated and needs to be interpreted in the context of data from other assays (e.g., bafilomycin A1 treatment and the expression of p62) [230, 264]. The relative expression of autophagy-related proteins in the presence of autophagy stimulation and inhibition is, therefore, an important surrogate to assay functional autophagy dynamics [230]. A common method to visualise the autophagy pathway is GFP-labelled LC3 proteins under fluorescent microscopy, however, it has its disadvantages [230]. Monodansylcadaverine (MDC) has been used as a dye for the study of autophagic vacuoles [265], but it has been found later to be a non-specific marker of autolysosomes with off-target staining of lysosomes and it does not stain autophagosomes [263, 266]. Thus, MDC staining may fail to reflect autophagosome maturation or degradation [267]. The development of efficient and specific autophagy-related dyes such as Cyto-ID have facilitated the study of autophagy with live staining of the autophagic compartment in a more specific and efficient manner [268]. Nevertheless, the identification of the archetype structure of double-layer membrane autophagosomes with transmission electron microscope (TEM) is still the gold-standard method to determine the presence of autophagy although it is not quantitative [230, 263].

The autophagy substrate protein p62 is also known as sequestosome 1/SQSTM1. It is a ubiquitin protein and only expressed in animals and humans. It binds directly to LC3-II

and is incorporated into the autophagosome [269]. Accumulation of p62 is observed when autophagy is impaired, and one of the consequences of this is the formation of large cellular aggregates in the cells [270]. The p62-positive aggregate is found in diseases such as various neurodegenerative disorders, liver disorders and cancers [271-273]. Genetically modified ATG animal studies have shown that p62 is required for the formation of the cellular aggregates [274]. *In vitro,* p62 is necessary for the clearance of M. tuberculosis infection through autophagy and without p62, the organism is not efficiently eliminated [275]. In homeostatic condition, p62 is found in the regulation of inclusion body formation and elimination of p62 can nullify damage caused by autophagy deficiency in mice [270].

To study basal autophagy or the functional dynamic of activated autophagy, late-phase autophagy blockers are normally used (e.g. bafilomycin A1). Bafilomycin A1 is an inhibitor of the v-type ATPase that blocks the fusion of the autophagosome and lysosome by inhibiting lysosomal acidification [276]. By blocking the autophagosome degradation, neither LC3-II nor p62 proteins will be degraded through the autophagy-lysosome pathway. Therefore, the accumulation of the autophagy marker (LC3-II) by bafilomycin A1 represents the "autophagy activity" in cells or the autophagic flux (calculated by the changes of LC3-II and p62 expression) [230].

1.3.4 Common mechanisms for autophagy in lung diseases

Many lung diseases manifest processes including ER stress, oxidative stress, hypoxia and inflammation that in turn are implicated in the autophagy pathway [17].

ER stress has been demonstrated as a modulator of the autophagy response [277]. Cigarette smoke [278], hypoxia [279] and LPS [280] have all been shown to induce ER stress. In the lung fibroblast cell line WI-38, ER stress increased LC3-II expression [281].

The lungs are particularly susceptible to the oxidative stress as they are exposed to both a relatively high oxygen environment and inhaled toxins [282]. The elevated oxidative stress has been shown to be associated with the activation of autophagy [283] and it is thought that autophagy in smoking-related lung conditions, such as COPD, are related

to oxidative stress [7, 284]. Cigarette smoke extract has been shown to increase oxidative stress in human bronchial epithelial cells that increased LC3-II expression [285]. In starvation-induced autophagy, Atg-4 has been identified as the potential target for oxidative stress [286] and the regulation of intracellular superoxide has been proposed as a mechanism of starvation-induced autophagy [287].

Hypoxia is associated with autophagy activation in many contexts, especially in tumours, and HIF-1 has been presented as a regulator in hypoxia conditions [279]. Protein-kinase-C (PKC) δ has been implicated in the autophagy induction under hypoxic conditions [288].

Inflammation regulates the autophagy pathway through the activation of Toll-like receptors (TLR)[289]. In RAW264.7 mouse macrophages and human alveolar macrophages, it has been shown that the induction of autophagy was related to the activation of TLR-4 [250]. Other TLRs, such as TLR-7 and TLR-3, have also been involved in autophagy in RAW264.7 macrophages [290].

1.3.5 Autophagy, wound healing and fibrosis

The association of autophagy with fibrosis is complex. It is generally believed that the disruption of homoeostasis is the initiation of a dysregulated wound healing process which leads to the failure of normal wound healing and results in tissue fibrosis [175, 222]. Autophagy, a fundamental process of maintaining cellular homoeostasis, is likely implicated in the regulation of the fibrotic process and there is some evidence that ECM may instruct cells through the autophagy pathway [215, 291, 292].

Induction of autophagy by trifluoperazine (TFP), an autophagy inducer, in primary mesangial cells from mice decreased collagen-I protein levels induced by TGF-β *in vitro* [293]. More recently, the newly approved drug for IPF, nintedanib was shown to have an anti-fibrotic effect on lung fibroblasts from IPF patients *in vitro* through three independent mechanisms which included the induction of non-canonical autophagy [294]. Animal studies provide more evidence to suggest that a functional autophagy pathway is critical for the normal wound healing process. In a genetically manipulated kidney experimental model, lack of autophagy resulted in excessive collagen in mouse kidneys *in vivo* and the activation of mTOR was accompanied with autophagy

resolution and renal repair [295]. In lung fibrosis, IL-17A antagonism improved both bleomycin- and silica-induced pulmonary inflammation and fibrosis in mice, which was abolished by inhibiting the activation of the autophagy pathway [296]. Researchers also showed that, in the bleomycin-treated mouse model of lung fibrosis, rapamycin-induced autophagy decreased the level of hydroxyproline and alpha-smooth muscle actin (alpha-SMA) and increased survival in treated mice [297, 298]. These data all suggest autophagy induction is associated with the resolution of lung fibrosis. There is evidence however, that autophagy may be a "double-edged sword" in organ fibrosis. In liver fibrosis, enhanced autophagy can attenuate liver fibrosis by inhibiting tissue inflammation, but can also activate hepatic stellate cells (HSCs) and increase collagen synthesis [299]. It has also been suggested that autophagy has a dual role in the lung epithelial injury which is proposed as one of the important mechanisms of lung fibrosis [300].

In patients with IPF, previous studies suggested that autophagy is depressed even with the known autophagy-regulating mechanism being upregulated [297, 298, 301]. Whole lung homogenate or tissue section from IPF patients have decreased levels of LC3 and p62 as determined by western blotting and fluorescent microscopy [297]. Immunohistochemistry staining showed that the accumulation of p62 was specifically increased in type-II epithelial cells within the fibroblastic foci (FF) and with no expression of autophagy markers in (myo)fibroblasts or type-I epithelial cells [301]. An mTOR downstream effector protein, p-S6, was weakly expressed in healthy lungs but was found strongly expressed in IPF lung myofibroblasts suggesting that autophagy induction was suppressed in IPF lungs which might be the result of activation of mTOR signalling that inhibits the activation of the autophagy pathway. [298]. In these three studies, AM were not specifically described. However, there are AM found in the alveolar space in these images and the immunohistochemistry (IHC) showed similar staining of p62, ubiquitin and beclin in AM as in type-II epithelial cells [301].

Excessive ECM deposition is a hallmark of tissue fibrosis including lung fibrosis (e.g., IPF). ECM components are biologically relevant and regulate many cellular processes including autophagy [302]. The pathways linking ECM and autophagy are largely unknown but cell surface integrins, lysosome motility and position, and soluble ECM

may be relevant to the cross-talk between the two pathways [215, 291]. ECM increases basal autophagy in epithelial cells through focal adhesion kinase (FAK) [216]. The proposed mechanism is that FAK tyrosine phosphorylates an upstream mTOR regulator (TSC2) which suppresses the activation of mTOR and leads to autophagy activation [303]. On the other hand, the detachment of epithelial cells from ECM (anoikis) induces autophagy which has been proposed as a mechanism to enhance cell survival and reattachment [291]. Indeed, cells cultured on low-attachment surfaces have shown increased autophagy due to the lack of integrin adhesion [304, 305]. Furthermore, adhesion to ECM promoted morphology changes of cells [216], which affects the redistribution of lysosomes and enhances the motility of lysosomes [306]. Lysosome positioning includes the dynein-mediated retrograde transport of lysosomes which promotes its fusion with autophagosomes. Thus, the changes of lysosome positioning by the interaction with ECM may affect the degradation of autophagosomes [306]. ECM may also modulate many processes in the lungs, such as oxidative stress, that are relevant to the autophagy pathway [154, 215].

In summary, autophagy as a fundamental mechanism of maintaining cellular homoeostasis, is involved in wound healing and tissue repair. Its exact role in IPF needs to be closely investigated.

1.4 Exosomes: mediating the intercellular communication

Exosomes are small vesicles that are released by almost all cell types. In recent years, exosomes have drawn much attention regarding their physiological and pathological roles in health and diseases.

1.4.1 Exosomes, microvesicles and apoptotic bodies

Intracellular communication is crucial for the maintenance of homoeostasis and the response to pathological factors. Exosomes are novel mediators for cell-cell communication. They are a group of small vesicles that are composed of a bilayer lipid membrane with protein and RNAs contents. Exosomes are released by parent cells and captured by recipient cells. Cells produce exosomes continuously under resting conditions, but the release of exosomes can be enhanced under certain conditions [307]. The release of exosomes causes biological effects in both the parent and the recipient cells [308, 309].

Cells can ‘talk’ to each other through direct contact or by the secretion of certain molecules. It is well-known that during apoptosis, apoptotic bodies are released and can serve as mediators between cells. The earliest observation of extracellular vesicles (EVs) can be traced back to 1946 when Chargaff and West observed pro-coagulant platelet-derived particles in plasma [310]. In 1983, the release of exosomes by the fusion of multivesicular bodies (MVBs) with plasma membrane was observed during the maturation of red blood cells [311, 312]. Later, these vesicles, released from lymphocytes, were proven to be functional material that could mediate the antigen-presentation process [313]. Around a decade ago, different RNAs were found within such vesicles and also demonstrated important functions that affect cell biology [314]. The significance of these nano-sized vesicles are now well-acknowledged and the subject of a new era of studies in many areas relating to health and diseases [315-320].

The biogenesis of exosomes is through the endocytic pathway. Exosomes are released by the fusion of MVBs with cell membrane [311, 321, 322]. MVBs are also known as late endosomes or multivesicular endosomes (MVEs) that are matured from early endosomes. Early endosomes are generated by endocytosis through the endocytic

transport pathway [322-324]. Late endosomes can be either directed to lysosomes for membrane recycling or they can be signalled to the cell membrane for the release of exosomes [322].

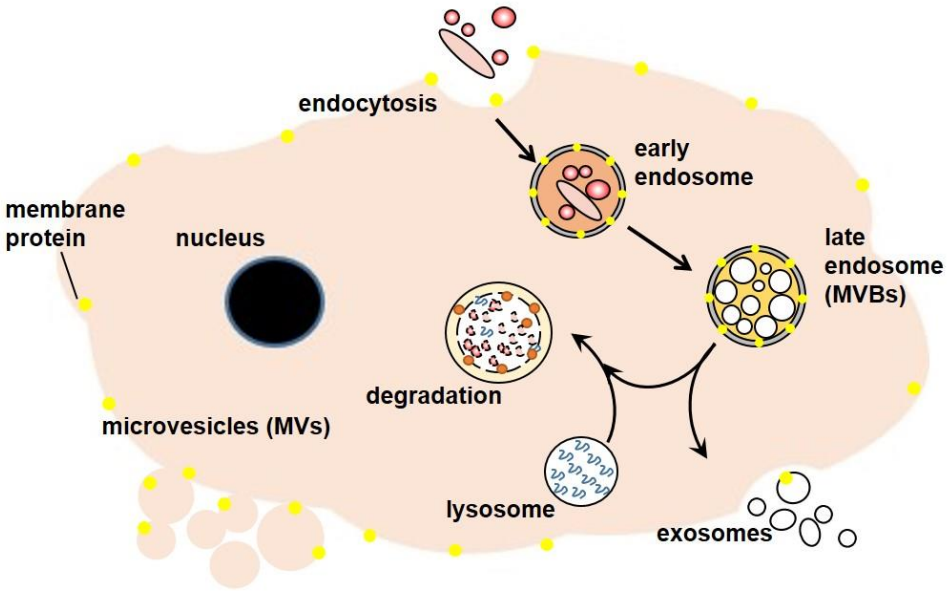

Figure 1-3 Secretion of exosomes and microvesicles.

Exosomes are released by the fusing of MVBs with plasma membrane; otherwise, MVBs can be directed to lysosomes for degradation. Microvesicles are released by the shedding of the plasma membrane. Both exosomes and MVs may carry membrane proteins of their parent cells.

MVs and apoptotic bodies are generated by the shedding of the plasma membrane. MVs (100 - 1,000 nm) are produced by healthy cells, while the apoptotic bodies (50 - 5,000 nm) are generated when cells undergo apoptosis [324]. The distinguishing features of exosomes, microvesicles and apoptotic bodies are largely dependent on their sizes. The size-definition of exosomes reported in the literature has been evolving, but there is an agreement that exosomes are small lipid bilayer vesicles ranging from 20 nm to 150 nm [324-326]. The most commonly described exosomes are between 40 nm to 100 nm as first defined in reticulocyte differentiation [311].

Besides the difference in size, these three types of vesicles also have different biological properties and functions [324]. As exosomes are produced from the endosomal compartment, they express shared proteins even if derived from different parent cells. The commonly expressed proteins are better described in exosomes than other vesicles. These proteins include transmembrane proteins like tetraspanins (e.g., CD9, CD63 and CD81); MHC class I and MHC class II; cytosolic proteins (e.g., heat shock proteins-70

and actin); and specific proteins that are associated with the endosomal sorting complex required for transport (ESCRT), such as tumour susceptibility gene 101 (TSG101) and Alix [323]. However, at present, there are no such proteins that can specifically distinguish exosomes from other large vesicles [327]. DNA fragments, e.g. double-stranded DNA (dsDNA) and genomic DNA, are often present on microvesicles and apoptotic bodies but are rarely found on the surface of exosomes. DNA is found both inside and on the membrane of EVs. The dsDNA is the most common form of DNA that located outside the EVs [326, 328-330].

EVs also carry surface proteins of their parent cells which may help identify their origins. Studies suggested that cellular membrane proteins are likely to be expressed on MVs. Sometimes, the membrane proteins can also be integrated on exosomes during their endosome formation [331, 332].

1.4.2 Current tools to study exosomes

Exosomes are released from almost all types of cell. They have been isolated from many types of body fluid including semen, blood, urine, saliva, breast milk, cerebrospinal fluid bile and bronchoalveolar lavage (BAL) fluid [324]. Exosomes can be studied by several methods and each method has its own advantages and limitations in the detection and measurement of exosomes [333, 334].

The most widely accepted practice to purify exosomes from bio-fluids or tissue culture media is ultracentrifugation after the sequential centrifugations of removing contaminating cellular products. Sequential centrifugations before the isolation of exosomes are highly recommended by the International Society for Extracellular Vesicles (ISEV). Missing steps between each centrifugation may compromise the results [325]. Purified exosomes can be directly visualised under transmission electron microscopy (TEM) which provides the physical evidence, i.e. the sizes of the vesicles. However, TEM is not a quantitative method and it often requires a lot of material (large volumes of fluid) to study. The purified exosomes can also be further studied for different purposes. For example, the protein profile of exosomes can be studied by western blotting or proteomics and RNAs can also be extracted for RNA analysis.

Nanoparticle tracking analysis (NTA) is a relatively new technique to study MVs and exosomes [335]. NTA is designed on the principle of Brownian motion and it can visualise and analyse vesicles in real time. The advantage of NTA is that it can distinguish vesicles of different sizes in the same solution [325, 336]. The concentrations of the tracked vesicles can be calculated based on the distance they move during a period of time. The concentrations of vesicles within the range of exosomes can be calculated and presented as the value of "area under curve" representing the level of exosomes.

Flow cytometry has been used to study the EVs in bio-fluids. Traditional cytometers cannot detect vesicles that are smaller than 300 nm. Newly developed cytometers specifically designed for MV studies are mainly used to study large vesicles and are not useful for exosomes [325]. The most common strategy to study exosomes with flow cytometry is to couple exosomes with micrometre-sized beads by targeting specific exosome surface proteins. This strategy facilitates the study of exosomal surface proteins and an optimised protocol may also be used for exosomal concentration study. It has been tested in several types of bio-fluids, but so far there is no study of its application in the BAL fluid samples from IPF patients [333, 337].

1.4.3 Biogenesis of exosomes

The biogenesis of exosomes has several steps including the formation of MVBs, the transportation of MVBs to the plasma membrane, docking, and fusion with the plasma membrane to release exosomes.

As described, MVBs can be either directed to the plasma membrane (for the release of exosomes) or to lysosomes (for degradation). Yeast mutants led to the discovery of the molecular machinery that regulates the biogenesis of MVBs for lysosome degradation. However, there is very limited understanding of the mechanisms of secretory MVBs for exosome production [330]. In mammals, the ESCRT is the key component for MVBs production. There are four evolutionarily conserved members of the ESCRT complexes: ESCRT-0, -I, -II and –III. Other accessory proteins, such as Alix and VPS4, are also implicated in the process [338].

Besides the ESCRT pathway, MVBs can also be formed through alternative mechanisms that are ESCRT independent. The first reported ESCRT-independent exosome production mechanism was observed in oligodendroglial cells. It was found that in these cells, the release of exosomes was sphingomyelinase dependent. As a result, the ceramide level in these exosomes was increased [339]. Furthermore, cells were still able to release CD63-positive MVBs even if the four ESCRT protein complexes were depleted by targeted siRNA [340]. Studies in melanocytes suggested that there might be other mechanisms of MVBs formation that are independent of both ESCRTs [341] and ceramide [342].

Following the formation of the MVBs, there are a few more steps before the release of exosomes including the traffic/ mobilisation of MVBs to the plasma membrane, docking and fusion with the cell surface. There is very little known about the exact mechanisms of how MVBs are directed to the plasma membrane. However, MVBs following different paths may have different biochemical and morphological properties. For example, cholesterol-rich MVBs are prone to be fused with plasma membrane for exosome secretion and cholesterol-poor MVBs are targeted by lysosomes for degradation [343]. Studies also showed that Rab GTPases, such as Rab 11, Rab 27 and Rab 35, are involved in exosome secretion [344-346]. ALIX and VPS4, the accessory proteins of the ESCRT pathway, may also play a role in exosome secretion [324, 347].

1.4.4 Autophagy in the regulation of exosome production

Exosomes are produced via the endosomal pathway and they interact closely with the autophagy-lysosome pathway to maintain cellular homoeostasis [348, 349].

The first piece of evidence linking autophagy and the exosome pathways is the observation of amphisomes. Amphisomes are formed when autophagosomes fuse with late endosomes [350]. There are more complex amphisome-related structures that are observed, but the function and mechanism are not yet understood. However, it is believed that these structures are formed during autophagosome–endosome interaction and they might be important for the maturation of autophagosomes. Furthermore, Rab-7 and Rab-11 have been demonstrated with essential roles for the interaction between autophagosome and the endocytic pathway [351, 352].

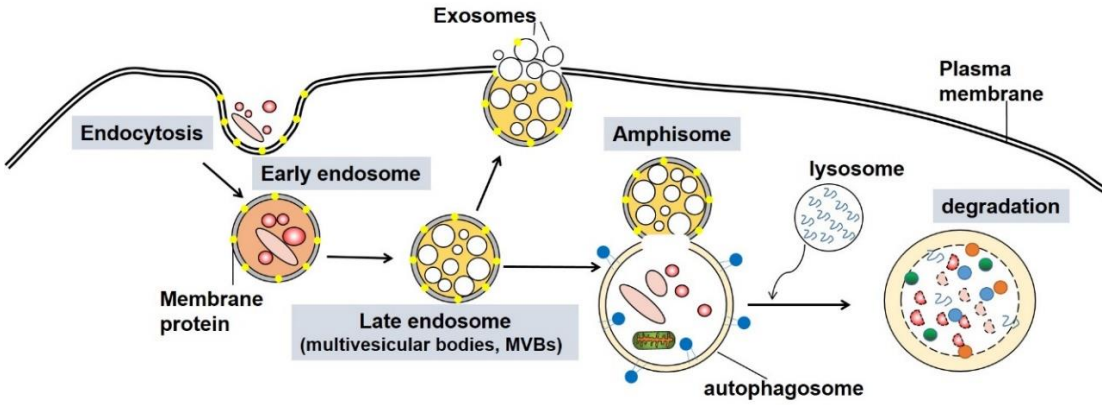

Figure 1-4 The interaction between autophagy and the exosome pathways.

The formation of the amphisome is the first piece of evidence suggests that the two pathways are closely linked.

Studies have shown that the changes in the autophagy-lysosome pathway affect exosome secretion. Fader and colleagues showed that autophagy induction promoted the fusion of MVBs with autophagosomes and therefore decreased the secretion of exosomes in K562 cells [353]. On the other hand, blockage of autophagosome-lysosome fusion by bafilomycin A1 increased the secretion of exosomes [354-356]. More recently, there is direct evidence showing that Atg12 and Atg3 interact with ALIX and regulate late endosome distribution, exosome biogenesis and the fusion of autophagosomes with MVBs [357]. Thus, dysregulated autophagy affects the MVBs transportation path and thereby affects exosome secretion.

The status of lysosomes, the common destination for the degradation of both autophagosomes and MVBs, also have an impact on the exosome production [327]. In conditions of lysosomal dysfunction, MVBs are more likely to be directed away from lysosomes to the plasma membrane and eventually increase exosomes secretion [327]. Mutations that affect lysosomal functions, such as mutations in Tau and VPS4, increased the secretion of EVs and the expression of disease-related proteins [358, 359]. More evidence is emerging from the studies in lysosome storage disorders (LSDs) where the lysosomes are dysfunctional [327].

Furthermore, there are pathways that regulate both the EVs secretion and autophagy. Several ESCRT proteins, for example, ALIX, HRS and TSG101, are implicated in both autophagy regulation and EVs secretion [360, 361]. In addition to that, ceramide, which has been demonstrated as an ESCRT-independent pathway of exosome secretion, also functions through the autophagy pathway. Sphingosine 1-phosphate (S1P) is the metabolite of ceramide. It has been shown that the activation of S1P receptor on MVBs facilitates the release of exosomes [362]. S1P signalling also affects the autophagy pathway and may play a role in pulmonary fibrosis. S1P treatment attenuated LC3 expression and autophagosome formation in primary lung fibroblasts isolated from IPF patients. The upregulated overexpression of S1P lyase (S1PL) found in the fibrotic lung tissues is believed to act as a protective mechanism by promoting autophagy [363].

Lastly, exosomes might have similar roles to autophagosomes in terms of recognising toxic proteins or RNAs and releasing them outside of the cells for homeostatic purposes. Thus, when the autophagy pathway is over-occupied or compromised, exosome production may serve as an alternative method for handling cellular waste [349]. For example, exosomes have been shown to assist in the sharing of pathological proteins between cells in many neurodegenerative conditions where autophagy is impaired [364].

1.4.5 Mediating the intercellular communication: exosomal lipids, proteins, RNAs and DNA

Exosomes are found modulating many key biological processes such as immune functions, metabolic regulation, and the communication between neurons and stem cells [319, 330, 365-367]. They perform these functions via the major components of exosomal lipids, proteins, and RNAs.

Lipids are specifically sorted structural and functional constituents of EVs. They form the bilayer membrane of EVs and maintain their stability in the extracellular environment [330]. In general, EV lipids contain higher levels of sphingomyelin, cholesterol, phosphatidylserine, and glycosphingolipids. The lipid composition varies between exosomes from different parent cells [368]. EV lipids can pass the cellular information between cells. Some lipids, for example, eicosanoids, fatty acids, and cholesterol, can be transferred between cells and affect their functions [368]. Other

lipids, such as cholesterol, can regulate the formation and release of EVs [369]. Furthermore, vesicle-bound lipid molecules even have more functions, such as dendritic cell maturation [370], lymphocyte chemotaxis [370], modulation of the cellular signalling pathways [371], induction of cell death [372], mediating angiogenesis [373] and facilitating the reproduction activity [374].

Exosomes express a group of conserved but distinct proteins as described earlier in section 4.1. Exosomes also carry and share disease-relevant proteins between cells. The release of exosomes has been proposed as an additional mechanism of removing the toxic proteins to alleviate cellular stress. In neurodegenerative diseases, the identified toxic proteins include Aβ, APP C-terminal fragments, α-synuclein, SOD1, the prion protein (PrP) and many others [375]. For example, the disease protein α-synuclein was found in exosomes of Parkinson's disease and may be associated with disease progression [376]. The amyloid protein is found on exosomes in Alzheimer diseases [377].

Exosomal RNA cargos are also carefully sorted and packed into exosomes for intercellular communication. Exosomal microRNA and messenger RNA (mRNA) contain genetic information from the parent cells. Exosomal RNAs can be delivered to the recipient cells, thus affecting their RNA expression, protein synthesis and function [314]. It is reported that cells increased the sorting and release of microRNA through exosomes when treated with endogenous RNAs [378]. Cancer cells not only secrete more exosomes but also with increased distinct exosomal microRNAs [379]. Exosomal RNAs can be used as specific markers associated with certain diseases. For example, exosomal microRNAs have been associated with Alzheimer's disease and have been proposed as diagnostic biomarkers [380]. Exosomal RNAs that are associated with tumour progression can affect healthy cells and drive tumorigenesis [381]. The RNA contents could also affect the immune system and affect the identification and clearance of cancer cells [382]. They can induce stromal cell activation, angiogenesis, immune escape and drug resistance in cancer [383]. Exosomes have also been associated with cancer metastasis and facilitate the formation of a pre-metastatic environment [384].

DNA is also found in exosomes and it can be found both inside and outside the exosomes [326, 385]. Similar to RNA, DNA carries genetic information and can be

delivered to other cells through exosomes. It has shown that exosomes can carry the modified DNA in cancers and deliver the mutations to other cells [385]. Mutated exosomal DNA may be used as biomarkers for diseases. The DNA in exosomes are different from that of the MVs and apoptotic bodies [386]. The physiological and pathological roles of exosomal DNA are largely unknown.

Exosomes are proposed as biomarkers in many diseases. In pathological conditions, the cellular profile is affected which then changes the exosome profiles. Exosomes serve as mediators for cell-cell communication and their presence is associated with many pathological conditions such as inflammation, infection, cancer, neurodegenerative disorders and tissue fibrosis [333, 387-389]. It has shown that when inflammation is active, the production of exosomes and MVs are promoted. For example, Mycobacterium tuberculosis (Mtb) infection [390], inflammasome activation [267] and in human diseases such as sarcoidosis, the production of exosomes is enhanced [391]. Exosome profile is changed in cancers, the adaptation of cells to the adverse environment triggered the aberrant exosomal process to promote the survival of cancer cells [387].

There is ongoing active research investigating exosomes as novel therapeutic tools in the areas such as drug delivery, anti-tumour therapy, pathogen vaccination, and immune-modulatory and regenerative therapies [392].

1.4.6 Exosomes in the lung and lung fibrosis

At present, only a handful of studies have been published regarding exosomes in the human lung. Exosomes in BAL fluid isolated from the healthy lungs expressed MHC-I, MHC-II, CD54, CD63, and CD86, but the role of exosomes was not studied [393]. BAL fluid exosomes in patients with allergic asthma may contribute to the cytokine and leukotriene production [394]. The microRNA profile in BAL fluid exosomes from asthma patients showed distinct microRNA patterns and significant changes of 24 miRNAs and when compared to the healthy controls [395]. BAL exosomes from sarcoidosis patients showed an increased level of exosomes and their pro-inflammatory role in the lungs when compared to healthy individuals [391]. BAL fluid exosomes from sarcoidosis patients also showed significantly higher expression of MHC class I and II,

tetraspanins CD9, CD63, and CD81. They also had increased level of neuregulin-1 which had been associated with cancer progression. PBMC incubated with the sarcoidosis exosomes had increased level of IFN-γ and interleukin (IL)-13 compared to the controls [391].

The role of lung exosomes was focused on immunity and it has been studied in different models. This includes the response of the lung to different stimuli such as infection with different pathogens [396] and nanoparticles [397]. Exosomes from different sources in the allergic airways can stimulate systemic immune response in mice [398-400]. Mycobacterial pathogen-associated molecular patterns (PAMs) were detected from BAL fluid exosomes isolated from mice lungs that were infected with pathogens. A mouse model of LPS induced acute lung injury (ALI) suggested that the mouse alveolar macrophage-derived EVs (F4/80 and CD11c positive vesicles) were the major population in the early phase of ALI and a major contribution to the inflammatory process [401].

Macrophages are critical for the normal wound healing and they can release microvesicles as other immune cells. Macrophage-derived exosomes mediate many biological processes [402-404]. Exosomes released from human macrophages contain enzymes that are related to the pro-inflammatory cytokine and leukotriene biosynthesis and promote granulocyte migration [405]. Macrophage released MVs contain MHC class II and have antigen presentation function [406]. In addition, macrophage-derived EVs contain high levels of miR-223 which regulates the proliferation and differentiation of myeloid cells. Macrophage MVs can induce the differentiation of macrophages and promote the transfer of miR-223 [407]. Macrophage MVs cause inflammation-induced programmed cell death in vascular smooth muscle cells via transfer of functional pyroptotic caspase-1 [408].

Inflammation and infection can change the profile and function of macrophage-derived exosomes [396, 402]. Exosomes released by macrophages that are pre-treated with a few different types of pathogens caused inflammatory responses *in vitro* and *in vivo*. When macrophages are infected with microbial pathogens, the production of EVs have been shown to be enhanced and the contents were changed [409]. Mycobacterial products, such as cell wall components, can be sorted to the EVs and promote

inflammatory responses in resting macrophages [396]. These EVs also stimulated the expression of pro-inflammatory cytokines and chemokines that drive the inflammation by facilitating the migration of immune cells and causing tissue damage [410, 411]. EVs released by macrophages that are infected with parasites showed down-regulation of the immune functions, such as by the inhibition of complement activation and the release of TGF-β [412]. In fact, different phenotypes of macrophages release specific exosomes with distinct properties [396]. A study of mouse macrophages showed that activated macrophages release microvesicles that contain polarised M1 or M2 mRNAs *in vitro* [413].

In lung diseases, exosomes are proposed as potential biomarkers for the diagnosis of asthma, lung cancer, chronic obstructive pulmonary diseases (COPD) and other pulmonary diseases [317]. In non-small cell lung cancer, a total of 9 exosomal proteins were identified as potential independent makers on the overall survival in the plasma from 276 patients and one protein, NY-ESO-1 was validated as a prognostic biomarker of survival after the required adjustments [414].

The persistence of inflammation caused by cigarette smoking in COPD makes exosomes a good candidate for a biomarker of the disease [415]. It is found that the endothelial-derived MVs are increased in COPD patients. Furthermore, the level of these MVs has been correlated with the lung functions [415]. The CYR61/CTGF/NOV family 1 (CCN1) has an important role in tissue repair and remodelling in COPD [416]. When lung epithelial cells are treated with cigarette smoke (CS), they released CCN1-enriched exosomes. Exosomes may also serve as a marker for COPD [415]. The level of circulating epithelial cell-derived exosomes is increased in CS-treated mice [417]. Muscular wasting is a common comorbidity of COPD [418]. Muscle-specific miRNAs is different in COPD patients and exosomal miRNA in plasma can be used as a biomarker to reflect the changes in the muscles in COPD patients [419]. BAL fluid miRNAs were also found to be different in COPD patients than healthy controls [420].

With the potentially important role of exosomes in lung diseases, little is known about exosomes in lung fibrosis and IPF [317, 421-423]. However, evidence suggests that exosomes can mediate fibrotic diseases. Exosomes have been proposed as a useful tool for diagnostic and therapeutic purposes in kidney and liver fibrosis [318, 424]. TGF-β1,

a key mediator of fibrosis, has been found enclosed in exosomes upon epithelial injury in a model of kidney fibrosis. These TGF-β1 enclosed exosomes further increased tissue injury [425]. Epithelial-mesenchymal-transition is regarded as one of the potential mechanisms for lung fibrosis and a role of exosomes in EMT has been proposed in cancer [426]. Furthermore, a small study showed that in IPF serum exosomes miR-141 (anti-fibrotic) had decreased and miR-7 (fibrogenic) had increased [422]. Accumulating evidence suggests that the autophagy-lysosome pathway, which has a regulatory role in exosome secretion, is impaired in the IPF lungs [297, 298, 301]. The increased deposition of extracellular matrix (ECM) in the lung has a tremendous impact on the structure of the lungs and the resident cells. The aberrant, bioactive ECM in IPF could affect the homeostatic and cell signalling and communication among the resident cells. However, little is known about the role of autophagy and exosomes in lung fibrosis and IPF, thus requiring further investigation.

Hypothesis and aims

The primary goal of this study was to investigate the autophagy pathway in alveolar macrophages in the setting of lung fibrosis and the effect of increased fibrotic ECM on the autophagy pathway. Furthermore, I aimed to define the consequences of an altered autophagy pathway on exosome production in the fibrotic lungs and to test the feasibility of utilising exosomes as a marker for fibrotic lung diseases.

The overarching hypothesis of this study was that fibrotic ECM modulates exosome biogenesis in alveolar macrophages through the regulation of the autophagy-lysosome pathway.

The following research aims were addressed in the study:

- To establish an 'easy-detach' method for the differentiation of human primary monocytes into macrophages
- To determine the effect of collagen-I and collagen-IV on macrophage autophagy
- To assay LC3 and p62 expression in alveolar macrophages from patients with fibrotic and non-fibrotic interstitial lung diseases (ILD)
- To measure the effect of primary lung fibroblast-derived ECM on macrophage autophagy
- To study the concentrations of alveolar macrophage-released exosomes *in vitro*
- To determine effect of modulating autophagy pathway (activation or blockage) on exosomes release in macrophages
- To compare the concentration of exosomes in BAL fluid from ILD patients with or without lung fibrosis
- To establish a flow cytometry assay for exosomal protein study in BAL fluid from patients with ILD conditions

Chapter 2 Materials and Methods

2.1 Monocyte-derived macrophage: culture and detachment techniques

2.1.1 Cell isolation from whole blood of healthy volunteers

Blood from healthy donors was collected into 50 mL Falcon tubes containing 3.8% sodium citrate (Sigma, PHR1416) to achieve a final concentration of 0.38%. After centrifugation (350 g, 20 minutes, low acceleration, no brake), the platelet-rich plasma was removed from the remaining cells. Leucocytes were isolated after removal of erythrocytes by sedimentation using 6% (w/v) dextran (Sigma, 31387) which was topped up to 50 mL with pre-warmed (37°C) 0.9% NaCl (UKF7124, Baxter). The leucocyte-rich layer was collected and washed with 0.9% NaCl (350 g, 10 minutes). Peripheral blood mononuclear cells (PBMC) and granulocytes were separated by centrifugation (700 g, 20 minutes) through a discontinuous Percoll® gradient (Sigma, P1644). Isotonic Percoll solutions (49.5%, 63%, and 72.9%) were made in Ca^{2+}/Mg^{2+}-free PBS (CMFPBS, ThermoFisher, 14190250). Leucocytes were re-suspended in 3 mL 49.5% Percoll and laid on top of 4 mL of 72.9% and 63% Percoll solution. After the centrifugation, mononuclear cells were aspirated from the 49.5%/ 63% interface and neutrophils from the 63%/ 72.9% interface. Cells were washed twice in PBS before other applications.

2.1.2 Isolation of $CD14^+$ monocytes from PBMC

$CD14^+$ monocytes were isolated from the mononuclear cell fraction using MACS® monocyte selection kit and the supplied LS columns (Miltenyi Biotec). Briefly, PBMC were counted and resuspended to the appropriate concentration in phosphate-buffered saline (PBS) with 5% heat-inactivated foetal bovine serum (FBS). Cells were incubated with Fc receptor (FcR) inhibitor and CD14 antibody cocktail before the incubation with MACS® beads, then cells were washed and passed through an LS column. $CD14^+$ monocytes were passed through the column and collected in the efflux. Monocytes were washed again with PBS before use.

2.1.3 Monocyte-derived macrophages (MDM) on standard tissue culture (TC) plates

PBMC were counted, pelleted and resuspended at 4.0×106 cells/mL in Iscove's Modified Dulbecco's Media (IMDM) without FBS. PBMC were plated out in tissue culture (TC) 24-well plates with 0.5 mL/well and left for 45 minutes at 37°C to enrich monocytes by adhesion. After adhesion, the non-adherent lymphocytes were washed away with PBS and complete medium was added to the monocytes. Monocytes were then cultured for 7 days in the complete medium at 37°C in a 5% CO_2 atmosphere. The medium was changed every 3 days before day-7. The complete medium is IMDM containing 10% FBS, 1% L-glutamine and 100 units/mL (1%) penicillin and streptomycin (pen/strep).

2.1.4 Differentiation of $CD14^+$ monocytes in ultra-low attachment flasks

The purified $CD14^+$ monocytes were counted, pelleted and then resuspended at 1×10^6/ mL in complete IMDM medium. Cells were transferred into ultra-low attachment flasks (Corning CLS3814) with 5 mL culture medium and differentiated for 7 days in a humidified incubator 37 °C (95% O_2 and 5% CO_2). The additional 5 mL fresh medium was added into the flask on day-4 of culture. For long-term culture, medium was collected and centrifuged at 300 g for 5 minutes to collect any floating monocytes and then resuspended in completed IMDM and transferred back to the original flask for culture.

2.1.5 Detachment of $CD14^+$ monocyte-differentiated cells from the ultra-low attachment flasks

On day-7 or the end of culture, the culture medium was collected and replaced with cold PBS. The flask with cells was placed on ice and left for 15 minutes to let cells detach. After the incubation on ice, cells were further detached by tapping on the side of the flasks. Then the cells were collected and centrifuged at 300 g for 5 minutes.

2.1.6 Detachment of MDM on standard TC plates with enzymatic disassociation solutions

Trypsin and ethylenediaminetetraacetic acid solution (trypsin-EDTA, 0.25%, ThermoFisher, 25200056) was warmed up to 37°C in a water bath before use. Accutase

(Sigma, A6964) was warmed up to room temperature before use. MDM were rinsed twice with CMFPBS before the pre-warmed disassociation solutions were added. Cells were incubated for 15 minutes in a 37°C incubator (trypsin/EDTA) or at room temperature (accutase) for up to 30 minutes before the detached cells were collected. The remaining cells in plates were washed off by applying PBS against the cells with repeated pipetting for three times.

2.1.7 Detachment of MDM on standard TC plate with enzyme-free disassociation solutions

MDM were washed with cold CMFPBS before the disassociation solutions or control solutions were added to the plate for the incubation on ice to detach. After the incubation of up to 30 minutes, cells were collected by repeated pipetting for 3 - 5 times with cold CMFPBS. The enzyme-free solutions were as follows, Gibco buffer (Gibco, 13151014), Sigma buffer (Sigma, C5914) and 5 mM EDTA solution.

2.1.8 Flow cytometry

Flow cytometry was performed with all incubations conducted on ice unless stated otherwise. All antibodies were purchased from BioLegend if not specified otherwise.

CD14+ monocytes derived macrophages were detached and stained for cell surface markers on day-7 of culture. Cells were incubated with specific antibodies at 1 in 20 dilutions. The following antibodies were used CD3-PE (321106), HLA-DR (FITC), CD14-PerCP/Cy5.5 (302018), CD-16-APC/cy7 (302018), CD206-PE (141706), CD163-APC (333610), 25F9-FITC eFluor 660 (eBio-sciences, 50-0115-42). Cells were incubated with the antibody on ice for 30 minutes and then washed in PBS containing 0.5% FBS. Cells were gated to exclude cell debris and analysed on 5-LSR Fortessa flow cytometer (Beckton Dickenson). Data were analysed using Flowjo software (Treestar, Oregon, USA).

2.1.9 Cytocentrifuge preparations and Diff-Quik® stain

Cells were counted and re-suspended in PBS. For each slide of the cytocentrifuge preparation, 50,000 cells were loaded into each of the chambers. Cells were centrifuged onto the slide at 300 g for 3 minutes. After the centrifugation, the cells on the slides

were fixed with methanol and then followed by the staining with Diff-Quik® staining kit (FisherScientific, NC0674866).

2.1.10 Phagocytosis assay

Neutrophils were isolated from peripheral blood of healthy donors by Percoll gradient method as described above. Cells were counted and resuspended to 4×10^6/mL in IMDM without serum and stained with CellTracker™ Orange (Invitrogen, C2927) for 30 minutes. Autologous serum was prepared from the platelet-rich plasma by adding 220 µL of 1 M $CaCl_2$ (Sigma, 449709) per 10 mL plasma in glass tubes and incubated at 37°C for 60 minutes. Autologous serum (10%) was then added to IMDM and cells were incubated for 24h in an incubator to become apoptotic. Neutrophils were collected by centrifugation at 230g (Acc 9/ Dec 5) for 5 minutes. Cells were washed with pre-warmed PBS (37°C) and counted before adding to macrophages at a ratio of 5:1 (neutrophils *vs* macrophages) and incubated for 30minutes. After the incubation, cells were gently rinsed for a couple of times using pre-warmed PBS (37°C) with calcium to remove unengaged neutrophils. The samples were then observed under a microscope.

2.1.11 Macrophage stimulation with LPS/ IFN-γ

Monocytes were cultured for 7 days to be differentiated into unpolarized macrophages ("M0"). M0 macrophages were then washed with PBS before adding the culture media with a cocktail of lipopolysaccharides (LPS) (Sigma, 100 ng/mL) and interferon (IFN)-γ (Life Technologies, 20 ng/mL) and cultured for 48 hours to be stimulated to the classically activated macrophages ("M1"). Cells were stimulated in standard TC plates or in the ultra-low attachment flasks.

2.2 BAL fluid preparation and alveolar macrophage study

2.2.1 Edinburgh lung fibrosis cohort and Patient information

The study is part of the Edinburgh Lung Fibrosis Cohort project which was registered and had been approved by University of Edinburgh /NHS Ethics Committee (regional ethic committee numbers are 07/S1102/02 and 06/S0703/81). All patients participated in this study had been fully informed and consent forms were signed.

Patients were referred to the interstitial lung disease clinic in the Royal Infirmary of Edinburgh by local general practitioners. The diagnosis of fibrotic ILD (mainly IPF) was made following the ATS/ERS guidelines by a multidisciplinary team including lung physicians and radiologists. The diagnosis was primarily based on the HRCT scans with the typical feature of lung fibrosis, including reticulation, architectural distortion, and honeycombing. Patients with ILD but no features of lung fibrosis on HRCT scans (such as "ground-glass") were served as controls. Both groups of patients were cared for a special clinical team. Details of patients in this study can be found in Appendix-B.

2.2.2 Bronchoalveolar lavage and isolation of the BAL fluid cells

Bronchoscopy with bronchoalveolar lavage (BAL) (five aliquots of 50 mL saline) was performed routinely by a dedicated team under the supervision of a consultant in respiratory medicine. The BAL fluid was then strained through a 40 μm double layer of Dacron strainers (Millipore, Bedford, Ireland), and centrifuged at 300 g for 5 minutes at 4°C.

2.2.3 Purification of BAL fluid exosomes by ultracentrifugation

BAL fluid supernatant was collected after the removal of tissue debris and cells. The supernatant was transferred to a fresh tube and then centrifuged at 3,000g for 20 minutes to pellet dead cells and apoptotic bodies (50 - 50,000 nm). The remaining BAL fluid

was centrifuged at 10,000 g (30 minutes, 4°C) to remove cell debris and large vesicles (100 - 1,000 nm). Exosomes, remaining in the BAL fluid after the sequential centrifugation, were pelleted at 100,000 g (70 minutes, 4°C) when a gel-like pellet was observed at the bottom of the tube. Pelleted exosomes were washed once by resuspending in 6 mL PBS and pelleted again at 100,000 g (70 minutes, 4°C). The total protein concentrations of the re-suspended exosomes were measured with bicinchoninic acid (BCA) assay (Pierce®, Thermo, USA).

2.2.4 BAL fluid exosome RNA extraction and Nano-drop®

Exosomes were purified from the same volume (6 mL) of BAL fluid samples by ultracentrifugation after the sequential centrifugations. Pelleted exosomes were re-suspended in 250 µL of PBS after an additional wash. Exosome RNA was extracted with Trizol reagent (ThermoFisher, 15596026) by following the manufacturer's manual. Extracted RNA was dissolved in 60 µL RNAase free water before the determination of concentration with Nanodrop® (Life Technology) and stored at -80°C.

2.2.5 Purification and culture of AM

To purify alveolar macrophages from the BAL fluid cells, the cells were resuspended in IMDM (5×10^6/mL) and plated out at 5×10^5 in each well in a 24-well plate. AM were purified by adhesion to the standard tissue culture plate for 45 minutes. The non-adherent cells were washed away with pre-warmed PBS (37°C). The remaining cells were purified AM (as examined with cytocentrifuge preparations) and they were maintained in IMDM with full supplements.

2.2.6 Transmission/ scanning electron microscope (TEM/ SEM)

Pelleted exosomes from ultracentrifugation were fixed in 2% paraformaldehyde (PFA) before the examination under TEM. Pelleted exosomes were compared against their size-definition (40 nm to 100 nm) in diameter. Or, exosomes were captured by the incubation with anti-CD9 magnetic beads and washed once with PBS before they were resuspended in 2% PFA and examined under TEM in parallel with control beads (without incubation with exosomes).

AM were purified by adhesion to plastic coverslips (Thermonox® Nunc, USA) in a 24-well TC plate for 45 minutes in IMDM media without serum. Purified AM were extensively washed with PBS to remove any non-adhesive BAL fluid cells. AM were then fixed for 1-2 hours in 0.1 M sodium cacodylate buffer containing 3% glutaraldehyde. Samples were the delivered for further processing by the TEM/SEM lab. Basically, the plastic coverslips were fixed in 1% osmium tetroxide, embedded in araldite resin and before they were cut into ultra-thin sections (around 60 nm thick). Samples were then were examined by TEM (JEOL, JEM-1400 Plus). Under TEM, autophagosomes were identified as classic double layer membrane structure. Other organelles with double membranes, mainly mitochondria were excluded by their feature of cristae/ ridges.

For SEM, samples were fixed as TEM in 3% glutaraldehyde and further processed by TEM/SEM lab before the examination under SEM (Hitachi S-4700). Basically, samples need to be dried by the critical point drier and mounted on the stubs to be studied.

2.2.7 Flow cytometry

Bronchoalveolar lavage (BAL) fluid was collected from the clinic and transported to the lab on ice. BAL fluid was first filtered through 0.45 µm filters to remove large pieces of tissue and debris before the centrifugation at 300 g for 10 minutes to pellet BAL fluid cells. BAL fluid cells were stained with Cyto-ID (Enzo, ENZ-51031) alive following the manufacturer's manual and analysed with BD FACSCalibur™ (with 488 nm laser). Otherwise, BAL fluid cells were fixed and permeabilised with a commercially available kit (BD Cytofix/Cytoperm, 554714) and stained with anti-LC3 antibodies (MBL, PM036) overnight. Samples were stained with secondary antibody (Alexa Fluor® 594 Phalloidin anti-rabbit) for 30 minutes and washed with PBS on the following day before the analysis with FACSCalibur™ (with 635 nm laser).

2.3 ECM and macrophage autophagy study

2.3.1 Compounds and reagents

Rapamycin (R8781), bafilomycin A1 (B1793), DMSO (D4540) and phorbol 12-myristate 13-acetate (PMA, P8139) were purchased from Sigma. The proteinase inhibitors leupeptin (L2884), pepstatin (P5318) and PMSF (93482) were also purchased from Sigma. All cell culture media and other reagents were purchased from Life Sciences.

2.3.2 Tissue culture-ware used in the study

Standard 24-well tissue culture plates (Sigma, Corning®, CLS3524), standard 35 mm tissue culture dishes (Sigma, Corning®, CLS430165), BioCoat™ Collagen type-I precoated 35 mm dishes (Scientific Laboratory Supplies, 354456) and BioCoat™ Collagen type-IV precoated 35 mm dishes (Scientific Laboratory Supplies, 354459). The Corning® ultra-low attachment cell culture flasks were purchased from Sigma (CLS3815).

2.3.3 Tissue culture and sub-culture of macrophages

RAW264.7 mouse macrophages and THP-1 human monocytic cells were kindly provided by Prof. Sarah Howie (University of Edinburgh, UK). RAW264.7 cells were cultured in DMEM and THP-1 cells were maintained in Roswell Park Memorial Institute (RPMI)-1640 medium both with supplements. Cells were grown in media with full supplements to the mid-logarithmic stage before they were seeded in plates or dishes for treatment protocols. For adherent cells, when they grew to 80% confluent approximately, cells were washed with CMFPBS and detached by trypsin-EDTA. THP-1 cells were cultured in suspension with complete RPMI medium and passaged every 3 days at a splitting ratio of 1:3.

THP-1 cells were treated with phorbol 12-myristate 13-acetate (PMA) to be differentiated into macrophage-like cells. After the cells were centrifuged at 300 g for 5 minutes. They were then resuspended in pre-made different complete RPMI-1640 media containing PMA at different concentrations at 1×10^6/mL. For each well of a

standard 24-well tissue culture plate, 0.5×10^6 cells were seeded. Cells were cultured 3 days for macrophages differentiation.

Tissue culture supplements included 10% FBS, 1% L-glutamine and 100 units/mL (1%) penicillin and streptomycin (pen/strep). All cells were maintained in a humidified incubator (Thermo Scientific, USA) 37°C with 95% O_2 and 5% CO_2.

2.3.4 Autophagy induction

For starvation-induced autophagy, once the cells were ready for treatments the culture media was discarded. Cells were gently washed with pre-warmed PBS (37°C) for a minimum of 3 times before the addition of the starvation agents. Hank's Balanced Salt Solution (HBSS, 14025050) and Earle's Balanced Salt Solution (EBSS, 24010043) were used as the starvation buffer.

For rapamycin-induced autophagy, rapamycin was diluted in complete culture media with full nutrients and supplements and added to the cells after the removal the previous media.

2.3.5 Confocal microscopy

After treatment, RAW 264.7 macrophages were gently rinsed with PBS before they were fixed and permeabilised with a commercially available kit (BD Cytofix/ Cytoperm, 554714). Then the cells were stained with rabbit anti-LC3 antibodies (1 in 200 dilution, MBL, PM036) overnight. On the next day, cells were washed and incubated with an anti-rabbit secondary antibody (1 in 200 dilution, Alexa Fluor® 594 Phalloidin anti-rabbit) for 45 minutes in the fridge. Cells were washed with Cytoperm buffer and analysed by confocal microscopy (Leica SP5).

2.3.6 Live cell staining of autophagic vacuoles and lysosomes

Cyto-ID (Enzo, ENZ-51031) was purchased and aliquoted and stored at -20°C before use. Fresh BAL fluid cells were stained alive with Cyto-ID for subsequent flow cytometry analysis. For fluorescent microscopy, purified AM were cultured at the standard condition for 20 hours before they were stained with Cyto-ID for analysis.

The staining for both flow cytometry and fluorescent microscopy was done by following the manufacturer's instruction. Briefly, for flow cytometry, 1 µL of Cyto-ID detection reagent was diluted with 1 mL assay buffer supplemented with 5% FBS. For fluorescent microscopy, another 1 µL detection reagent and 1 µL Hoechst nuclear stain (included in the Cyto-ID kit) were added. Cells were stained for 30 minutes at 37°C before they were washed and analysed with a flow cytometer (with a 488nm laser, BD FACSCalibur) or a fluorescent microscope (FITC filter, EVOS FL, ThermoFisher).

Lysosomes were stained with LysoTracker Red DND-99 (working concentration 50 nM, ThermoFisher, L7528) for 30 minutes at 37°C. They were also stained together with Cyto-ID. After the staining, cells were washed with PBS (37°C) before they were visualised with EVOS FL Cell Imaging System (ThermoFisher).

2.3.7 Culture of primary human lung fibroblasts

Primary lung fibroblasts were isolated from the surgical lung biopsies of patients for diagnostic purposes. Biopsy tissues were cut into small pieces (approximately 2×2 millimetres in size) while emerging in complete culture medium using forceps and scalpel under a biological safety cabinet. Pieces of small lung tissues were seeded in a 6-well tissue culture plate with a minimum amount of complete medium (0.5 -0.75 mL). Fibroblasts were grown out of the tissue before they were detached and passaged. Once the cell line were generated, they were frozen in freezing medium (20% DMSO and 80% FBS) and kept in liquid nitrogen. Primary human fibroblasts were generated throughout the years due to the low biopsy rate by different members of the group including myself.

For the experiments, fibroblasts were brought back from liquid nitrogen and maintained in a humidified incubator (Thermo Scientific, USA) 37°C with 95% O_2 and 5% CO_2. Normally, cells can be passaged for 5 times before they were rounded up and lost the morphology of normal fibroblasts. The complete culture medium included Dulbecco's Modified Eagle Medium (DMEM) with 10% FBS, 1% L-glutamine and 100 units/mL (1%) penicillin and streptomycin (pen/strep).

2.3.8 Primary human lung fibroblast-derived ECM

Fibroblasts were maintained at low passage numbers (up to 5) to keep their fibroblast phenotype as described above. Fibroblasts were plated in 24-well plate at 0.25×10^6/well and cultured until confluent which was observed with an inverted light microscope. Confluent fibroblasts were cultured for another 72 hours to enhance ECM deposition.

After the ECM deposition, the culture medium was removed and cells were washed with warm PBS (37°C). The cells in the plates were de-cellularized with 6 freeze-thaw cycles (freeze 40 minutes at -80°C and thaw 15 minutes at room temperature). ECM left on the plate was washed with sterile water between each cycle. Any remaining cells were checked with DAPI (D1306, ThermoFisher) staining. After the de-cellularization, the remaining ECM scaffold was washed with 25 mM NH_4OH aqueous solution (Sigma, 221228) and incubated for 20 minutes on a slowly moving four-way shaker at room temperature to remove any cell debris. The synthesised ECM was washed with sterile water for 3 times and then washed again with PBS for 3 times. Before use, ECM was treated with 20U/mL DNase I (ThermoFisher, EN0525) in sterile H_2O for 60 minutes at 37°C and washed with PBS for 3 times.

2.4 Protein extraction and western blotting

2.4.1 Protein extraction

To extract proteins from cells, once the treatment was finished, the supernatant was collected. Then, the culture plates containing cells were put on a tray of ice and cells were washed with ice-cold PBS for 3 times before adding RIPA Buffer (Thermo, 89900) with proteinase inhibitors to extract proteins. The proteinase inhibitors included: leupeptin (1 µg/mL), pepstatin (1 µg/mL) and phenylmethylsulfonyl fluoride (PMSF, 1 mM). Cells were lysed on ice for 30 minutes and then scraped off the plates. Cell lysate was centrifuged at 10,000 g for 30 minutes at 4°C. The supernatant was collected and the protein concentrations were measured with bicinchoninic acid (BCA) assay (Pierce®, Thermo, USA) before they were stored at -20°C.

2.4.2 Western blotting

Total protein concentrations were measured by BCA Protein Assays (Pierce®, Thermo, USA). Same amount of proteins (20 µg or 30 µg) from each sample was aliquoted and mixed with loading buffer (NuPAGE™, NP0007) and reducing agent (NuPAGE™, NP0004) and heated at 95°C for 5 minutes. Then the samples were quickly centrifuged at room temperature for a few seconds at the maximum speed of a bench-top centrifuge. Samples were loaded into the each of the wells of a 4-12% Bis-Tris protein gel (NuPAGE™, NP0321). The proteins were separated using Mini-Cell Electrophoresis System® (ThermoFisher, XCell SureLock™, EI0001) in 1× MES SDS running buffer (NuPAGE™, NP0002) with a pre-stained protein standard (SeeBlue™ Plus2, LC5925) as an indicator. After the electrophoresis, the proteins on the gel were transferred to a piece of pre-activated PVDF membrane (GE, 10600023) with the XCell II™ Blot Module (ThermoFisher, EI9051) transfer system while immersed in the transfer buffer (NuPAGE™, NP0006) at 32V for 70 minutes.

The PVDF membrane with proteins was kept moisture between the procedures. It was blocked in 5% non-fat milk protein (Marvel, UK) in PBS. The membrane was then incubated with primary antibody overnight at 4°C with 5% non-fat milk proteins in

PBS. Proteins were visualised with an appropriate horseradish peroxidase-conjugated secondary antibody and chemiluminescent substrate (Thermo 32109). Densitometry analysis on the immunoblots was quantified by Image-J software. Results were expressed in arbitrary units.

2.4.3 Antibodies for western blotting

Exosome antibodies (CD9, CD63 and CD81) were purchased from SBI (EXOAB-KIT-1) and used at 1:1000 dilution. TSG-101 (ab30871), HSP-70 (ab2787), and β-actin (ab8227) were purchased from Abcam and used at 1:1000 dilution.

Monoclonal antibody to LC3B (NanoTool, 0231-100/LC3-5F10) was used at 1:1000 dilution. Anti-p62/SQSTM1 antibody (Sigma, P0067) was used at 1:70,000 dilution and anti-GAPDH antibody (Santa Cruz, sc-25778) was used at 1:5000 dilution.

HRP-conjugated secondary antibodies goat anti-rabbit IgG-HRP (Santa Cruz, sc-2004) and goat anti-mouse IgG-HRP (Dako, P044701-2) were used at 1:5000 dilution.

2.5 Exosome study

2.5.1 Nanoparticle tracking analysis (NTA)

NTA LM10 (NTA Ltd., Amesbury, United Kingdom), was used to determine the concentration of exosomes. A video of 60 seconds was taken for each of the samples and at least 6 measurements were performed with each sample. Data were analysed with NTA software on a frame-by-frame basis and the concentrations were calculated based on the Brownian movement and Stokes-Einstein equation. The concentrations of vesicles of interest (40 – 100 nm) were represented as a value of "area under curve" and the mean of 6 measurements was used for statistical analysis.

2.5.2 Exosome labelling

Following the manufacturer's protocol, Qtracker® 655 Cell Labelling Kits (Q25021MP) was used for the exosome labelling. Briefly, the working solution (10 nM labelling solution) was prepared before use and added to the pelleted exosomes and incubated for 60 minutes at 37ºC. After the labelling, the exosomes were further diluted (final volume 0.75 mL) with complete IMDM culture media and incubated with MDM for 24 hours. After the incubation, stained exosomes were examined with EVOS microscope under RFP filter (531/40 nm excitation; 593/40 nm emission).

2.5.3 Exosome treatment assay *in vitro*

Monocytes were derived for 7 days to become mature macrophages in standard tissue culture plate before they were treated with pelleted exosomes (30 µg) purified from the BAL fluid samples. Final volumes of BAL fluid from different samples were topped up to 0.75 mL with complete IMDM media. Macrophages were incubated with BAL fluid exosomes for 24 hours before they were lysed for western blotting.

2.5.4 Anti-CD9 beads coupling

Human anti-CD9 pre-coated magnetic beads were purchased from ThermoFisher (10620D). The product was vortexed for 1 minute before adding 10 µL beads into 100 µL (1:10 dilution) of the solution with BAL fluid exosomes. The samples were mixed on an end-over-end rotator at 4°C for the time required. Then the magnetic bead-

captured exosomes were removed from the solution using a magnet before further analysis or experiment.

2.5.5 Flow cytometry

For the anti-CD9 beads captured exosomes, after the bead-captured exosomes were washed with PBS, they were resuspended in PBS and stained for CD9-FITC (312104), CD63-PE (353004), MHC-I-PE (BD, 565291), Sytox blue® nucleic acid stain (ThermoFisher, S11348), or the corresponding isotype controls at room temperature for 30 minutes. Samples were washed and resuspended in PBS for flow cytometry analysis.

2.5.6 Repeated freeze-thaw cycle of BAL-fluid samples

Frozen BAL fluid samples were defrosted and aliquoted for the coupling with anti-CD9 beads for flow analysis. Another aliquot was returned to -80°C and defrosted again 24 hours later to study the effect of "repeated freeze-thaw cycle" on BAL-fluid exosomes.

2.6 Statistical analysis

Data are presented as mean ± SEM (standard error of the mean) unless otherwise stated. Statistical analysis was performed with GraphPad Prism (GraphPad Software, La Jolla, CA, USA) using one-way ANOVA with Tukey's Multiple Comparison Test or student t-test as indicated. Statistical significance was taken at $p \leq 0.05$.

Chapter 3 An easy-detach method to differentiate human monocytes into macrophages

3.1 Abstract

Monocyte-derived macrophages (MDM) are very difficult to detach from surfaces (e.g., plastic or matrix-coated surfaces) *in vitro*. Thus, an easy-detach method of macrophage differentiation was developed and investigated.

Current protocols to detach MDM using enzymatic and non-enzymatic disassociation solutions resulted in a very limited harvest of cells. None of the disassociation solutions achieved 50% recovery of macrophages and increase of the incubation time did not improve recovery.

In order to avoid the difficulties in detaching macrophages after differentiation, $CD14^+$ cells were isolated by negative bead-selection and cultured in ultra-low attachment flasks to be differentiated to mature macrophages. They formed cell aggregates when first seeded in the flasks, but on day-3 they migrated away from each other and spread out as a monolayer of cells. On day-7 of differentiation, cells increased in size and acquired macrophage morphologies such as "fried-egg" and "spindle" shapes. To achieve 50 - 70% confluence on day-7, the initial density of $CD14^+$ monocytes was determined as 3 - 4 million cells per flask. Cell morphology started to change after 4 weeks of culture, multinucleated foreign body giant cells started to appear in the flask. After differentiation, cells were easily detached by replacing culture media with ice-cold PBS and incubated on ice for 15 minutes. The recovery rate was more than 95%.

$CD14^+$ monocyte-derived cells in the low-attachment flasks were CD14, CD16 and HLA-DR positive. Flow cytometry showed that they were $CD163^-/CD206^+/Mac\text{-}2^+/25F9^+$ macrophages. MDM from this easy-detach method (MDM-ED) displayed macrophage morphology when observed by microscopy of cytocentrifuge preparations. MDM-ED were also functional macrophages in that they phagocytosed apoptotic human neutrophils. MDM-ED responded to IFN-γ/LPS stimulation and changed

morphology towards the spindle-shaped, "classically activated" macrophages on standard tissue culture (TC) plates.

In summary, an easy-detach method to acquire macrophages was successfully developed which harvested over 95% of morphological and functional macrophages with polarisation plasticity.

3.2 Introduction

Macrophages are versatile immune cells that are often the first cells involved in immune cell defence. They can engulf and degrade apoptotic cells, debris, pathogens and foreign materials and can initiate the inflammatory process [427, 428].

Monocytes/macrophages are strongly adhesive cells and monocytes require adhesion processes to successfully differentiate into macrophages [429, 430]. MDM are strongly adhesive to the TC plastic that researchers often find difficult to detach without compromising cell viability and function [431, 432]. The typical differentiation time of MDM is a period of 7 days. It has been demonstrated that MDM are metabolically and morphologically stable for at least 4 weeks in culture [431, 433, 434]. Human autologous serum or heat-inactivated foetal bovine serum (FBS) can facilitate macrophage differentiation [434, 435]. Autologous serum contains different levels of cytokines and growth factors which might affect macrophage differentiation *in vitro* between different donors [436]. Adding supplements to the differentiation media may polarise the cells to different phenotypes [436, 437]. Macrophage colony-stimulating factor (M-CSF) promotes macrophages towards the alternatively activated (anti-inflammation, "M2") phenotype; while granulocyte-macrophage colony-stimulating factor (GM-CSF) leads to classically activated macrophages (pro-inflammation, "M1") [438, 439].

The most common practice to detach cells is to use disassociation solutions. In general, there are two types of disassociation solutions: solutions with enzymes such as trypsin or accutase, and solutions without enzymes (enzyme-free) such as ethylenediaminetetraacetic acid (EDTA) solution. Trypsin breaks the linking peptide chains by cleaving the peptide chains at the carboxyl side of the amino acids lysine or arginine unless followed by proline which makes the cells detached and individualised

in a suspension. However, trypsin can cause damage to the cells and even cause cell death. Accutase is a relatively newly found mixture of marine-origin enzymes that has proteolytic and collagenolytic activity thus can individualise cells. Accutase does not need a neutralising solution and it auto-inhibits at 37°C. Accutase maintains high cell viability and can be incubated with cells for a longer period which makes it an ideal candidate for detaching macrophages. EDTA alone can detach and de-clump cells and by weakening the function of adhesion molecules, such as cadherins. EDTA also binds to Mg^{2+} and Ca^{2+} which can weaken function of calcium-dependent adhesion molecules. Cells can also be detached by mechanical approaches, such as using cell scrapers or by vigorous shaking. However, these procedures may introduce cell death and cause cell aggregation which is not ideal for subsequent experiments.

To avoid the firm attachment of MDM to the standard TC plates, the alternative is to have monocytes differentiated on a non- or less adhesive surface in the first place [431]. Among these surfaces, plastic dishes [430, 433], Teflon-coated pots/ bags [431, 432, 440] and low-attachment expansion bags [441] have been used. Though many methods were studied, none of them had been used for regular laboratory practice. A relatively newly designed ultra-low attachment surface has been designed to avoid cell attachment for 3-D cell culture [442]. The ultra-low attachment surface has a covalently bound hydrogel layer which is hydrophilic and neutrally charged. This design inhibits the attachment of proteins and biomolecules via passive hydrophobic adsorption and ionic interactions. The coating is biological, non-cytotoxic, stable and non-degradable. Similar materials have shown temperature sensitivity [443]. In fact, leaving the culture plate on ice facilitated macrophage detachment [444].

Macrophages are highly heterogeneous and plastic cells. They represent a spectrum of different phenotypes that include pro-inflammatory (M1) and anti-inflammatory (M2) macrophages [427]. They can respond to the local signals and rapidly change their phenotype and function [427]. They can even switch from one phenotype to another in response to the signals in the local microenvironment [445-449]. Upon the stimulation of IFN-γ and LPS, MDM can change their morphology to a “spindle” shape M1 macrophage *in vitro* [436]. Commonly used human macrophage surface markers include Mac-2 and 25F9. CD68 is predominantly expressed intracellularly but can be

found on cell surface of both M1 and M2 macrophages [441, 450]. CD206 and CD163 are used to phenotype M2 macrophages subgroups [451].

Differentiation of macrophages on ultra-low attachment surface may affect their phenotype, functions, and plasticity. By addressing all these questions, this potential method may bring good technical advantages to understand the basics of human macrophage biology.

3.3 Hypotheses and aims

3.3.1 Hypotheses

- Human monocytes can differentiate to mature macrophages on ultra-low attachment surface

- Macrophages differentiated on ultra-low attachment surface can be easily detached by changing the environmental temperature

- $CD14^+$ monocyte-derived cells on ultra-low attachment surface are functional macrophages with polarisation plasticity

3.3.2 Aims

- To compare different methods of detaching macrophages derived in standard tissue culture plates

- To optimise the protocol of cell density, time of differentiation and detachment method of $CD14^+$ monocytes derived cells on ultra-low attachment surface

- To culture and characterise $CD14^+$ monocytes derived cells on ultra-low attachment surface

- To test the phagocytosis and polarisation plasticity of $CD14^+$ monocytes derived cells on ultra-low attachment surface

3.4 Results

In the first place, the efficiency of detaching MDM using enzymatic (Fig 3-1) and non-enzymatic (Fig 3-2) disassociation solutions was studied. Data showed MDM were very difficult to be detached after differentiation.

Since the results showed different disassociation solutions achieved poor recovery of macrophages (less than 50%), a protocol of culturing $CD14^+$ monocytes in ultra-low attachment flasks was designed and then optimised. Firstly, $CD14^+$ monocytes were purified and the purity was examined by flow cytometry (Fig 3-3). When these cells were cultured in ultra-low attachment flasks, they underwent unique morphological changes (Fig 3-4). Secondly, the cell density (Fig 3-5), time of differentiation (Fig 3-6) and method of detachment were optimised (Fig 3-7). The recovery rate of differentiated MDM from low-attachment flasks was more than 95% which was significantly higher when compared to the rates achieved by other methods (Fig 3-7).

After the establishment of the protocol, the expression of macrophage markers on the $CD14^+$ monocyte-derived cells was studied. The differentiated cells were characterised as mature macrophages by the expression of macrophage markers including $CD206^+$, Mac-2^+ and $25F9^+$ on flow cytometry (Fig 3-8). Furthermore, the function of MDM-ED macrophages was examined by the successful phagocytosis of apoptotic human neutrophils (Fig 3-9). Finally, the plasticity of MDM-ED was studied by stimulating them with IFN-γ and LPS on different surfaces (Fig 3-10).

3.4.1 MDM derived on standard TC plate were difficult to detach by enzymatic disassociation solutions

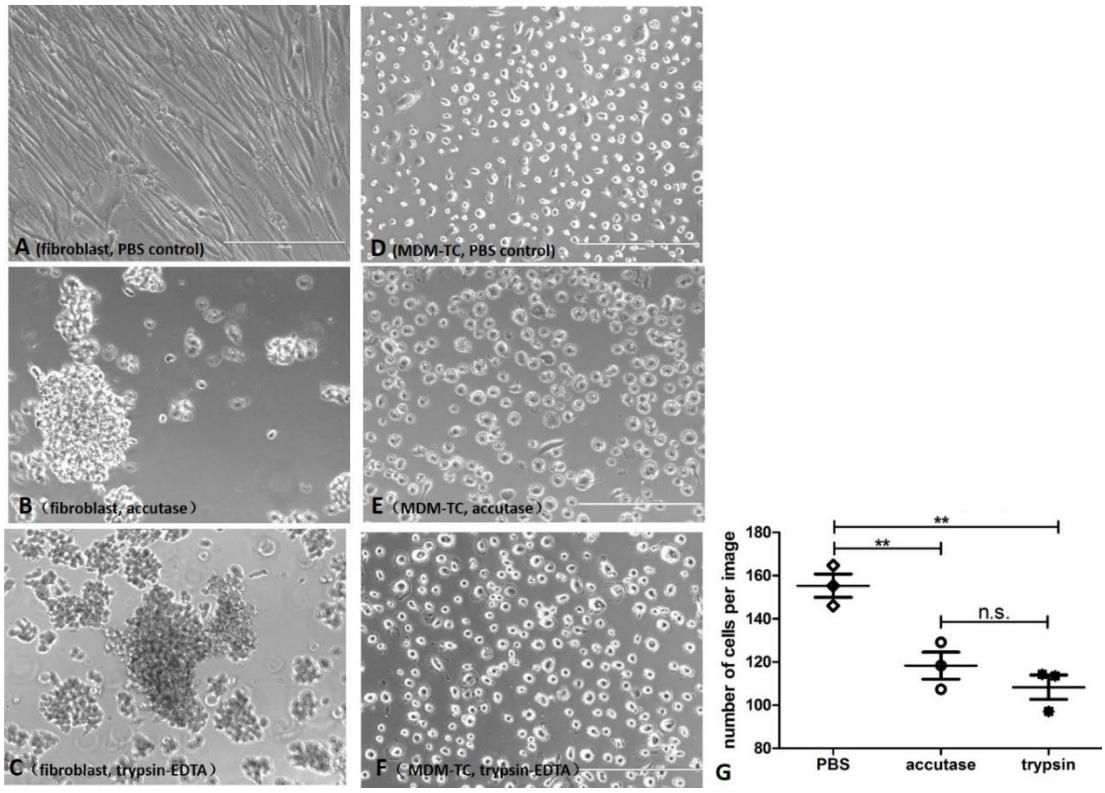

Figure 3-1 MDM derived on standard TC plate were difficult to detach by enzymatic disassociation solutions.

Fibroblasts were disassociated by accutase (B) and trypsin-EDTA (C) within a couple of minutes but not by PBS control (A); MDM were washed with PBS and treated with either solution for up to 15 minutes (trypsin-EDTA, F) or 30 minutes (accutase, E). Neither solutions detached MDM efficiently, as there were many MDM remaining on the plates (D), though statistically the number of cells per image was decreased (G). ** $p<0.01$, one-way ANOVA with Tukey's Multiple Comparison Test, n=3, scale bar=200 μm.

3.4.2 MDM derived on standard TC plates were difficult to detach by enzyme-free disassociation solutions

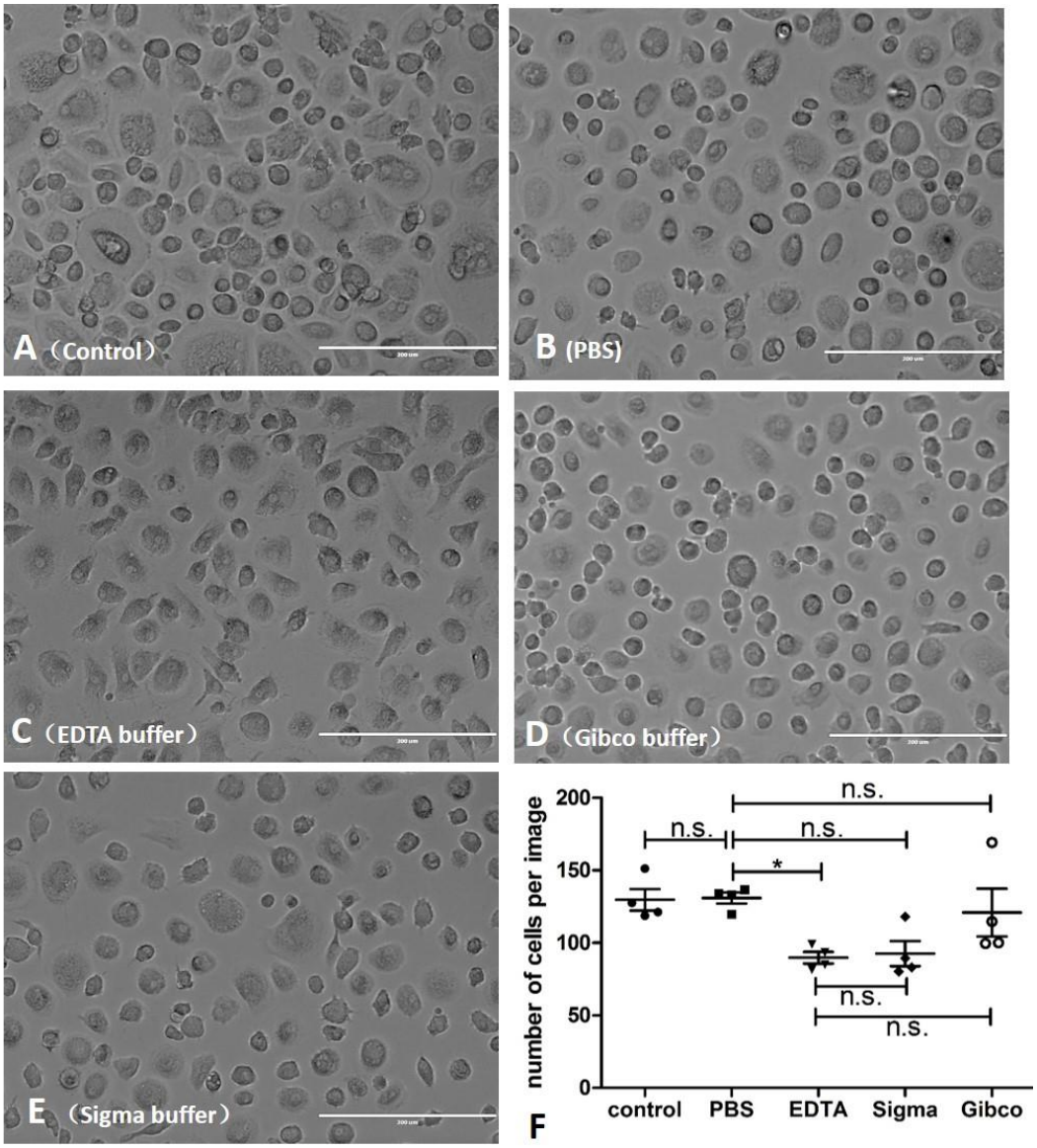

Figure 3-2 MDM derived on standard TC plates were difficult to detach by enzyme-free disassociation solutions.

MDM were incubated with enzyme-free solutions for 30 minutes while the plate was placed on ice. MDM were incubated in culture media (A) as a negative control, or in PBS (B), EDTA (5 mM, C), Gibco buffer (D) and in Sigma buffer (E). The number of the remaining MDM adherent to the plates was compared (F). Gibco: enzyme-free disassociation buffer from Gibco; Sigma: non-enzymatic disassociation solution from Sigma. ** $p<0.01$, one-way ANOVA with Tukey's Multiple Comparison Test, n=3, scale bar=200 µm.

3.4.3 Isolation of CD14$^+$ monocytes from peripheral blood mononuclear cells (PBMC)

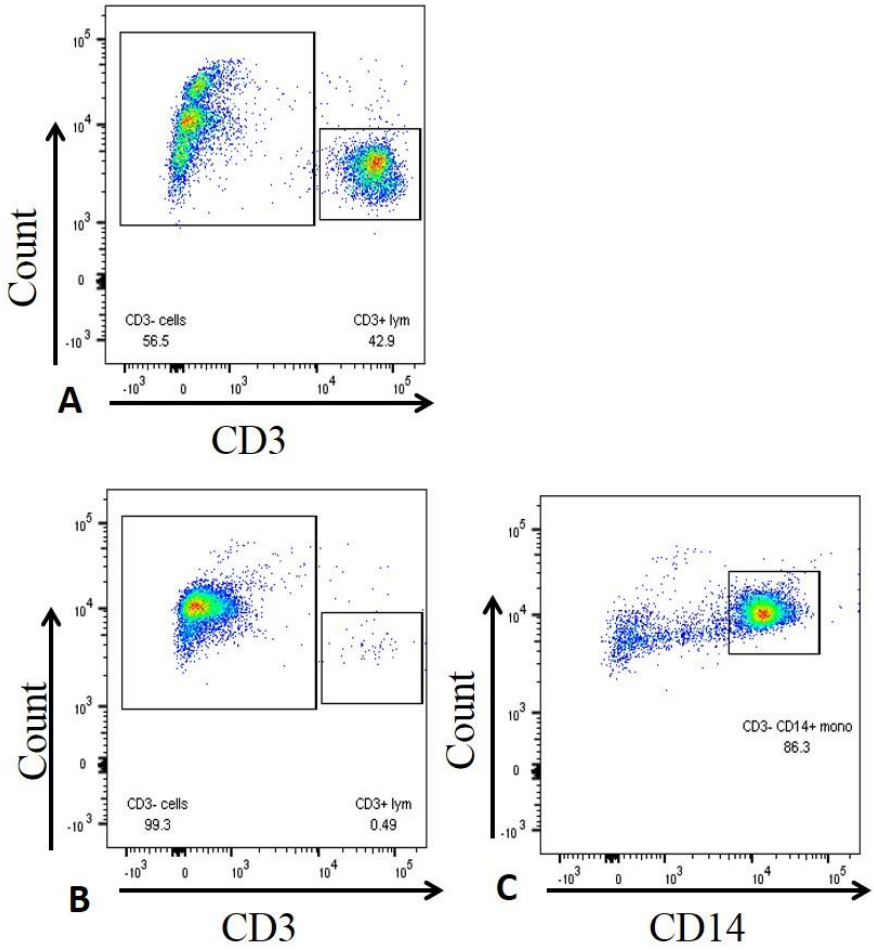

Figure 3-3 Isolation of CD14$^+$ monocytes from the PBMC.

The monocyte pan isolation kit was used to purify CD14$^+$ monocytes from PBMC after the separation of leucocytes using Percoll gradients. (A) Before the isolation, there were CD3$^+$ lymphocytes (42.9%) among the PBMC; (B) after the isolation, there were very few CD3$^+$ lymphocytes (0.49%); (C) the remaining cells were mainly CD14$^+$ monocytes (86.3%). Representative flow cytometry analysis of the CD14$^+$ and CD3$^+$ cells before and after the isolation (n=3). Gates were set up based on the isotype-control antibody stained cells.

3.4.4 Morphology changes of CD14$^+$ monocytes in the ultra-low attachment flask during the 7-day differentiation

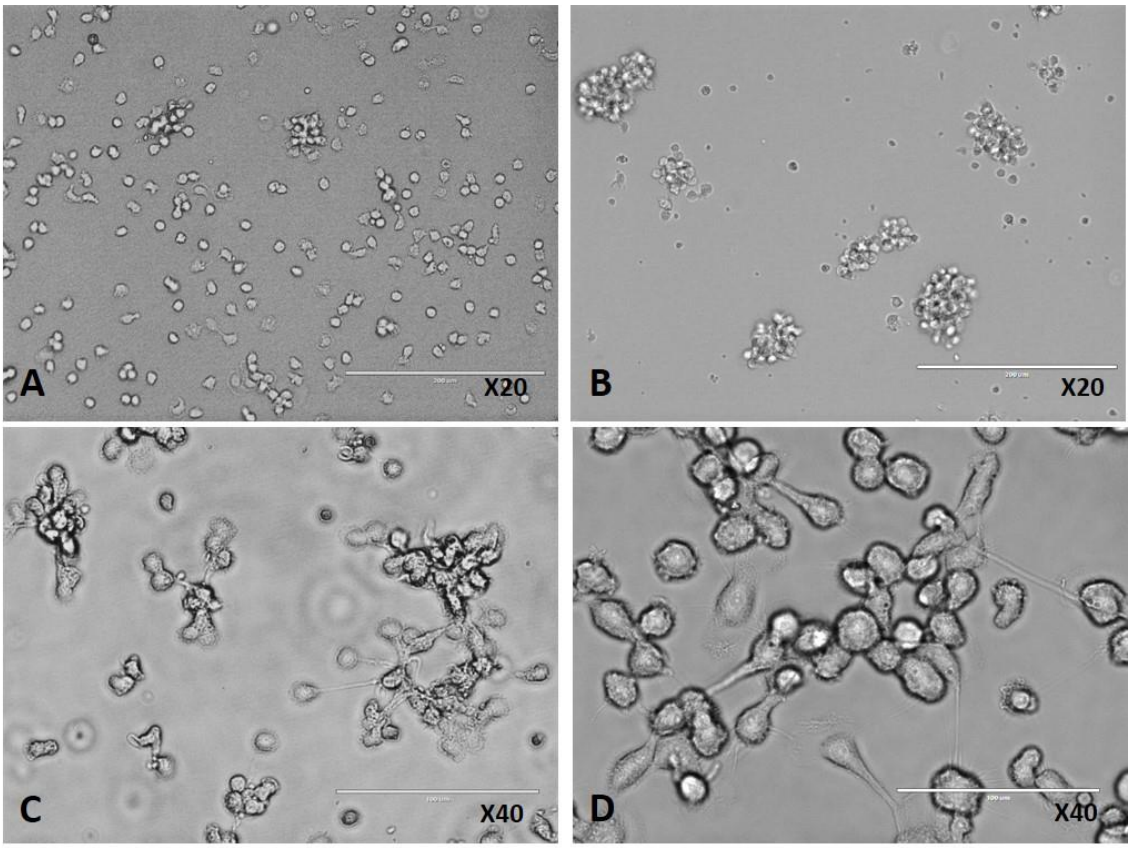

Figure 3-4 Morphology changes of CD14$^+$ monocytes in the ultra-low attachment flasks during the 7-day differentiation.

(A) On day-0, when CD14$^+$ monocytes were seeded in the ultra-low attachment flasks, cells were spread out evenly; (B) on day-1, cells formed aggregates and clumped together after the overnight incubation; (C) from day-3 or 4, cells started to migrate away from the centre of the aggregation and spread out to form a monolayer of individual cells; (D) on day-7, cells took over their individual spaces in the flask and their sizes were increased.

3.4.5 Defining the cell density of CD14$^+$ monocyte for macrophage differentiation in the ultra-low attachment flask

To determine the density of CD14$^+$ monocyte to culture in the ultra-low attachment flasks, different numbers of cells were seeded and cultured for 7 days.

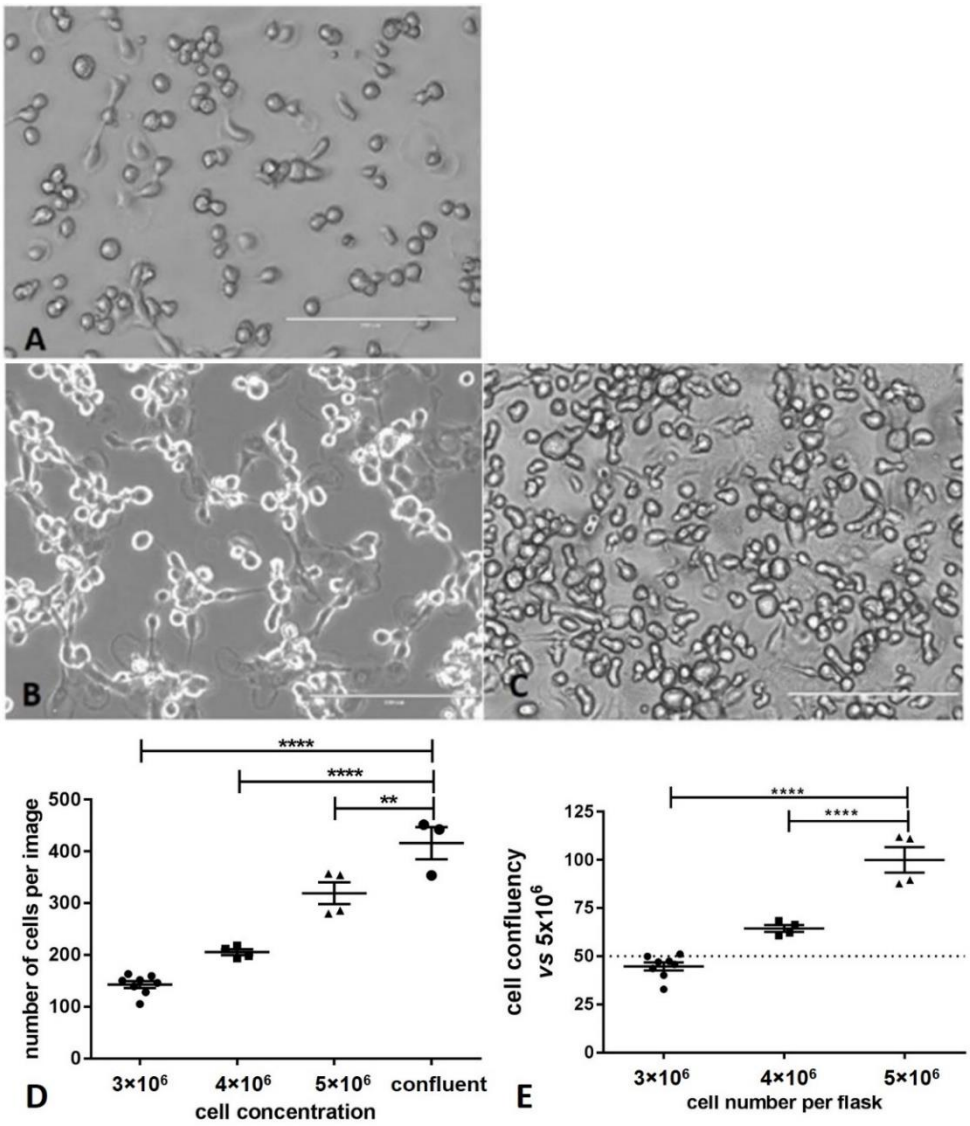

Figure 3-5 Defining the cell density of CD14$^+$ monocyte for macrophage differentiation in the ultra-low attachment flask.

Different numbers of CD14$^+$ monocytes were seeded and cultured in the flasks for 7 days before the images were taken (magnification ×20). (A-C) The numbers of cells in each flask on day-0 were 3×10^6 (A), 4×10^6 (B) and 5×10^6 (C) cells; (D) the number of cells per image on day-7; (E) cell confluence was calculated by comparing to the number of cells per image against that of 5×10^6 per flask on day-0. One-way ANOVA with Tukey's Multiple Comparison Test, ** $p<0.01$, *** $p<0.001$.

3.4.6 Long-term (beyond 4 weeks) culture of $CD14^+$ monocytes on ultra-low attachment flask formed multinuclear foreign body giant cells

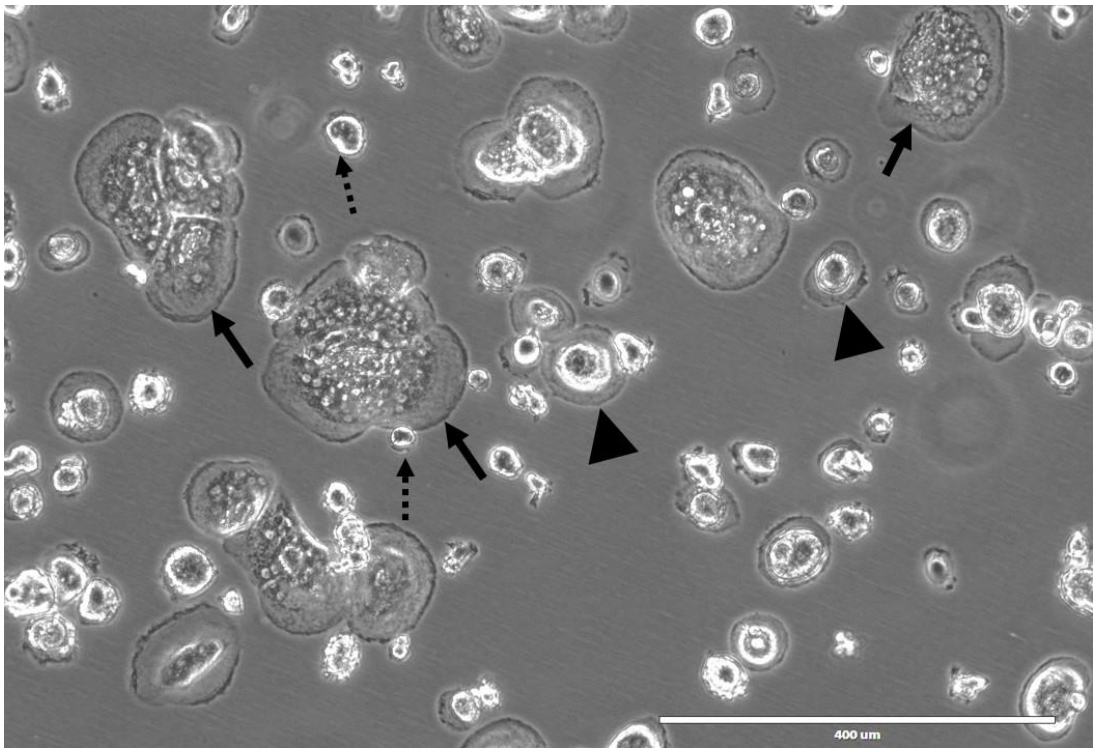

Figure 3-6 Long-term (beyond 4 weeks) culture of $CD14^+$ monocytes on ultra-low attachment flask formed multinuclear foreign body giant cells.

Cell morphology dramatically changed when $CD14^+$ monocytes were cultured for a period longer than 4 weeks. Some cells became very large cells with a multinuclear feature (solid arrow) which were recognised as foreign body giant cells; other cells shrunk in size (dashed arrow) and getting disappeared. A small number of macrophages with normal morphology were also observed (arrowhead) (magnification ×40).

3.4.7 CD14^{+} monocyte-derived cells were easily detached from ultra-low attachment flask after differentiation

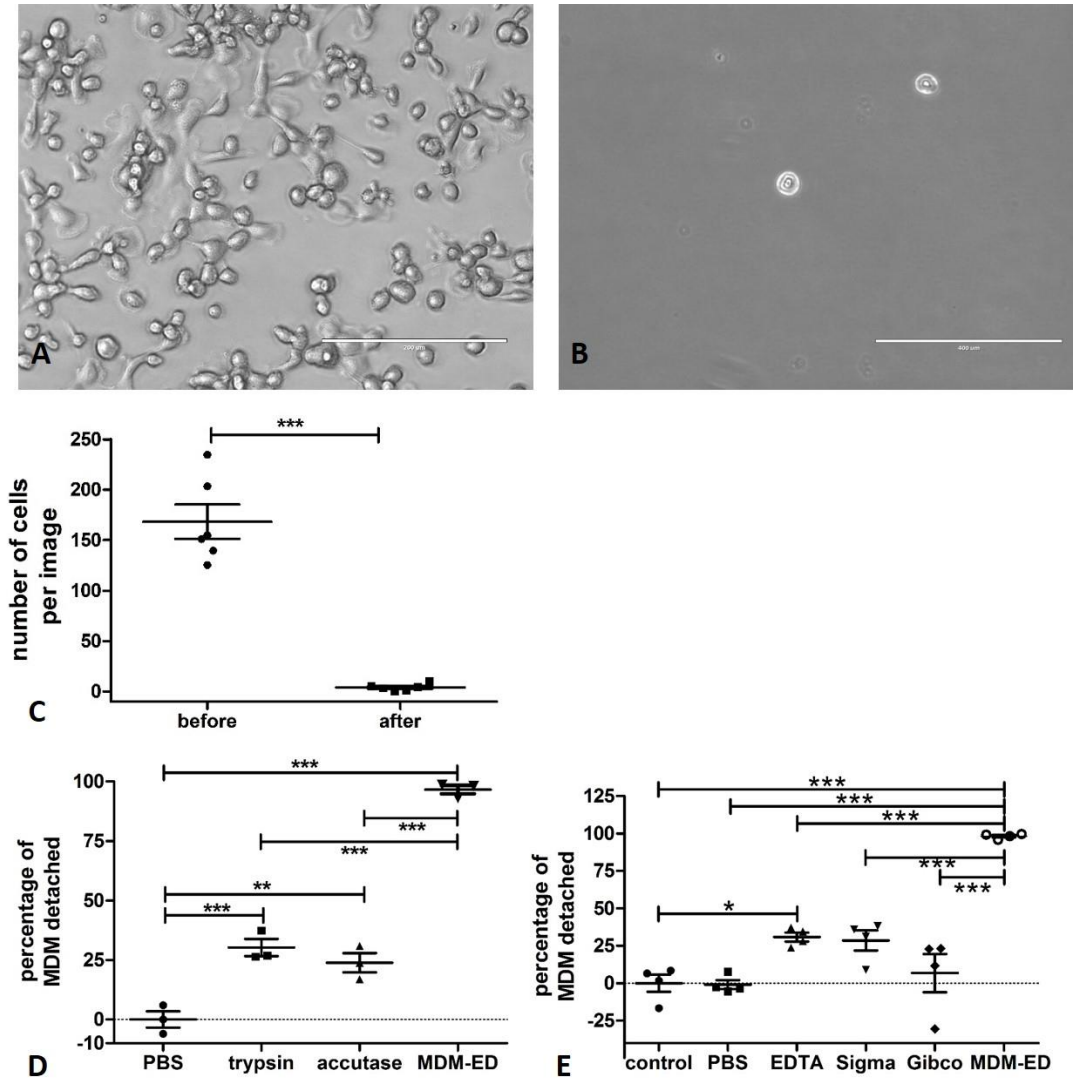

Figure 3-7 CD14^{+} monocyte-derived cells were easily detached from the ultra-low attachment flasks after differentiation.

Culture media was replaced with ice-cold PBS and the flask with cells was left on ice for 15 minutes. (A) CD14^{+} monocyte-derived cells in ultra-low attachment flasks on day-7 before detachment; (B) image of the remaining cells after the detachment; (C) the number of cells per image before and after detachment was compared, n=6; (D) comparing the percentage of detached cells (n=4) with that of the enzymatic solutions (n=3); (E) comparing the percentage of detached cells with that of the enzyme-free solutions, n=4. Gibco: enzyme-free disassociation buffer from Gibco; Sigma: non-enzymatic disassociation solution from Sigma. *p<0.05. ** p<0.01, *** p<0.001, student t-test (C), one-way ANOVA with Tukey's multiple comparison test (D & E).

3.4.8 CD14$^+$ monocyte-derived cells from the easy-detach method were CD163$^-$/CD206$^+$/Mac-2$^+$/25F9$^+$ cells

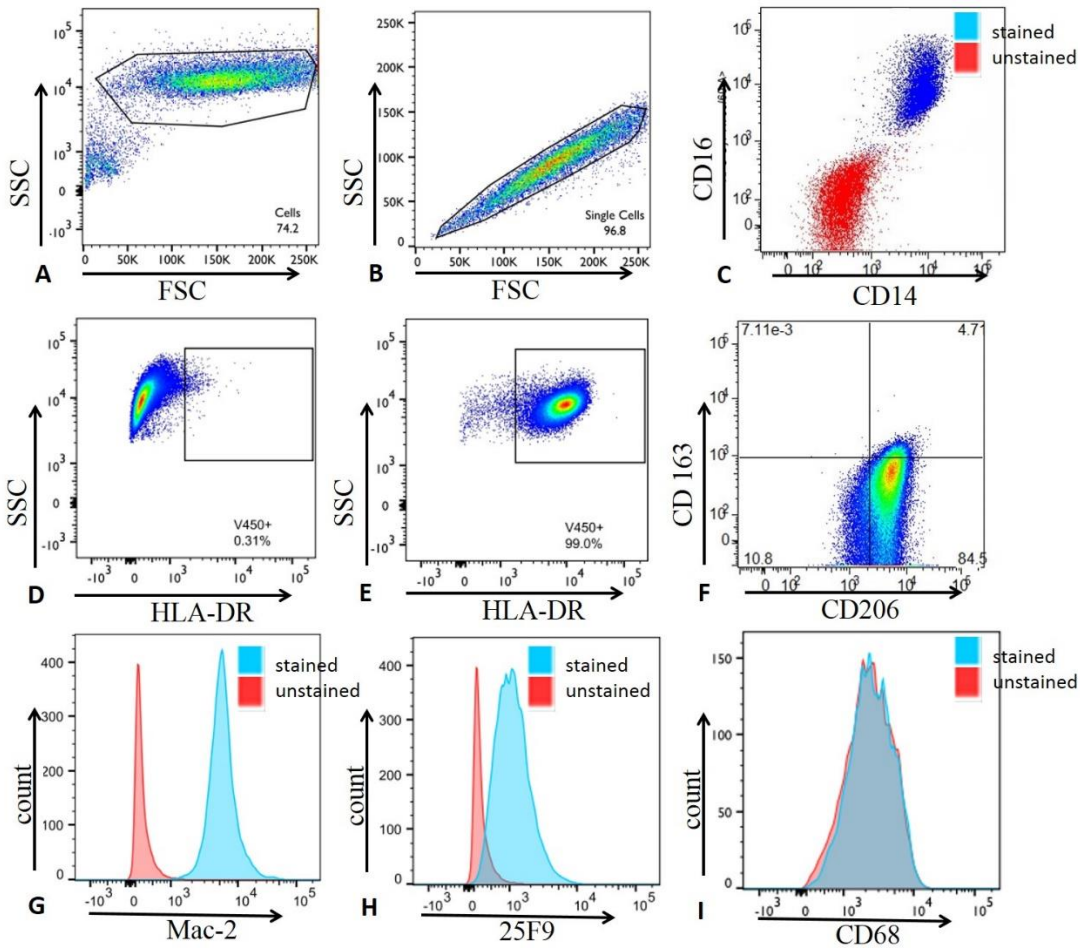

Figure 3-8 CD14$^+$ monocyte-derived cells from the easy-detach method were CD163$^-$/CD206$^+$/Mac-2$^+$/25F9$^+$ macrophages.

CD14$^+$ monocytes were differentiated using the easy-detach method and collected for flow cytometry analysis. (A) MDM-ED displayed on forward and side scatters; (B) singlets were gated for analysis; (C) MDM-ED were CD14$^+$ and CD16$^+$; (D) HLA-DR positive gate was set up based on isotype controls; (E) MDM-ED were HLA-DR$^+$; (F) the majority of MDM-ED were CD206$^+$ and CD163$^-$ cells; (G) MDM-ED were Mac-2$^+$; (H) MDM-ED were 25F9$^+$; (I) MDM-ED were CD68$^-$ on surface. A representative of n=4 experiments on different occasions.

3.4.9 Phagocytosis of apoptotic neutrophils by MDM-ED *in vitro*

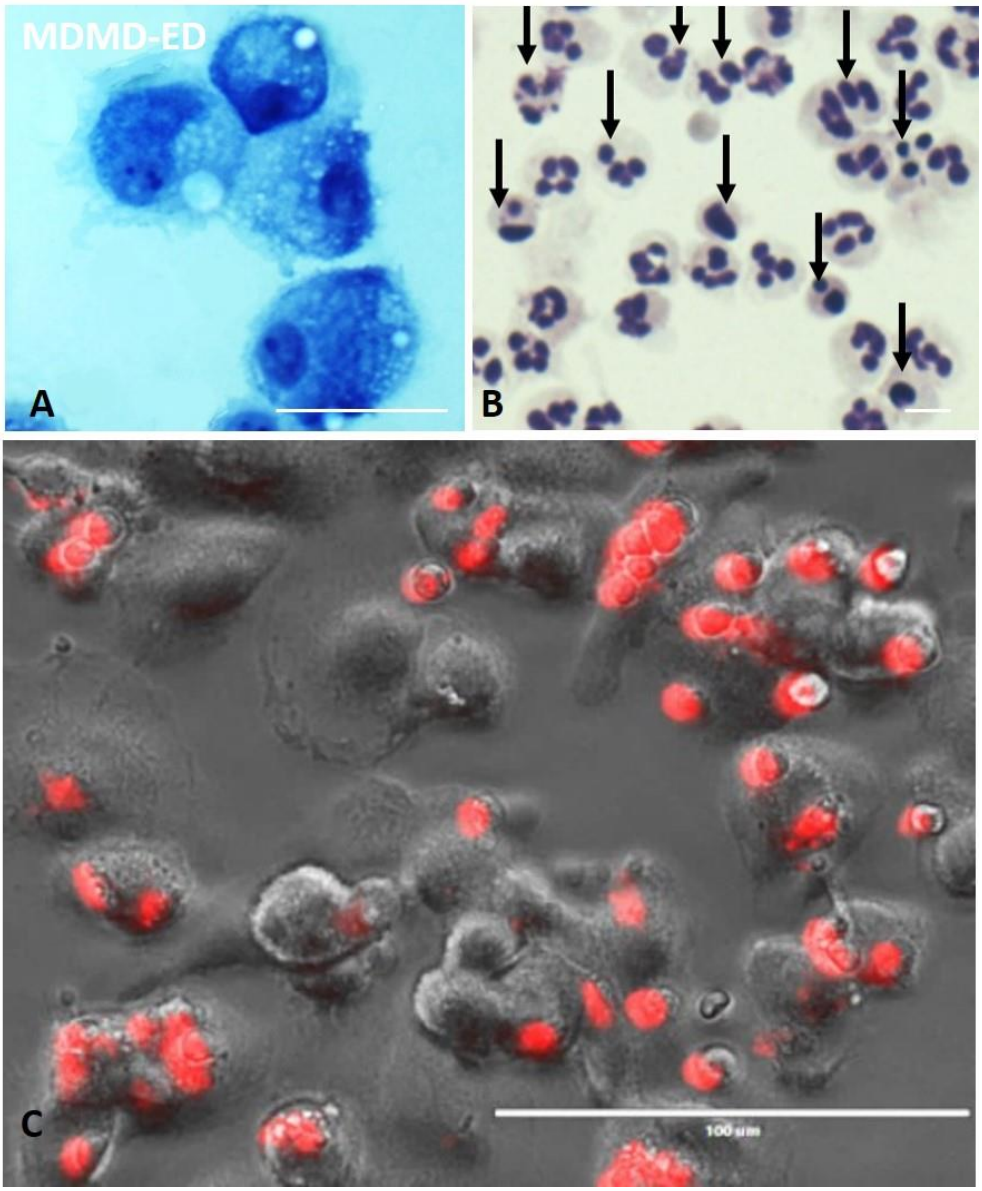

Figure 3-9 MDM-ED successfully phagocytosed apoptotic neutrophils *in vitro*.

MDM-ED (250,000 per well) were plated out in each well of a standard 24-well TC plate and apoptotic neutrophils (1.25×10^6 per well) were incubated with MDM-ED for 30 minutes. Cells were prepared as described in section 2.1.10 and 2.1.9 in the Materials and Methods. (A) Diff-Quick stain of MDM-ED cytocentrifuge preparation on day-7 showed ruffles and blebs on the cell surface with abundant cytoplasm (magnification ×40); (B) apoptotic neutrophils (arrows) after the 24 hours ageing process showed the loss of multi-lobed nucleus and nuclear condensation and fragmentation (magnification ×40); (C) apoptotic neutrophils (red, pre-stained with CellTracker™ Orange) were phagocytosed by MDM-ED during co-culture. Scale bars, A (20 µm); B (10 µm) and C (100 µm).

3.4.10 MDM-ED in response to IFN-γ and LPS

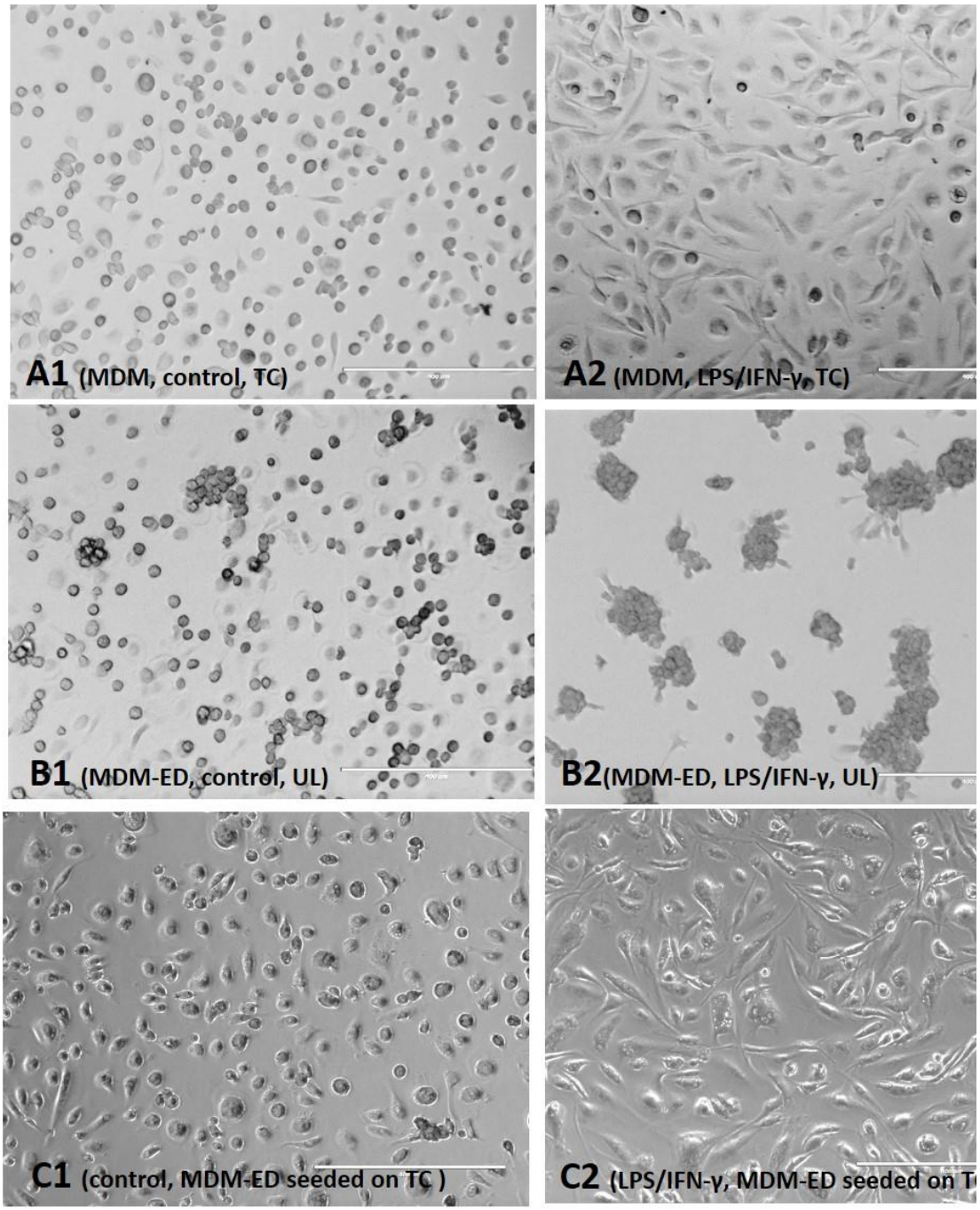

Figure 3-10 MDM-ED in response to IFN-γ (20 ng/mL) and LPS (100 ng/mL).

(A1) unstimulated MDM in standard TC plates (TC); (A2) IFN-γ/ LPS stimulated MDM in standard TC plates; (B1) unstimulated MDM-ED in ultra-low attachment flask (UL); (B2) IFN-γ/ LPS stimulated MDM-ED in ultra-low attachment flask. MDM-ED were detached and plated out in normal TC plates the day before IFN-γ/ LPS treatment and then treated with control media (C1) or IFN-γ/ LPS (C2). All treatments were for 48 hours. Scale bar = 400 µm.

IFN-γ and LPS are the archetypal M1 macrophage-polarising stimuli. MDM cultured on standard TC plates were treated with IFN-γ/ LPS (A2) or media control (A1) for 48 hours. By the end of the treatment, IFN-γ/ LPS treated MDM changed their morphology to a dominating "spindle" shape as shown in A2.

MDM-ED on day-7 contained a variety of macrophages with "fried-egg" and "spindle" shapes in the ultra-low attachment flask (B1). When they were stimulated with IFN-γ and LPS in the ultra-low attachment flasks, the evenly spread-out monolayer of cells before the treatment (B1) were disrupted and became cell aggregates (B2).

MDM-ED were detached and seeded in the standard TC plates the day before the treatment. IFN-γ/ LPS treatment changed the morphology of MDM-ED to a dominating "spindle" shape (C2) similar to that of A2. Thus, macrophages differentiated from low-attachment flask were able to adopt morphology change when stimulated with type-1 cytokines IFN-γ and LPS.

3.5 Summary and Discussion

In this study, I closely studied and optimised an easy-detach method to differentiate monocytes into macrophages using low-attachment flasks. Cells recovered from this method were characterised as CD206-positive macrophages. They were functional macrophages in that they engulfed apoptotic neutrophils and they exhibited polarisation plasticity.

3.5.1 Easy-detach method, a technical advantage

It has been speculated that adhesion is critical in the differentiation of monocyte to macrophages. The attachment of monocytes to plastic is commonly used to differentiate these cells into macrophages. However, the differentiated macrophages are too adhesive and cannot be easily detached

In this study, I compared the performance of different disassociation solutions on detaching MDM from standard TC plates. In general, all the methods resulted in less than 50% recovery (Fig 3.1 and Fig 3.2). Increasing the incubation time with disassociation solutions did not enhance the recovery. The best results were with 5 mM EDTA which on average detached just over 40% of MDM (Fig 3.1 and Fig 3.2). Earlier studies showed that the overall yield of macrophages on plastic was 35% [431]. Although a recent study showed better results of detaching MDM from plastic (over 80% recovery) with extended incubation time, the viability was compromised and the expression of certain receptors on the cell surface was reduced [452]. Furthermore, studies have shown that incubation with trypsin inhibits protein production by macrophages [453] and trypsin may decrease the response of macrophages to the pro-phagocytosis or pro-migration signals [454]. It is clear that the adherence-structures formed during macrophage differentiation are very difficult to disrupt and thus the cells are difficult to detach [431, 432].

With ultra-low attachment flasks, MDM were easily detached by leaving on ice. Furthermore, more than 95% of attached cells were collected (Fig 3.7). The cell loss was about 5% and this may be due to pipetting as not all the cells can be rinsed off and collected from the flask. The detachment of MDM by the easy-detach method was effortless and more predictable (about 15 minutes) than other methods. Technically, this

easy-detach method of macrophage differentiation is a great improvement and could serve as a good tool for macrophage study.

3.5.2 Macrophage differentiation and the development of adhesion molecules

In the protocol, CD14-positive monocytes were cultured in ultra-low attachment flasks to differentiate into macrophages (Fig 3.3). On day-0, the cells were more adherent to each other than to the surface of the flask (Fig 3.4-B). On day-3, the cells began to migrate away from each other and started to attach to the low-attachment surface (Fig 3.4-C). As the hydrophilic and neutrally charged attributes of the culture surface were not altered, it was more likely that the cells started to acquire more adhesion abilities by the development of specific adhesion molecules (Fig 3.4-D). Furthermore, when MDM-ED were detached and seeded back to an unused low-attachment flask, they attached well to the surface (data not shown). This suggested that differentiation of macrophages in ultra-low attachment flask had increased the expression of certain adhesion molecules on macrophages rather than forming a structure between the cells and the surface. In fact, a study has closely investigated the changes of adhesion molecule expression during the differentiation to macrophages on standard conditions [455].

Clearly, during the differentiation to macrophages, monocytes started to acquire some features of macrophages and may be accompanied by the expression of specific adhesion molecule(s). Indeed, the exact mechanisms and specific molecules of the attachment during macrophage differentiation need to be further studied. Such adhesion molecules could be used as potential phenotyping and functional markers for macrophages in the future.

3.5.3 MDM-ED are functional and plastic CD206^{+} macrophages

MDM-ED were morphologically macrophage-like cells (Fig 3.8 and Fig 3.9). Phagocytosis assays showed that MDM-ED were able to uptake apoptotic neutrophils *in vitro*, demonstrating these cells are phagocytically functional macrophages. Importantly, these cells expressed coldmmon macrophage markers including HLA-DR, CD14, CD16, Mac-2 and 25F9. They uniformly expressed CD206, a macrophage marker that is present on M2 polarised cells but did not express CD163 or CD68 (Fig

3.8). It is documented that alternatively activated or M2 macrophages (CD206-positive) are the most common type of macrophages related to fibrosis and tissue repair [151, 157]. In our group, AM from patients with IPF are shown to be CD206-positive cells (unpublished data), though with different expressions of CD163. This suggests that macrophages from the easy-detach method may have some similarities with the general phenotype of AM from IPF patients.

Multinucleated giant cells (MGC) were observed after the prolonged culture after 4 weeks (Fig 3.6). It is known that MGC are at the terminal stage of macrophage differentiation and they are formed by the fusion of highly differentiated macrophages [456, 457]. In other studies, MGC was also observed when cells were cultured for more than 4 weeks [433, 458, 459]. This suggested that the macrophage differentiation course of this easy-detach method is comparable to the traditional and standard process.

As previously mentioned in the introduction, macrophages are heterogeneous and plastic cells. The change of their environment can switch the cells from one phenotype to another [445-449]. When macrophages are stimulated with LPS/IFN-γ, they are activated to a "pro-inflammation" (M1) type and normally change their morphology to a "spindle" shape [436]. When MDM-ED were plated out on the standard TC plates, they adhered well and showed round shaped macrophages (Fig 3.10-C1). Upon the stimulation with LPS/IFN-γ, the cells changed their morphology accordingly to an M1 type (Fig 3.10-C2). Interestingly, when the cells were treated with LPS/IFN-γ in the ultra-low attachment flasks, they aggregated together into clumps shortly after the stimulation and stayed as aggregates until the end of the 48 hours stimulation without adopting a typical spindle shape. (Fig 3.10-B2). This suggested that when macrophages are poorly attached or in a low-attachment environment they may fail to adopt an M1 phenotype with stimulation. However, when MDM-ED cells were transferred to normal plastic and stimulated with LPS/IFN-γ, these cells adopt a typical spindle-shaped morphology. It could be that cells differentiated on ultra-low attachment surface lack IFN-γ receptors. Addressing such questions will offer helpful information for macrophage biology in diseases such as IPF which the microenvironment is altered.

In summary, macrophages derived from this easy-detach method are functional CD206-positive macrophages with polarisation plasticity.

Chapter 4 Developing an anti-CD9 bead-based flow cytometry assay for exosome study in BAL fluid from ILD lungs

4.1 Abstract

This study was designed to establish a flow cytometry assay for the investigation of exosomes in human bronchoalveolar lavage (BAL) fluid samples retrieved from patients with interstitial lung diseases (ILD).

Exosomes were purified from fresh BAL-fluid samples by ultracentrifugation after the removal of cells, cell debris and large vesicles by sequential centrifugation steps. Transmission electron microscope (TEM) showed that the pelleted vesicles were small in size (less than 100 nm in diameter) which were within the size definition of exosomes. Western blotting experiments confirmed the expression of exosome surface markers in these vesicles including CD9, CD63, TSG-101 and HSP-70, but they did not express CD81. Exosomes pelleted from defrosted BAL-fluid samples showed a consistently strong CD9 expression, however, the other exosome markers were hardly detectable. Thus, CD9 was chosen as the target protein for exosome isolation in BAL fluid. There was no recognised pattern of expression of exosomal proteins in the BAL-fluid exosomes in relation to lung fibrosis.

The anti-CD9 bead-based flow cytometry assay showed good specificity and sensitivity in the isolation of pelleted exosomes. Exosomes captured by anti-CD9 beads were confirmed by the expression of CD63 and MHC-I. A simplified method was also developed which spared the ultracentrifugation step as exosomes were shown as the major $CD9^+$ vesicles in the BAL fluid with little contamination of other $CD9^+$ vesicles. Using the simplified method, BAL-fluid exosomes were stable for exosomal surface protein study within the first 72 hours of retrieval when they were stored at 4°C. Time-course experiments defined 5 hours as the optimal time point for determining exosome concentration. In addition, the concentration of exosomes was decreased to 2/3 of the original value after the freeze-thaw cycle when the BAL fluid was stored at -80°C.

In summary, I carefully studied the exosomes in BAL fluid from patients with ILD and present a simple and powerful method for the isolation and analysis of BAL-fluid exosomes.

4.2 Introduction

Exosomes are recently discovered biological entities that are important in biological and pathological conditions [322, 326]. The size of exosomes that have been reported in the literature has been varied although there is agreement that exosomes are small lipid bilayered vesicles [324-326]. In this study, I chose to define exosomes by the most widely reported range of size (40 - 100 nm) which avoids the "smaller" exosomes (< 40 nm) or the "bigger" ones (> 100 nm) reported in a few studies.

Exosomes are released from cells by the fusion of multi-vesicular bodies (MVBs) with the cell membrane [322]. MVBs are also known as the late endosomes and they are generated through endocytosis and processed from early endosomes to be matured as late endosomes by the endocytic transport pathway [322-324]. Late endosomes can be directed to lysosomes for membrane recycling or signalled to merge with the cell membrane and release their internal vesicles as exosomes [322]. Besides exosomes, there are two other members in the extracellular vesicle (EVs) family which are 1) microvesicles (100 - 1,000 nm) and 2) apoptotic bodies (50 - 5,000 nm) [324]. The latter two are also lipid bilayered vesicles, but they are secreted from the cells by shedding of the plasma membrane and results in vesicles with bigger sizes when compared with exosomes [324].

These three types of vesicles also have different biological properties and functions [324]. Exosomes are a more defined population with distinct RNAs and proteins. The commonly used markers for exosomes are better described than other vesicles which include: transmembrane proteins like tetraspanins (e.g., CD9, CD63, and CD81); MHC class I and MHC class II proteins; cytosolic proteins (e.g., heat shock proteins -70/ HSP-70); and specific proteins that are associated with the endosomal sorting complex required for transport (ESCRT), such as tumour susceptibility gene 101 (TSG101) protein [323, 324]. There is no such protein that specifically distinguishes exosomes from other large vesicles at present [327]. However, nucleic acid materials (e.g., DNA

fragments) are often present in the other two EVs, especially apoptotic bodies, but not on the surface of exosomes [326, 328, 329].

Bronchoalveolar lavage (BAL) fluid is a very important material to study lung diseases [147, 460]. It gives useful information for the lung conditions and the nature of the diseases under scrutiny. The cell types and mediator levels (especially cytokines) in BAL fluid are generally used as important clinical data for diagnosis, monitoring progression and the effectiveness of treatments for diseases such as idiopathic pulmonary fibrosis (IPF) [460]. In IPF, the most common type of lung fibrosis, the BAL cell differential count has been correlated to disease progression, and it is useful evidence for differential diagnosis and making treatment plans [50, 66, 68]. So far, exosomes have been studied in different types of bio-fluids and their presence is associated with many diseases including cancer, neurodegenerative disorders and kidney fibrosis [333, 387-389]. At present, only a handful of studies have been published regarding exosomes in human lung BAL fluid which included a study in healthy lungs [393] and in conditions such as asthma and sarcoidosis [391, 395]. With the potential pathological role of exosomes in lung diseases, little is known about exosomes in IPF lungs [317, 421-423]. This is largely due to the technical barriers and lack of specific tools to study these biologically important nano-size vesicles [327].

Isolation of exosomes is achievable in many types of fluid using different methods [333, 334]. Ultracentrifugation after the removal of the other cellular products by sequential centrifugation is the widely accepted practice to purify exosomes from bio-fluids or tissue culture media. The sequential centrifugation steps are highly recommended by the International Society for Extracellular Vesicles (ISEV) and missing steps could compromise the results [325]. Nanoparticle tracking analysis (NTA) is relatively a new technique to study MVs [335]. NTA is designed on the principle of Brownian motion. NTA can visualise and analyse the vesicles in real time and can distinguish vesicles with different sizes in the same solution [325, 336].

Flow cytometry has been used to study EVs in bio-fluids. However, exosomes (40 - 100 nm) cannot be detected reliably by current flow cytometry. There are newly developed micro-vesicle cytometers which are expensive and they are used to study mainly large vesicles and not useful for exosome measurement [325]. In fact, binding with

micrometre-sized beads targeting on specific exosome surface proteins can enable the study of exosomes by flow cytometry. It has been tested in several types of bio-fluids, but there is no study of its application in ILD/IPF BAL-fluid samples [333, 337].

4.3 Hypotheses and aims

4.3.1 Hypotheses

- Exosomes are present in BAL-fluid samples from ILD patients
- Lung fibrosis may affect the expression of exosomal proteins in BAL-fluid exosomes
- Targeting abundantly expressed protein(s) on the surface of BAL-fluid exosomes can be used for exosome isolation and enable the analysis by flow cytometry

4.3.2 Aims

- To enrich and confirm exosomes in ILD/IPF BAL-fluid samples
- To detect and compare the expression of proteins on ILD BAL-fluid exosomes
- To identify candidate target protein(s) for immuno-beads isolation of exosomes
- To develop a flow cytometry assay to study BAL-fluid exosomes
- To determine the stability of BAL-fluid exosomes
- To optimise the bead-based flow cytometry assay for exosome concentration study

4.4 Results

To develop an immuno-magnetic bead assay for flow cytometry study of exosomes in ILD BAL fluid, a number of technical challenges were solved by the following experiments.

Alveolar exosomes were firstly isolated and purified from BAL fluid using sequential centrifugation and ultracentrifugation. Purified exosomes were confirmed by their sizes with TEM (Fig 4-1) and the expression of exosome markers by western blotting (Fig 4-2). A candidate target surface protein (CD9) for flow cytometry assay was determined by comparing the expression of exosome proteins (Fig 4-3 and Fig 4-4). The specificity and reproducibility of the designed assay were studied (Fig 4-5, Fig 4-6, and Fig 4-7). The expression of exosome surface proteins of BAL fluid exosomes captured by anti-CD-9 beads was confirmed (Fig 4-8 and Fig 4-9).

Then, a simplified method of the established protocol was designed (Fig 4-10) and the results were reproducible (Fig 4-11). The purity of exosomes was tested by the staining of DNA which can be found on the surface of large extracellular vesicles (Fig 4-12).

To apply the established method as a tool for studying exosomes in BAL fluid, the established assay was used to determine the efficiency of ultracentrifugation and the contamination of free exosome proteins (Fig 4-13). Furthermore, the stability of exosomes in BAL fluid (Fig 4-14) was studied. The optimal incubation time for exosome concentration study was determined (Fig 4-15) and the concentrations of fresh BAL fluid sample and the effect of the freeze-thaw cycle was investigated (Fig 4-16 and Fig 4-17).

4.4.1 Pelleted BAL-fluid exosomes were confirmed by TEM

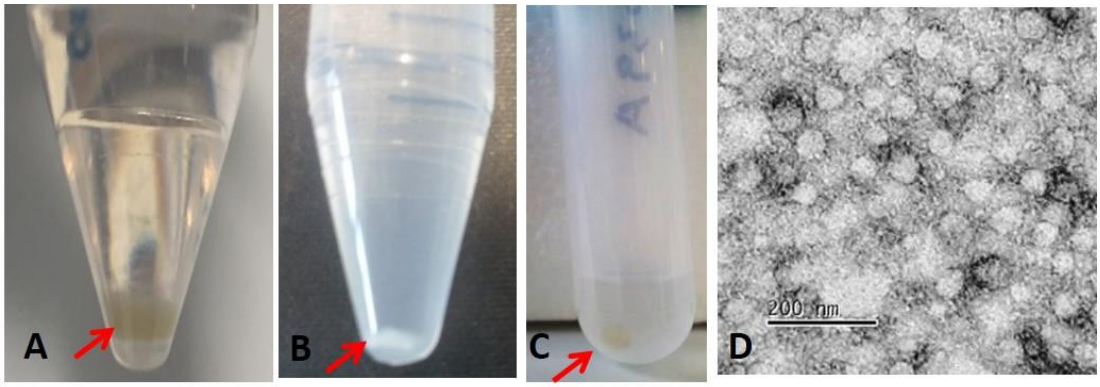

Figure 4-1 Ultracentrifugation pelleted BAL-fluid exosomes were confirmed by TEM.

BAL fluid was collected and kept on ice before sequential centrifugations and then ultracentrifugation at 100,000g to collect exosomes. (A) Pelleted BAL-fluid cells (300g); (B) pelleted dead cells and apoptotic bodies (3,000g); (C) pelleted exosomes (100,000g); (D) pelleted exosomes visualised by TEM (scale bar =200 nm).

BAL fluid was collected from the clinic and transported to the laboratory on ice. BAL fluid was first filtered through 0.45 μm filters to remove large pieces of tissue before it was centrifuged at 300g for 10 minutes to pellet BAL cells (A). The supernatant was transferred into a new tube and then centrifuged at 3,000g for 20 minutes to pellet dead cells, cell debris and apoptotic bodies (B). After the removal of cell debris and large particles at 10,000g for 30 minutes at 4°C (not shown as the pellet was invisible), exosomes were finally pelleted at 100,000g (70 minutes, 4°C) when a pellet was observed at the bottom of the tube (C) which was difficult to be broken up and resuspended by pipetting.

Exosomes were resuspended in 6 mL of PBS and pelleted again at 100,000g (70 minutes, 4°C) before the fixation with 2% PFA. Fixed samples were visualised and examined by TEM (D). Pelleted exosomes were confirmed by the sizes of the vesicles as the diameters of the vesicles were smaller than 100 nm when compared to the scale bar.

Then, the expression of exosome marker proteins was probed in the pelleted exosomes using western blotting. Furthermore, banked exosomes in frozen BAL fluid were isolated and probed for candidate target protein for the immuno-magnetic bead isolation protocol.

4.4.2 Pelleted exosomes from fresh BAL-fluid samples expressed common exosomal markers

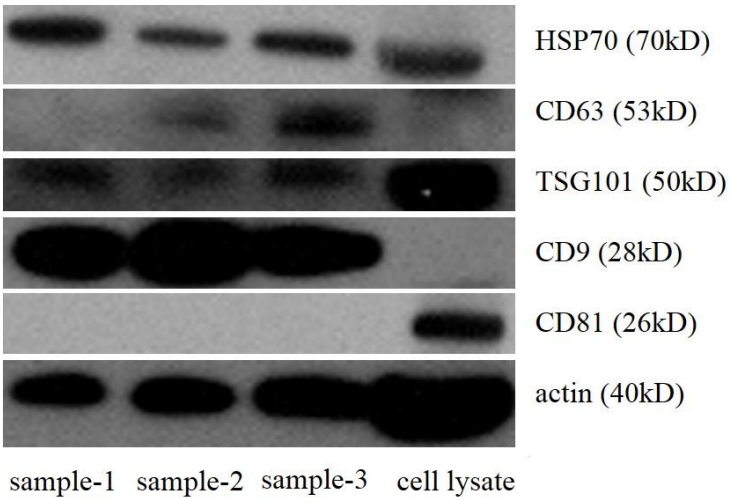

Figure 4-2 Pelleted exosomes from fresh ILD BAL-fluid samples expressed common exosome proteins.

Sample-1, sample-2, and sample-3 were pelleted exosomes from three different ILD BAL-fluid samples. Western blot showed that the pelleted vesicles express some common exosomal proteins, including HSP-70, TSG-101, CD63, and CD9. CD81 was not detected in any of the samples. The RAW264.7 macrophage cell lysate was used as positive control.

4.4.3 Pelleted exosomes from defrosted BAL fluid consistently expressed CD9

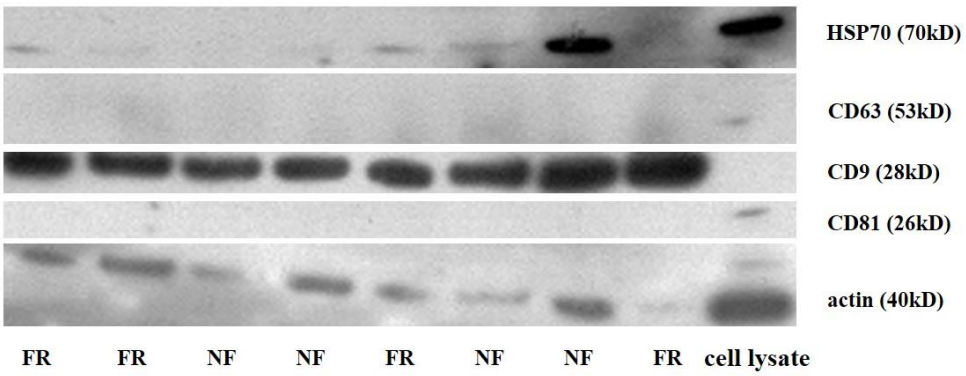

Figure 4-3 Pelleted exosomes from defrosted BAL-fluid samples consistently expressed CD9.

Exosomes were pelleted from defrosted BAL-fluid samples, washed and analysed by western blotting and a panel of exosome proteins was analysed. FR: fibrotic ILD (n=4); NF: non-fibrotic ILD (n=4); positive control: RAW264.7 cell lysate.

4.4.4 Protocol design: isolation of BAL-fluid exosomes with anti-CD9 beads for flow cytometry analysis

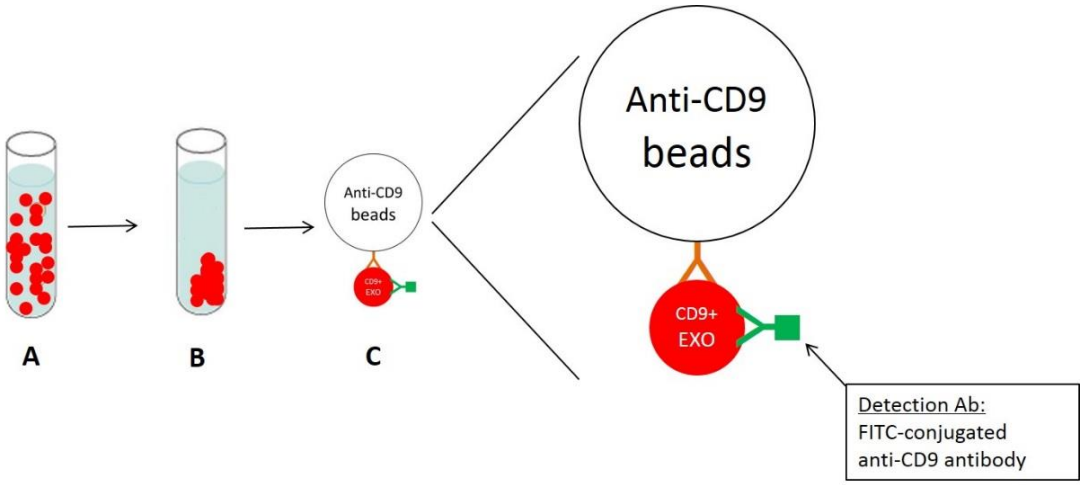

Figure 4-4 Isolation of BAL-fluid exosomes with anti-CD9 magnetic beads.

(A) Fresh BAL fluid with exosomes; (B) pelleted BAL-fluid exosomes by ultracentrifugation; (C) the bead-coupled exosomes for the staining with detection antibody (anti-CD9 FITC) before the analysis with flow cytometry.

By targeting CD9 on exosomes, an immuno-magnetic bead isolation protocol was designed. BAL-fluid exosomes were pelleted after the removal of cells, cell debris and large particles. Pelleted BAL-fluid exosomes were washed in PBS before they were resuspended in 250 µL PBS. Resuspended exosomes were coupled with pre-coated anti-CD9 beads (2.7 µm) for 24 hours at 4°C on a rotator. After the coupling, beads were washed and incubated with the anti-CD9-FITC antibody (detection antibody) for 30 minutes at room temperature. Samples were washed and analysed by flow cytometry.

The following experiments were done to test the efficiency and specificity of the designed method. Furthermore, by comparing the expression of CD9-positive population between each of the purification steps, a simplified method was designed and studied.

4.4.5 Anti-CD9 beads displayed three populations by flow cytometry whereas pelleted exosomes were depicted as debris

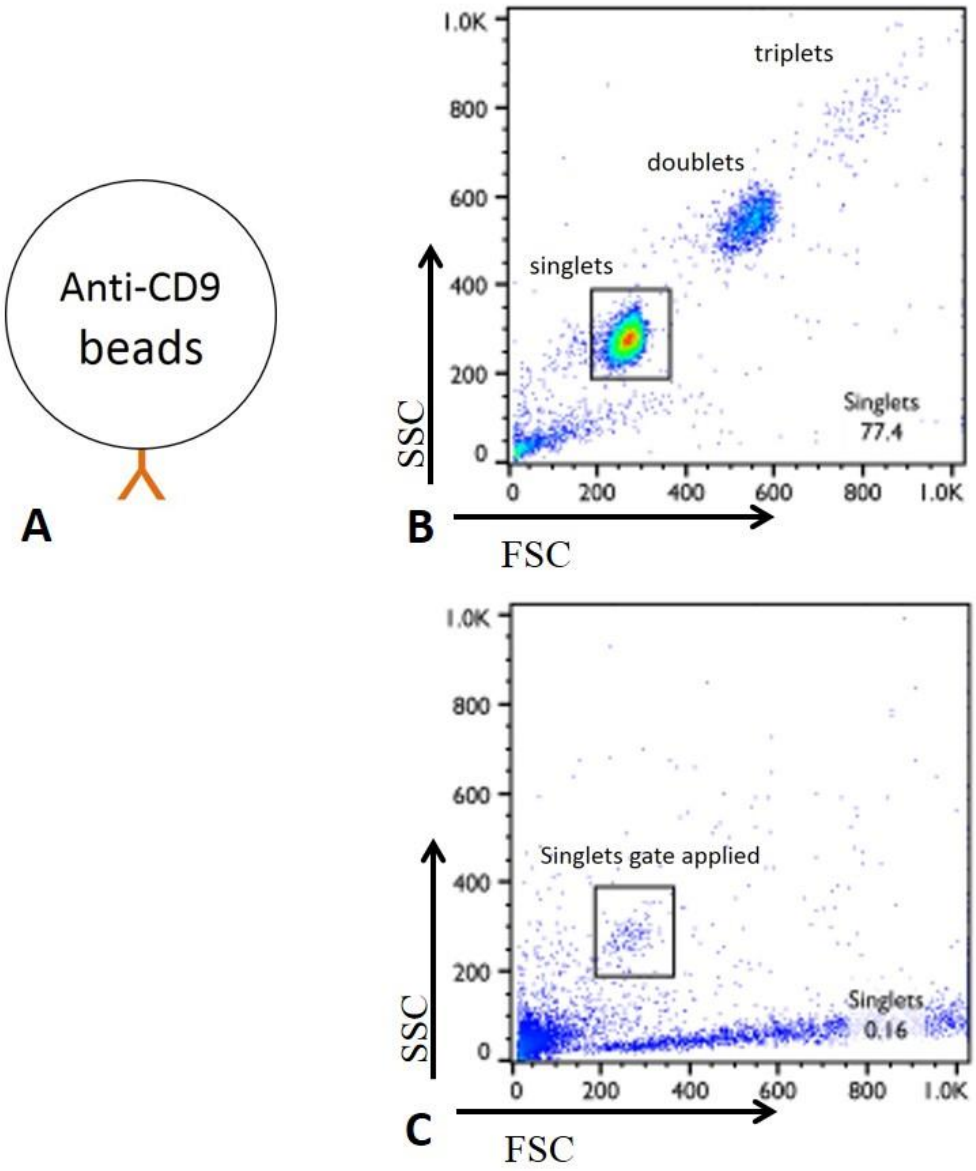

Figure 4-5 Anti-CD9 beads displayed three populations by flow cytometry.

(A) Diagram of the structure for flow analysis: anti-CD9 beads pre-conjugated with anti-CD9 antibody; (B) flow cytometry analysis of the structure; (C) pelleted BAL-fluid exosomes showed as debris. Representative data of experiments performed 3 times on different occasions (n=3).

4.4.6 Anti-CD9 beads were not auto-fluorescent and did not bind to the detection antibody

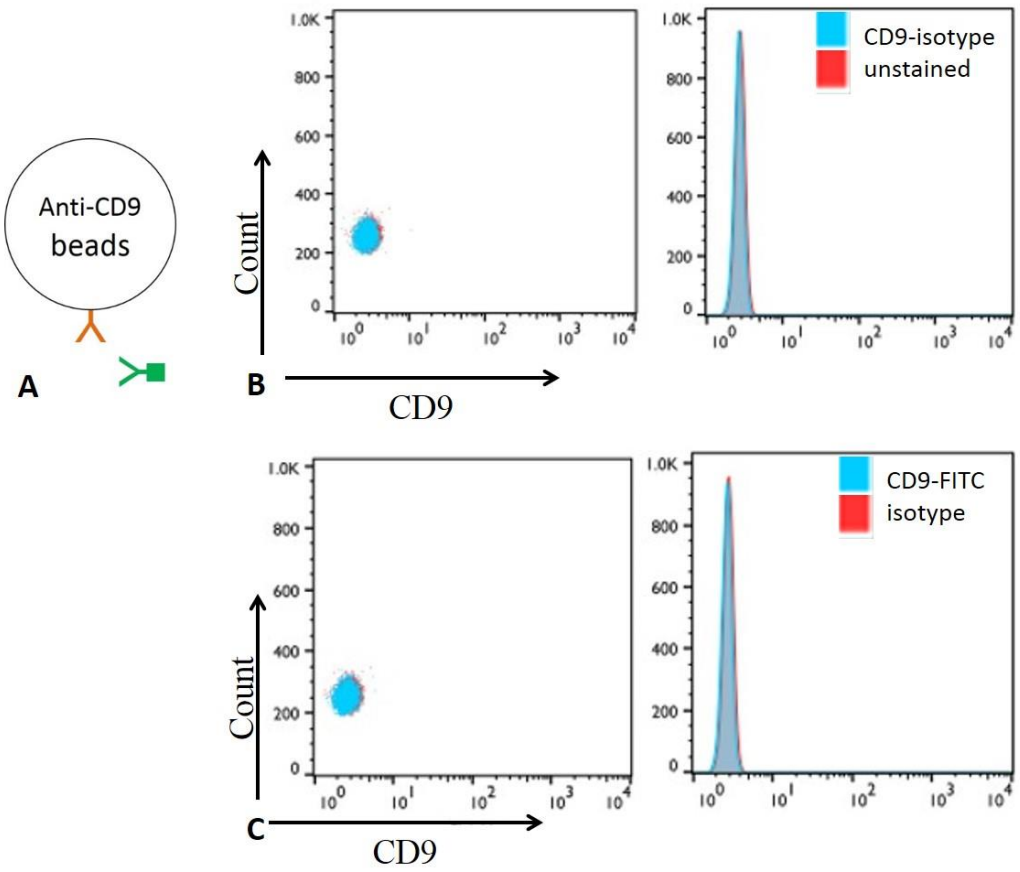

Figure 4-6 Anti-CD9 beads were not auto-fluorescent.

(A) Diagram of the structure for flow analysis: anti-CD9 beads stained with detection antibody (anti-CD9-FITC antibody) or its isotype control; (B) flow analysis of the structure with isotype staining; (C) flow analysis of the structure with anti-CD9-FITC staining. Representative data of experiments performed 3 times on different occasions (n=3).

4.4.7 Anti-CD9 bead-coupled exosomes were not auto-fluorescent

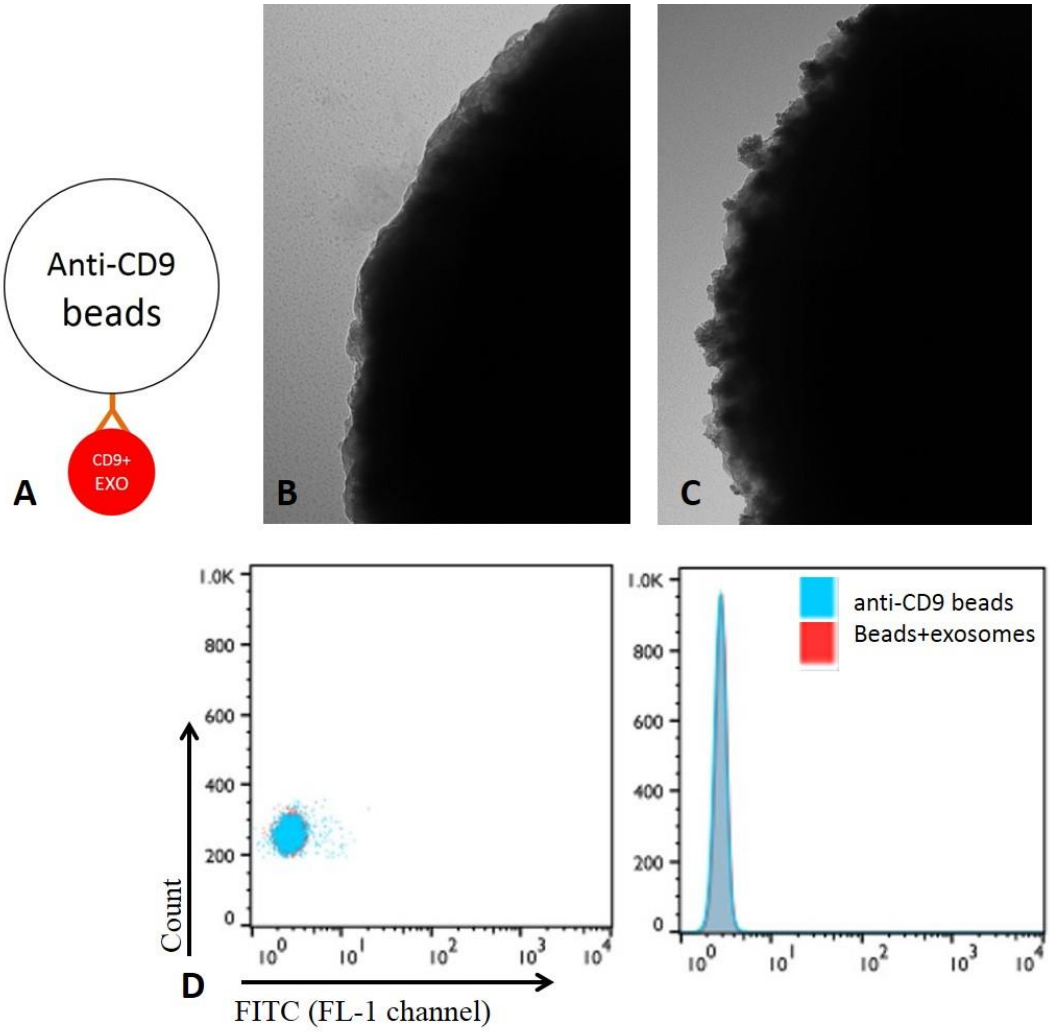

Figure 4-7 Anti-CD9 bead-coupled exosomes were not auto-fluorescent.

(A) Diagram of the structure for flow analysis: anti-CD9 beads were coupled with pelleted BAL-fluid exosomes; (B & C) TEM image of the surface of anti-CD9 beads before (B) and after (C) the coupling with pelleted exosomes; (D) flow cytometry analysis of the structure. Representative data of experiments performed 3 times on different occasions (n=3).

4.4.8 Anti-CD9 bead-coupled BAL-fluid exosomes were analysed by flow cytometry

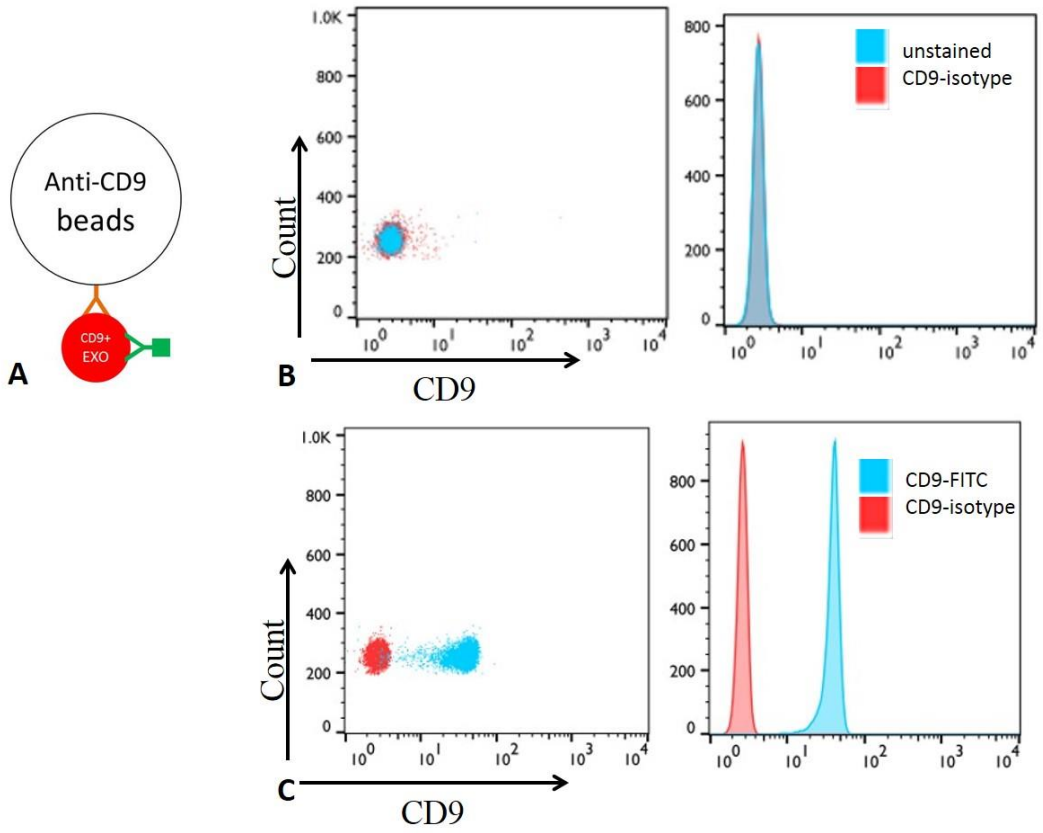

Figure 4-8 Anti-CD9 bead-coupled BAL-fluid exosomes were analysed by flow cytometry.

(A) Diagram of the structure for flow analysis: bead-coupled pelleted exosomes stained for CD9-FITC or isotype; (B) Flow analysis of the structure with isotype antibody staining; (C) Flow analysis of the structure with anti-CD9-FITC staining. Representative data of experiments performed 3 times on different occasions (n=3).

4.4.9 Pelleted BAL-fluid exosomes were CD63$^+$ and MHC-I$^+$ vesicles

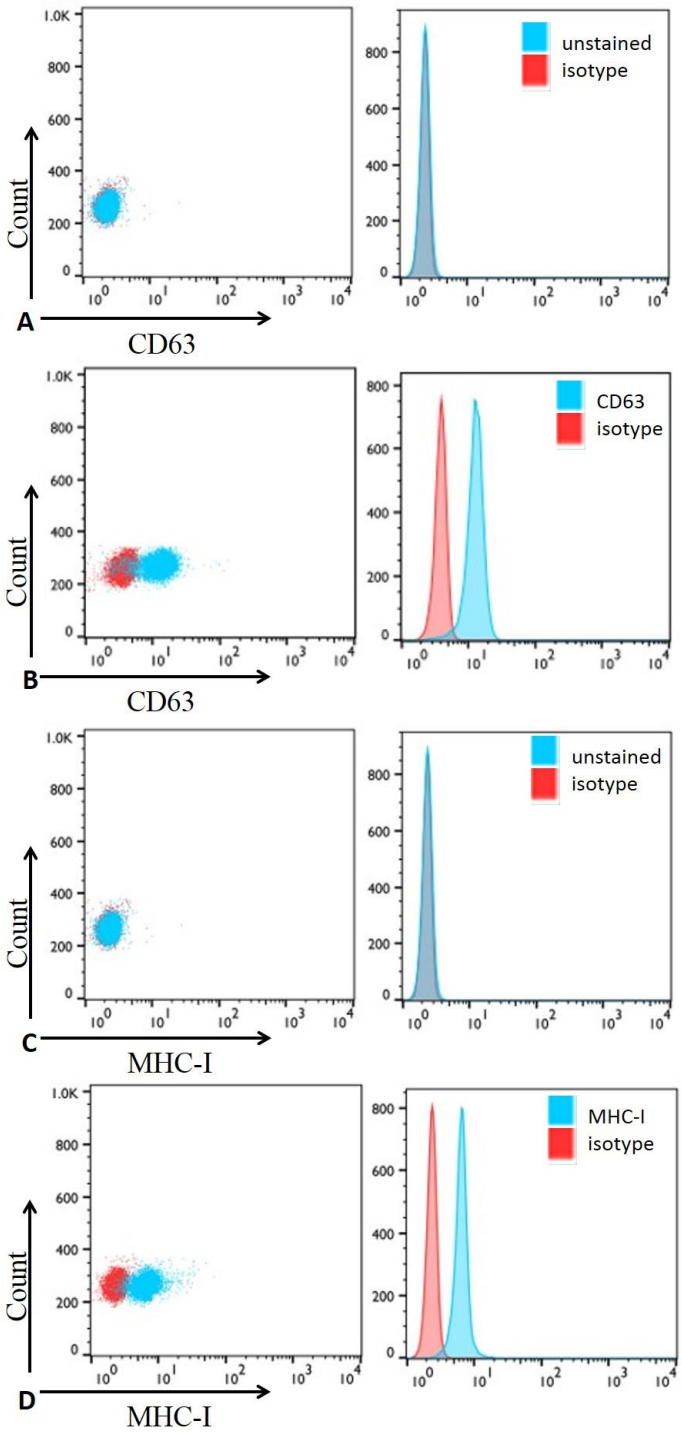

Figure 4-9 Pelleted BAL-fluid exosomes were CD63$^+$ and MHC-I$^+$ vesicles.

Bead-captured exosomes were CD63$^+$ (B) and MHC-I$^+$ (D) when compared to their isotype controls (MHC-I, A or CD63, C). Representative data of experiments performed 3 times on different occasions (n=3).

4.4.10 Simplified method: anti-CD9 bead-captured CD9$^+$ vesicles from BAL fluid after the sequential centrifugations

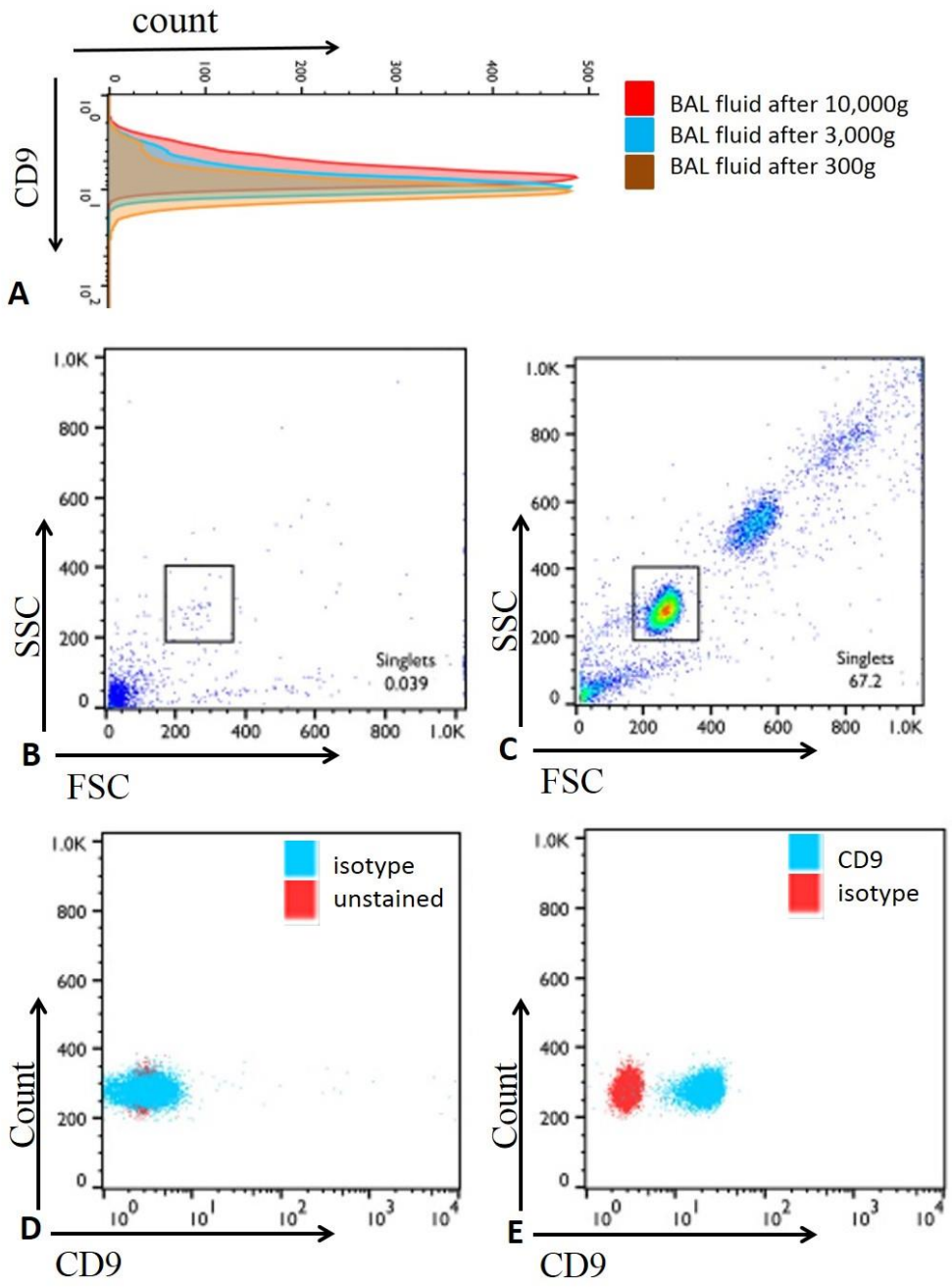

Figure 4-10 Simplified method: anti-CD9 bead-captured CD9$^+$ vesicles from BAL fluid after sequential centrifugations.

(A) Exosomes were the major CD9$^+$ vesicles in ILD BAL fluid; (B) BAL-fluid exosomes was shown as debris on flow cytometer; (C) bead-captured CD9$^+$ vesicles were identified as three populations; (D) isotype control staining showed no CD9$^+$ population; (E) anti-CD9 bead-captured vesicles were CD9$^+$. Representative data of experiments performed 3 times on different occasions (n=3).

Exosomes in BAL fluid from each of the centrifugation steps were coupled with anti-CD9 beads and analysed for the CD9 expression by flow cytometry (A). It showed that dead cells and apoptotic bodies (before 3,000g) contributed to the $CD9^+$ population (brown). The overlapping histograms of CD9 expression of the BAL fluid after 3,000g (blue) and 10,000g (red) suggested that there were very few large vesicles in the BAL fluid. Thus, exosomes were the major $CD9^+$ vesicles in the ILD BAL fluid.

Exosomes in the BAL fluid could not be identified by flow cytometer (B), but after the incubation with anti-CD9 beads, the bead-coupled exosomes were identified as three populations by flow cytometry (C). Most of them were identified as singlets (gated). Anti-CD9-FITC staining confirmed the bead-captured vesicles express CD9 when compared to the isotype staining (D).

For the validation of the simplified method, the expression of exosome surface proteins was probed. Furthermore, the contamination of large vesicle was studied by the staining of DNA which was more likely bound to their surface. To further validate the immuno-magnetic bead method, the level of exosomes before and after ultracentrifugation was compared.

4.4.11 Simplified method: anti-CD9 bead-captured CD9$^+$ vesicles were CD63$^+$ and MHC-I$^+$

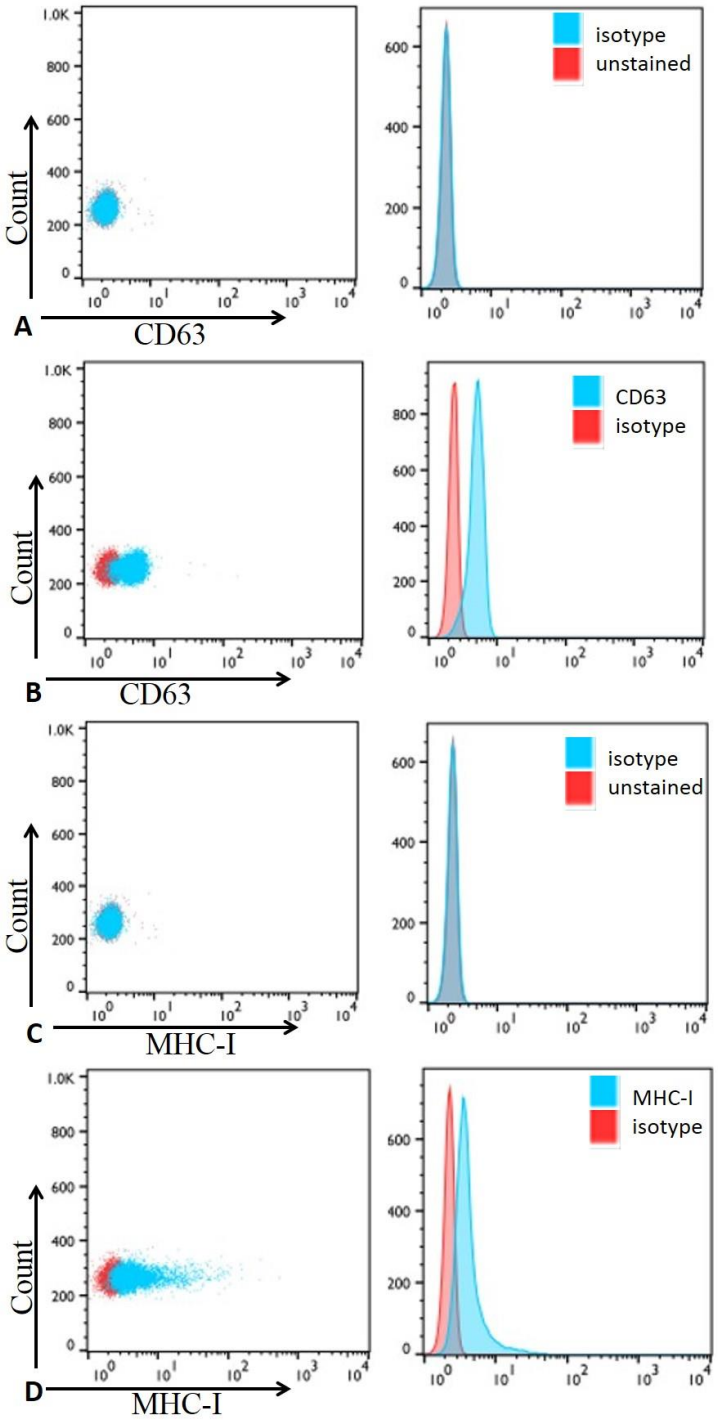

Figure 4-11 Anti-CD9 bead-captured vesicles from BAL fluid were CD63$^+$ and MHC-I$^+$.

CD9$^+$ vesicles captured by the simplified method were CD63$^+$ (A & B) and MHC-I$^+$ (C & D). Representative data of experiments performed 3 times on different occasions (n=3).

4.4.12 Simplified method: anti-CD9 bead-captured vesicles from BAL fluid were free of nucleic acid on their surface

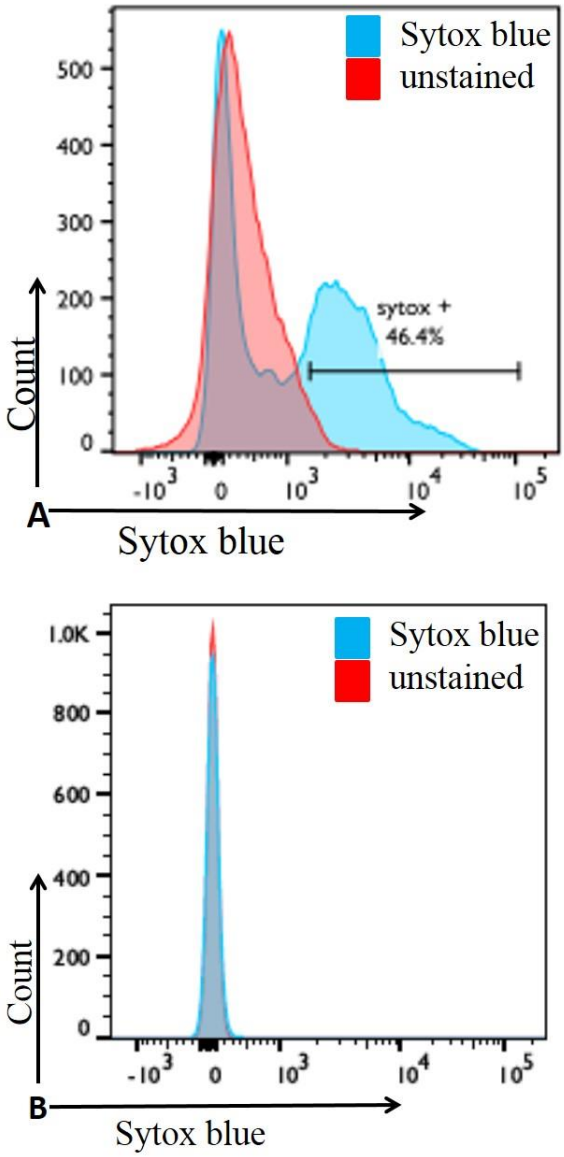

Figure 4-12 Anti-CD9 bead-captured vesicles from BAL fluid were free of surface nucleic acid.

(A) Apoptotic neutrophils were stained with Sytox blue as a positive control; (B) bead-captured $CD9^+$ vesicles were Sytox blue negative. Representative data of experiments performed 3 times on different occasions (n=3).

4.4.13 Ultracentrifugation enriched exosomes

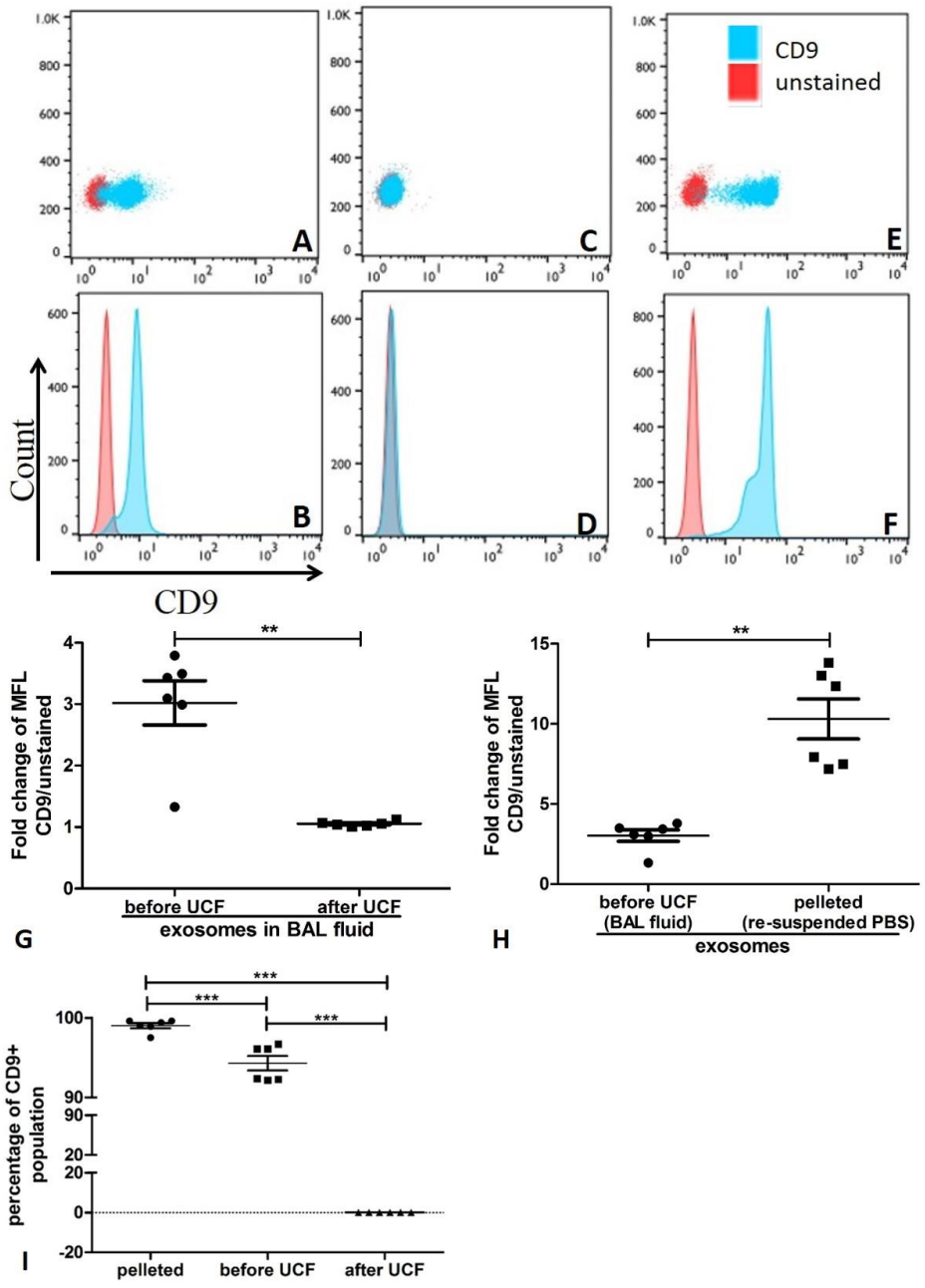

Figure 4-13 Ultracentrifugation enriched exosome concentrations.

The expression of CD9 of exosomes captured in BAL fluid before (A, B) and after (C, D) ultracentrifugation. Pelleted BAL exosomes were re-suspended in 250 µL PBS before analysed by flow cytometry (E, F). The statistical analysis of CD9 expression and the percentage of $CD9^+$ population (G-I). Student paired t-test (G & H), one way ANOVA (I), Tukey's Multiple Comparison Test, **p<0.01, ***p<0.001. Representative data of experiments performed 6 times on different occasions (n=6).

BAL fluid (containing vesicles) after the sequential centrifugations was incubated with anti-CD9 beads before (A, B) and after (C, D) ultracentrifugation to capture the exosomes before the analysis with flow cytometry. The expression of CD9 showed a significant decrease after the ultracentrifugation (G).

Pelleted exosomes were washed and resuspended in 250 µL PBS, then analysed with anti-CD9 beads flow assay (E, F). As expected, ultracentrifugation enriched the concentration of exosomes and increased the shift of CD9 fluorescence (E, F). CD9 expression was increased in the re-suspended exosomes (H).

The percentage of $CD9^+$ population was increased from 95% before ultracentrifugation to approximately 100% in the resuspended solution of pelleted exosomes (I). After the ultracentrifugation, there were no $CD9^+$ vesicles in the remaining BAL fluid (I), which also suggested that there was no soluble/ free CD9 protein in the BAL fluid.

These data suggested that before the ultracentrifugation, the anti-CD9 beads were sensitive enough to bind with the exosomes in BAL fluid even though they are at low concentrations. The isolation of exosomes from the BAL fluid without ultracentrifugation is achievable.

To expand the application of this anti-CD9 bead-based method, especially for the study of alveolar exosomes in IPF/ILD patients, a few other experiments were carried out. These experiments included the stability of exosomes for surface protein studies, defining the coupling time for exosome-concentration studies and the freeze-thaw effect on alveolar exosomes in BAL fluid.

4.4.14 Simplified method: exosomes in BAL fluid were stable in the first 72 hours for surface protein study

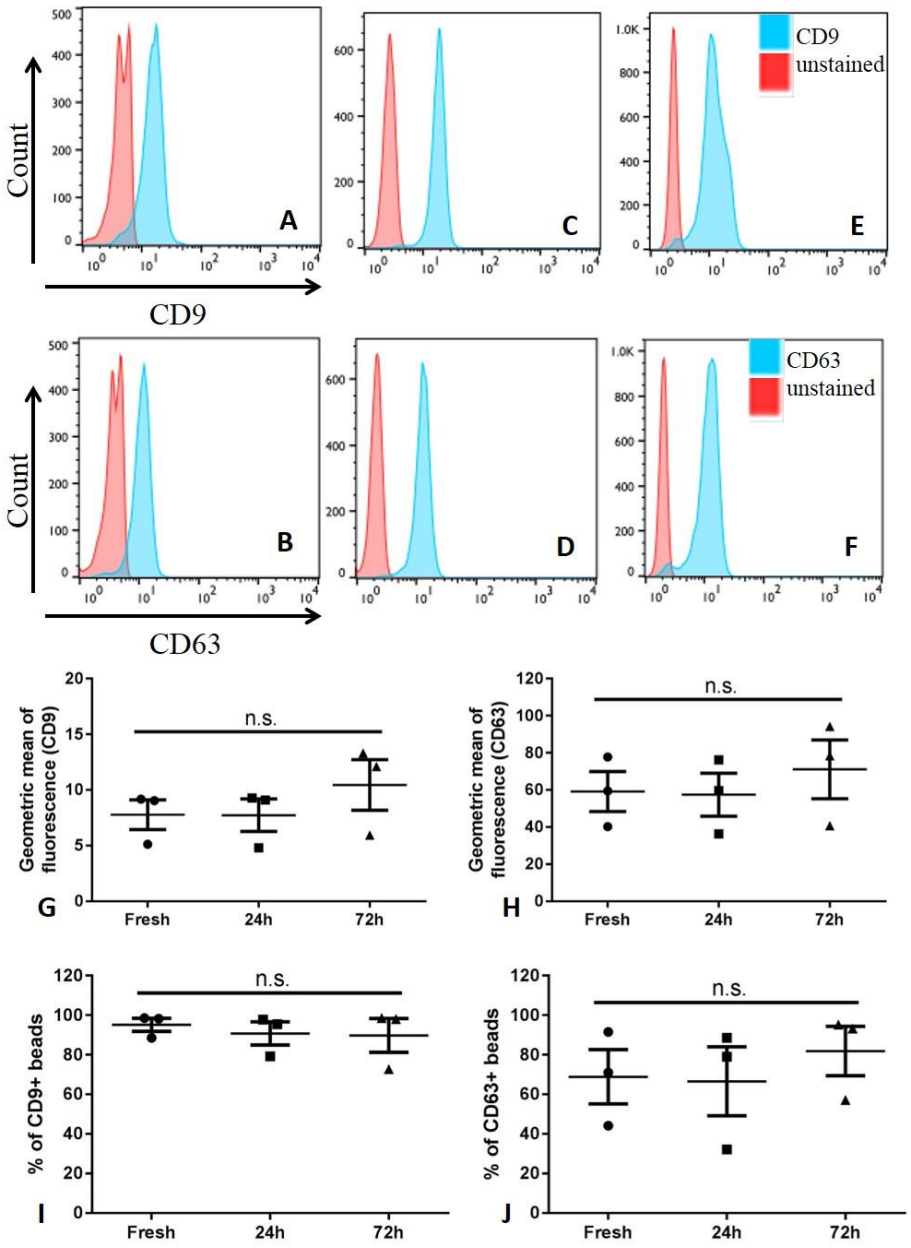

Figure 4-14 Exosomes in BAL fluid were stable in the first 72 hours.

Anti-CD9 beads were coupled with exosomes in fresh BAL fluid (A & B), after 24 hours (C & D), and again after 72 hours (E & F) before the analysis of CD9 and CD63 expression. The mean fluorescence of CD9 (G) and CD63 (H) expression or the percentage of $CD9^+$ (I) and $CD63^+$ (J) population were analysed which showed no difference. One-way ANOVA, Tukey's Multiple Comparison Test, n.s., not significant. Representative data of experiments performed 3 times on different occasions (n=3).

4.4.15 Simplified method: defining the beads coupling time for exosome concentration study

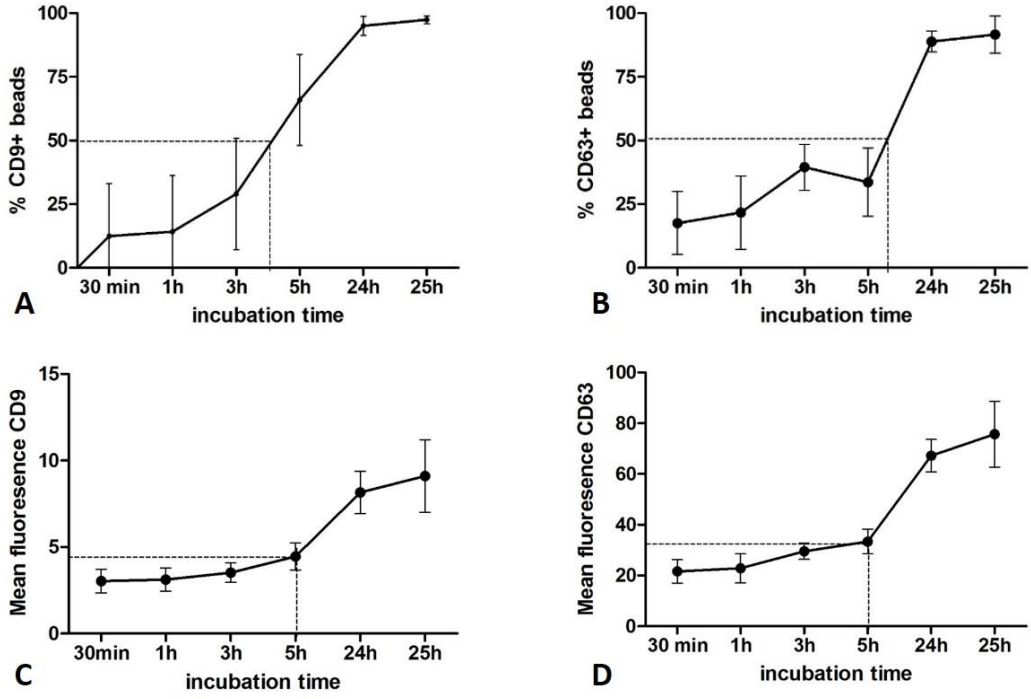

Figure 4-15 Defining the beads coupling time for exosome concentration study.

Half of the beads were coupled with BAL-fluid exosomes at approximately 5 hours. (A & B) Percentage of $CD9^+$ (A) and $CD63^+$ (B) populations. (C & D) Incubation of 5 hours reached about half of the maximum mean fluorescence of CD9 (C) and CD63 (D). Representative data of experiments performed 4 times on different occasions (n=4).

4.4.16 Simplified method: BAL fluid from fibrotic lungs may have less exosomes than non-fibrotic lungs

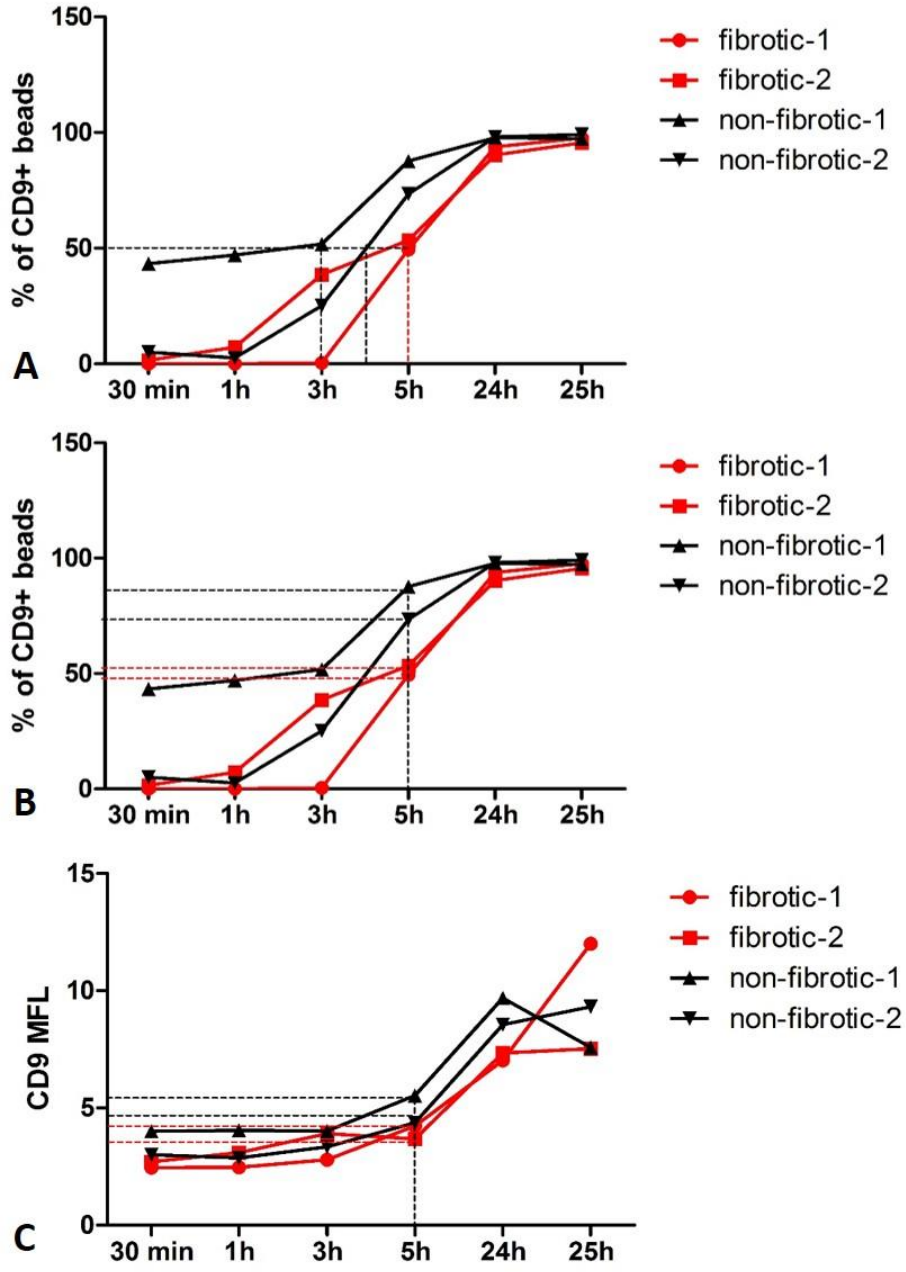

Figure 4-16 BAL fluid from fibrotic lungs may have less exosomes than non-fibrotic lungs.

(A) BAL fluid from fibrotic lungs needed longer coupling time to reach 50% of $CD9^+$in the whole population; (B) coupling for 5 hours showed lower percentages of the $CD9^+$ population with fibrotic BAL fluid; (C) coupling for 5 hours showed lower mean CD9 fluorescence with fibrotic BAL fluid. Fibrotic ILD n=2 (in red), and non-fibrotic ILD n=2 (in black).

4.4.17 Simplified method: the number of exosomes decreased after repeated freeze-thaw cycle in ILD BAL fluid

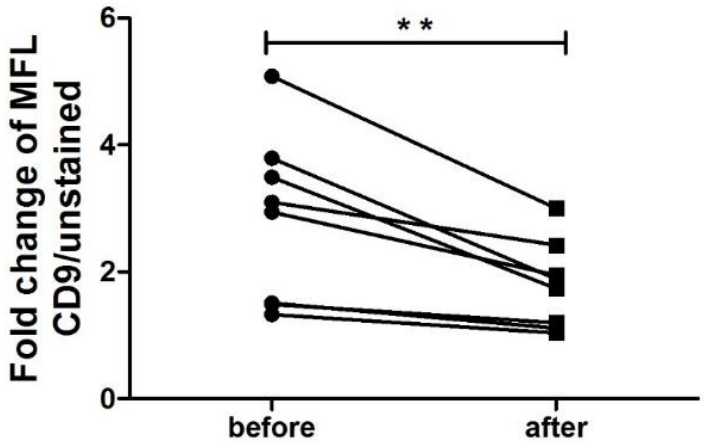

Figure 4-17 The number of exosomes decreased in human ILD BAL fluid after repeated freeze-thaw cycle.

BAL-fluid exosomes were analysed by anti-CD9 beads flow cytometry assay. Fold change of CD9 fluorescence was compared before and after the repeated freeze-thaw cycle. **p<0.01, paired student t-test, n=7.

BAL fluid was defrosted and coupled with anti-CD9 beads for CD9 staining. The same set of samples were returned to -80°C and defrosted again 24 hours later for analysis. The fold change of CD9 fluorescence between stained and unstained was calculated to represent the exosome concentrations. Statistical analysis showed that the CD9 expression dropped 2.84±1.32 to 1.79±0.68 after the freeze-thaw cycle ($n=7$, $p<0.01$). The CD9 expression was decreased by 33.05 ± 12.80 % on average which suggested that 1/3 of the vesicles was lost during the freeze-thaw cycle.

4.5 Summary and Discussion

In this study, I have presented an easy but powerful tool to assist in the investigation of BAL-fluid exosomes, particularly in ILD/IPF patients.

Using immuno-magnetic beads is a common method to "enlarge" the size of exosomes and make them visible by flow cytometry [325, 333]. In fact, a number of different immuno-magnetic beads have been used for the isolation of exosomes in different samples. This includes anti-CD9, anti-CD63, anti-CD81, anti-MHC-I, anti-HLA-DR and anti-EpCAM magnetic beads [461-463]. Immuno-magnetic bead isolation is designed according to the protein expression on exosomes, and thus using this technique may not capture the whole exosome population [325]. In order to capture the majority of exosomes, the pre-coated beads should target the most common protein that is expressed on the exosome surface. Prior to this study, there were no established immuno-magnetic bead protocols for the study of BAL-fluid exosomes in ILD/IPF.

In this study, I have shown that exosomes from ILD/IPF BAL fluid did not express CD81, weakly expressed CD63 but expressed CD9 abundantly (Fig 4.2 and Fig 4.3). Thus, CD9 was identified as the target for exosome immuno-magnetic beads isolation. The materials used for the assay did not cause unspecific binding or generate false positive signals such as auto-fluorescence (Fig 4.4 – Fig 4.7). Anti-CD9 bead-captured exosomes also expressed CD63 and MHC-I on flow cytometry, common exosome-associated proteins, which further confirmed these were indeed captured exosomes. A simplified method was further developed to make it a more efficient technique.

The stability of exosomes is critical for experimental studies of exosomes [325, 337]. Exosomes in ILD/IPF BAL fluid were abundant in proteins with different molecular weights (SDS-PAGE silver stain, data not shown), however, the freeze-thaw cycle may lose a significant amount of exosomes. In fact, this study showed repeated freeze-thaw cycle have lost 30% of the original exosomes when stored in BAL fluid (Fig. 4.17) at -80°C. For the surface protein study, exosomes were stable in BAL fluid at least in the first 72 hours (Fig 4.14) when they were stored at 4 °C.

The protein expression on exosomes gives information such as their origins, functions and whether they are disease relevant [322, 388, 391, 461]. The cellular proteins are actively sorted to exosomes for different purposes and the exosome pathway also coordinates with other mechanisms such as autophagy to maintain cellular homoeostasis [349]. CD81, a tetraspanin protein that expresses on almost all exosome varieties, was not present in ILD/IPF BAL-fluid exosomes. CD81 is essential for T cell development at early stages [464] and CD81 knockout mice showed compromised immune responses *in vivo* [465]. CD81 also mediates the signal transduction and cell adhesion of immune cells [466] and can also form molecular complexes with CD9 that may have specific roles in many cellular functions [467]. CD9- and CD81-null mice resulted in multinucleated cells, and CD9/CD81 double-null mice spontaneously developed multinucleated giant cells in the lungs, which highlighted the function of both tetraspanin proteins in monocyte/ macrophage biology [468]. CD81 has also been shown crucial in liver HCV infection and female fertility [469, 470]. *In vitro*, it has been shown that the expression of CD9, CD81 and CD63 changes during the differentiation of monocyte to macrophages [471]. The role of CD81 and CD9 in ILD/IPF exosomes needs to be further studied. CD81 negative exosomes might be used for the profile of this distinct exosome population in ILD/IPF lungs. The high expression of CD9 and the absence of CD81 may offer clues to identify the parent cells of the BAL fluid exosomes. Furthermore, cells in ILD/IPF lungs may also have been affected which led to the lack of CD81 in the alveolar exosomes. For future studies, it will be useful to examine the expression of CD81 and CD9 in the alveolar cells. It might be very useful to compare the protein expression of alveolar exosomes of other lung conditions with ILD/IPF as well, for example, COPD, acute lung injury (ALI) and lung cancer.

Regardless of their protein composition, the actual concentration of exosomes may be very informative and disease-relevant. In fact, the level of exosomes in plasma had been correlated with the stage of lung cancer and plasma exosomal RNA has shown a fibrotic profile in IPF which was also correlated with disease severity [422, 423]. The level of BAL fluid exosomes which better represent the condition of the diseased lungs compared to plasma exosomes may be more sensitive and thus more informative. Prior to my study, there was no established methodology for quantifying exosomes in IPF BAL fluid. In this study, the optimal ‘coupling time’ (that is the incubation time for

CD9-immuno-magnetic beads to couple with CD9-expressing exosomes) was shown to be 5 hours. This is important for the standardisation of measuring exosome concentrations in the ILD/IPF BAL fluid between samples. The standardised anti-CD-9 bead-assay also suggested fewer exosomes in BAL fluid from patients with lung fibrosis (Fig 4.16), which has been confirmed with larger number of samples by NTA as presented in chapter 7 of this thesis.

In summary, by observing that CD9 was abundantly expressed on ILD BAL-fluid exosomes, an easy and user-friendly method was developed and tested to study the BAL-fluid exosomes by flow cytometry. This technique could be used as a reliable tool to study exosome protein expression and concentrations in BAL fluid, particularly in ILD/IPF.

Chapter 5 Collagen-I and collagen-IV modulate both the formation and degradation of autophagy in macrophages

5.1 Abstract

This study was designed to establish an *in vitro* model in which to investigate the role of extracellular matrix (ECM), specifically collagen-I and collagen-IV, on macrophage autophagy.

The formation and degradation of autophagosomes were studied with starvation (limited nutrients), rapamycin and bafilomycin A1 in three types of macrophages: RAW264.7, THP-1 and human peripheral blood monocyte-derived macrophages (MDM). Confocal microscopy and western blotting were used to measure the expression of microtubule-associated protein light chain 3 (LC3) and p62.

Starvation induced weak LC3-II expression. Rapamycin-induced autophagy achieved robust and reproducible LC3-II expression in a time- and concentration-dependent manner. The optimal condition for autophagy induction with rapamycin was determined as 25 μM for 4 hours. Bafilomycin A1 blocked LC3/p62 degradation and 50 nM was determined as the optimal concentration for 4 hours treatment. Bafilomycin A1 increased the LC3-II expression in rapamycin-induced autophagy. The classic pattern of LC3 changes, the increase in LC3-II and decrease in LC3-I, were observed in RAW264.7 macrophages upon autophagy induction. In human monocyte/ macrophages, only LC3-II was observed whereas LC3-I was not detected.

Differentiation up-regulated autophagy in MDM which was reduced to basal level by collage-I and collagen-IV ($p<0.001$). Collagen-I and collagen-IV increased basal autophagy in RAW264.7 macrophages ($p<0.001$ and $p<0.05$) but only collagen-I increased basal autophagy in MDM ($p<0.05$). Collectively, ECM, particularly collagen-I, regulates both the formation and degradation steps of autophagy in macrophages.

These data suggest that the surrounding environment of cells can dictate their autophagic response, a finding that is relevant in diseases where ECM composition is altered.

5.2 Introduction

The excessive deposition of ECM is a feature of idiopathic pulmonary fibrosis (IPF) and the composition of ECM changes at different stages of IPF. Collagen type-I, III and IV may be associated with early stage of lung fibrosis [203]. At the later stage of IPF, type-I collagen is found increased and type-IV collagen, the major collagen in the basement membrane, is found decreased [204].

Macrophages are key regulators of the wound-healing process which is likely impaired in IPF [15, 136]. In IPF, the number of alveolar macrophages (AM) is greatly increased, and they also exhibited a distinct “wound-healing” phenotype [151, 157].

Studies have suggested that ECM plays an important role in determining innate cell function in inflammation [156]. It is known that the interaction between macrophages and ECM influences the inflammation effector functions of macrophages [214]. ECM increases basal autophagy in epithelial cells through adhesion molecules [216] and the detachment from ECM also induces autophagy[217]. ECM also modulates many processes that are relevant to autophagy in the lungs [154, 215].

Autophagy is necessary for macrophage biology. Intact autophagy is required for monocyte differentiation to macrophages [472, 473], the antigen presentation process [474, 475] and the polarisation of macrophages (against and in favour of the alternative activation) [476, 477]. The impaired autophagic activity can lead to the accumulation of protein aggregates and damaged organelles which may impair macrophage function. Monick and colleagues have demonstrated that AM isolated from smokers have compromised autophagy [478]. Studies in bleomycin-induced lung fibrosis have shown that the degree of lung fibrosis was improved by inducing autophagy [297, 298, 479].

The primary feature of autophagy is the formation of autophagosomes upon its activation through mTOR-dependent and -independent pathways. Both starvation and rapamycin can induce autophagy by inhibiting the mTOR [256]. Once autophagy is

activated, the cytosolic LC3-I is conjugated with phosphatidylethanolamine (PE) to form LC3-II by an ubiquitination-like enzymatic reaction. LC3-II, but not LC3-I, associates with both the outer and inner membranes of autophagosomes. And, therefore, LC3-II is regarded as the marker of autophagosomes and autophagy activation [237, 480, 481]. The archetypical cellular response in active autophagy is an increase in LC3-II expression and a decrease in LC3-I expression. Autophagy substrate protein, p62, also known as SQSTM1/ sequestosome-1, is selectively incorporated into autophagosomes through direct binding to LC3-II [269, 482-484]. Bafilomycin A1 is an inhibitor of the v-type ATPase that blocks the fusion of the autophagosome and lysosome by inhibiting lysosomal acidification [276]. By blocking the autophagosome degradation, neither LC3-II nor p62 proteins can be degraded. Therefore, the accumulation of the autophagy marker (LC3-II) by bafilomycin A1 represents the "autophagy activity" in cells.

Taken together, the interaction between ECM and macrophages might regulate macrophage autophagy and result in functional consequences that may be relevant to lung fibrosis.

5.3 Hypothesis and aims

5.3.1 Hypothesis:

Extracellular matrix proteins modulate autophagy in macrophages

5.3.2 Aims:

- To demonstrate autophagy induction in mouse and human macrophages

- To determine the effect of different ECM proteins (type-I and type-IV collagens) on the autophagy pathway in macrophages

5.4 Results

In this chapter, I first established the consistent autophagy induction in RAW264.7 mouse macrophages by targeting the mTOR using the starvation medium (Fig 5-1) and rapamycin (Fig 5-2 and Fig 5-3). Results showed that successful autophagy induction with rapamycin was dose- and time-dependent. Bafilomycin A1 increased the expression of LC3-I, LC3-II, and p62 by blocking the fusion of autophagosomes and lysosomes (Fig 5-4 and Fig 5-5) which can be used to study the dynamic of the autophagy pathway.

The same effect of rapamycin and bafilomycin was observed in human monocytic cell THP-1-derived macrophages (Fig 5-6 and Fig 5-7) and human peripheral blood monocyte-derived macrophages (Fig 5-8 and Fig 5-9).

With the established model of autophagy induction, the effect of ECM, specifically type-I and type-IV collagen, was studied with RAW264.7 mouse macrophages (Fig 5-10) and human monocyte-derived macrophages (Fig 5-11 and Fig 5-12).

5.4.1 Starvation-induced autophagy in RAW264.7 macrophages

Starvation, or nutrient depletion, is a classic stimulus for the activation of autophagy in mammalian cells. Without amino acids or serum proteins, Hanks' Balanced Salt Solution (HBSS) and Earle's Balanced Salt Solution (EBSS) were used as starvation media for autophagy induction in RAW264.7 mouse macrophages.

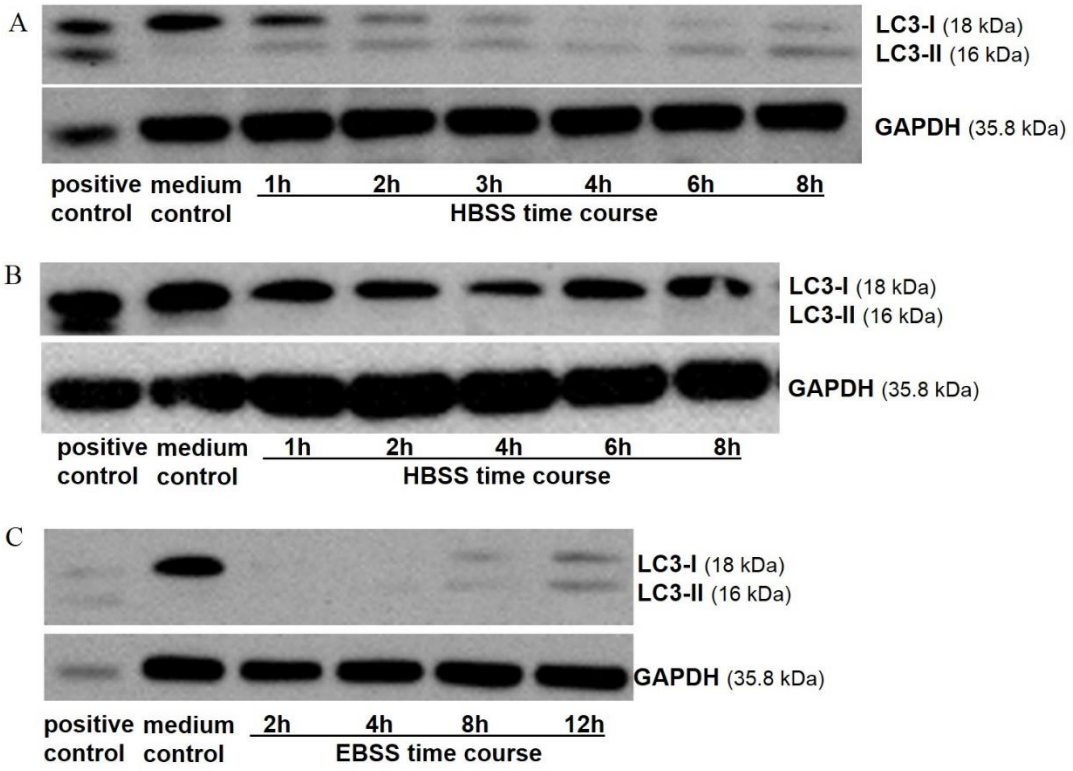

Figure 5-1 Starvation-induced autophagy in RAW264.7 mouse macrophages.

Cells (1×10^6) were seeded in a six-well plate the day before starvation treatment. The following day, cells were rinsed with pre-warmed (37°C) PBS 3 times before starvation with HBSS (A, B) or EBSS (C) for different lengths of time. Cell lysates were prepared and subjected to western blotting. Positive control: Neuro-2A cell lysate; medium control: DMEM with 10% FBS. Representative blots are shown for A (performed once) and for B and C (each performed 3 times on separate occasions).

When the culture medium was removed and replaced with HBSS or EBSS starvation medium, autophagy, as determined by the changes of LC3-I and LC3-II expression, was induced (A and C) in RAW264.7 macrophages.

HBSS starvation showed the classic pattern of LC3 expression in autophagy induction: the increase of LC3-II expression and the decrease of LC3-I expression (A). Cells left in medium control did not have any expression of LC3-II, but in the starvation medium, LC3-II expression was observed. The longer the cells were starved, the more LC3-II expression was observed on the blot.

The induction of autophagy with HBSS, however, was not consistent (B). As mentioned in the figure legend, this experiment was repeated several times (n=3), however, LC3-II expression was barely detachable. On the contrary, LC3-I was consistently expressed and easily visualised.

EBSS is another commonly used starvation medium for autophagy induction. As shown in the blot (C), LC3-I was expressed in the medium control, but no LC3-II was detected. When the cells were cultured in EBSS medium, the LC3-I level was decreased and gradually weak LC3-II expression was detected from 8 hours of incubation onwards. This again showed the changes of the LC3-I and LC3-II proteins during autophagy induction. Furthermore, autophagy induction with EBSS was more consistent and was repeated on 3 separate occasions.

To establish a consistent model of autophagy induction, rapamycin was used in experiments. LC3-II expression was not observed with low concentrations of rapamycin at different time points of treatment (additional data in Appendix-A), so higher concentration of rapamycin was used.

5.4.2 Rapamycin-induced autophagy in RAW264.7 macrophages in a concentration-dependent manner

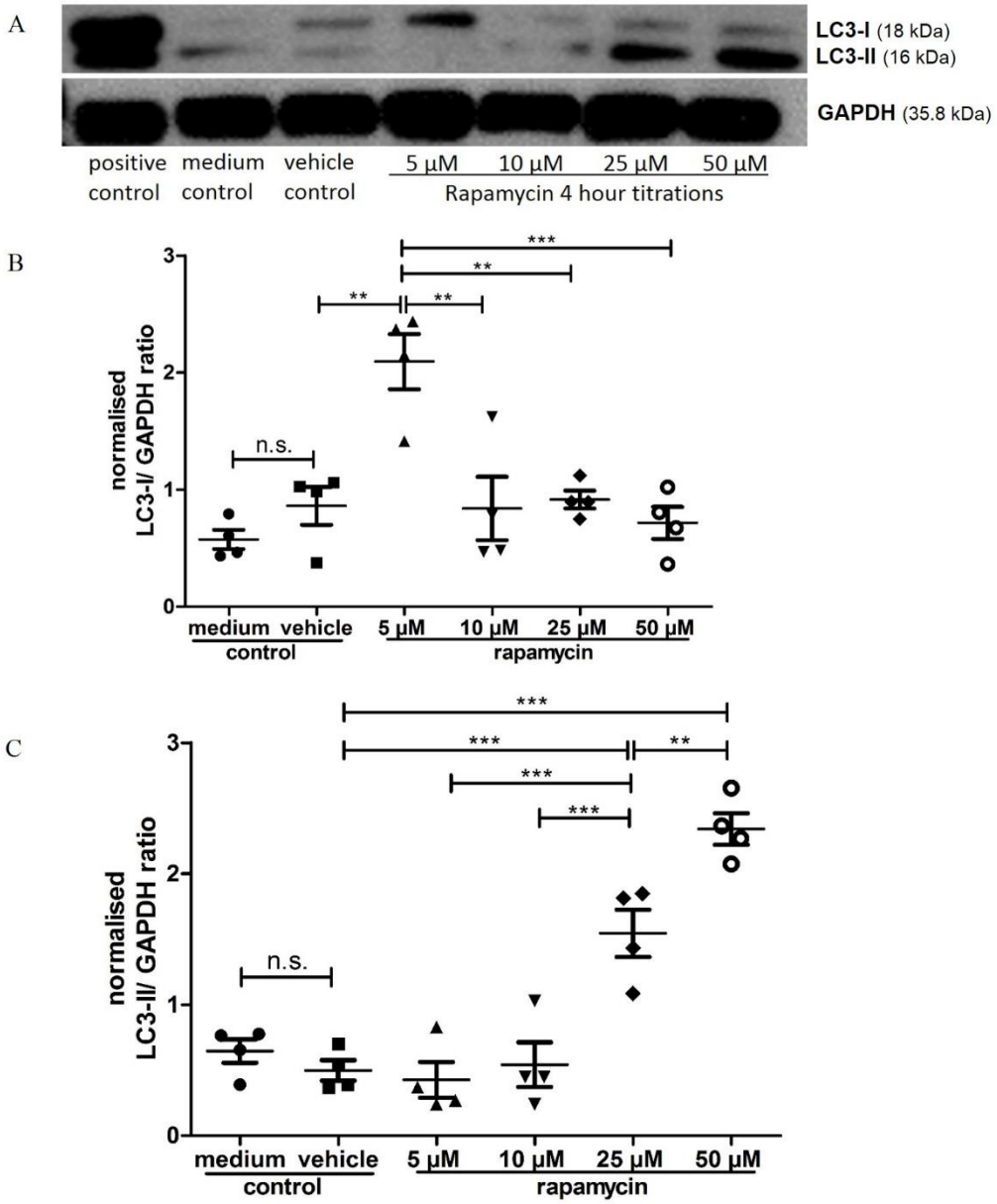

Figure 5-2 Rapamycin-induced autophagy in RAW264.7 mouse macrophages in a concentration-dependent manner.

(A) Representative blot of experiments performed 4 times on different occasions (n=4); (B-C) densitometry analysis of LC3-I and LC3-II expression. Cells were treated as indicated for 4 hours before the cell lysates were prepared for western blotting. Positive control: Neuro 2A cell lysate; vehicle control: DMSO diluted in complete DMEM medium (as 50 µM rapamycin). One-way ANOVA, Tukey's Multiple Comparison Test, ** $p<0.01$, *** $p<0.001$, n.s. not significant.

RAW264.7 macrophages were treated for 4 hours with rapamycin or control media. As shown in the blot and densitometry graphs (A & C), at lower concentrations of rapamycin there was no expression of LC3-II, but LC3-II protein was increased when treated with 25 µM and 50 µM rapamycin.

The expression of LC3-I (A & B), the free cytosolic LC3 protein, also changed. LC3-I expression was higher at lower concentrations of rapamycin (eg. 5 µM) and decreased at higher concentrations of rapamycin (25 µM and 50 µM).

The rapamycin titration experiments (4 hours of incubation), showed that rapamycin-induced autophagy in RAW264.7 macrophages was concentration-dependent.

5.4.3 Rapamycin-induced autophagy in RAW264.7 macrophages in a time-dependent manner

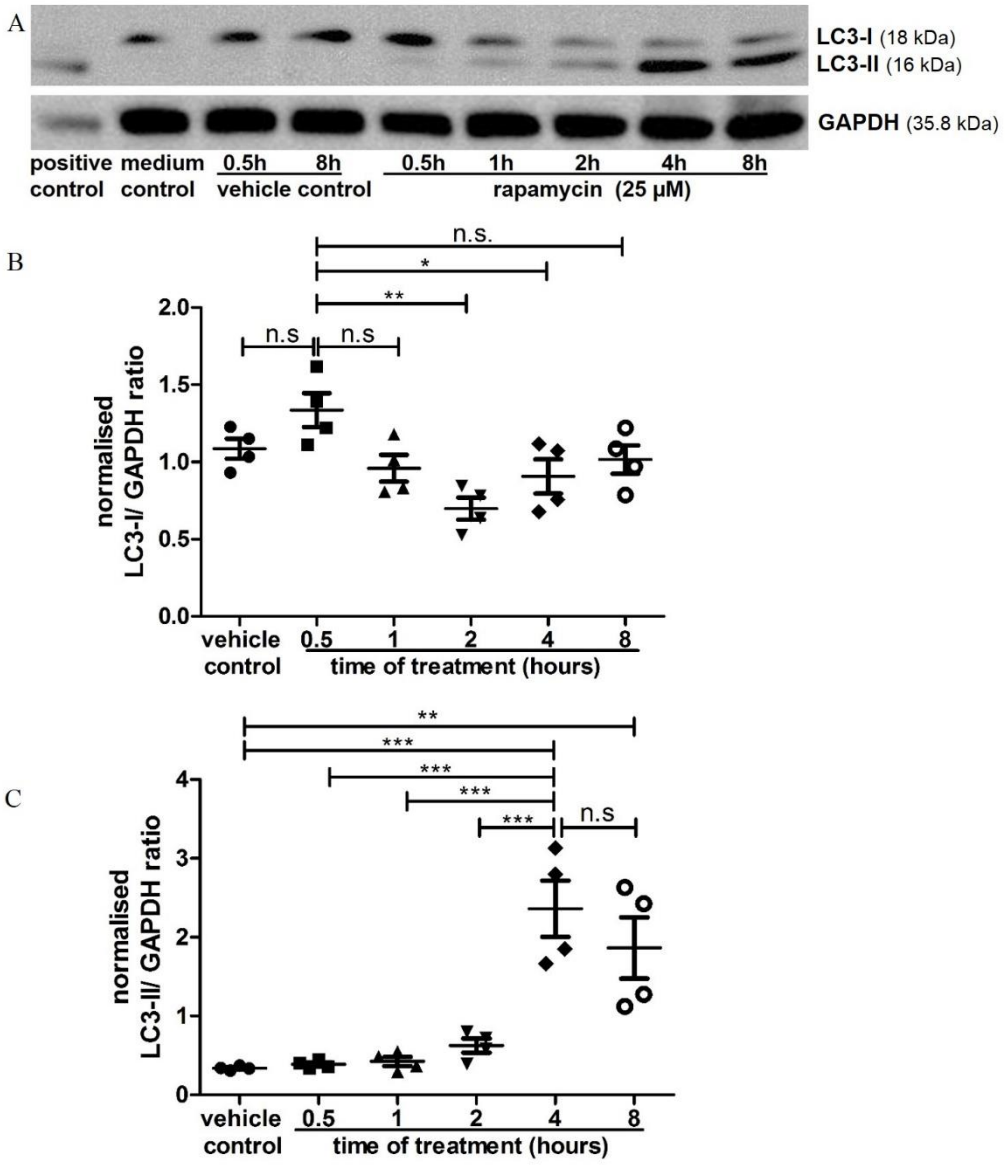

Figure 5-3 Rapamycin-induced autophagy in RAW264.7 mouse macrophages in a time-dependent manner.

(A) Representative blot of experiments performed 4 times on different occasions (n=4); (B-C) densitometry analysis of LC3-I and LC3-II expression. Cells were treated with 25 µM rapamycin at the indicated lengths of time before the cell lysates were prepared for western blotting. Positive control: Neuro 2A cell lysate; vehicle control: DMSO diluted in complete DMEM medium (as 25 µM rapamycin). One-way ANOVA, Tukey's Multiple Comparison Test, *p<0.05, ** p<0.01, *** p<0.001, n.s. not significant.

To determine the optimal time-point for 25 μM rapamycin treatment, RAW264.7 cells were treated with 25 μM rapamycin for different time period.

As shown in the representative blot (A), there was no LC3-II expression under culture media control or vehicle control, but consistent LC3-I expression was observed. With 25 μM of rapamycin, LC3-I started to convert to LC3-II. From 1-hour onwards, LC3-I expression began to decrease and LC3-II expression started to increase. By 4 hours there was significant LC3-II detected in the cells. Incubation for an additional 4 hours (8-hour treatment) did not increase the LC3-II expression.

Densitometry analysis confirmed the observation on the blots, that during autophagy induction, LC3-I decreased from early time-point (0.5-hour) to later time-point (4 hours); and LC3-II increased during the incubation with different lengths of time. Thus, rapamycin-induced autophagy in RAW264.7 macrophages was time-dependent

Collectively, with the results from the rapamycin titration experiments, the optimal autophagy induction was achieved with rapamycin at 25 μM by 4 hours in RAW264.7 cells. Thus, in the following experiment, the concentration of blocking the autophagosome degradation by bafilomycin A1 was determined at different concentrations of 4-hour incubation.

5.4.4 Bafilomycin A1 blocked LC3 and p62 degradation in RAW264.7 macrophages

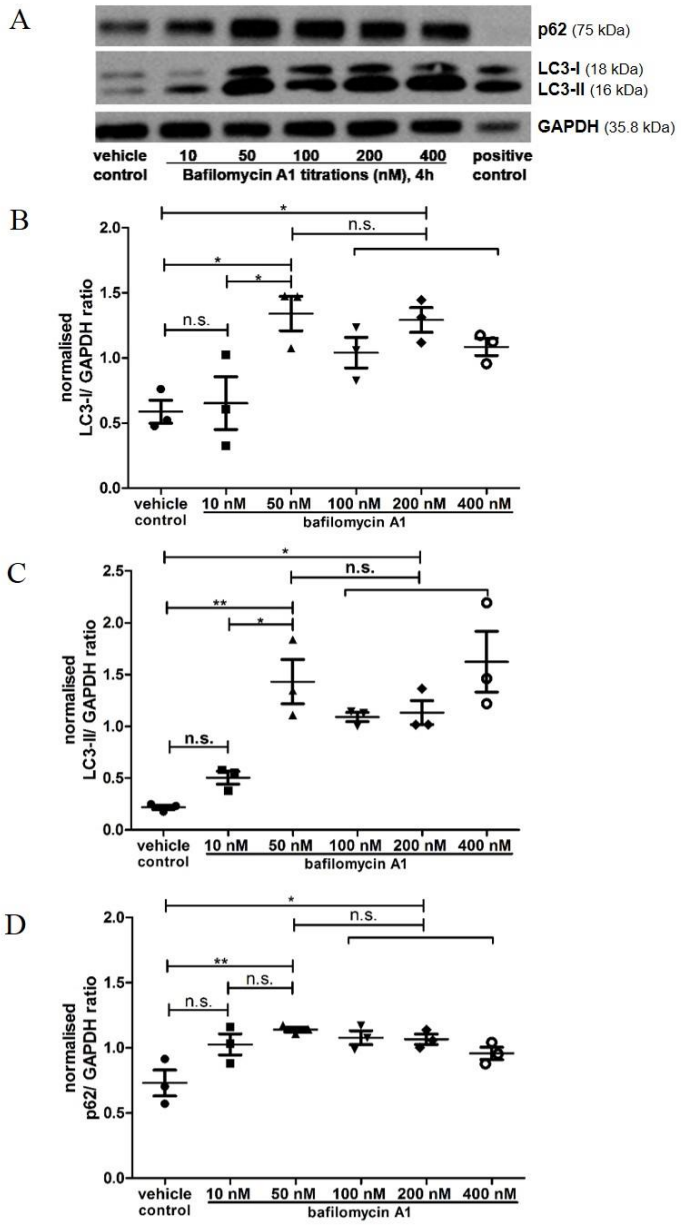

Figure 5-4 Degradation of LC3 and p62 was blocked by bafilomycin A1 at 50 nM by 4 hours.

(A) Representative blot of experiments performed 3 times on different occasions (n=3); (B-D) densitometry analysis of LC3-I, LC3-II, and p62 expression. RAW264.7 cells were treated as indicated for 4 hours. Positive control: Neuro 2A cell lysate; vehicle control: DMSO diluted in complete DMEM (as 400 nM bafilomycin.). One-way ANOVA, Tukey's Multiple Comparison Test, *p<0.05, ** p<0.01, n.s. not significant.

Bafilomycin A1 blocks the fusion of autophagosome with lysosome by inhibiting vacuolar H^+-ATPase (V-ATPase) through changing the cellular pH values. Blocking the degradation step results in the accumulation of p62 and LC3 proteins.

As shown in the rapamycin experiments, the optimal time-point for autophagy induction was 4 hours, thus it was used as the end-point for bafilomycin A1 treatments.

As shown in the blot (A), there was a very little expression of both LC3-I and LC3-II in the cells cultured in vehicle control media. Both LC3-I and LC3-II proteins began to accumulate in cells when they were treated with bafilomycin A1 at different concentrations. From 50 nM onwards, LC3-I (B) and LC3-II (C) expression were both significantly higher than the controls.

There was p62 expressed in the vehicle control as shown in the example blot (A) and treatment with bafilomycin A1 increased p62 expression. At 50 nM of bafilomycin A1, p62 expression was significantly higher than the controls (D). From 50 nM of bafilomycin A1 onwards, there was not much difference in p62 expression, which suggested that fusion of autophagosome with lysosome was completely blocked.

For the next experiment, the effect of using rapamycin and bafilomycin was further studied to establish the methodology of studying the dynamic autophagy activities, especially the formation and degradation of LC3 proteins.

5.4.5 Bafilomycin A1 increased rapamycin-induced LC3 expression in RAW264.7 cells

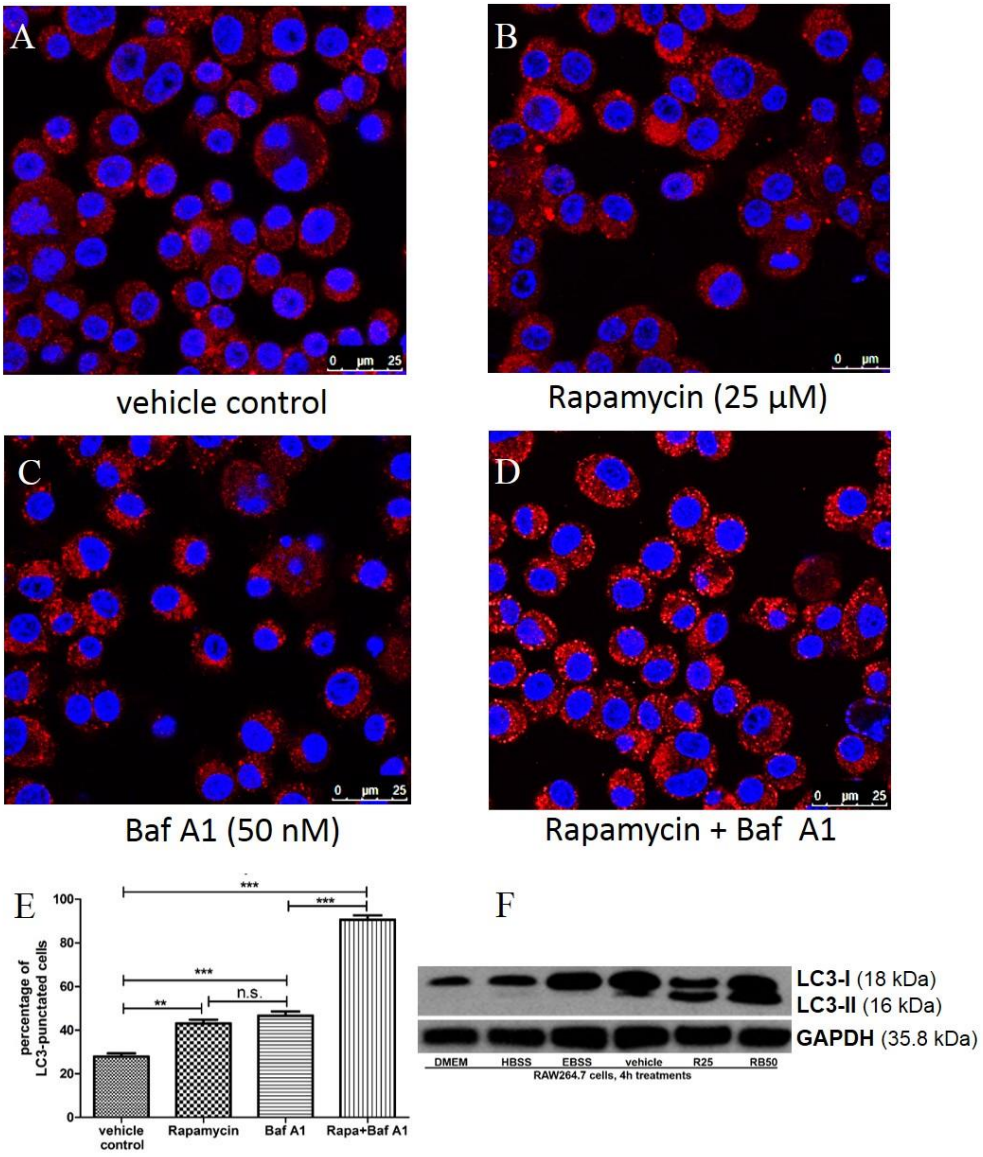

Figure 5-5 Bafilomycin A1 enhanced rapamycin-induced LC3 expression in RAW264.7 macrophages.

RAW264.7 cells were treated as indicated for 4 hours before they were fixed and stained for LC3.Cells were processed as described in section 2.3.5 in the Materials and Methods chapter. Representative images of experiments performed 3 times on different occasions (n=3). (A) vehicle control, DMSO diluted in completed DMEM (as rapamycin + Bafilomycin.A1); (B) rapamycin, 25 µM; (C) Bafilomycin A1 (Baf. A1), 50 nM; (D) double treatment with 25 µM rapamycin and 50 nM Bafilomycin A1; (E) percentage of LC3 punctated cells. punctated cells in each of the frame was counted, the average percentage of three frames were used for statistical analysis; (F) western blotting comparing different treatments for autophagy induction. ** $p<0.01$; *** $p<0.001$, n.s. not significant, one-way ANOVA, Tukey's Multiple Comparison Test.

Adding bafilomycin A1 to rapamycin, in theory, should block the degradation of the increased LC3-II expression by rapamycin.

To test this hypothesis, RAW264.7 macrophages were treated with individual compound alone or in combination (A-D). Results showed (E) that the percentage of LC3-puncta positive cells was significantly increased in the double treatment compared with vehicle control, rapamycin alone and bafilomycin A1 alone (90.60% ± 2.04% vs 27.90% ± 1.50% vs 43.10% ± 1.74% vs 46.63 ± 1.96%).

Western blot results (F) confirmed the confocal data. As shown in the blot, there was almost no LC3-II expressed in the medium control or vehicle control. LC3-II expression was not increased when cells were cultured in HBSS or EBSS media. Increased LC3-II and decreased LC3-I was observed when RAW264.7 cells were treated with rapamycin. Both LC3-I and LC3-II expression was further increased when bafilomycin A1 was added into the culture medium containing rapamycin.

With the results of successfully modulating and measuring the autophagy pathway in mouse RAW264.7 macrophages, the autophagy pathway with human monocyte-derived macrophages (THP-1 monocytic cell-line and primary peripheral blood monocyte from healthy donors) were further investigated.

5.4.6 Rapamycin induced autophagy in THP-1 macrophages

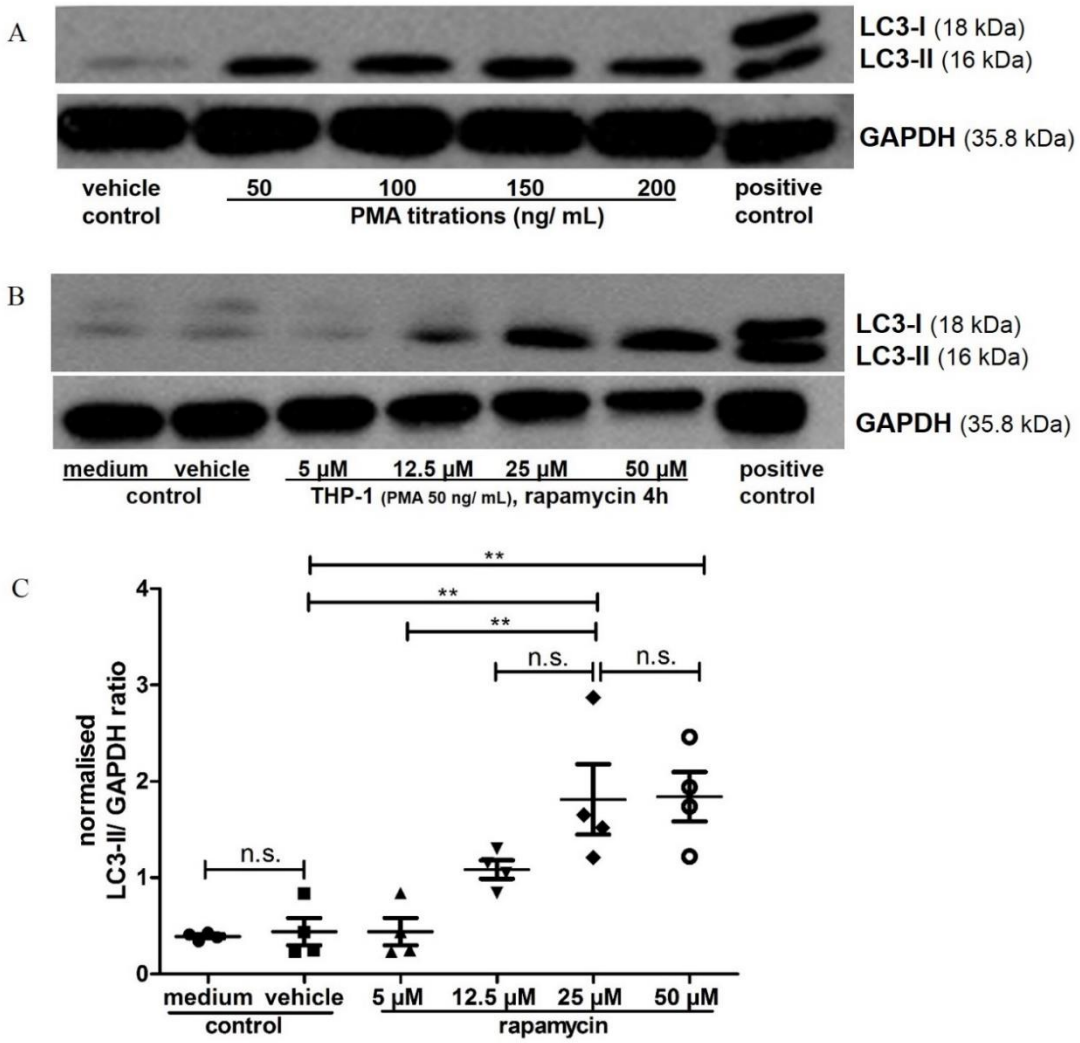

Figure 5-6 Rapamycin induced autophagy in THP-1 macrophages.

THP-1 monocyte-derived macrophages were treated as indicated and the cell lysates were prepared for western blotting. (A) PMA differentiation increased LC3-II expression. (B) rapamycin-induced autophagy by 4 hours of incubation. (C) densitometry analysis of LC3-II expression. THP-1 cells were incubated with 50 ng/ mL PMA for three days before rapamycin treatment. Medium control: RPMI1640+10%FBS; vehicle control: DMSO diluted in complete RPMI medium (as 50 μM rapamycin). Positive control: Neuro 2A cell lysate. **p<0.01, n.s. not significant, one-way ANOVA, Tukey's Multiple Comparison Test. Representative blots are shown for (A) performed 3 times (n=3) and (B) performed 4 times (n=4) on different occasions.

THP-1 human monocytic cells were differentiated to macrophages with PMA for 3 days. When THP-1 cells were treated with PMA, they became adherent and began to differentiate to mature macrophages. In the study, it is found that THP-1 cells only became adherent when treated with PMA at 50 ng/ mL or higher concentrations.

Western blot (A) showed that the increased LC3-II expression was observed in all THP-1 macrophages differentiated with PMA at different concentrations. LC3-II was barely detected in THP-1 cells that were cultured in vehicle control medium. It suggested that the successful differentiation of THP-1 macrophages by PMA inevitably upregulated the LC3-II expression.

THP-1 macrophages, with up-regulated LC3-II expression, were treated with rapamycin at different concentrations for 4 hours (B & C). THP-1 macrophages responded to rapamycin in a concentration-dependent manner. LC3-II was barely detected in the controls but increased when they were treated with rapamycin at different concentrations. Densitometry analysis showed that at 25 μM and 50 μM, the LC3-II expression induced by rapamycin was significantly higher than the expression in vehicle control.

Of note, LC3-I was barely detected in THP-1 macrophages in all the experiments (A & B). Referring to the consistent expression of LC3-I in RAW264.7 mouse macrophages, results suggest that LC3-I may be at very low levels in this human macrophage.

5.4.7 Blockage of autophagosome degradation increased p62 and LC3-II expression in THP-1 macrophages

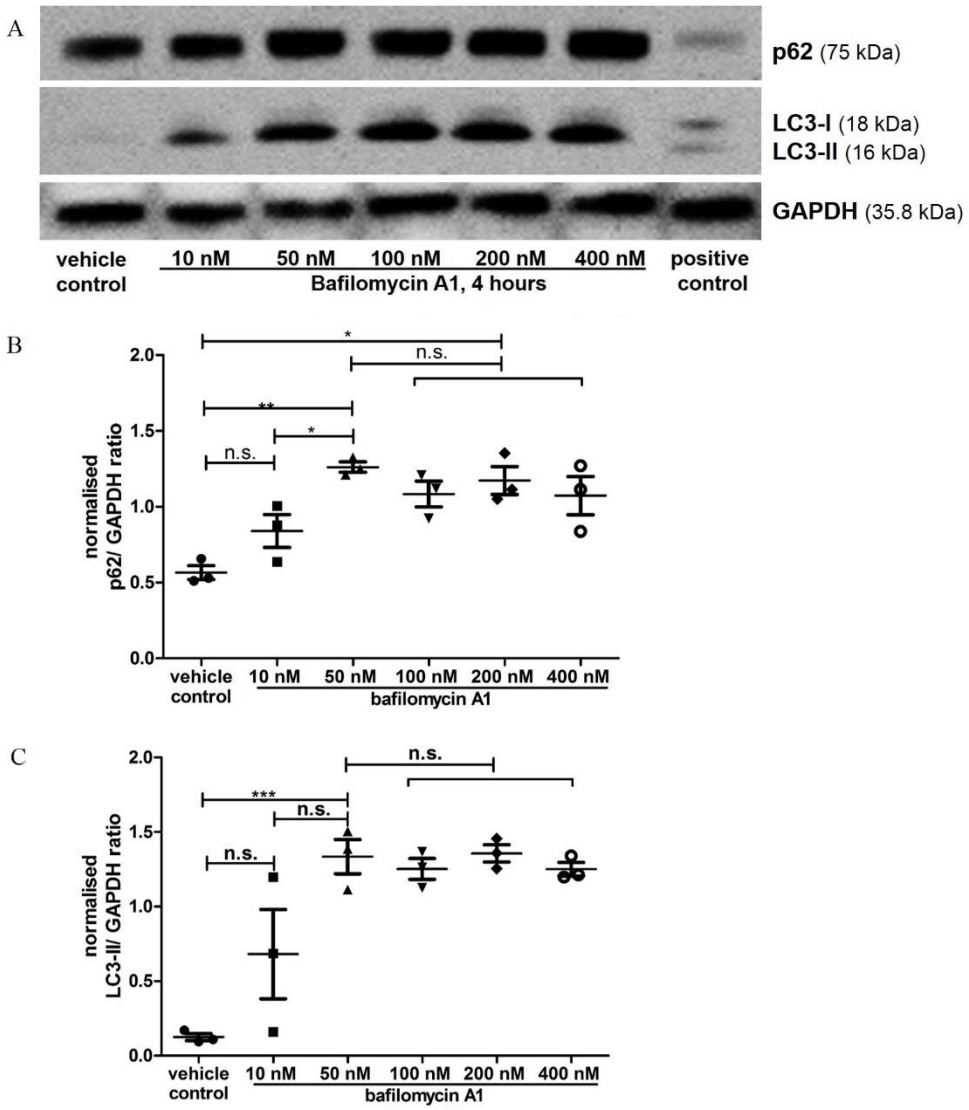

Figure 5-7 Blockage of autophagosome degradation showed increased LC3-II but no LC3-I expression in THP-1 macrophages.

THP-1 macrophages were treated with bafilomycin A1 at indicated concentrations for 4 hours and the cell lysates were prepared for western blotting. (A) Representative blot of experiments performed 3 times on different occasions (n=3); (B-C) densitometry analysis for p62 and LC3-II expression. Vehicle control: DMSO diluted in culture medium (as 400 nM bafilomycin A1); Positive control: Neuro 2A cell lysates. THP-1 cells were differentiated with 50 ng/mL PMA for 3 days before use. *p<0.05, **p<0.01, ***p<0.001, n.s. not significant, one-way ANOVA, Tukey's Multiple Comparison Test.

THP-1 macrophages were treated with bafilomycin A1 at different concentrations for 4 hours to study the changes in the expression of LC3 proteins. The expression of p62 was probed as an indicator for the successful blockage of autophagosome degradation.

The expression of p62 was increased when THP-1 macrophages were cultured in bafilomycin A1 for 4 hours (A & B). Densitometry analysis showed that the autophagosome degradation was blocked by bafilomycin A1 at 50 nM and higher concentrations (B).

After bafilomycin A1 treatment, the LC3-II expression was also increased (A & C). At 50 nM of bafilomycin, LC3-II expression was significantly higher than the vehicle control (C). Higher concentrations of bafilomycin did not further increase the expression of LC3-II (C).

LC3-I expression, however, was barely detected when autophagosome degradation was successfully blocked (A). This confirmed that LC3-I was not highly expressed in human THP-1 macrophages, otherwise by blocking its degradation the existing LC3-I would have been detected.

Leaving aside LC3-I, both rapamycin and bafilomycin A1 had successfully modulated the autophagy pathway in this human THP-1 macrophages.

5.4.8 Rapamycin-induced autophagy in MDM in a concentration-dependent manner

As shown in RAW264.7 macrophages and THP-1 macrophages, rapamycin induced autophagy in a concentration- and time-dependent manner. Thus the same strategy was extended to human MDM.

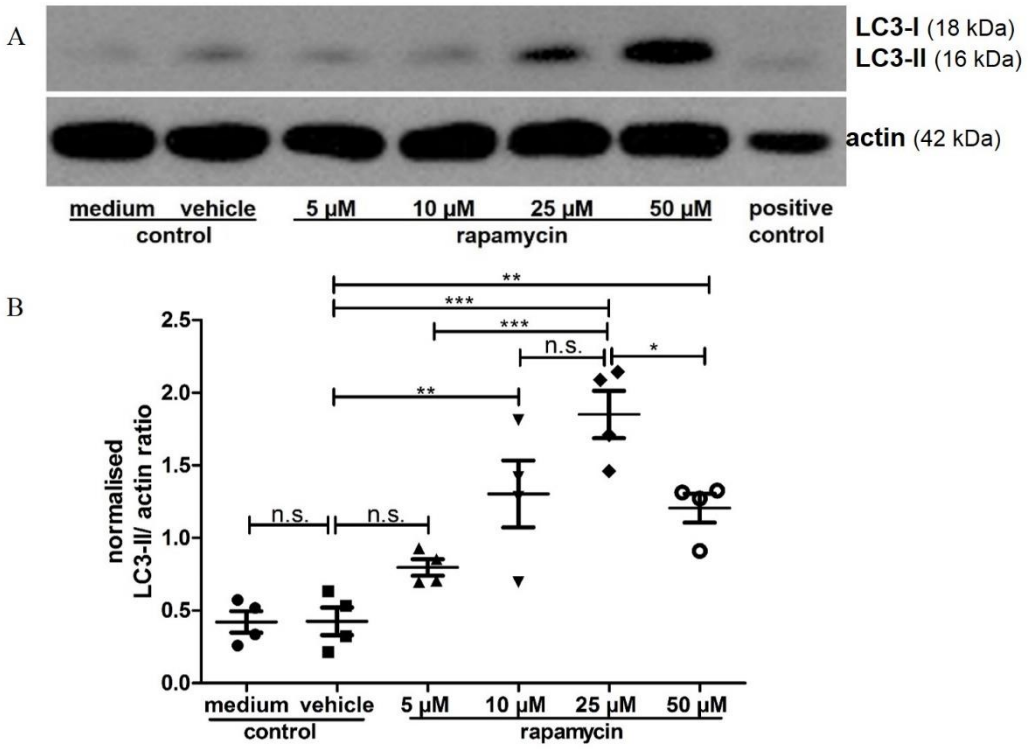

Figure 5-8 Rapamycin-increased autophagy in MDM.

MDM were treated with rapamycin at the indicated concentrations for 4 hours and cell lysates were prepared for western blotting. (A) Representative blot of experiments performed 4 times on different occasions (n=4); (B) densitometry analysis of LC3-II expression. Medium control: IMDM + 10% FBS; vehicle control: DMSO diluted in culture medium (as 50 μM rapamycin); positive control: Neuro 2A cell lysate. *p<0.05, **p<0.01, ***p<0.001, n.s. not significant, one-way ANOVA, Tukey's Multiple Comparison Test.

Monocytes were isolated from peripheral blood and differentiated to mature macrophage on standard tissue culture (TC) plates for 7 days before the rapamycin treatment.

As shown in the blot (A), there was little LC3-II expressed in MDM when cells were cultured in the control medium or the vehicle control. LC3-II expression was increased in MDM when they were cultured in rapamycin at 25 μM, and the expression was further increased at 50 μM.

Densitometry analysis (B) of the blots suggested that the optimal concentration for autophagy induction in MDM was 25 μM with 4-hour of incubation.

Of note, again LC3-I was not detected in the human peripheral blood MDM, which was observed in the human THP-1 macrophages.

5.4.9 Blockage of autophagosome degradation increased p62 and LC3-II expression in MDM

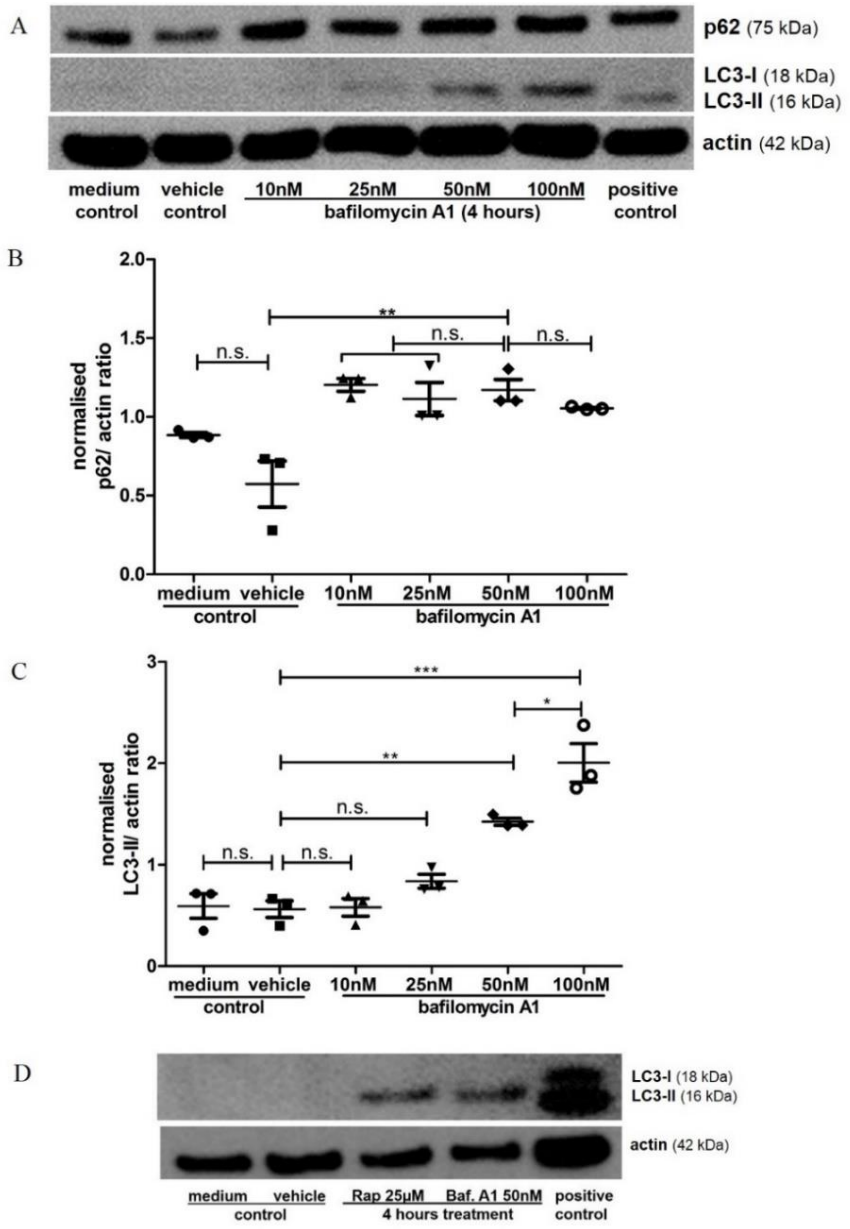

Figure 5-9 Blockage of autophagosome degradation increased p62 and LC3-II expression in MDM.

MDM were treated as indicated for 4 hours before the cell lysates were prepared for western blotting. (A) Bafilomycin A1 blocked the degradation of autophagosomes in MDM; (B & C) densitometry analysis of p62 and LC3-II; (D) LC3-I was not expressed in human peripheral blood. Medium control: IMDM+10%FBS; vehicle control: DMSO diluted in culture medium (as 100 nM Baf.- A1). Positive control: bafilomycin A1 treated RAW264.7 cells (50 nM, 4 hours). *p<0.05, **p<0.01, ***p<0.001, n.s. not significant, one-way ANOVA, Tukey's Multiple Comparison Test. Representative blots were shown for A and D, both were performed 3 times on different occasions (n=3).

The expression of p62 was probed as another indicator of autophagy following bafilomycin A1 treatment. Increased expression of p62 was observed in MDM from 10 nM of bafilomycin onwards (A & B). The expression of p62 remained constant (A) and the densitometry analysis did not show any statistical significance (B).

LC3-II expression, however, was not detected at 10 nM of bafilomycin (A). LC3-II expression began to increase from 25 nM and was significantly increased at 50 nM and 100 nM of bafilomycin (A & C).

Collectively, the expression of p62 and LC3-II data suggested that the accumulation of p62 happened earlier than the accumulation of LC3-II. The optimal concentration for bafilomycin A1 treatment in MDM was 50 nM.

The expression of LC3-I was not detected in MDM by blocking the degradation of autophagosomes (A).

To address whether the differentiation process from monocyte to macrophages had changed the LC3 protein profile, human peripheral blood monocytes were isolated and treated with rapamycin or bafilomycin A1.

As shown in the example blot (D), LC3 proteins were not detected in monocytes that were cultured in the control media and the vehicle control. LC3-II expression was detected in cells that were treated with rapamycin (25 μM) and bafilomycin A1 (50 nM). LC3-I protein, however, was not detected. Thus, similar to the data with THP-1 cells, LC3-II protein may be the major LC3 protein presented in human monocytes/ macrophages with the absence of LC3-I protein.

As a consistent model of studying the autophagy in macrophages was established with rapamycin and bafilomycin A1, the effect of ECM, particularly type-I and type-IV collagen, was investigated in the following experiments with RAW264.7 mouse macrophages and MDM from the easy-detach method. As the differentiation to macrophages had increased LC3-II expression, the baseline autophagy level was measured in MDM-ED.

5.4.10 Type-I and type-IV collagens increased basal autophagy (autophagosome formation) in RAW264.7 macrophages

RAW264.7 macrophages were treated with 50 nM bafilomycin A1 in the presence of type-I and type-IV collagen to study the effect of ECM on basal autophagy.

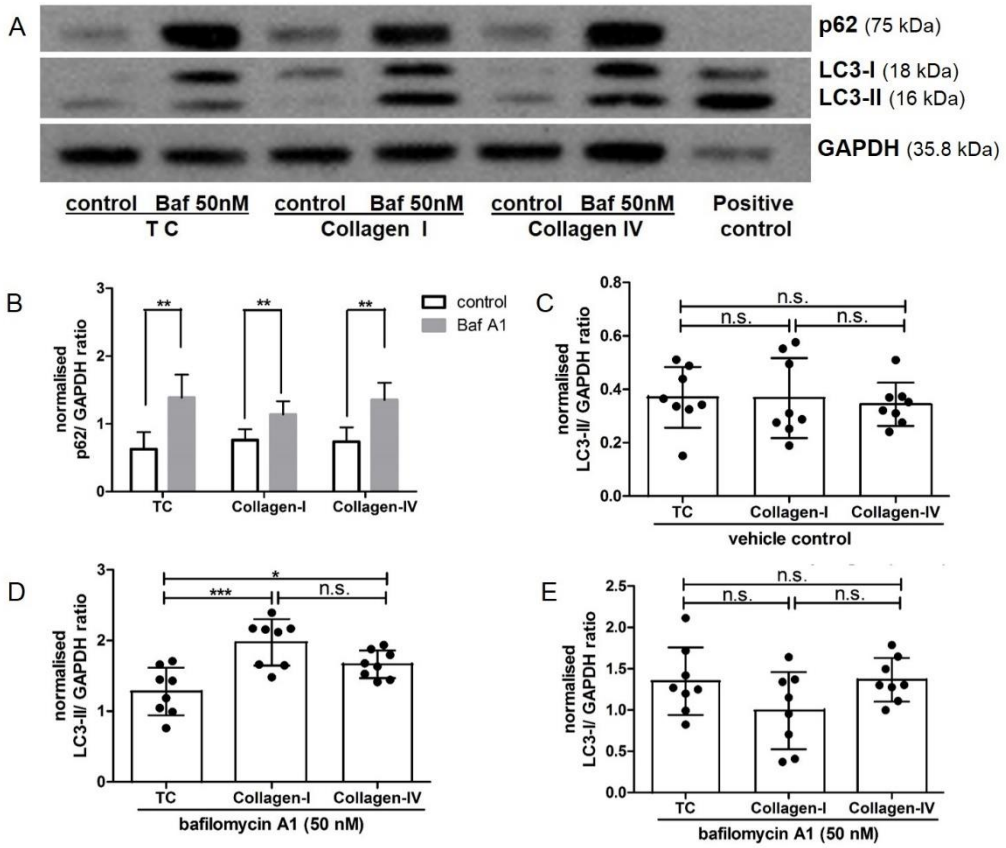

Figure 5-10 Type-I and type-IV collagens increased basal autophagy in RAW264.7 cells.

RAW264.7 macrophages were seeded on TC dishes or dishes pre-coated with type-I or type-IV collagen before the cells were treated as indicated (with 50 nM bafilomycin A1 or vehicle control) for 4 hours. The cell lysates were prepared and subjected to western blotting. (A) Representative blot of 8 experiments performed on different occasions (n=8); (B-E) densitometry analysis of p62 (B), LC3-II in cells under vehicle control condition (C), LC3-I in cells under Baf.- A1 condition (D), and LC3-II in cells under Baf.- A1 condition (E). Control: DMSO diluted in culture medium (as 50 nM Baf.- A1); Baf 50 nM: Bafilomycin A1, 50 nM for 4 hours. Positive control: Neuro 2A cell lysate. *p<0.05, **p<0.01, ***p<0.001, n.s. not significant, paired student t-test (B) and one-way ANOVA, Tukey's Multiple Comparison Test (C, D & E).

As shown in the representative blot and densitometry analysis (A & B), RAW264.7 macrophages had increased p62 expression on all culture dishes after bafilomycin A1 treatment. The increased p62 expression confirmed that the autophagosome degradation was blocked. Thus, the basal autophagy can be studied with LC3-II expression.

LC3-II was barely expressed in RAW264.7 macrophages that were cultured with the vehicle control (A). Densitometry analysis showed there was no difference in LC3-II expression on the three types of culture dishes in vehicle control media (C). This showed that neither the vehicle control medium nor the contact with collagen had induced autophagy in RAW264.7 cells.

Compared to the low LC3-II expression in the control media, LC3-II expression was increased in RAW264.7 cells when they were treated with bafilomycin A1 (A). Densitometry analysis (D) showed that LC3-II expression was increased in cells when they were in contact with both type-I and type-IV collagens compared to cells on TC dishes (1.98 ± 0.12 vs 1.66 ± 0.07 vs 1.28 ± 0.12). In addition, there was no difference in LC3-II expression between cells that were cultured on type-I and type-IV collagens (D). These data suggested that the basal autophagy was increased in RAW264.7 cells in the presence of type-I and type-IV collagens.

LC3-II was synthesized from LC3-I, thus the level of LC3-I might have been decreased if LC3-II was increased. However, the densitometry analysis showed that the LC3-I expression was not statistically different among the conditions (E).

5.4.11 Differentiation to MDM by the easy-detach method up-regulated autophagy

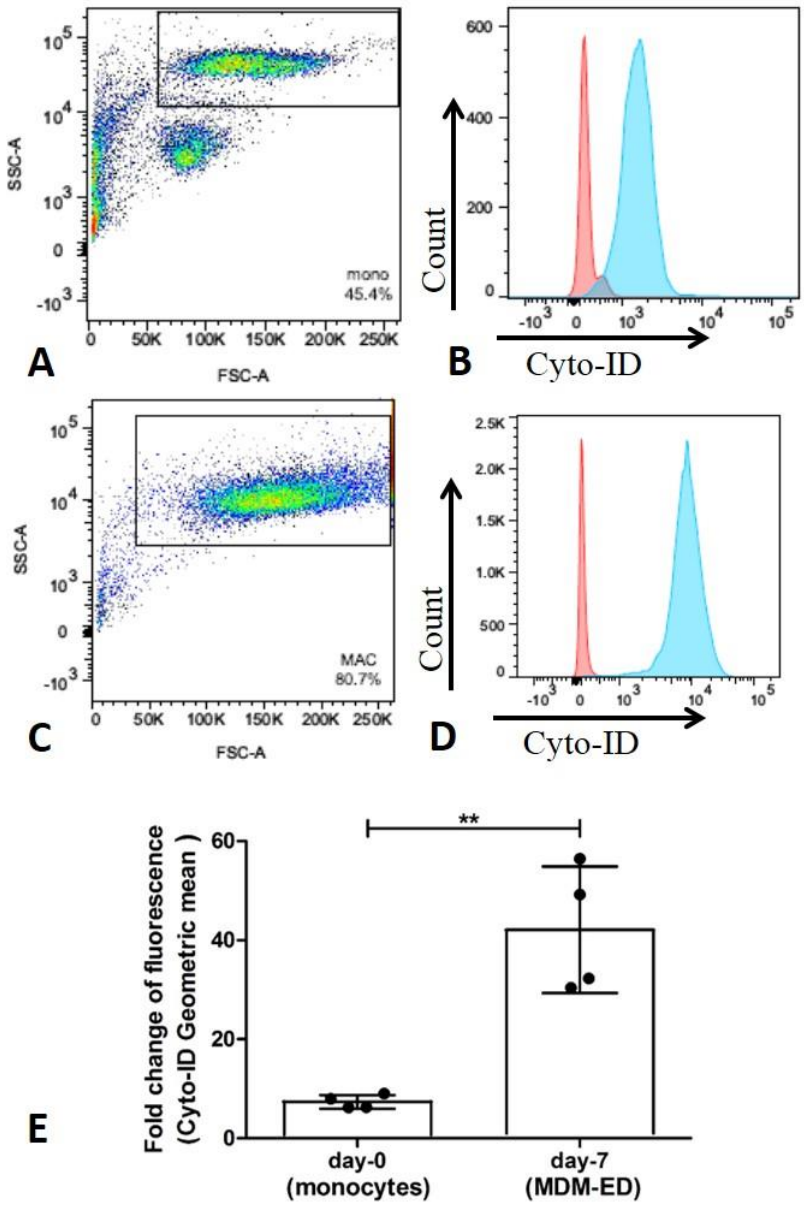

Figure 5-11 Differentiation to MDM by the easy detach method (MDM-ED) up-regulated autophagy.

(A & B) Cyto-ID staining of monocytes before culture to macrophages (day-0); (C & D) cyto-ID staining of MDM-ED on day-7; (E) analysis of fold changes of Cyto-ID mean fluorescence (n=4). **p<0.01, student t-test.

To examine the baseline level of autophagy after the differentiation process, macrophages from the easy-detach method were stained with Cyto-ID and compared with freshly purified monocytes from the peripheral blood mononuclear cells (PBMC).

Monocytes were gated from the PBMC population (A) and compared with the unstained cells. Flow cytometry analysis (B) showed an increased Cyto-ID expression in monocytes.

MDM-ED showed a uniformed population (C) and when compared the Cyto-ID expression with the unstained cells, the histogram shifted further to the right (D).

When comparing the fold changes of Cyto-ID expression to the unstained (E), MDM-ED had up-regulated autophagy and increased fold change of Cyto-ID fluoresce than the freshly isolated monocytes (42.08 ± 6.39 vs 7.37 ± 0.69, $n=4$, $p<0.01$, unpaired student t-test). The Cyto-ID expression in MDM-ED was almost 6 times higher after the differentiation.

5.4.12 Collagen modulated both autophagosome degradation and formation in MDM-ED

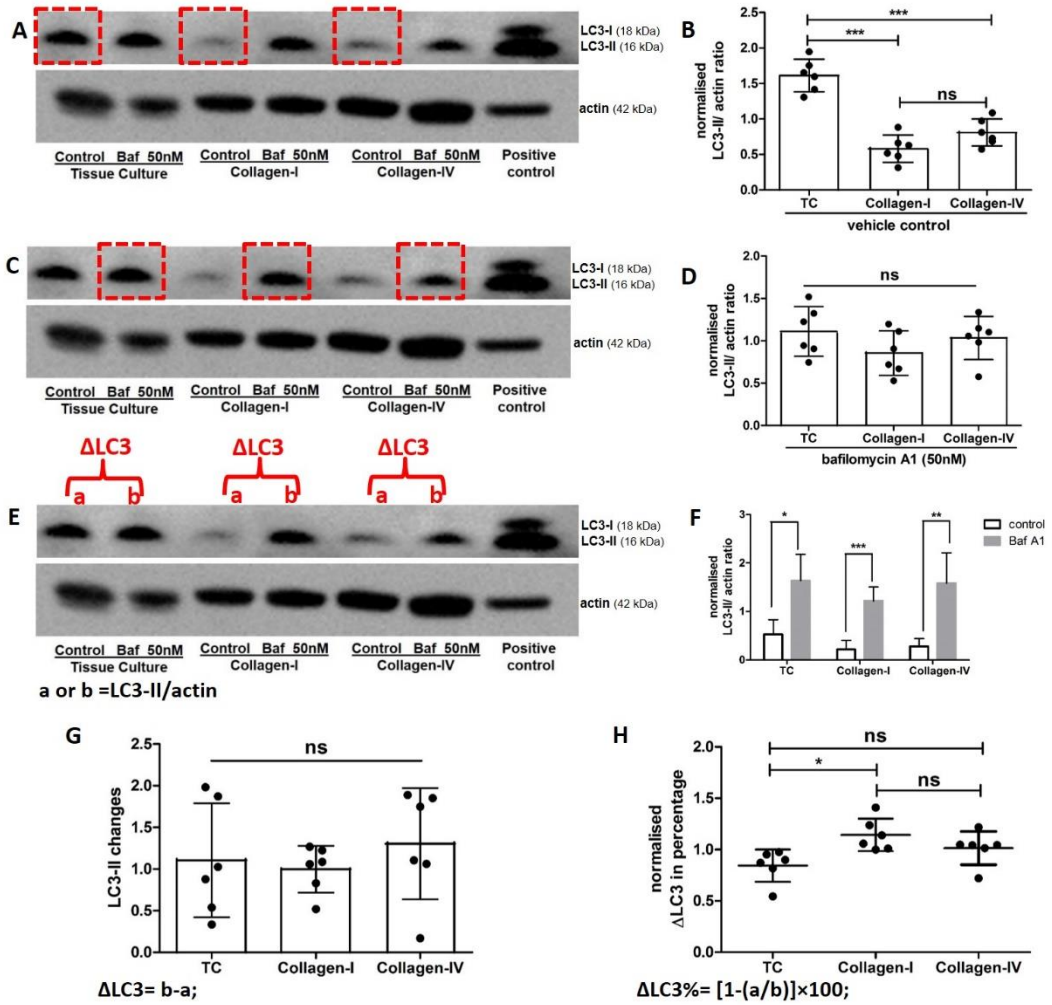

Figure 5-12 Collagen modulated autophagy in MDM-ED.

(A & B) analysis of LC3-II expression cultured in the control media; (C & D) analysis of LC3-II expression cultured in 50 nM bafilomycin A1 for 4 hours; (E) calculations for the change of LC3-II expression (ΔLC3); (F) Experiment control:bafilomycin A1 increased LC3-II expression compared with vehicle control; (G & H) ΔLC3 presented as values of subtraction (G) or percentage (H). MDM-ED were seeded on different culture dishes and cultured for 20 hours before Baf.- A1 or vehicle control treatments as indicated. Cell lysates were prepared and proteins were extracted after the treatments and the expression of LC3 was analysised by western blotting. Control: DMSO in culture medium (as Baf.- A1); Baf 50 nM: bafilomycin A1, 50 nM. Positive control, human neuro-2A cell lysate. *p<0.05, **p<0.01, ***p<0.001, n.s. not significant, paired student t-test (F) and one-way ANOVA, Tukey's Multiple Comparison Test (B, D, G & H). Representative blot of 6 experiments performed on different occasions (n=6).

MDM from the easy-detach method (MDM-ED) were seeded on the culture dishes (TC, collagen type-I and type-IV) the day before and cells were cultured for 20 hours before the experimental treatments.

As shown on the blot and densitometry (A), the expression of LC3-II was different in MDM-ED on the three surfaces when they were cultured in the control media. The upregulated autophagy in MDM-ED (Figure 5.11) was decreased in the presence of type-I and type-IV collagen compared with cells from TC dishes (1.61 ± 0.09 vs 0.58 ± 0.08 vs 0.81 ± 0.08, $n=8$, $p<0.001$). Thus, both type-I and type-IV collagens assisted in the decrease of up-regulated autophagy, by enhancing autophagosomes degradation.

When compared with the LC3-II expression in MDM-ED that were treated with bafilomycin A1 (C & D), no difference was observed on the 3 surfaces. After the down-regulation of autophagy on collagen dishes (A & B), there were active autophagic activities in MDM-ED and blockage of LC3 degradation revealed the underlying active LC3-II formation (C & D).

Since the initial LC3-II expression was higher in cells on the TC dishes (A & B), the change of LC3-II (ΔLC3) was calculated to demonstrate the accumulation of LC3-II after bafilomycin treatment (E, G &H) during the 4 hours.

Bafilomycin treatment had increased the LC3-II expression in MDM-ED on all the three dishes (F), which enabled the calculations of ΔLC3.

When ΔLC3 was presented as a value of subtraction, the analysis showed no difference on the 3 surfaces (G). When ΔLC3 was presented as a percentage (F), it made the values more comparable to each other. Results (F) showed that ΔLC3% was significantly higher when MDM-ED were in contact with collagen-I than in the TC control ($p<0.05$). There was no difference in ΔLC3% between cells cultured on type-I and type-IV collagens or between cells cultured on type-IV and the TC control (1.14 ± 0.06 vs 1.01 ± 0.07 vs 0.84 ± 0.06, $n=6$).

The ΔLC3% results suggested that 1) contact with collagen-I had increased the basal autophagy; 2) the existing up-regulated autophagy in MDM-ED on TC control (B) may have affected the formation of LC3-II in basal autophagy.

5.5 Summary and Discussion

The interaction between ECM and the surrounding cells has been investigated intensely over recent years. Collagen-I is the most common type of fibrotic ECM found in late-stage IPF [204] and it may influence macrophage autophagy and lead to important consequences. This study has demonstrated that ECM, particular type-I collagen, participates in both the formation and degradation steps of autophagy in macrophages.

5.5.1 Macrophages may be refractory to autophagy induction through mTOR

Normally, autophagy is rapidly induced by starvation or low concentration of rapamycin in different types of cells**.** However, this study shows starvation induced very weak LC3-II expression in RAW264.7 macrophages. LC3-II expression only became consistent and robust when macrophages were treated with relatively high concentrations of rapamycin.

Starvation and rapamycin activate the autophagy pathway by inhibiting the mTOR [256]. In my experiments, both rapamycin- and starvation-induced LC3-II formation in macrophages, but this required relatively high concentrations of rapamycin (25 μM or higher). Lower concentrations of rapamycin (250 nM to 5 μM) was also used to induce autophagy in macrophages for 24 hours (additional results in Appendix-A), but the results were not reproducible and the LC3 expression was similar to that induced by starvation (Fig 5.1). In fact, in many other types of cells, LC3-II is successfully induced with 100 nM to 400 nM of rapamycin or by starvation for a period of 24 hours [485-487]. It is known that low concentrations of rapamycin (0.5–100 nM) act through mTOR complex-1 (mTOR1) and high concentrations of rapamycin (0.2 μM and above) targets at mTORC2 [488]. In fact, the inhibition of both mTORC1 and mTORC2 activates autophagy. mTORC1 is associated with autophagy which is induced by starvation, reduced growth factors and stress, whereas mTORC2 is responsible for the autophagy that is achieved by affecting autophagy gene expression mainly via a downstream transcription factor of Akt, i.e., FoxO3 [256]. High concentrations of rapamycin (10 μM and above, including 25 μM) has been used as positive controls of inhibiting mTOR, however, higher concentrations may also activate other mechanisms

that are independent of autophagy induction and need to be further understood [489]. Nevertheless, these data imply that macrophages may be relatively refractory to mTOR-targeted autophagy or it may be related to the mTOR complexes and their functions within macrophages.

In contrast, and consistent with other studies, LC3-II was found rapidly accumulated in macrophages when they were treated with bafilomycin A1 within a short period of time (4 hours) and at low concentrations [483, 490]. The rapid accumulation of LC3-II proteins implies that the formation of LC3 is active within the macrophages. Thus, the response of macrophages to starvation and rapamycin might appear to be refractory, but in fact, the autophagy machinery within macrophages is very active as demonstrated by blocking the downstream autophagy pathway by bafilomycin A1.

A further observation that normal macrophages have enhanced autophagy machinery is that macrophages are abundant in lysosomes [491]. Autophagosomes, once formed, are directed to lysosomes and are then rapidly degraded. Lysosomes have been described as the “Achilles' heel” in the autophagy-lysosome pathway because disruption at this stage leads to a complete break-down in the autophagy machinery [492]. An abundant lysosomal stock suggests that macrophages have high capacities to support the very active formation and degradation of LC3-II proteins.

5.5.2 Autophagy and macrophage differentiation

In human THP-1 macrophages, consistent LC3-II expression was observed after the treatment with PMA. Adjusting PMA concentrations did not modify the increased LC3-II expression. Other studies also have shown that the LC3-II expression was increased with PMA treatment, although Behura suggested that with 50 ng/ mL of PMA only limited LC3-II expression was detected [493, 494]. In neutrophils, the activation of autophagy is required for their production of neutrophil extracellular traps (NETs) which can be triggered by PMA through the PKC pathway [495, 496]. However, a study with HEK-263 cells showed that the inhibition of PKC increased LC3-II expression, but activation by PMA attenuated the conversion of LC-I to LC-II [497]. However, the mechanism of PMA induced autophagy needs to be further studied.

The exact mechanism for macrophage differentiation is not yet elucidated, but accumulating evidence suggested that autophagy may be involved. Many monocyte maturation strategies have increased autophagy in cells, such as vitamin D3 [498], GM-CSF [499], PMA (Fig 5.6) [493, 494] and on the low-attachment surface (Fig 5.11). The activation of autophagy during macrophage differentiation is inevitable in these strategies but the mechanisms might be different. Though autophagy is observed in these conditions, it needs to be clarified whether autophagy is involved in the differentiation or the differentiation activates autophagy.

5.5.3 LC3 proteins in human monocyte/ macrophages

In this study, I found consistent LC3-I expression in RAW264.7 mouse macrophages, but not in human monocyte/ macrophages where LC3-I was not detected. In previous studies, LC3-I is found weakly expressed or absent in THP-1 cells [494] and human macrophages [478]. However, LC3-I was consistently present in THP-1 cells in the data presented by Behura [493]. The expression of LC3 proteins and their roles in monocyte/ macrophages needs to be better understood.

In this study, different antibodies against human LC3 proteins were tested and LC3-I was not detected in human monocyte/ macrophages. In fact, the LC3 antibody worked very well with human Neuro-2A cell lysate, which was supplied from the supplier as the positive control, and both LC3-I and LC3-II proteins were consistently detected. Furthermore, lysate from rapamycin-treated HeLa cells, a human epithelial cell line, was also used to test the antibodies and both LC3-I and LC3-II were detected (data not shown). Increasing the exposure time for the luminescence detection step in western blotting did not reveal any expression of LC3-I (data not shown).

There were very few occasions in these experiments when LC3-I was observed those were when MDM were left in “extreme” conditions such as treated with Bafilomycin A1 for 24 hours (data not shown). These “extreme” conditions may lead to cell death and in fact, dysregulation of autophagy is implicated in cell death [500]. These data suggested that in “normal homeostatic” conditions, LC3-I is rapidly conjugated to form LC3-II in macrophages. However, in “extreme” conditions more LC3-I proteins can be synthesized to enhance the autophagy pathway. The failure of the completion of

autophagy may lead to cell death [500]. Thus, in human macrophages, LC3-II is the "pro-survival" signal and LC3-I might be more relevant to the "pro-cell death" signal but need to be further studied.

LC3-I converting to LC3-II requires other Atg proteins such as Atg4, Atg7, Atg5 and Atg12 [226]. Bafilomycin A1 blocked the fusion of autophagosomes but did not stop the conjugation of PE to LC3-I for LC3-II production. To better understand LC3-I and LC3-II in human macrophages, future work should probably focus on the Atg proteins responsible for the conjugation process. Nevertheless, a lack of LC3-I expression has been observed and the LC3-II proteins might be the major LC3 proteins in human macrophages in "normal homeostatic" conditions. These data suggest LC3 proteins may have unique functions in macrophages.

5.5.4 ECM regulates LC3 formation and degradation

The pathways linking ECM and autophagy remain elusive and the function of ECM in cellular biology is largely unknown. The cell surface integrins, lysosome motility and position, and soluble ECM may be relevant to the cross-talk between ECM and autophagy-lysosome pathway [215, 291].

The integrin-mediated cell adhesion is required for many cellular processes [501]. The main mechanism of cell-matrix interaction is through integrins which are heterodimers of associated α subunit and β subunit [502]. There are 24 distinct integrins and they are clustered to form focal adhesions (FAs) on cell surface which are the areas for cell-ECM adhesion [503]. A similar study to ours has shown that collagen-IV, not collagen-I, had increased basal autophagy in HeLa cells. Silencing of the FA kinase (FAK) using siRNA had diminished the effect of increased autophagy in HeLa cells on collagen-IV [216]. The proposed mechanism is that FAK tyrosine phosphorylates an upstream mTOR regulator (TSC2) and thus suppresses the activation of mTOR and leads to autophagy activation [303]. The data in my study showed that contact with both type-I and type-IV collagens increased basal autophagy in macrophages, and collagen-I had a greater influence. The mechanism could also be related to the FAs that are formed when macrophages attached to collagen surfaces.

The detachment of epithelial cells from ECM (anoikis) induces autophagy and it is proposed as a mechanism to enhance cell survival and reattachment [291]. In fact, cells cultured on low-attachment surfaces have showed increased autophagy due to the lack of integrin adhesion [304, 305]. In this study, I also showed that the autophagy level was upregulated in human macrophages after the low-attachment differentiation (Fig 5.11). Low-attachment and lack of FAs could be at least part of the reason of the upregulated autophagy.

More interestingly, my data also suggested that ECM modulates LC3-II degradation as the upregulated autophagy in MDM returned back to the normal level rapidly in the presence of type-I and type-IV collagens. The degradation of LC3/autophagsosomes occurs when they fused with lysosomes. Adhesion to ECM promoted changes in cellular morphology [216] which can trigger the redistribution of lysosomes and enhance the motility of lysosomes [306]. The lysosome positioning includes the dynein-mediated retrograde transport of lysosomes which promotes their fusion with autophagosomes and eventually could enhance the degradation of LC3 [306].

When macrophages attached to ECM, they do not just adhere, they can also digest ECM proteins by releasing MMPs and part of ECM can be recognized and engulfed by macrophages for further degradation [504-506]. The proteolysis of ECM by macrophages not only promote the degradation pathways within the cells, but also increase the production of bio-active peptides (termed 'matrikines') [507]. Proteolysis of collage-I and collagen-IV also generate matrikines and collagen-I derived DGGRYY can activate human neutrophils [508]. Such bioactive peptide might also be able to mediate the autophagy pathway. For example, there is evidence that soluble matrix constituents can modulate the autophagy pathway both positively (eg. decorin, collagen VI and endostatin) and negatively (eg. laminin a2) [215].

In summary, ECM components actively regulate the autophagy pathway regarding both LC3-II formation and its degradation in macrophages. The underlying mechanisms and the effect on macrophage biology are yet to be addressed.

Chapter 6 Fibrotic ECM potentiates the impairment of the autophagy pathway in AM in the setting of dysfunctional lysosomes

6.1 Abstract

This study was designed to investigate the autophagy pathway in alveolar macrophages (AM) and determine the role of fibroblast-derived ECM in macrophage autophagy.

A range of techniques was used to study the autophagy-lysosome pathway in AM from patients with interstitial lung diseases (ILD). Transmission electron microscopy (TEM) confirmed the presence of double-layer membrane autophagosomes in AM. Flow-cytometry showed that AM were the major autophagic cells in the BAL fluid cell population. AM were purified by adhesion and rested *ex vivo* for 20 hours. With fluorescent microscopy, AM from fibrotic ILD patients were shown to have a significantly higher percentage of autophagic vacuole positive cells than AM from non-fibrotic ILD patients ($p<0.01$). Western blotting showed increased LC3-II ($p<0.001$) and p62 ($p<0.001$) expression in fibrotic AM. TEM revealed the presence of membranous cytoplasmic bodies (MCBs) in fibrotic AM and dual staining of autophagic vacuoles and lysosomes showed co-localisation of these two structures. These data suggest that AM from fibrotic ILD have impaired autophagy through blockage of processing of autophagic vacuoles.

Lung fibroblasts were purified from human lung biopsies with (fibrotic) or without (non-fibrotic) lung fibrosis. TEM confirmed the presence of synthesised 3-dimensional extracellular matrix (ECM) by primary lung fibroblasts *in vitro.* Culture of healthy monocyte-derived macrophages on ECM showed that fibrotic ECM increased both basal autophagy ($p<0.05$) and rapamycin-induced autophagy ($p<0.001$) in MDM but did not show ECM caused blockage of autophagy.

This study demonstrated that the autophagy pathway was blocked in AM from patients with fibrotic ILD. Fibrotic ECM does not cause blockage of autophagy, but potentiates

the upstream autophagy pathway and thus may further impair macrophage function in cells that exhibit blockage of autophagy.

6.2 Introduction

Autophagy is a constitutive and continuous homeostatic process. It is a rapid process and in yeast an autophagy cycle takes about 7-9 minutes [253]. The formation of autophagosomes takes about 4-5 minutes in yeast and in mammals it takes about 5-10 minutes [252-254]. Disrupted autophagy may have pathological consequences [229]. In fact, some of the pathological processes associated with lung fibrosis are known to activate autophagy, such as high levels of endoplasmic reticulum (ER) stress, elevated reactive oxygen species (ROS), significant low oxygen (hypoxia) and accumulated protein aggregates and/or malfunctioning cellular organelles. Exposure to these autophagy activators should provide the alveolar space with a "pro-autophagic microenvironment".

The association of autophagy with fibrosis is complex. Collagen and ECM deposition is a hallmark of IPF and other fibrotic lung diseases. In patients with IPF, previous studies have shown that autophagy is reduced, as measured by immunohistochemistry and western blotting of LC3 expression in whole lung tissue section or homogenate compared to patients with COPD [297]. In bleomycin-treated mice, rapamycin-induced autophagy decreased the level of hydroxyproline and alpha-smooth muscle actin (alpha-SMA) and increased survival in treated mice [297, 298]. In a genetically manipulated Beclin-1 deficient mice model, lack of autophagy showed increased collagen deposition in mouse kidneys *in vivo*. Induction of autophagy by TFP, an autophagy inducer, in primary mesangial cells from these mice decreased TGF-β-induced collagen-I protein level *in vitro* [293]. There is evidence, however, that autophagy can be a "double-edged sword" in organ fibrosis. In liver fibrosis, enhanced autophagy can attenuate liver fibrosis by inhibiting tissue inflammation, but can also active hepatic stellate cells (HSCs) and increase collagen synthesis [299].

The autophagy pathway and fibrosis are thought to be linked but "the cause and effect" relationship needs to be better understood. Autophagy is tissue- and cell-dependent, and

autophagy may have distinct roles at different stages of fibrosis. There is very little information regarding the autophagy-lysosome pathway in AM in lung fibrosis.

6.3 Hypothesis and aims

6.3.1 Hypothesis

Contact with extracellular matrix modulates the autophagy-lysosome pathway in AM from patients with lung fibrosis

6.3.2 Aims

- To assay the autophagy pathway in AM by multiple methods
- To optimise the protocol of human lung fibroblast-derived ECM for *in vitro* studies
- To determine the effect of lung fibroblast-derived ECM on the autophagy pathway in macrophages

6.4 Results

In chapter 6, the autophagy pathway in AM was investigated using several methods.

The autophagy structure, autophagosome, was identified and confirmed using TEM (Fig 6-1). The autophagy level of AM from ILD conditions with or without lung fibrosis was further studied with flow cytometry by the staining of autophagic vacuoles and LC3 proteins (Fig 6-2). To stabilise the AM and reveal the function/dysfunction of the autophagy pathway, cells were rested for 20 hours before they were further studied. The percentage of autophagic vacuole positive AM (Fig 6-3) and the expression of LC3-II and p62 in AM from the fibrotic and non-fibrotic ILDs were compared (Fig 6-4). The results suggested a blockage of autophagosome degradation in AM from ILD patients with lung fibrosis. Furthermore, dysfunctional lysosomes were observed with TEM (Fig 6-5 and Fig 6-6) and the colocalisation of lysosomes with autophagosomes confirmed the blockage of autophagosome degradation was primarily due to dysfunctional lysosomes (Fig 6-7).

Then a few experiments were designed to understand the role of fibrotic ECM on the regulation of macrophage autophagy in fibrotic lungs. Lung fibroblasts were derived from lung biopsies with or without lung fibrosis. ECM was derived from these lung fibroblasts (Fig 6-8) and different ECM did not change the adhesion of MDM (Fig 6-9-1). Finally, the effect of ECM on basal level autophagy (Fig 6-9-2) and rapamycin-induced autophagy (Fig 6-10) in MDM were studied.

6.4.1 The presence of autophagosomes in alveolar macrophages were confirmed with TEM

The observation of autophagosomes with TEM is the gold standard method to confirm the presence and occurrence of autophagy. AM from ILD patients were purified, fixed and examined under TEM.

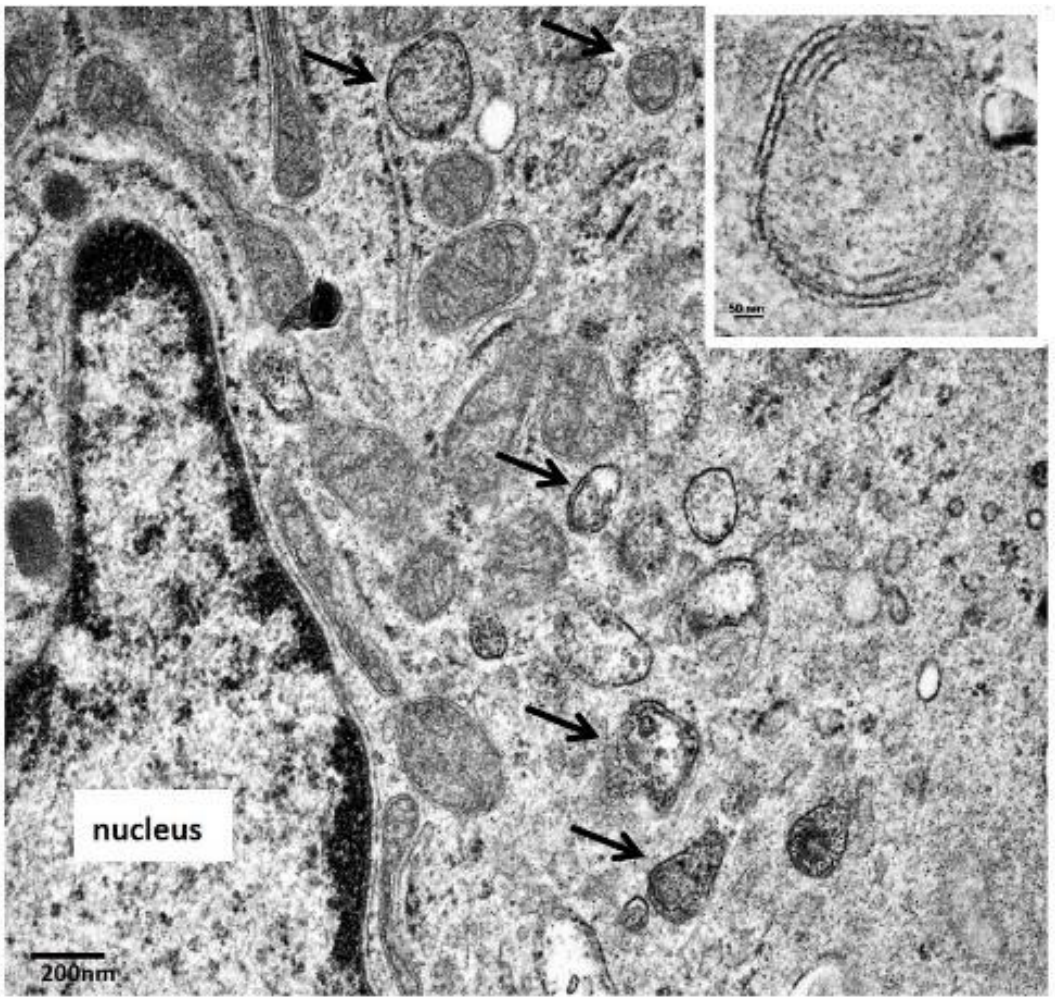

Figure 6-1 Presence of autophagosomes in AM were confirmed with TEM.

AM in human BAL fluid were purified and fixed for TEM. Autophagosomes and autophagy-related double-layer membrane structures (autophagic vacuoles) were observed (arrowed). The presence of "classic" autophagosome containing cargos for degradation was also observed (top right insert). Scale bar = 200 nm.

Autophagosomes and autophagy-related double-layer membrane structures (autophagic vacuoles) were observed under TEM. “Classic” functional autophagosomes (Fig 6.1) were seen confirming the presence of an autophagy pathway in AM. Thus, the autophagy pathway in AM was further studied by quantitative methods in the following experiments.

6.4.2 AM were autophagic positive (Cyto-ID and anti-LC3 staining)

To determine the autophagy in BAL fluid cell populations, freshly isolated BAL fluid cells were stained with Cyto-ID or anti-LC3 antibody for the detection of autophagic vacuoles and the autophagy protein LC3.

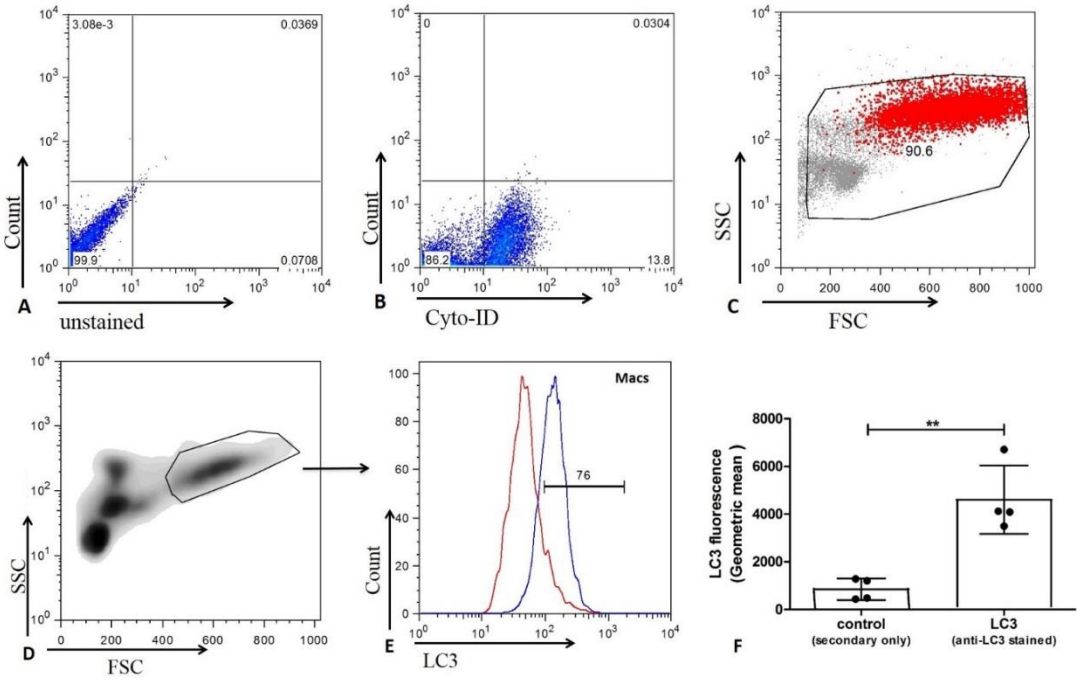

Figure 6-2 AM were autophagic positive (Cyto-ID and anti-LC3 staining).

BAL fluid cells from ILD patients were stained with Cyto-ID or anti-LC3 antibody. (A) Cyto-ID negative gates were set-up with unstained cells; (B) Cyto-ID positive cells were presented against the unstained; (C) Cyto-ID positive cells (in red) were shown on the forward and side scatter profiles to identify autophagic-positive population (n=3); (D) alveolar macrophages were gated based on their sizes on the forward and side scatter profiles; (E) Macrophages were LC3 positive cells (LC3 stained, blue; secondary antibody control, red), average of LC3 positive cells 71.25 ± 4.91% (n=4). (F) AM from ID patients were LC3 positive, ** $p<0.01$, paired student t-test, n=4.

The BAL fluid autophagic positive cells were gated back on the whole population and they appeared at the location of AM (Fig 6.2 A-C).

LC3 antibody staining (Fig 6.2 D & E) showed that the majority of macrophages were LC3 positive (71.25 ± 4.91% (mean ± SEM, n=4). The mean fluorescence of LC3 staining was significantly higher than the (secondary only) control (4605 ± 717.3 vs 850.0 ± 226.5, n=4).

Flow cytometry showed that AM from ILD were 'autophagic positive' cells. Because these cells were freshly isolated from BAL, the induction of autophagy markers may have been due to the BAL procedure or sample handling.

These data show that in AM from fibrotic ILD patients, there was increased LC3-II expression. The increased LC3-II expression could be the outcome of the increased autophagy induction, or the blockage of autophagosome degradation, or maybe both.

To address this, autophagy expression was measured in purified alveolar macrophages that were firstly 'rested' in tissue culture for 20 hours. This strategy was to minimise the effect of autophagy activation that might have been triggered by the BAL procedures or sample handling. Furthermore, it will help the functional autophagy process to be completed.

6.4.3 AM from fibrotic ILD patients had an increased percentage of Cyto-ID positive cells

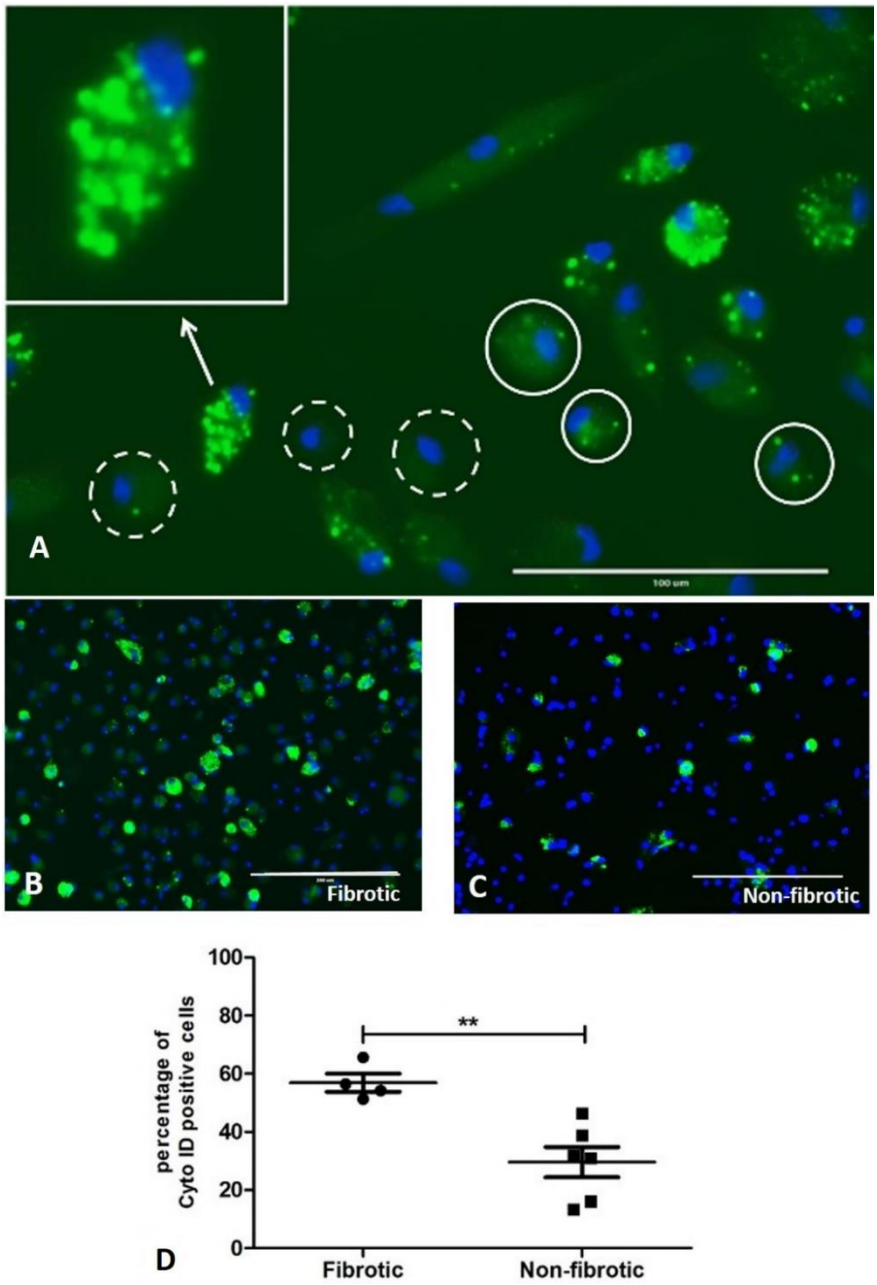

Figure 6-3 AM from fibrotic ILD patients had an increased percentage of Cyto-ID positive cells than cells from non-fibrotic ILD patients

AM were purified by adhesion and rested for 20 hours before the staining with Cyto-ID as described in section 2.3.6 in the Materials and Methods. Photos were taken and cells were analysed from at least 4 frames of each sample. An average of positive cells was used for analysis and the diagnosis was revealed just before the grouping of samples. (A) Purified AM were stained with Cyto-ID. Solid circle, Cyto-ID positive (puncta≥3) and dashed circle, Cyto-ID negative (puncta<3). Top left insert, an example of an extremely positive cell, magnified (2.5×). (B & C) examples of Cyto-ID staining of AM from fibrotic and non-fibrotic ILD; (D) analysis of Cyto-ID positive cells, student t-test, ** $p<0.01$. Green, Cyto-ID stain; blue, Hoechst stain for nuclei; scale bar =200 μm (A) and 100 μm (B & C).

As shown in the example (Fig 6.3A), both the occurrence and sizes of autophagic vacuoles (puncta) were different among AM. For analysis, cells were regarded as Cyto-ID positive only if they contained at least three puncta.

AM from the fibrotic ILD had a higher percentage of Cyto-ID positive cells (Fig 6.3B) than the AM from non-fibrotic ILD (56.91 ± 3.11%, n=4 vs 29.60 ± 5.21%, n=6, $p<0.01$).

Besides the live staining of autophagic-positive AM, the expression of LC3-II and p62 was compared using western blotting.

6.4.4 AM from fibrotic ILD had increased LC3-II and p62 expressions

Protein lysates of AM were prepared after 20 hours of tissue culture. The expression of LC3-II and p62 was analysed by western blotting.

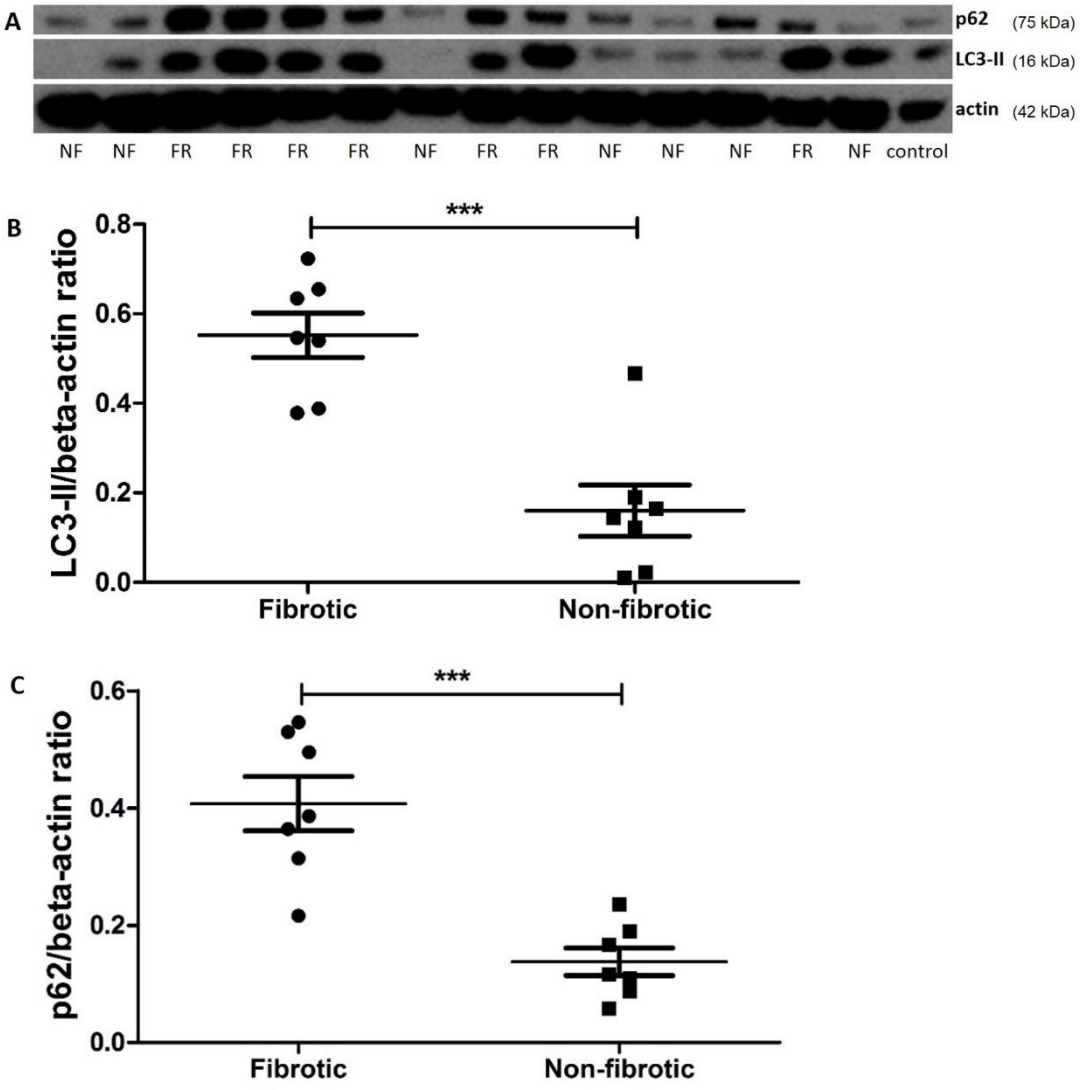

Figure 6-4 AM from fibrotic ILD (FR) had increased LC3-II and p62 expressions than AM from non-fibrotic ILD (NF).

AM were purified by adhesion, cells were rested for 20 hours before the extraction of proteins. The investigator was blinded from the diagnosis and the group of samples until analysing the data. (A) Western blotting probing for LC3-II, p62 and actin. (B & C) densitometry analysis of LC3-II and p62 expressions. Control: Neuro 2A cell lysate. Student t-test, *** $p<0.001$, n=7.

Samples were described as ‘fibrotic’ (FR) or ‘non-fibrotic’ (NF) ILD according to the patients’ HRCT pattern as described in the introduction. The data were normally distributed and thus a student’s t-test was employed for statistical analysis.

Densitometry analysis showed that in AM from the fibrotic ILD LC3-II and p62 expression was significantly higher than that from the non-fibrotic ILD (LC3-II, 0.55 ± 0.05 vs 0.16 ± 0.06, $n=7$, $p<0.001$) and p62 (0.41 ± 0.05 vs 0.14 ± 0.02, $n=7$, $p<0.001$).

The increased P62 expression in fibrotic AM implies that autophagy-pathway blockage was at probably at least in part least in part responsible for the increased LC3-II expression. The blockage of autophagosome degradation could be because of the fusion of autophagosomes and lysosomes or it could be because of lysosomes dysfunctions. This is further explored in the following experiments.

6.4.5 Undigested cargos were observed in lysosomes in AM from IPF lungs

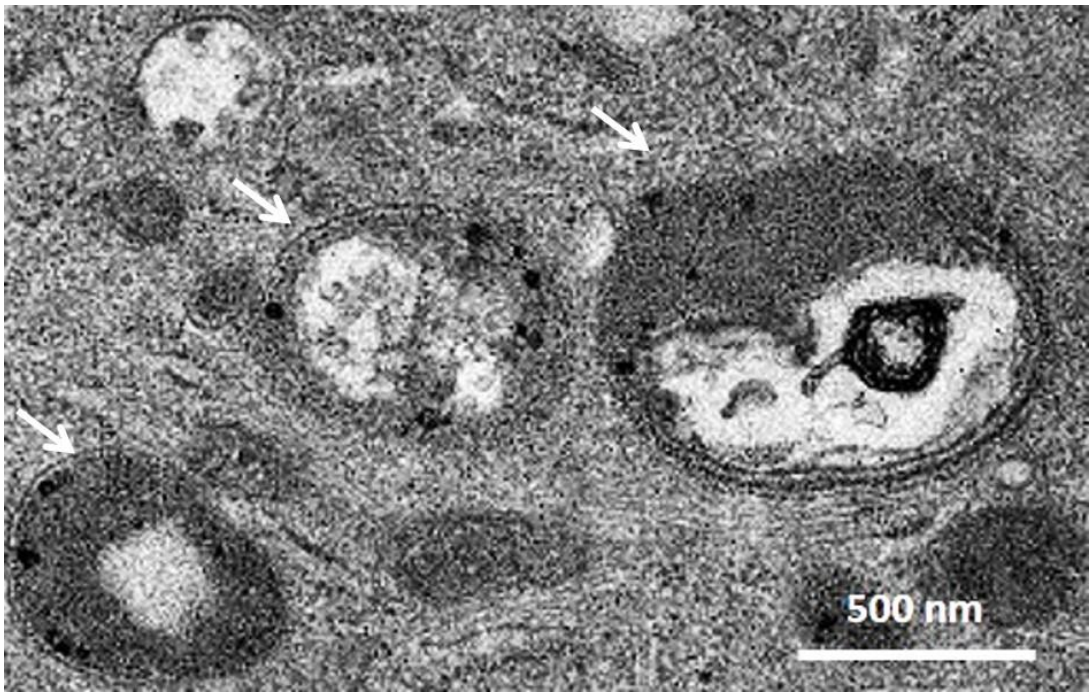

Figure 6-5 Undigested cargos were observed in lysosomes in AM from IPF lungs.

Lysosomes with undigested cargos (arrowed) were observed in AM from an IPF patient under TEM, scale bar = 500 nm.

6.4.6 Membranous cytoplasmic bodies in AM were observed under TEM

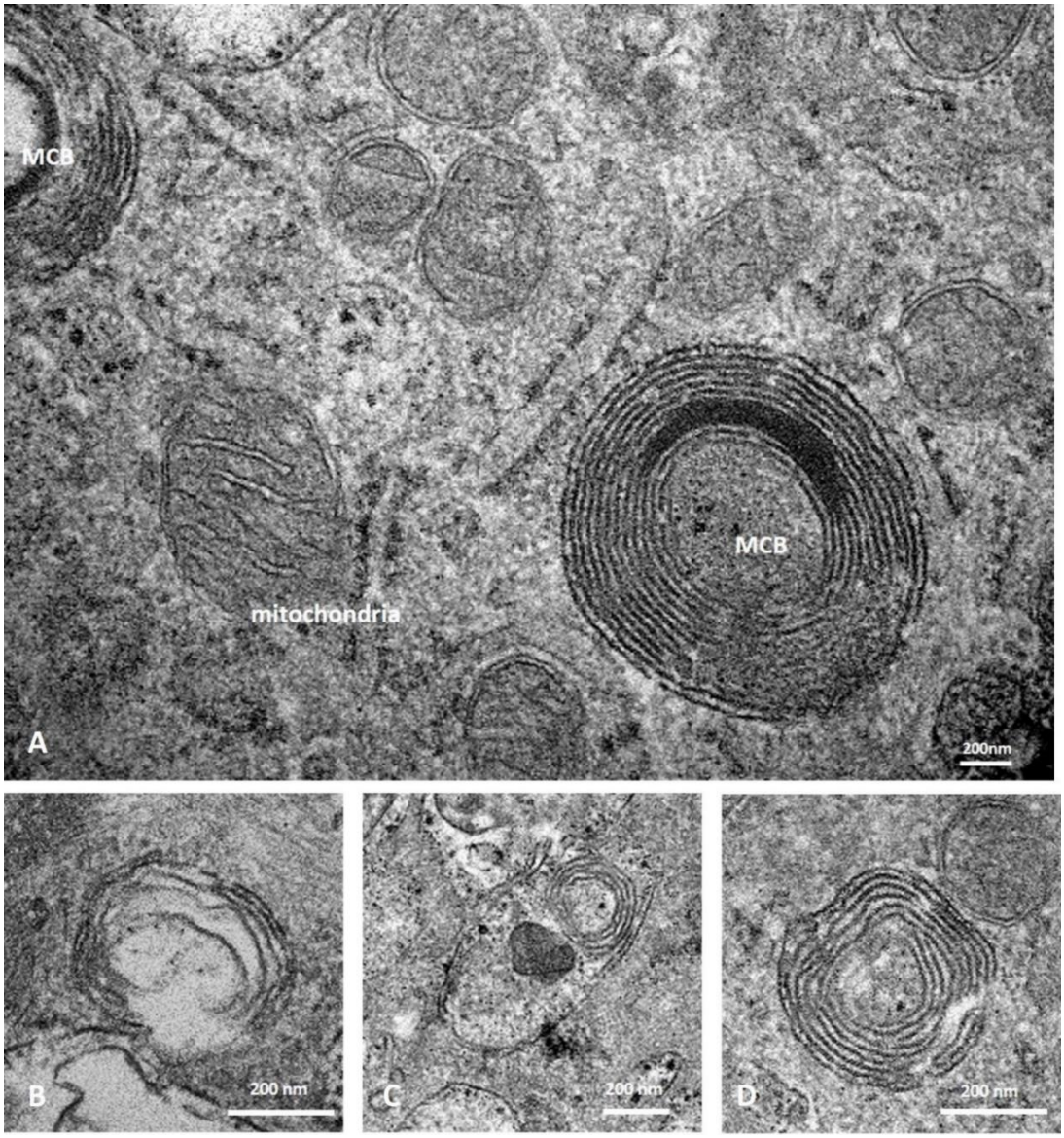

Figure 6-6 Membranous cytoplasmic bodies were observed under TEM in AM.

(A) "Classic" Membranous cytoplasmic bodies (MCBs) with sheets of stacked membranes were observed in AM; (B-D) MCBs were observed in different shapes/stages in AM, n=4. Scale bar = 200 nm.

Classic membranous cytoplasmic bodies, with sheets of stacked membranes (Fig 6.6A), were observed in AM. MCB is evidence of dysfunctional lysosomes and they were in different shapes/ at different stages (Fig 6.6 B-D). CMBs were present in AM from both fibrotic (n=2) and non-fibrotic (n=2) ILD patients.

The observation of undigested contents in (autophago)lysosomes and dysfunctional lysosome structures suggested a defect in the lysosomes. The localisation of autophagic structures and lysosomes were further studied with fluorescent microscopy.

6.4.7 Co-localisation of lysosomes and autophagic vacuoles in AM suggested the blockage of autophagosome degradation

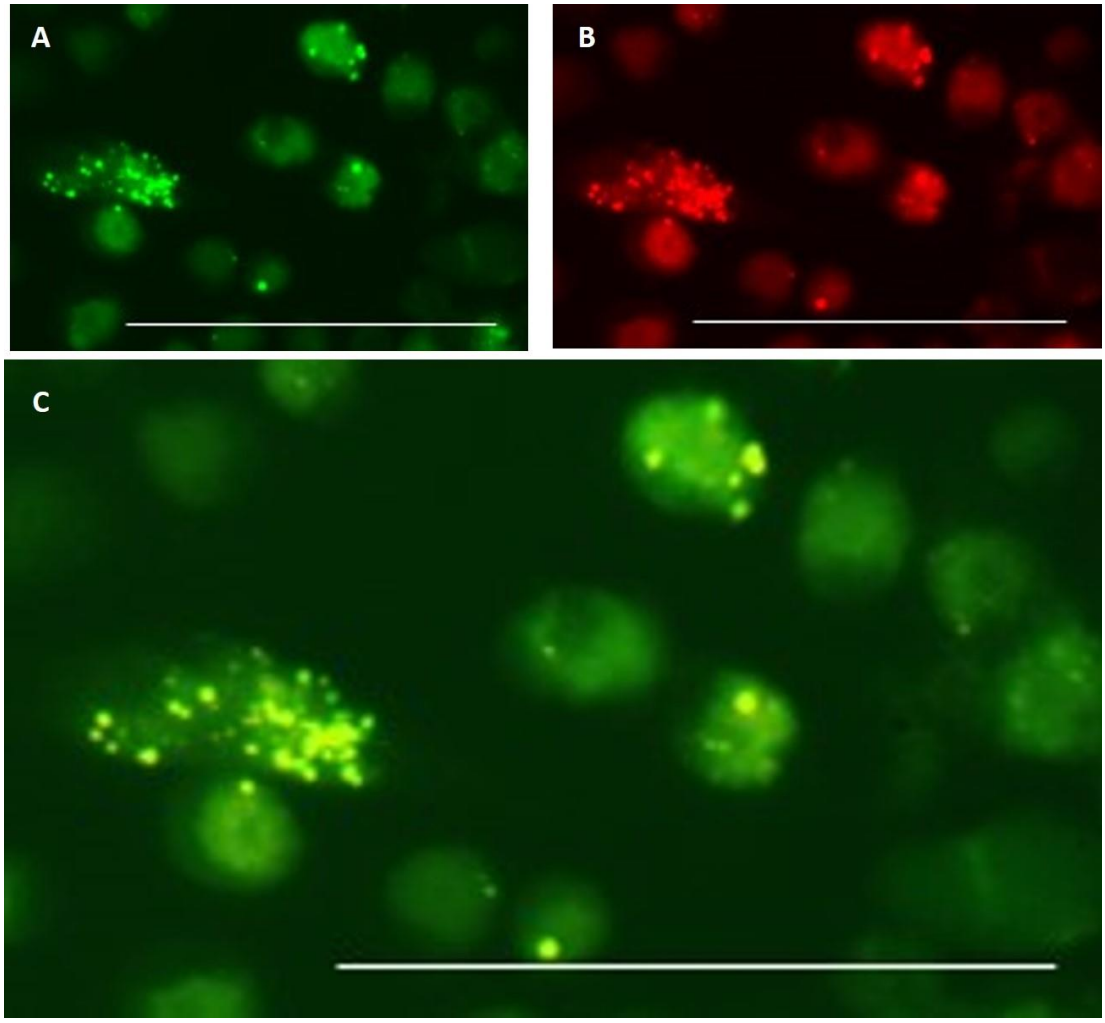

Figure 6-7 Co-localisation of lysosomes and autophagic vacuoles in AM suggested blockage of autophagosome degradation.

Cells were processed as described in section 2.2.5 and 2.3.6 in the Materials and Methods before imaging. Briefly, AM were purified by adhesion and rested for 20 hours before the staining of autophagic vacuoles and lysosomes. (A) Cyto-ID channel (green); (B) LysoTracker channel (red); (C) fused of both channels (yellow). Scale bar = 100 μm. This is a representative of AM that purified from 4 different patients.

AM were stained with Cyto-ID (Fig 6.7A, autophagic vacuoles) and LysoTracker (Fig 6.7B, lysosomes). Co-localisation of lysosomes and autophagic vacuoles were observed (Fig 6.7 C) in Cyto-ID positive cells which suggested the incomplete degradation of autophagosomes in AM even after 20 hours of culture *ex-vivo*.

Since the AM cells were rested for 20 hours after retrieval thus any form of functional autophagy should have been completed. These studies did not explain the contribution of the enhanced induction of autophagy to the increased autophagy in AM that are originally observed in fibrotic lungs. However, it clearly showed that the blockage of autophagy-degradation in AM in fibrotic lungs. Furthermore, the blockage of autophagy degradation was likely due to the lysosomes dysfunctions.

In the following experiments, the role of ECM on the autophagy pathway was investigated with MDM form healthy volunteers. ECM was derived from primary human lung fibroblasts as described in section 2.3.7 and 2.3.8 in the Materials and Methods chapter.

6.4.8 Deriving three-dimensional (3D) ECM from human lung fibroblasts

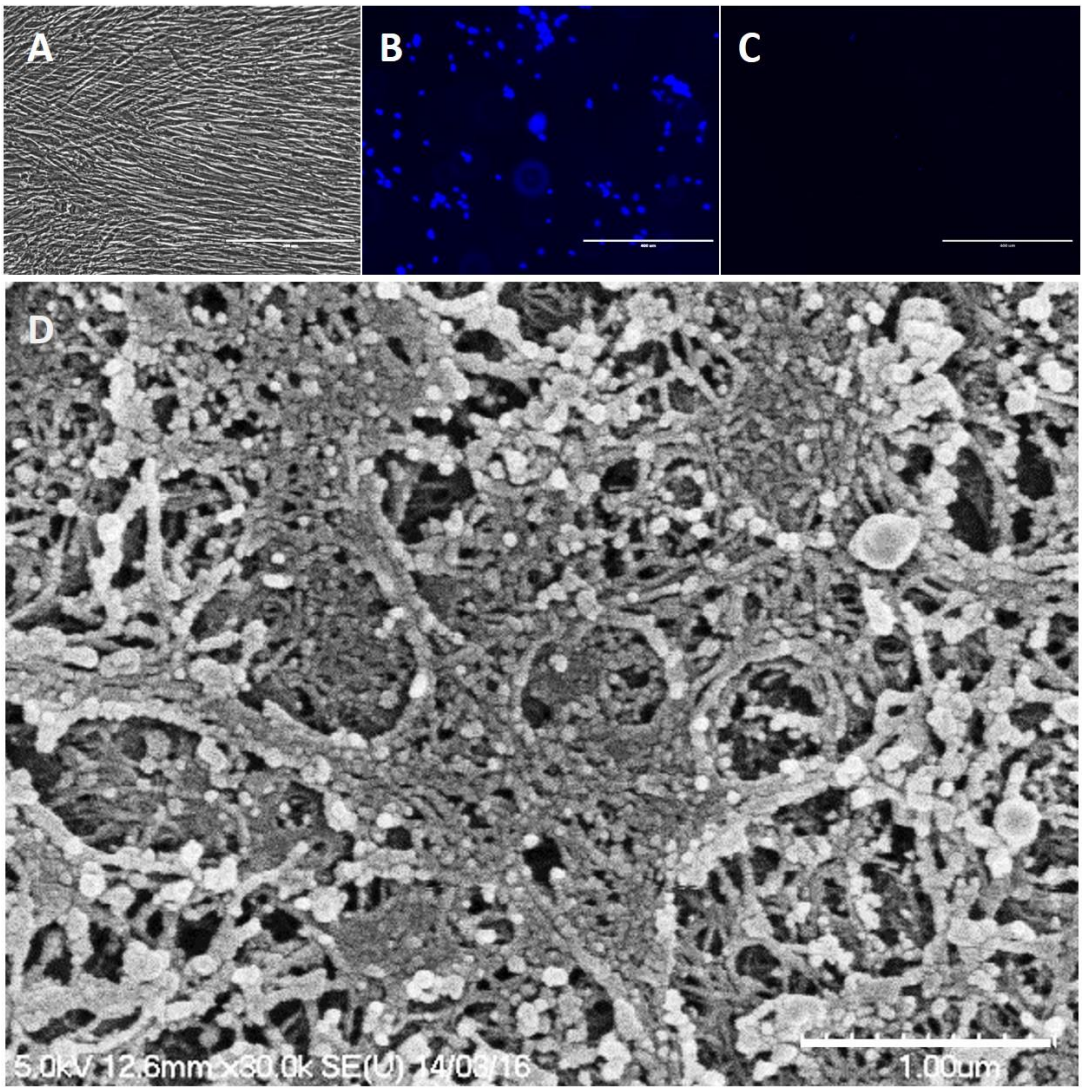

Figure 6-8 Primary human lung fibroblast-derived ECM.

Fibroblasts were cultured and processed for fluorescent imaging or SEM as described in section 2.3.7, 2.3.8, and 2.2.6. Briefly, cells were cultured for another 3 days when became confluent to enhance ECM production. ECM structures were left in situ after decellularisation by repeated freeze-thaw cycles. (A) The over-confluent culture of human lung fibroblasts; (B) DAPI (blue) staining for the quality control of freeze-thaw de-cellularization; (C) After 6 freeze-thaw cycles, cells were removed and confirmed by DAPI stain; (D) fibroblast-derived ECM were observed under SEM. Scale bar = 200 µm (A-C) and 1 µm (D).

The extracellular matrix structures derived from lung fibroblasts were confirmed by SEM. After the decellularisation (Fig 6.8 A-C), ECM derived from fibroblasts showed an interconnected meshwork of macromolecules (Fig 6.8 D).

Using this method, fibroblast-derived ECM was produced and used in the following experiments. Firstly, the effect of the structures on macrophage adhesion was compared between ECM derived from fibrotic and non-fibrotic fibroblasts. Then, the effect of different ECM on basal and rapamycin-induced autophagy was investigated.

6.4.9 Fibrotic ECM did not affect the attachment of MDM and increased basal LC3-II expression in MDM

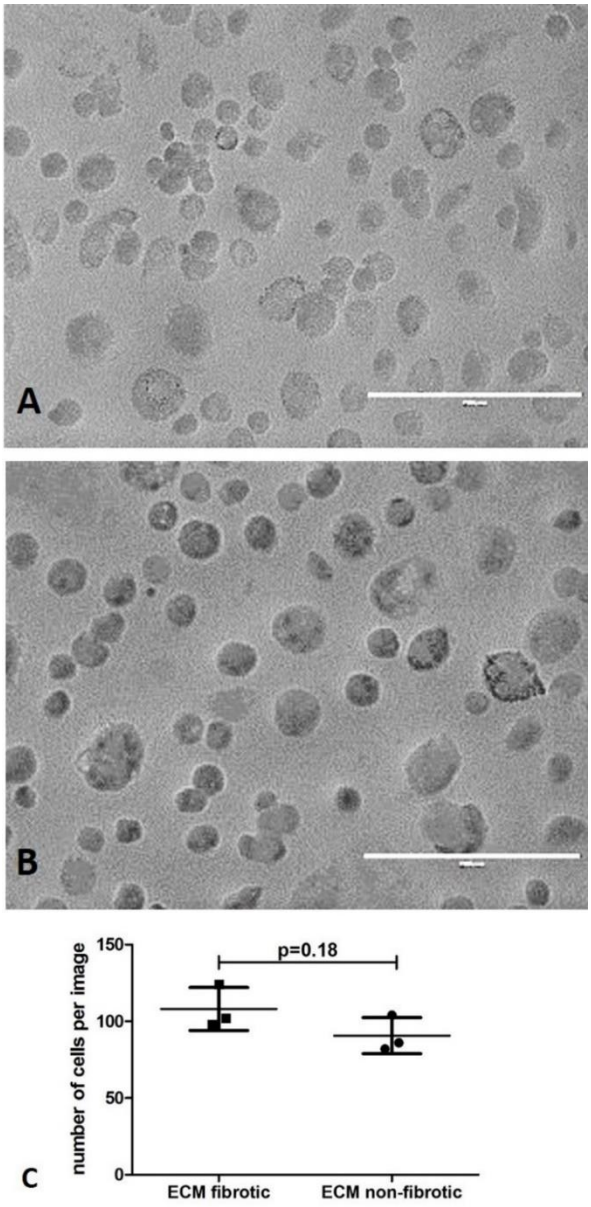

Figure 6-9-1 Fibrotic ECM did not affect the attachment of MDM.

Macrophages were acquired with the easy-detach method (MDM-ED) then plated on ECM derived from fibrotic (n=3) and non-fibrotic (n=3) fibroblasts. After adhesion for 24 hours, non-adherent cells were washed away with PBS before the images were taken. The number of cells in each frame was counted and an average of 4 frames of each sample was used for analysis. (A) MDM-ED attached to non-fibrotic ECM; (B) MDM-ED attached to fibrotic ECM; (C) analysis of the numbers of attached MDM-ED per image. Fibrotic vs non-fibrotic = 108.0 ± 8.1 vs 90.67 ± 6.8, n=3, p=0.18, student's t-test, scale bar = 200 μm.

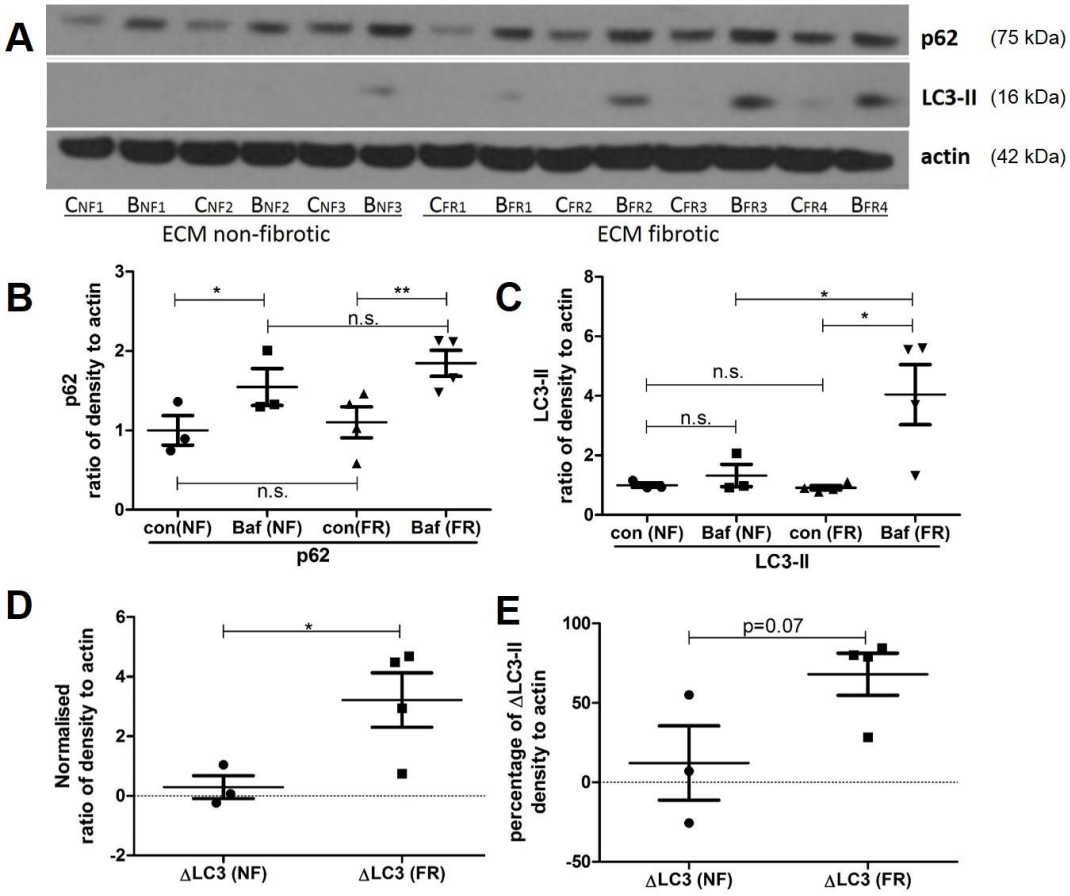

Figure 6-9-2 Fibrotic ECM increased basal LC3-II expression in MDM.

MDM-ED were seeded on human lung fibroblast-derived extracellular matrix. Cells were treated as indicated for 4 hours and proteins were extracted for Western Blotting. (A) Western Blot for p62, LC3-II and actin; (B & C) densitometry analysis of p62 and LC3-II; (D & E) densitometry analysis of ΔLC3-II (in subtraction and percentage). NF: non-fibrotic ECM; FR: fibrotic ECM. B: bafilomycin A1, 50 nM. C: vehicle control (DMSO in complete IMDM as Baf. A1 50 nM); *p<0.05, ** p<0.01, n.s. not significant, one-way ANOVA with Tukey's Multiple Comparison Test (B & C) and student t-test (D & E).

The expression of p62 was probed as an experimental control for the effectiveness (autophagosome blockage) of bafilomycin A1 treatment (Fig 6-9-2 A & B). The p62 expression was significantly increased in MDM-ED that were treated with Baf. A1 (Baf-NF vs con-NF = 1.55 ± 0.23 vs 1.00 ± 0.17, $p<0.01$, n=3 and Baf-FR vs con-Baf, 1.85 ± 0.16 vs 1.10 ± 0.20, n=4, $p<0.05$).

More importantly, there was no difference in p62 expression in MDM on non-fibrotic and fibrotic ECM when they were cultured in control media. This showed that fibrotic ECM itself did not block the degradation step of the autophagy pathway as the p62 expression was the same.

LC3-II protein was not detected in MDM-ED cultured in the control medium (Fig 6-9-2 A & C). There was no difference between the cells that were cultured on non-fibrotic and fibrotic ECM (con-NF, 1.00 ± 0.19, n=3 vs con-FR, 1.10 ± 0.20, n=4, Fig 6-9-2 C). This suggested that fibroblast-derived ECM alone did not induce LC3-II expression.

The LC3-II expression was significantly increased in MDM on fibrotic ECM after bafilomycin A1 treatment (Fig 6-9-2 A & C): con-FR vs Baf-FR = 0.91 ± 0.07, n=3 vs 4.04 ± 1.01, n=4, $p<0.05$, suggesting enhanced autophagy in MDM. In contrast, this was not observed in cells on non-fibrotic ECM (con-NF vs Baf-NF = 1.00 ± 0.08 vs 1.33 ± 0.37, n=3). Furthermore, the LC3-II expression after bafilomycin A1 treatment was significantly higher on fibrotic ECM than the non-fibrotic ECM (Baf-FR vs Baf-NF = 4.04 ± 1.01, n=4 vs 1.33 ± 0.37, n=3, $p<0.05$). This suggested that the formation of LC3-II through basal autophagy in MDM was increased on fibrotic but not non-fibrotic ECM.

The change in LC3 (ΔLC3) expression between control and bafilomycin A1-treated is another way of describing these data. ΔLC3 is presented as whole values (Fig 6-9-2 D) and as a percentage (Fig 6-9-2 E). Fibrotic ECM increased ΔLC3-II compared with non-fibrotic ECM: 3.22 ± 0.912, n=4 vs 0.29 ± 0.39, n=3, $p<0.05$ and ΔLC3%, 68.06 ± 13.31%, n=4 vs 12.18 ± 23.41%, n=3, $p=0.07$. This confirmed the increase in LC3 expression in MDM cultured on fibrotic ECM.

Collectively these data show that fibrotic ECM increased the basal autophagic activity.

6.4.10 Fibrotic ECM increased rapamycin-induced autophagy in MDM and recruited more p62

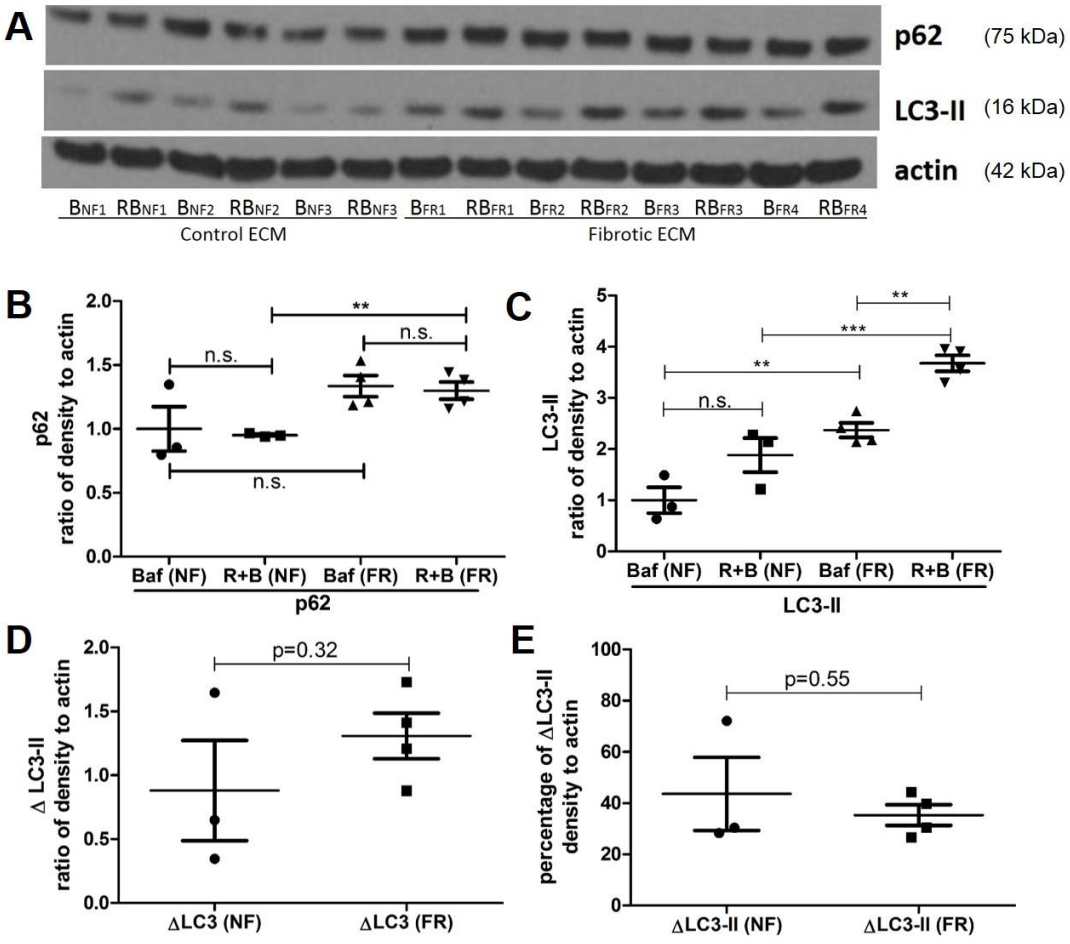

Figure 6-10 Fibrotic ECM increased rapamycin-induced autophagy in MDM.

MDM-ED were seeded on human lung fibroblast-derived ECMs. MDM-ED were treated as indicated for 4 hours and proteins were extracted for Western Blotting. (A) Western Blot for p62, LC3-II, and actin; (B & C) densitometry analysis of p62 and LC3-II; (D & E) densitometry analysis of ΔLC3 (in subtraction and percentage). B/Baf: Bafilomycin A1, 50 nM. RB/R+B: rapamycin (25 μM) with Baf. A1 (50 nM); NF: non-fibrotic ECM; FR: fibrotic ECM. **p<0.01, *** p<0.001, n.s. not significant, one-way ANOVA with Tukey's Multiple Comparison Test (B & C) and student t-test (D & E).

As shown in Fig 6-10-C, the basal LC3-II expression (bafilomycin A1 alone) was significantly higher on fibrotic ECM when compared with the non-fibrotic ECM (Baf-FR vs Baf-NF= 2.37 ± 0.14, n=4 vs 1.00 ± 0.25, n=3, $p<0.01$). This confirmed the results presented in Fig 6-9-2 and showed fibrotic ECM increased basal autophagy.

The rapamycin-induced LC3-II expression on fibrotic ECM was higher than that on non-fibrotic ECM (RB-FR vs RB-NF=3.68 ± 0.16, n=4 vs 1.88 ± 0.33, n=3, $p<0.001$). This showed that fibrotic ECM potentiated rapamycin-induced autophagy in MDM.

When autophagy was induced with rapamycin, however, p62 expression was also increased significantly when compared cells cultured on fibrotic ECM versus non-fibrotic ECM (RB-FR vs RB-NF = 1.30 ± 0.07, n=4 vs 0.95 ± 0.01, n=3, $p<0.01$). This suggested that more p62 may have been recruited for selective autophagy on fibrotic ECM when the autophagy pathway was activated.

Collectively these data show that fibrotic ECM enhances or potentiates the upstream autophagy pathway (increased LC3-II expression) and that if the downstream autophagy pathway is blocked, fibrotic ECM exacerbates autophagy impairment as shown by increased autophagosome accumulation (LC3-II and p62 expression).

There was p62 expressed in all conditions. Densitometry showed p62 expression was not significantly different when cells were cultured on the same surface: Baf-NF vs RB-NF =1.00 ± 0.17 vs 0.95 ± 0.01 (n=3) and vs Baf-FR vs RB-FR = 1.34 ± 0.08 vs 1.30 ± 0.07 (n=4). This means that on both fibrotic ECM and non-fibrotic ECM, the blockage of autophagy was successful and adding rapamycin to bafilomycin did not recruit more p62.

The change in LC3-II (ΔLC3) was not significantly different between the fibrotic and non-fibrotic ECM: ΔLC3, 1.31± 0.19, n=4 vs 0.88 ± 0.40, n=3 and ΔLC3 %, 35.33 ± 4.06%, n=4 vs 43.60 ± 14.27%, n=3. This suggested that LC3-II expression triggered by rapamycin were the same on both fibrotic and non-fibrotic ECMs. The higher LC3-II expression by rapamycin on fibrotic ECM was due to the nature of the fibrotic ECM and its effect on basal autophagy in MDM.

6.5 Summary and Discussion

The autophagy pathway in IPF is not fully understood. My study has shown that AM from fibrotic ILD patients had increased LC3-II and p62 expression which was primarily due to the blockage of autophagosome degradation. The colocalisation of autophagosome and lysosome suggested the fusion of the two compartments was not compromised. Thus, the blockage of autophagosome degradation was most likely the consequence of dysfunctional lysosomes.

Both fibrotic and non-fibrotic ECM facilitate the damping of upregulated autophagy and they do not cause blockage of the autophagy pathway. Fibrotic ECM also promotes basal LC3-II formation, and in the setting of dysfunctional lysosomes, the increased basal autophagy may exacerbate the impairment of the autophagy pathway.

6.5.1 AM express markers of autophagy in the fibrotic lung

Autophagosomes were observed in AM from ILD patients by TEM which is the gold standard method for the confirmation of the presence of autophagy. TEM is not readily quantifiable. Staining with Cyto–ID and LC3 proteins in fresh BAL fluid cells demonstrated that AM were positive in autophagic vacuoles and LC3 staining. On average over 70% of AM were LC3 positive in fresh AM from ILD patients. Autophagy could have been activated by lavaging and processing the BAL fluid cells. However, autophagy is a rapid process, and leaving cells in a unstimulated condition will quickly help them return to their basal status [257-260]. In order to reveal the genuine autophagy level in AM, purified AM were rested in tissue culture for 20 hours. Even after the 20-hour incubation, Cyto-ID showed significantly increased staining of autophagic vacuole positive cells and significantly increased LC3-II expression in AM from fibrotic ILD patients.

Previous studies showed that the ‘autophagy level’ was decreased in IPF lung tissue [297, 301]. Whole lung tissue section or homogenate from IPF patients had decreased levels of LC3 and p62 as determined by western blotting and fluorescent microscopy [297]. Immunohistochemistry staining also showed similar results but with no expression of autophagy markers in (myo)fibroblasts or type-I epithelial cells, but the accumulation of p62 was specifically increased in type-II epithelial cells within the

fibroblastic foci (FF) [301]. Although AM were not specifically described in this study, immunohistochemistry (IHC) images of IPF tissue in this paper showed p62, ubiquitin and beclin expression in AM, similar to that in type-II epithelial cells [301]. A mTOR downstream effector protein, p-S6, was weakly expressed in healthy lungs but was found strongly expressed in IPF lung myofibroblasts suggesting an activation of mTOR signalling in IPF lungs which suppressed autophagy induction [298]. Again in this study AM were not specifically described in the paper which only included a small number of IPF tissue samples [298]. My results showed that AM had increased LC3-II and p62 in fibrotic lungs, suggesting the occurrence of autophagy in these cells. My data also suggested that the contact with ECM can alleviate the upregulated autophagy. The low expression of autophagy-related proteins seen in the lung tissues from other studies could be because of contact with tissue ECM, and our *in vitro* studies of macrophages suggest that ECM modulated autophagy to maintain a low and homeostatic level.

6.5.2 Lysosome dysfunction, the primary cause of impaired autophagy in AM

In this study, I showed that MCBs are present in the AM of patients with ILD. These MCBs are the hallmark evidence of dysfunctional lysosomes. It is known that MCBs are related to conditions with dysfunctional lysosomes such as lysosomal storage disorders (LSDs) [509]. Studies showed that the accumulation of lipid body like structures in leucocytes, such as alveolar macrophages, is relevant in infection, cancer, and inflammation [510, 511]. The frequent observation of MCBs in AM suggested that the lysosome-degradation pathway was impaired. In these AM, lysosomes had difficulty in processing the cellular waste that had been delivered to them. Macrophages from only 4 ILD patients (n=2 with fibrosis, n=2 without fibrosis) were studied for the presence of MCBs so it cannot be determined if the presence of MCB correlates or is associated specifically with fibrosis or if MCBs are not present in healthy AM.

Macrophages express a range of factors mediating iron uptake and they play important roles in maintaining systemic iron homoeostasis [512]. Iron overload causes macrophage dysfunction, decreased cellular chemotaxis and phagocytosis [513, 514]. Kao and colleagues showed that the chronic iron overload increased lysosomal pH and caused an increased number of dysfunctional lysosomes which led to blockage of

autophagosome degradation with increased LC3-II and p62 expression [515]. In our group, we had shown increased expression of CD71 in AM from IPF patients which was also associated with disease progression [65]. CD71, also known as transferrin-iron-transferrin receptor-1 (TfR-1), is widely expressed in macrophages and it is proposed as a major route of iron uptake in the absence of RBC by mediating diferric transferrin endocytosis [516]. Thus, the increased CD71 which leads to chronic iron overload might be an underlying mechanism for lysosome dysfunction in AM in IPF.

The co-localisation of autophagic vacuoles and lysosomes was further evidence that the degradation step via lysosomes was impaired. Incomplete autophagosome degradation may either be the cause or the outcome of the accumulated MCBs in AM. Incomplete autophagosomes degradation may lead to repeated "capture-degradation" cycles which could lead to pathological consequences in AM (Fig 6.6-C). It is likely that the accumulation of autophagosomes was the outcome of dysfunctional lysosomes. The fusion of autophagosome and lysosome was not affected, however, this needs to be further studied.

The increased accumulation of autophagosome could also cause further lysosome damage by being an excessive waste burden. In fibrotic lungs, the rapid assembly of LC3-II in contact with fibrotic ECM in the setting of dysfunctional lysosomes may cause further accumulation of autophagosomes. The newly formed cellular waste (excessive autophagosomes) may lead to a pathological "capture-degradation cycle" and cause further damage to lysosomes.

As mentioned, autophagy can be activated in by many factors among which smoking and ageing are most relevant to IPF. In fact, as shown in Fig 6.3, there were autophagic positive cells in both groups. These autophagic cells after resting in tissue culture suggested common autophagy-inducing factors in both groups which might be smoking and ageing. As shown in Appendix-B (Fig A-2), there was no difference in smoking or age in the participants in the fibrotic and non-fibrotic groups. Thus, the increased LC3-II expression and blocked autophagosome degradation observed in fibrotic AM were the results of other factors such as lysosomal dysfunction as shown in this study. Nevertheless, both smoking and ageing could be contributing factors that lead to the observation in the established lung fibrosis.

6.5.3 Impaired autophagy-lysosome pathway may lead to other functional consequences in AM

Gaucher disease is a type of LSDs that mainly affects macrophages. It is caused by the systemic lack of lysosomal hydrolase β-glucocerebrosidase and with glucocerebroside restricted to the monocyte/macrophage lineage [509]. Gaucher macrophages (GMs) are shown as distinct "alternative" activated macrophages and do not express pro-inflammatory cytokines, such as tumour necrosis factor α, IL-6, IL-1β and IL-10 in patients' spleen tissues [517]. They are skewed towards the "alternative" activated macrophages as they expressed CCL18 and interleukin-1 receptor antagonist and CD163 by IHC staining [517]. Recently studies have shown that GMs are efficient in phagocytosis but compromised in reactive oxygen species production and have impaired chemotaxis [518]. Upon phagocytosis, GMs have decreased expression of Atg16L1 and increased expression of p62 which suggest impaired autophagy in these macrophages [519]. There is evidence showing different lysosome phenotypes modulate the function of peritoneal and bone marrow-derived macrophages from mice [520]. Thus the changes shown in AM in the present study could be the causes of the properties in AM in the fibrotic lungs.

Impaired macrophage autophagy affects macrophage immune response and may promote inflammation [521]. Autophagy also affects cell death and is relevant to pre-apoptotic signals due to the accumulation of damaged mitochondria which should be removed by autophagy [522]. It is known that AM from IPF patients release a variety of mediators and growth factors that may be pro-fibrotic [71] and impaired autophagy could be an underlying mechanism.

Thus, impaired autophagy-lysosome pathway in AM from IPF patients may create an environment that favours fibrosis. The cause of impaired autophagy in AM needs to be further studied. It may be that the fibrotic environment results in blocked autophagy or, alternatively, impaired autophagy may be the cause of lung fibrosis. Indeed some rare lysosomal disorders do cause ILD [523], although none of these has been shown to cause usual interstitial pneumonia (UIP) which is the pathological phenotype that is associated with IPF.

6.5.4 Fibrotic ECM potentiates autophagy-lysosome dysregulation and assist in autophagy degradation

As shown, contact with ECM modulates macrophage autophagy *in vitro*: 1) it reduces autophagy level (LC3-II expression) that is otherwise apparent in freshly isolated cells cultured on low attachment flask; 2) specifically fibrotic ECM enhances both basal autophagy and mTOR-dependent autophagy; and 3) fibrotic ECM does not specifically block autophagy but enhanced autophagy may be the mechanism for the increased recruitment of p62. In this case, p62 functions as an autophagy cargo receptor (termed selective autophagy) and mediates the degradation of ubiquitinated cargo material such as aggregated proteins or intracellular infective organisms [524].

Lung fibrosis occurs when the synthesis and degradation of ECM are dysregulated [175]. Formation of ECM is also dependent on the proliferation, activation and apoptosis of fibroblast which is the major cell for ECM production [176]. In IPF besides the excessive accumulation of the ECM, the components of ECM also changed. At the later stage of IPF, type-I collagen is found increased and type-IV collagen is found decreased [204]. As described in chapter-5, I had also shown the regulation of autophagy by collagen-I and collagen-IV *in vitro* and the effect of fibrotic ECM on autophagy is similar to collagen-I as presented here. Furthermore, the effect of adhesion molecules (e.g. integrins), morphology changes during the attachment to ECM and bioactive peptides (generated by ECM proteolysis) have already been discussed (chapter-5). However, the formation of fibroblast-derived ECM is more complex and versatile. My studies presented here used fibroblast-derived ECM from fibrotic and normal fibroblasts which is a highly relevant model to study ECM [525]. The specific properties of the fibrotic ECM need to be further elucidated and many factors should be considered. The stiffness of ECM [208], the organisation and orientation (e.g. cross-linking) of ECM [175], post-translational modifications [175, 209] and other physical/mechanical changes that may be different between the fibrotic ECM and the non-fibrotic ECM. Therefore, these factors could contribute to the regulation of autophagy by fibrotic ECM. In fact, IPF fibroblast-derived ECM can change the gene expressions of the fibroblast itself and form a positive feedback-loop of fibrosis [155]. The exact mechanism of fibrotic ECM in the regulation of autophagy still needs to be further understood.

Fibrotic ECM does not cause the blockage of autophagy pathway *in vitro* but increased the basal autophagosome formation. The increased autophagy in AM in IPF patients is associated with impaired lysosomes. It is possible that the impaired autophagy observed in fibrotic AM is a result of lysosomal dysfunction is similar to that observed in primary LSDs. Although specific lysosomal-disorder genetic defects have not been identified in IPF, the damage to lysosomes could be secondary to 1) factors in the local micro-environment in the fibrotic lungs (hypoxia and ER stress); 2) external factors (smoking, dust, inhalation of other materials or virus infection); and 3) host factors such as polygenetic traits and ageing [17]. More likely, all these factors may contribute to lysosomal dysfunction and lung fibrosis.

The persistent active basal autophagy in the setting of excessive fibrotic ECM could have different roles at different stages of fibrosis: 1) in the early stages of injury, with intact lysosomes, activation of basal autophagy leads to reduced cellular stress and maintains cellular homeostasis in AM; 2) in the later stages of established lung fibrosis where there is lysosomal impairment, the continuous activation of autophagy leads paradoxically to AM dysfunction and potentially a pro-fibrotic cellular phenotype.

To summarise, there is impaired autophagy in AM from fibrotic ILD which is caused by the blockage of autophagosome degradation due to dysfunctional lysosomes. ECM actively regulates autophagy in macrophages and contact with fibrotic ECM potentiates autophagy dysfunction by enhancing autophagosome formation through upregulated basal autophagy. Furthermore, lysosomal impairment, rather than autophagy induction or inhibition, may be a therapeutic target in IPF.

Chapter 7 Autophagy regulates exosome secretion in macrophages

7.1 Abstract

In this study, I examined the effect of altered autophagy on exosome secretion in macrophages and studied the profile of alveolar exosomes in IPF patients.

There were less multi-vesicular bodies (MVBs) observed in fibrotic AM (from fibrotic ILD) than non-fibrotic AM (from non-fibrotic ILD) under TEM. AM released extracellular-vesicles (EVs) *ex vivo* which were confirmed by TEM and SEM. Furthermore, the anti-CD9 bead-based flow cytometry assay showed that alveolar EVs expressed the exosome marker CD63. NTA analysis showed that fibrotic AM released less exosomes *ex vivo* than non-fibrotic AM ($p<0.05$).

In fresh BAL fluid, samples from fibrotic ILD showed consistent low level of exosomes and was 2.7 times lower than that in the samples from non-fibrotic ILD ($p<0.001$). Exosomes pelleted from the same volumes of BAL fluid showed lower concentrations of both total exosomal protein ($p<0.05$) and total exosomal RNA in fibrotic ILD ($p<0.05$). In a small cohort ($n=12$), the baseline level (0-month) of alveolar exosomes was lower in the progressed IPF patients than that in stable IPF patients ($p=0.07$). However, the changes in alveolar exosome levels between 0-month and 12-month were not significant ($p>0.05$). Human peripheral blood monocyte-derived macrophages (MDM) release exosomes *in vitro* and this was affected by the modulation of the autophagy pathway with rapamycin and bafilomycin A1.

Alveolar exosomes from ILD patients did not express monocyte/macrophages surface markers which included CD14, CD16, HLA-DR, Mac-2 and CD206. Pelleted alveolar exosomes can be internalised into MDM which decreased the original exosome level in the culture media ($p<0.001$) and increased LC3-II expression in MDM.

In summary, impaired autophagy in AM affected their exosome secretion *ex vivo* which might contribute to the low levels of alveolar exosomes in the fibrotic lungs in humans

that may be associated with disease progression in IPF. Autophagy and exosomes may be new targets for the management of IPF.

7.2 Introduction

Exosomes are small EVs (most commonly 40 nm to 100 nm in size) that are released when MVBs are directed to fuse with the plasma membrane [324]. They serve as mediators of cell-to-cell communication through their cargo proteins and RNAs. Exosomes are classified as a homogeneous population and they express a group of conserved but distinct proteins such as tetraspanin protein CD9, CD63 and CD81 [324, 361]. Furthermore, the cellular membrane proteins could also be integrated on exosomes during endosome formation [331]. Exosomes can also carry and spread disease-relevant proteins, for example, the amyloid protein can be found on exosomes in Alzheimer diseases [377].

Exosomes are produced via the endosomal pathway and they also interact with the autophagy-lysosome pathway [348, 349]. Identification of the amphisome, a structure when the autophagosome fuses with the endosome, was the first piece of evidence linking autophagy and the exosome pathway [350]. More recently, there is direct evidence showing Atg12 and Atg3 interact with Alix, an important protein of the endosome pathway, to promote basal autophagy and regulate the fusion of autophagosomes and MVBs [357].

Normally, MVBs are either directed to the plasma membrane (released as exosomes) or to lysosomes (for degradation). Any changes in the autophagy-lysosome pathway could affect exosome secretion. Fader and colleagues showed that autophagy induction promoted the fusion of MVBs with autophagosomes and therefore decreased the secretion of exosomes in K562 cells [353]. On the other hand, blockage of autophagosome-lysosome fusion by bafilomycin A1 increased the secretion of exosomes [354-356]. Furthermore, in conditions of lysosomal dysfunction, MVBs are more likely to be directed away from lysosomes to the plasma membrane and eventually increases the exosomes secretion [327]. The release of exosomes has been proposed as a mechanism to compensate for the removal of toxic proteins when the lysosome pathway is dysfunctional. More evidence is emerging from the studies in lysosome

storage disorders (LSDs) and certain neurodegenerative diseases to support exosomes as a mechanism to alleviate cellular stress [327]

Exosomes have been proposed as a useful tool for diagnostic and therapeutic purposes in kidney and liver fibrosis [318, 424]. TGF-β1, a key mediator of fibrosis, has been found enclosed in exosomes upon epithelial injury in a kidney model. These TGF- β1 enclosed exosomes further increased tissue injury [425]. Exosomes are proposed as potential biomarkers for the diagnosis of lung cancer and other pulmonary diseases [317] but little is known in lung fibrosis. A small study in IPF showed that in serum exosomes the expression of miR-141 (anti-fibrotic) had decreased and the miR-7 level (fibrogenic) had increased [422].

In fibrotic lungs, accumulating evidence suggests that the autophagy-lysosome pathway which has a regulatory role in the exosome secretion is impaired [97, 297, 301]. Furthermore, my data showed that in fibrotic AM the autophagy-lysosome pathway is blocked (chapter-6). Thus, the exosome biogenesis in AM and the overall exosomal profile in the fibrotic lungs might both be affected and require further investigation.

7.3 Hypotheses and aims

7.3.1 Hypotheses

- Impaired autophagy-lysosome pathway in AM affects their exosome secretion
- Impaired autophagy in fibrotic lungs affects alveolar exosome levels
- Modulation of the autophagy-lysosome pathway regulates exosome secretion in MDM

7.3.2 Aims

- To determine the pattern of AM-released EVs from ILD patients *ex vivo*
- To determine the level of exosomes in BAL fluid retrieved from ILD patients
- To determine the association of exosome level and disease progression in IPF
- To determine the effect of autophagy modulation on exosome secretion in MDM
- To determine the effect of BAL fluid exosomes on autophagy induction in MDM

7.4 Results

In this chapter, I first demonstrated the presence of MVBs in AM along with the autophagosomes and MCBs (Fig 7-1). The number of MVBs may be less in fibrotic AM than non-fibrotic AM (Fig 7-2). Thus, the effect of the impaired autophagy-lysosomes pathway on exosome release was further investigated.

The secretion of EVs by AM e*x vivo* was confirmed under TEM and SEM (Fig 7-3). AM-derived EVs were captured by anti-CD9 beads and they were CD63 positive (Fig 7-4). Fibrotic AM released less exosomes *ex vivo* measured by NTA analysis (Fig 7-4). These results led to the question of whether the total exosome level was decreased in the fibrotic lungs in general.

To address this, BAL fluid exosome level was determined with fresh samples by NTA analysis (Fig 7-5). The level of alveolar exosomes from fibrotic ILD was consistently low and was 2.7 times less than that in non-fibrotic ILD (Fig 7-6). Furthermore, exosomes pelleted from the same volumes of BAL fluid (Fig 7-6) showed lower concentrations of total exosomal protein and total exosomal RNA in fibrotic ILD. In a small cohort (Fig 7-7, n=12), progressed IPF showed lower baseline (0-month) alveolar exosome level than stable IPF. However, the changes of alveolar exosome levels between 0-month and 12-month were not different.

Thereafter, the origin of BAL fluid exosomes was investigated by targeting the monocyte/macrophage surface markers (Fig 7-8). Results showed that they did not express CD14, CD16, HLA-DR, Mac-2, 25F9 or CD206 on their surface.

Finally, *in vitro* experiments were designed to understand the role of autophagy on exosome release in MDM. Mimicking the observation in AM, MDM were treated with rapamycin (with or without bafilomycin A1) which showed increased MVBs under TEM (Fig 7-9) and increased exosomes in the culture medium (Fig 7-10).

Finally, to study the function of alveolar exosomes, the pelleted BAL fluid exosomes were found internalised by MDM (Fig 7-11) and increased LC3-II expression in MDM was observed (Fig 7-12).

7.4.1 Impaired autophagy and dysfunctional lysosomes in AM may affect their secretion of exosomes

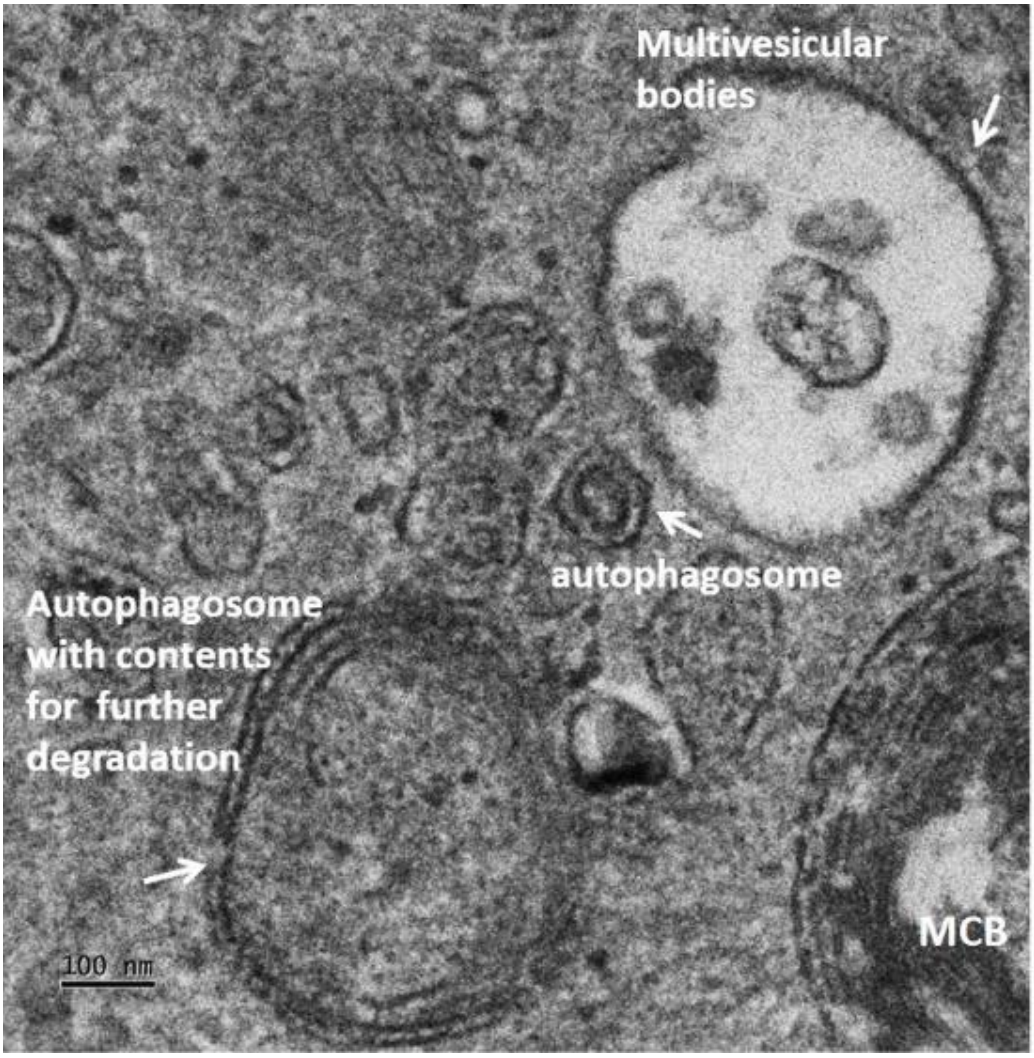

Figure 7-1 Impaired autophagy and dysfunctional lysosomes in AM may affect their secretion of exosomes.

The key compartments of exosome machinery (MVBs), autophagy-lysosome pathway (autophagosomes) and dysfunctional lysosome (MCBs) were observed besides each other in AM by TEM, scale bar = 100 nm.

7.4.2 AM from fibrotic ILD may contain less MVBs

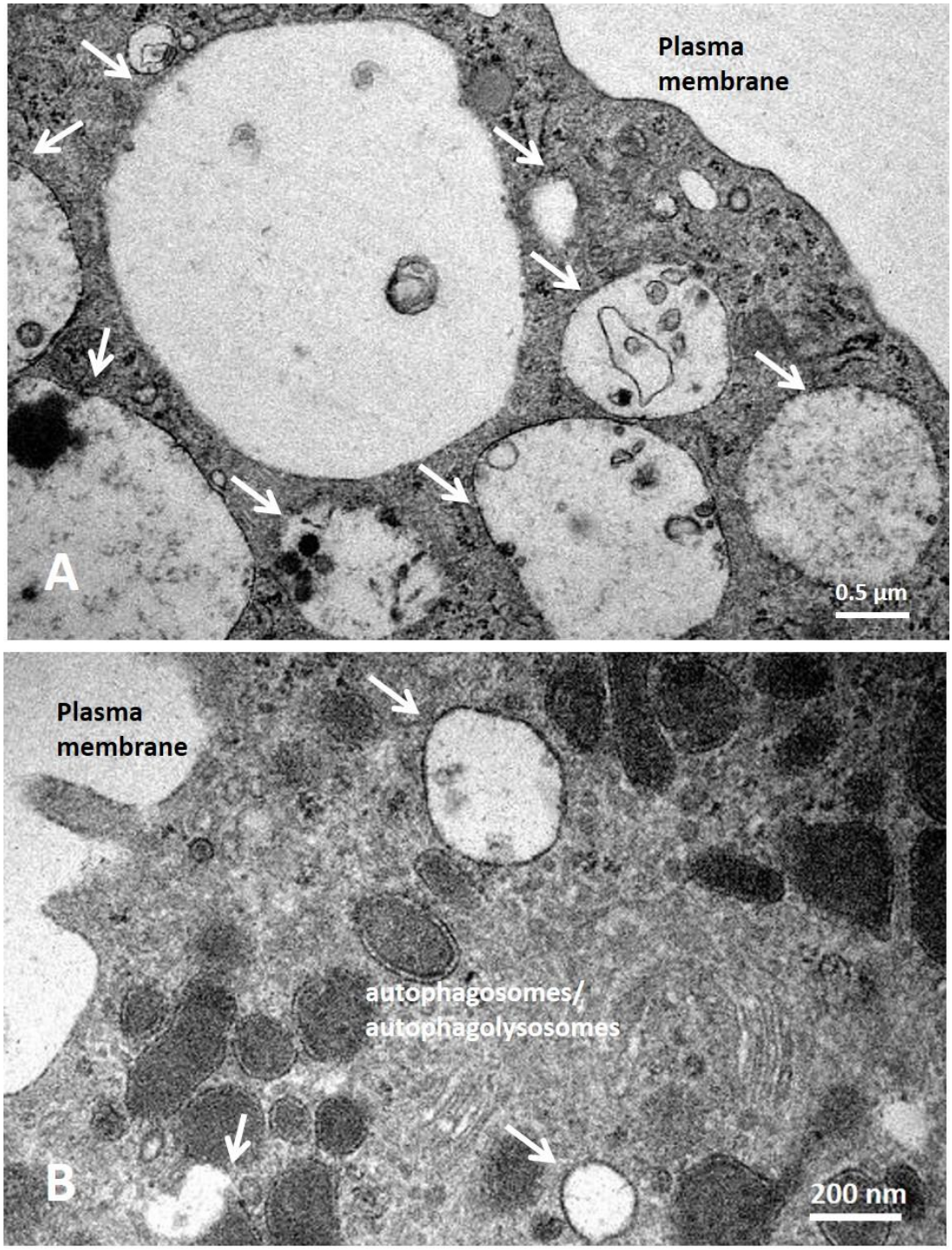

Figure 7-2 AM from fibrotic ILD may have less MVBs.

As shown in the example TEM images, fibrotic AM (B) had less MVBs than non-fibrotic AM (A), scale bar = 0.5 µm (A) and 200 nm (B). Representative images of patient samples who were diagnosed with fibrotic ILD (n=2) and non-fibrotic ILD (n=2).

7.4.3 AM-released EVs *ex vivo* were confirmed by TEM and SEM

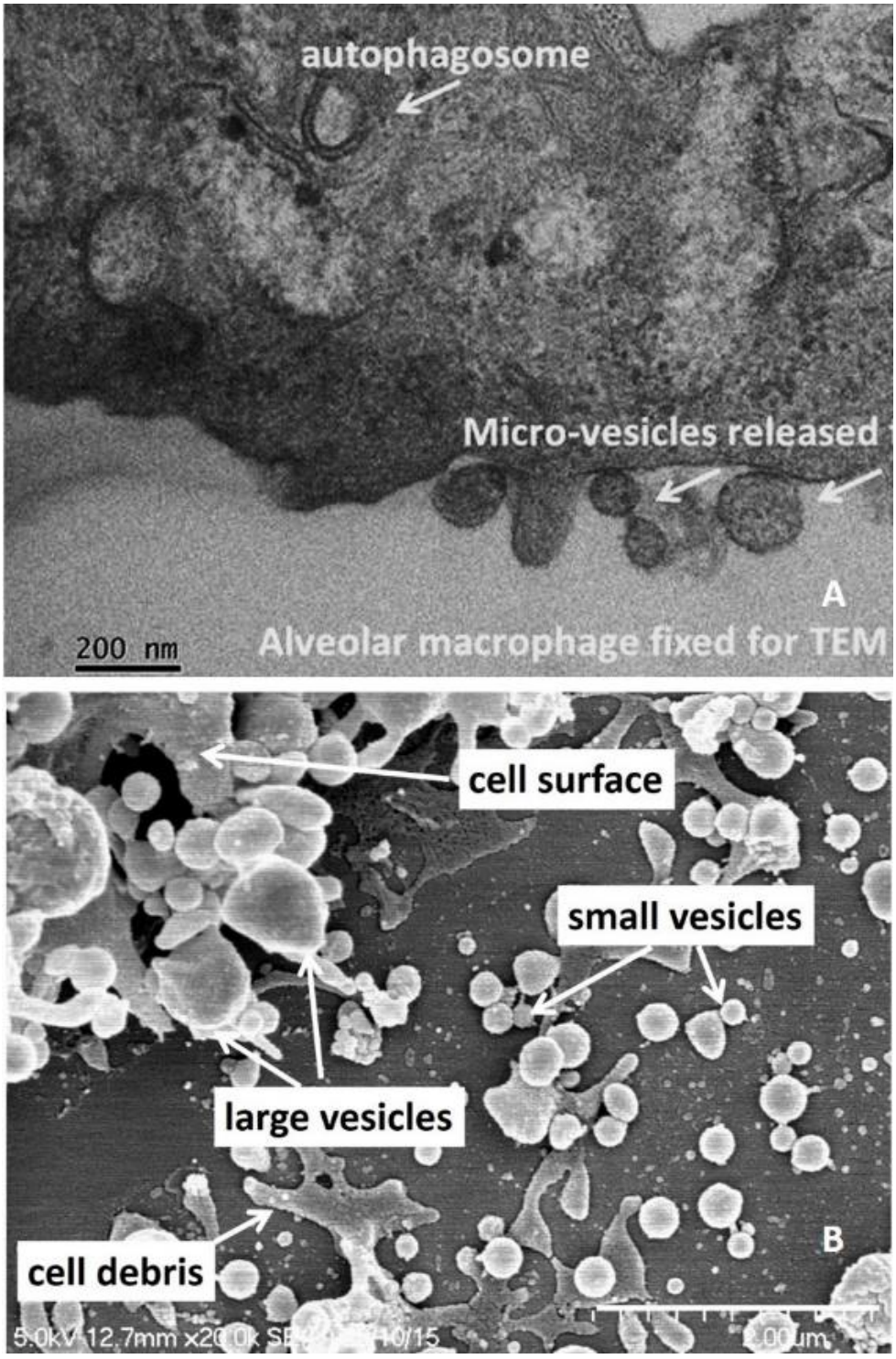

Figure 7-3 AM-released EVs were confirmed by TEM and SEM.

AM-released EVs were confirmed by TEM (A) and SEM (B). Scale bar = 200 nm (TEM) and 2.0 μm (SEM).

EVs (arrowed) appeared to be released from the cell surface as determined by TEM (A) and SEM (B).

In the TEM image, the released vesicles had clear boundaries with the cell membrane which suggested that they were not any surface structures of the cell but released from the cell. Compared to the scale bar, the diameters of the vesicles were approximately 100 nm, which is the size of exosomes by definition. Of note, part of the autophagosome (isolation membrane/ phagophore, arrowed) was also observed in the same cell.

EVs of different sizes released by AM were observed under SEM. Compared to the scale bar (2.00 μm), the sizes of EVs were variable and the majority of them were around 200 nm (small vesicles). Larger vesicles were also observed which had reached around 600 nm in diameter. This suggested that the released vesicles from AM *ex vivo* were a mixture of EVs which included: exosomes (40 nm to 100 nm) and microvesicles (100 nm to 1,000 nm).

The results from electron microscopy studies suggested that there might be more MVBs within the fibrotic AM and the release of different extracellular vesicles by the AM was active. The level of exosomes released by AM *ex vivo* was further studied using quantitative methods.

7.4.4 AM from fibrotic ILD released less exosomes *ex vivo*

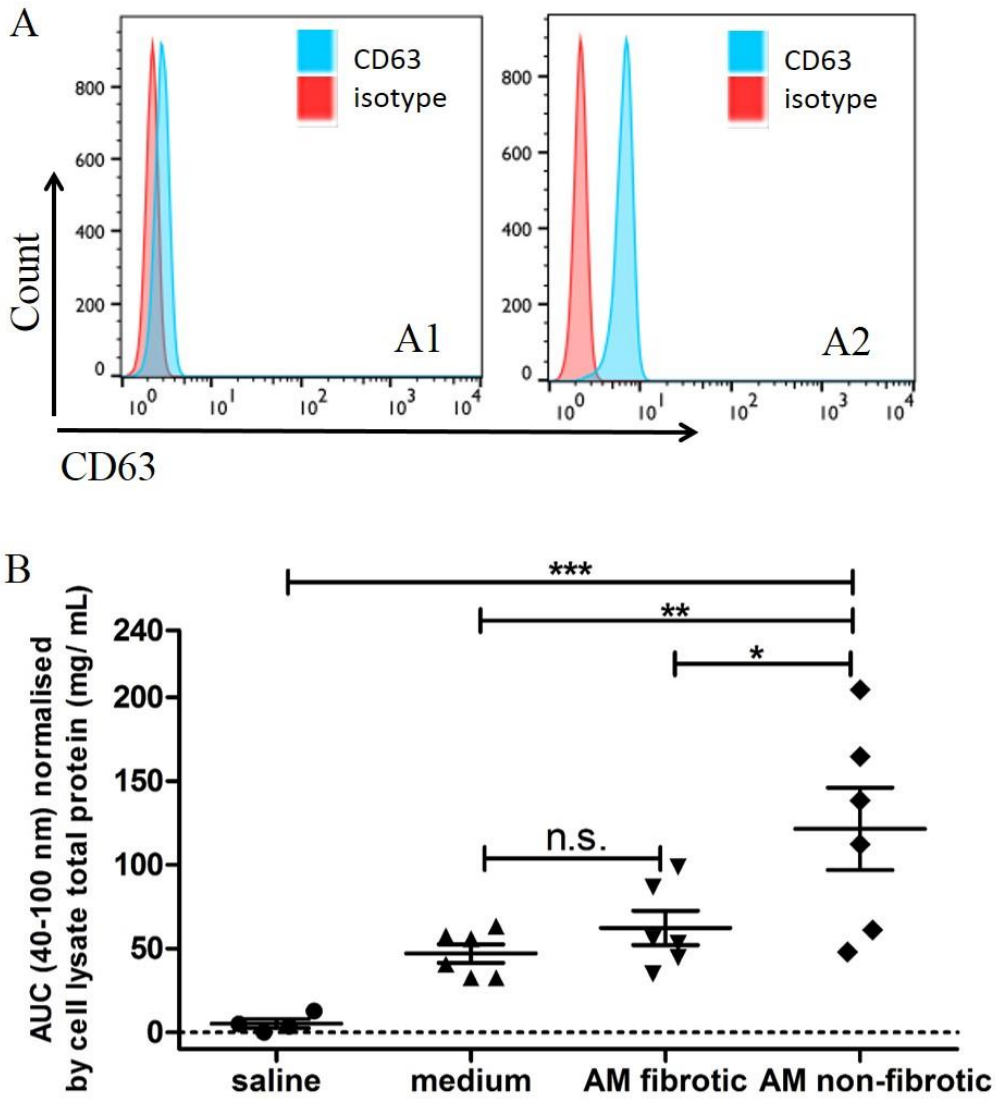

Figure 7-4 AM from fibrotic ILD released less exosomes *ex vivo*.

The same number of cells (0.5×10^6) were seeded in a 24-well plate and cultured for 20 hours before replacing with fresh medium (0.5 mL) and cultured for 4 hours. After the 4-hour incubation with AM, culture medium was collected and the cells were lysed in 120 µL RIPA buffer and the supernatant was collected for protein assay. (A) CD63 was expressed on CD9-beads captured EVs released by AM; (A1) CD9-beads selection in control medium; (A2) CD9-beads selection in the supernatant of AM cultured medium. (B) Exosome levels in AM cultured medium was determined by NTA (4 measurements of each sample) and represented as the mean of the area under curve (AUC) of vesicles with the sizes between 40 nm - 100 nm. *p<0.05, **p<0.01, ***p< 0.001, n.s. not significant. One way ANOVA, Tukey's Multiple Comparison Test.

Anti-CD9 beads flow cytometry assay showed that these vesicles expressed the exosome marker CD63 (A). The number of exosomes (B) released into the culture medium by fibrotic AM was less than the non-fibrotic AM (62.43 ± 10.20 vs 121.50 ± 24.62, n=6, $p<0.05$).

As AM are the dominant type of cell in the alveolar space, the different pattern of exosome secretion of AM might affect the level of exosomes in the lungs at real time. To test this hypothesis, fresh BAL fluid samples were collected from patients and analysed with NTA or exosomes were pelleted and the total protein and RNA were compared in the following experiments.

7.4.5 Measurement strategy and quality control for NTA

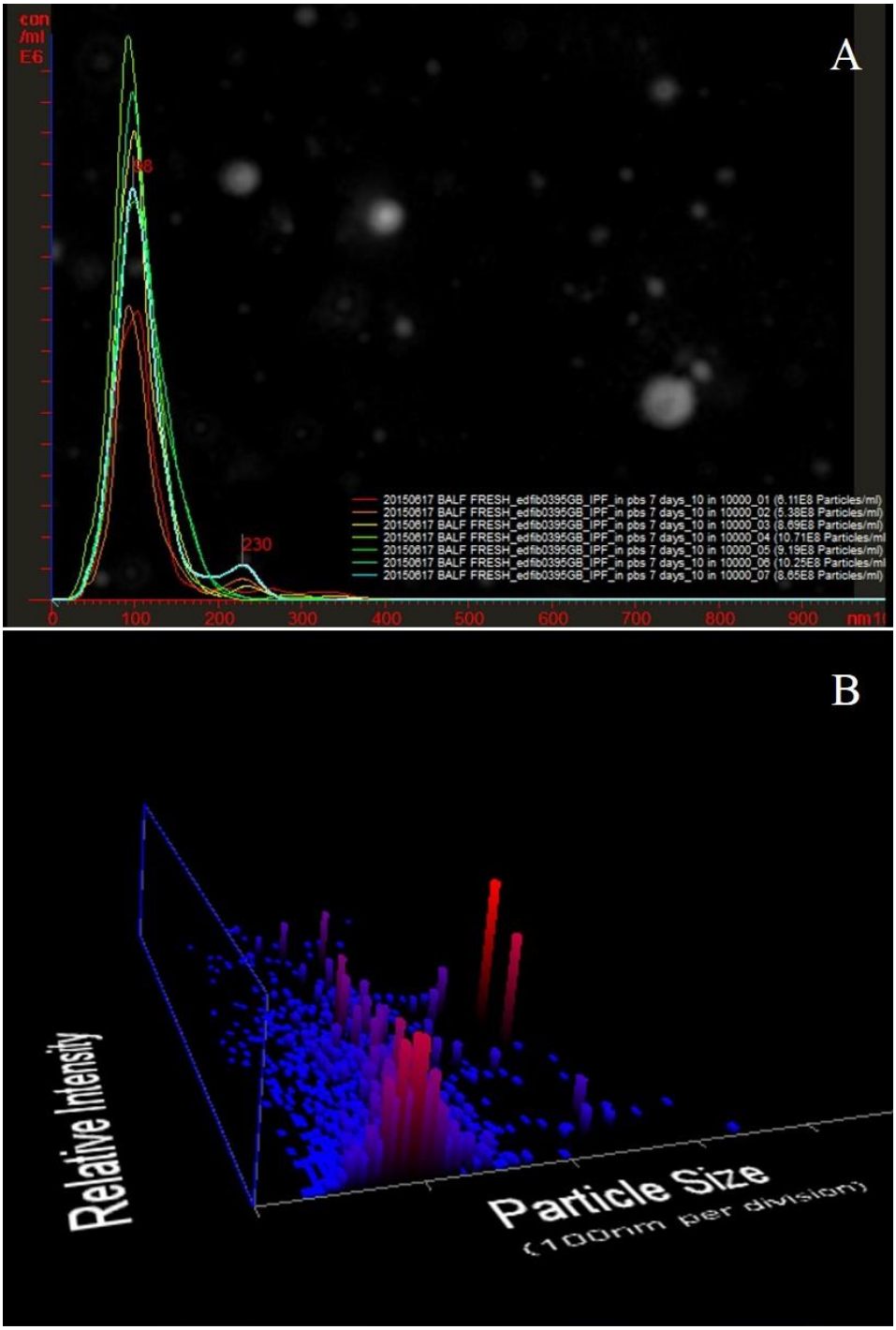

Figure 7-5 Measurement strategy and quality control of exosome study with NTA.

Normal distribution of BAL fluid vesicles. Each sample was measured at least 6 times and the area under curve of 40 nm - 100 nm was calculated to represent the exosome level and was used for analysis. (B) Small vesicles were the major EVs in the BAL fluid. Intensity against particle size: low level (blue & short), high level (red & tall).

7.4.6 BAL fluid from fibrotic ILD had low levels of exosomes, total exosomal proteins, and total exosomal RNAs

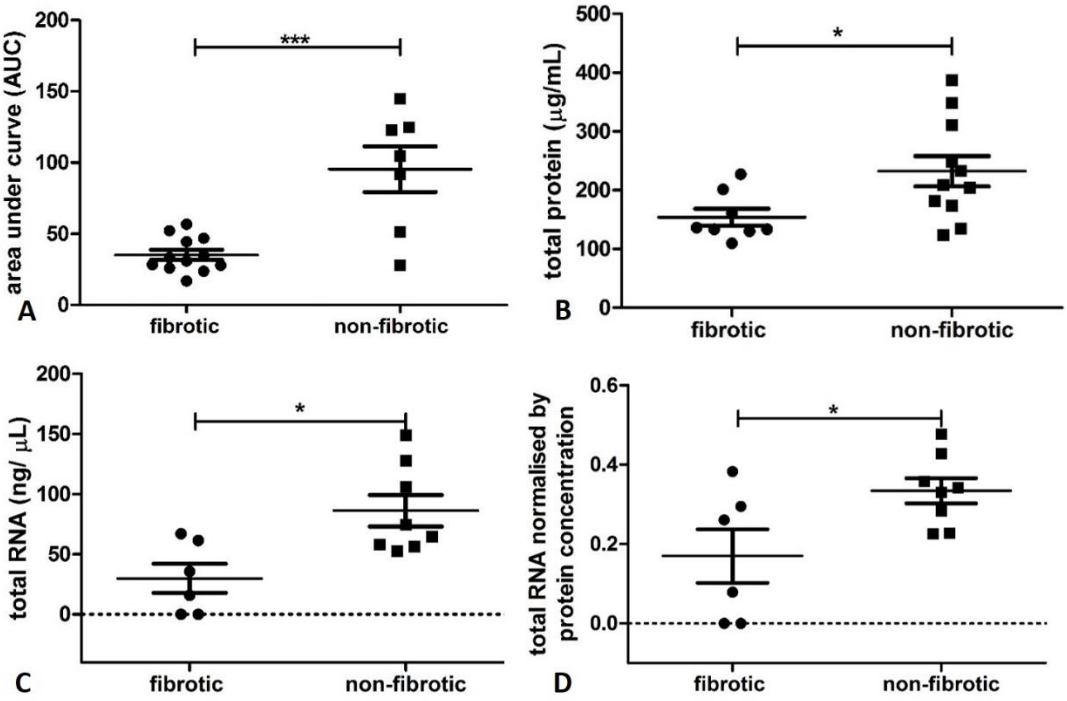

Figure 7-6 BAL fluid from fibrotic ILD had low levels of exosomes, total exosomal proteins, and total exosomal RNAs.

Fresh BAL fluid was retrieved from patients and kept on ice before further processing. (A) Exosome concentration was determined with NTA (fibrotic ILD n=12 and non-fibrotic ILD n=7). (B & C) Exosomes were isolated by ultracentrifugation from 6 mL of BAL fluid then re-suspended in 250 µL of PBS for total protein assay (B, fibrotic n=8, and non-fibrotic n=11) or the extraction of total RNA (C, fibrotic n=6, and non-fibrotic n=8) and the results were compared. (D) Normalised total RNA concentration with the total protein concentrations. * $p<0.05$, ***$p<0.001$, student t-test.

Results showed that the exosome concentration in alveolar space was significantly decreased in the fibrotic ILD compared with the non-fibrotic ILD (35.16 ± 3.54, n=12 vs 95.44 ± 15.95, n=7, $p<0.001$), and the exosome in non-fibrotic ILD was 2.7 fold higher.

BAL exosomes were isolated from the same volumes (6 mL) of fresh BAL fluid for total protein or total RNA. The protein concentration of pelleted exosomes was lower in fibrotic ILD than that of non-fibrotic ILD (154.10 ± 14.24 µg/ mL, n=8, vs 232.40 ± 25.73 µg/ mL, n=11, $p<0.05$).

The total RNA concentration of fibrotic ILD was lower than that of non-fibrotic ILD (30.00 ± 12.10 ng/ µL, n=6 vs 86.21 ± 13.05 ng/ µL, n=8, p=0.01). When normalised the total RNA with total protein, the results showed the same finding that in fibrotic ILD there was less RNA than the non-fibrotic ILD (1.70 ± 0.67, n=6 vs 3.34 ± 0.32, n=8, p=0.03). Given the nature of the BAL fluid and the isolation process, with 1.67 ± 0.07 (mean ± SD, n=14) as the A260/A280 for quality control, the results were acceptable.

Since the level of BAL fluid exosomes was lower in the ILD with lung fibrosis, the level of BAL fluid exosomes and its association with disease progression were studied with banked BAL fluid samples.

7.4.7 Low level of baseline BAL exosome may be associated with progressed IPF

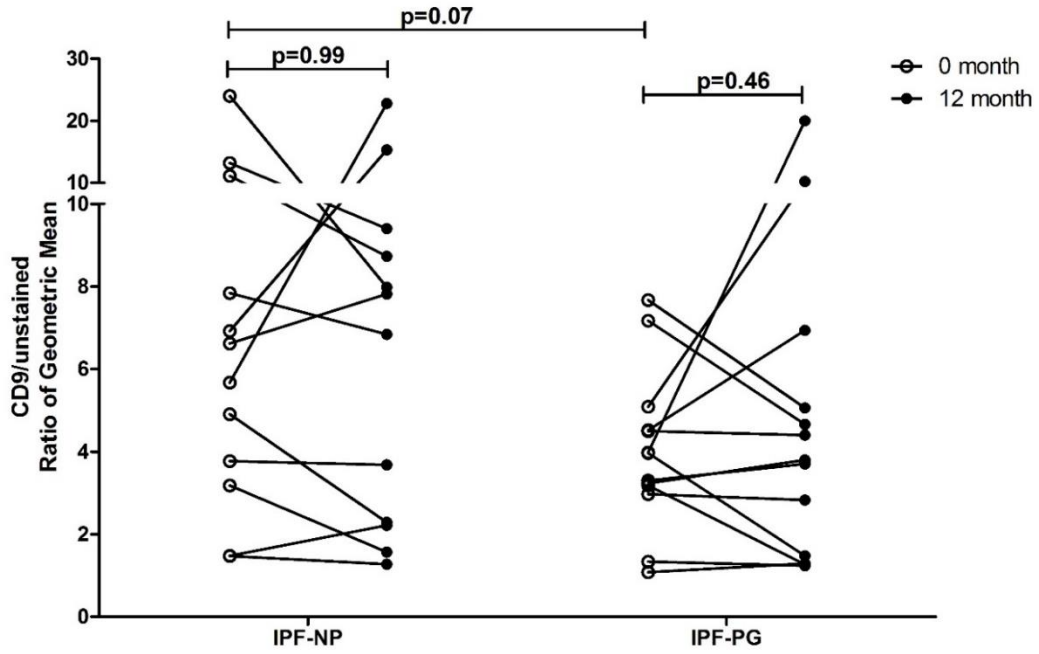

Figure 7-7 Low level of baseline BAL exosome may be associated with progressed IPF.

BAL fluid samples (stored at -80 ºC) were defrosted and the level of exosomes was measured using anti-CD9 beads flow cytometry assay. IPF-NP: stable IPF (non-progressor); IPF-PG: progressed IPF. Disease progression was defined as a ⩾10% decline in FVC or death within 12 months. Open circle: 0 months (baseline), solid circle: 12 month; Within the group paired student t-test, between stable IPF (n=12) and progressed IPF (n=13) unpaired student t-test.

The exosome level in defrosted BAL fluid was determined with anti-CD9 beads flow assay and represented as the fold change of CD9 fluorescence (stained against unstained).

From stable IPF patients, results suggested that there were no significant changes of exosome levels during the 12 month period (0-month vs 12-month = 7.51 ± 1.81 vs 7.49 ± 1.84, n=12, paired t-test, p=0.99).

With progressed IPF the changes of BAL fluid exosomes were not observed either: 0-month vs 12-month = 4.00 ± 0.53 vs 5.14 ± 1.43, n=13, paired t-test, p=0.46. However, the baseline BAL exosome level (0-month) in the progressed IPF was lower than that of stable IPF (p=0.07). This suggested that low baseline exosome level in BAL fluid might be associated with progressed IPF. However, these findings need to be better characterised and validated with a larger cohort.

Besides, the concentration of exosomes, another important question to be addressed was the origin of these exosomes. Particularly, in a macrophage dominating lung disease, the contribution of macrophages to the exosome pool in IPF lungs was studied with a panel of specific markers that expressed on immune cells in the alveolar space including monocyte/macrophage markers.

7.4.8 BAL fluid exosomes retrieved from ILD patients did not express common monocyte/ macrophage surface proteins

In order to study the origin of the alveolar exosomes, exosomes were coupled with anti-CD9 beads and a panel of monocyte/ macrophage markers were investigated. CD9 expression was used to confirm the successful isolation of exosomes (data not shown).

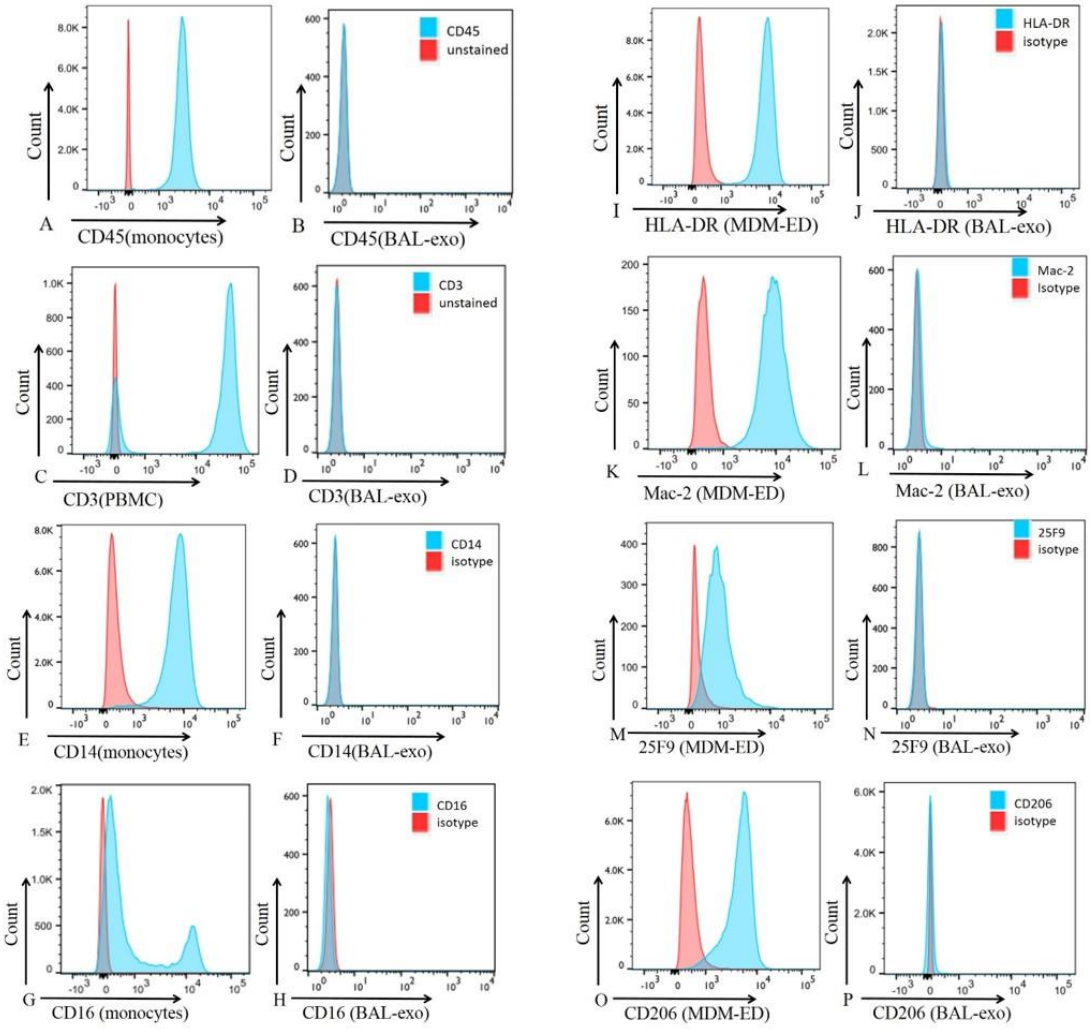

Figure 7-8 BAL fluid exosomes retrieved from ILD patients did not express common monocyte/ macrophage surface proteins.

Common monocyte/ macrophage surface proteins such as CD14 (F), CD16 (H), HLA-DR (J), Mac-2 (L), 25F9 (N), CD206 (P) were not detected on alveolar exosomes. General leucocyte protein CD45 (B) and lymphocyte marker CD3 (D) and were not detected. Different cells (PBMC, monocytes, MDM-ED macrophage) were used as positive controls as indicated in the figure. Representatives of n=6 experiments (fibrotic ILD, n=3, non-fibrotic ILD n=3).

So far, the impact of an impaired autophagy pathway on exosome release in the alveolar macrophages had been studied. Less MVBs were found in fibrotic AM and low concentration of exosomes were found in the culture medium in these macrophages. Low level of exosomes was found in BAL fluid from patients with lung fibrosis and may be associated with disease progression. Macrophage markers were not detected on exosomes.

In the following experiments, the interaction of autophagy-exosome pathways was further explored with *in vitro* models. The effect of exosome release by the modulation of the autophagy pathway in MDM was studied.

7.4.9 Rapamycin and bafilomycin A1 treated MDM contained MVBs and autophagic vacuoles

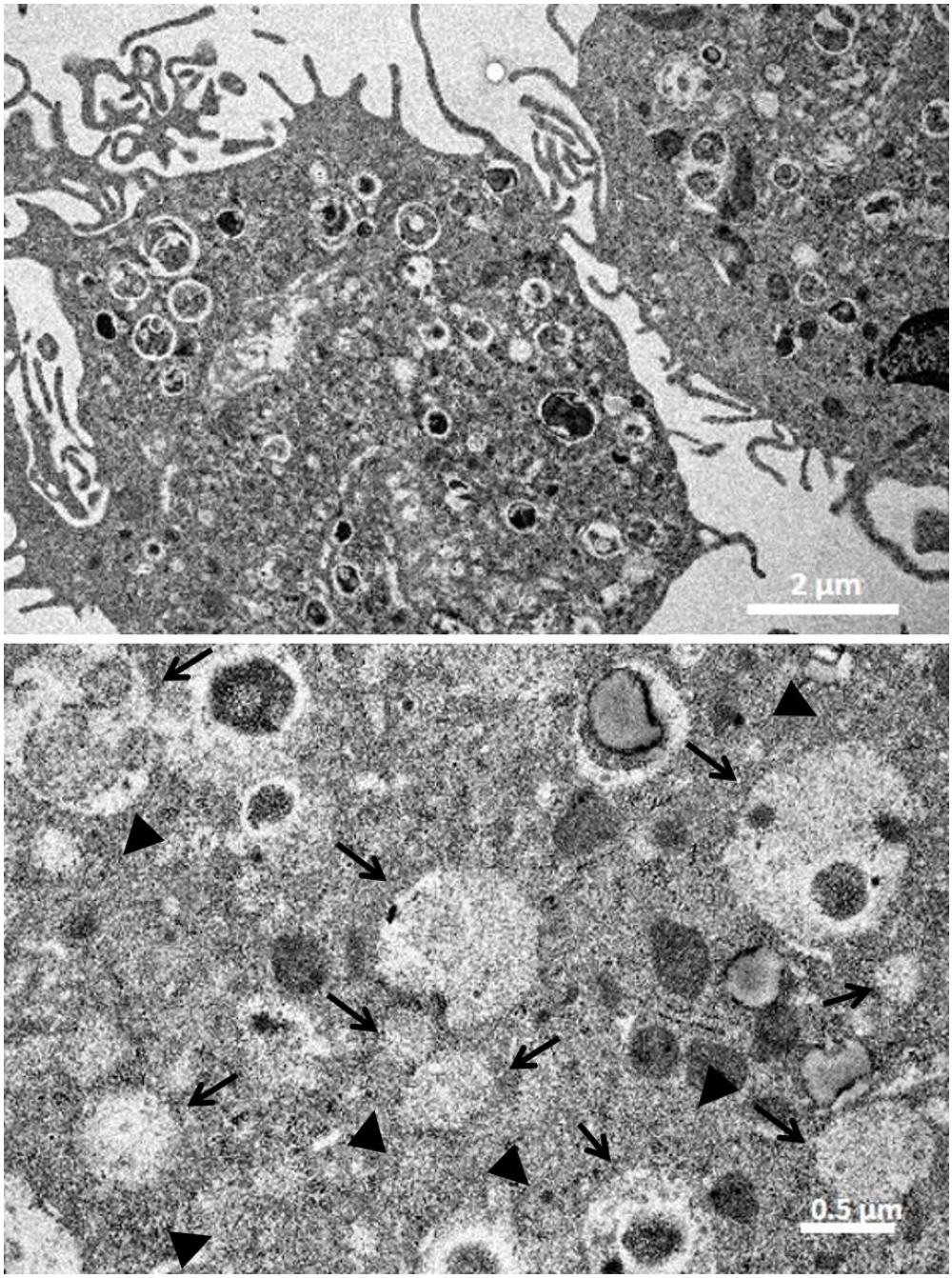

Figure 7-9 Rapamycin and bafilomycin A1 treated MDM contained MVBs and autophagic vacuoles.

Rapamycin and bafilomycin A1 treated MDM contained MVBs (arrowed) and autophagic vacuoles (arrowhead). MDM were treated with 25 µM rapamycin and 50 nM bafilomycin A1 for 4 hours before they were fixed and processed for TEM analysis. Scale bar =2 µm (A) and 0.5 µm (B).

7.4.10 Modulation of autophagy-lysosome pathway changed the concentration of MDM-released exosomes into culture media

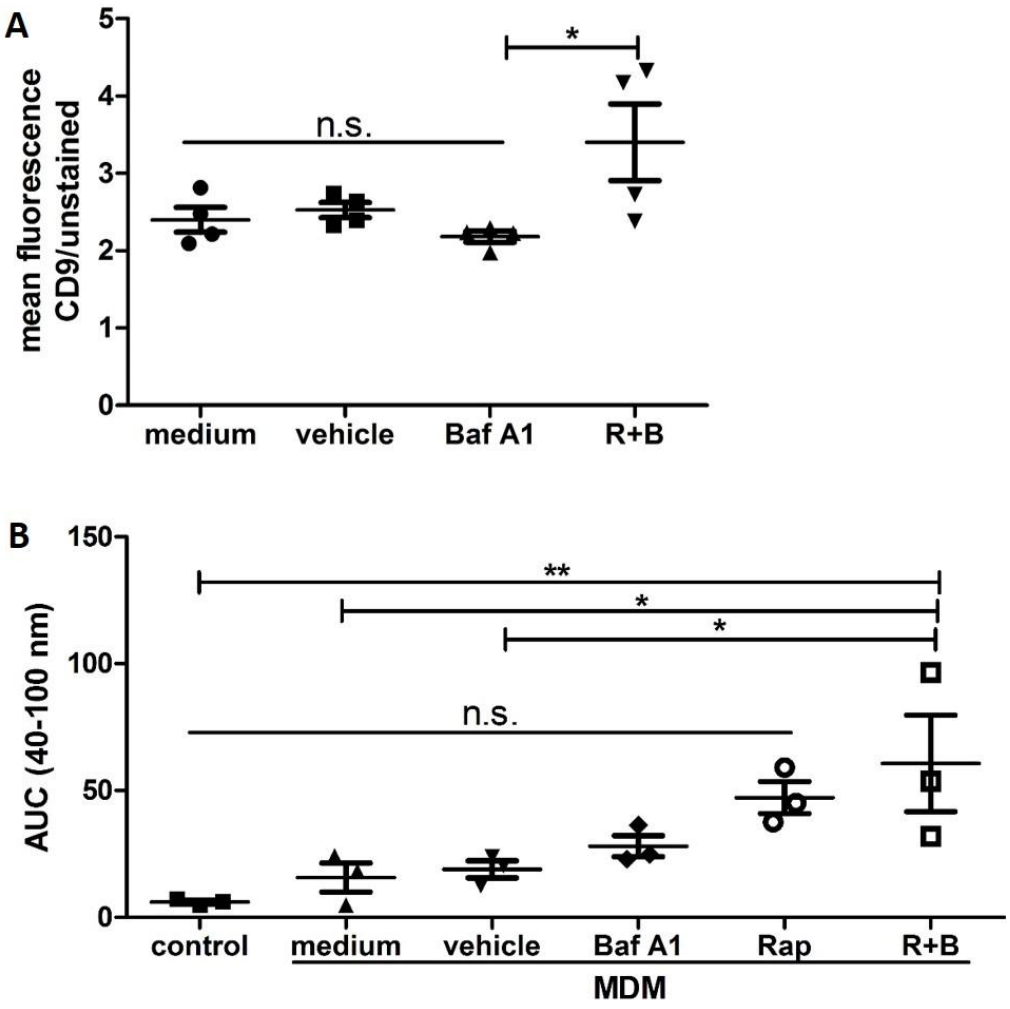

Figure 7-10 Modulation of autophagy changed the concentration of MDM-released exosomes into the culture media.

The concentration of exosomes was determined by (A) anti-CD9 beads flow assay and (B) NTA analysis of exosome levels in different conditions. Each sample was measured 4 times and a mean was used for statistical analysis. Control: distilled water. Monocytes were differentiated to macrophages (MDM) for 7 days and cells were treated as indicated conditions for 4 hours: medium: IMDM+10% FBS (filtered); vehicle: DMSO (as RB) diluted in culture medium; Baf A1: bafilomycin A1, 50 nM; Rap: rapamycin 25 μM; R+B: Baf A1 and Rap. *$p<0.05$, n.s. not significant, one-way ANOVA, Tukey's Multiple Comparison Test, n=4 (A) and n=3 (B).

Supernatants following treatments were coupled with anti-CD9 beads for flow cytometry analysis (A). Exosome levels were higher when MDM were treated with both rapamycin and bafilomycin comparing with bafilomycin alone (3.40 ± 0.50 vs 2.18 ± 0.07, n=4, $p<0.05$), whereas no difference was observed between bafilomycin A1 treatment and medium or vehicle control (2.18 ± 0.07 vs 2.40 ± 0.16 vs 2.53 ± 0.10, n=4, n.s.).

Another set of experiments were performed and exosome levels were measured by NTA (B). Results showed that MDM treated with rapamycin and bafilomycin A1 for 4 hours had increased exosome levels in the supernatant compared with treatment of the medium control or vehicle control (60.71 ± 18.97 vs 15.74 ± 5.74, $p<0.05$ and 60.71 ± 18.97 vs 18.94 ± 3.39, $p<0.05$). Although the exosome levels in the media treated only with bafilomycin A1 (28.04 ± 4.16) or only with rapamycin (47.24 ± 6.33) were not significantly changed compared with the controls.

Together both sets of data suggested that modulation of the autophagy pathway regulates the exosome secretion in macrophages. Furthermore, the effect of BAL fluid exosome on the autophagy pathway in MDM *in vitro* was studied.

7.4.11 Internalisation of BAL fluid exosomes into MDM

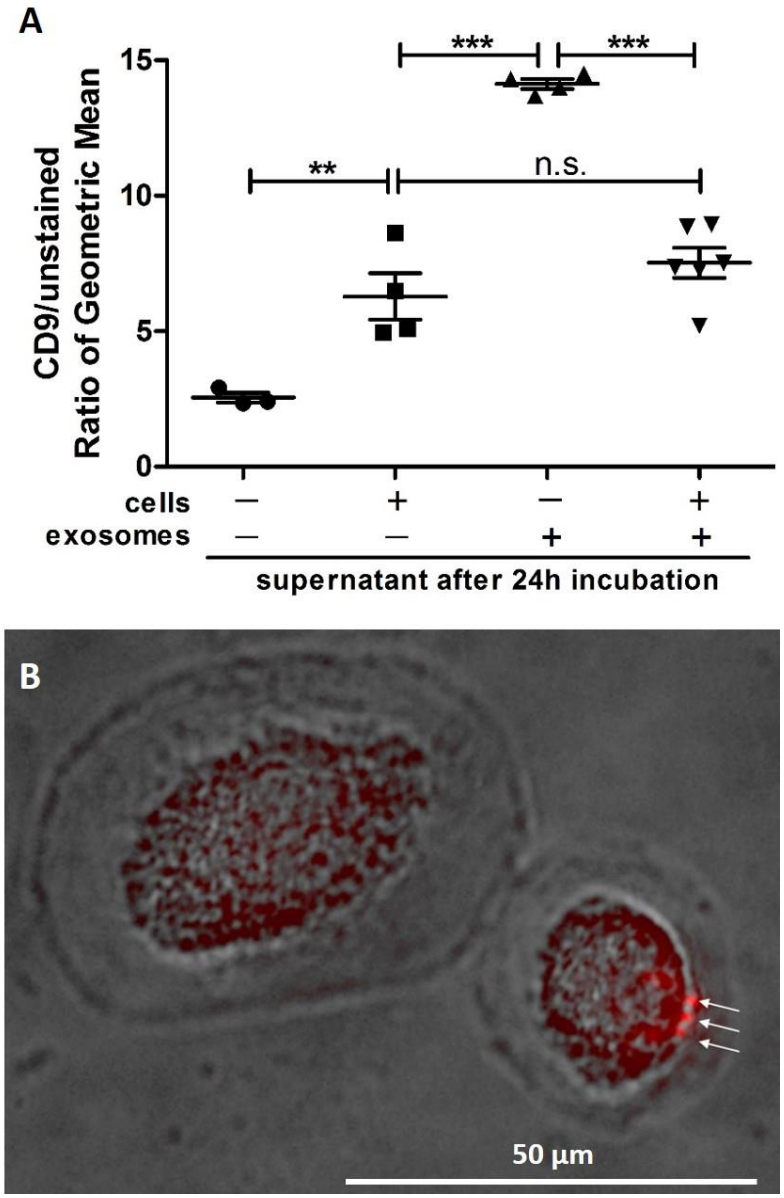

Figure 7-11 Internalisation of BAL fluid exosomes into MDM.

(A) The number of BAL fluid exosomes were decreased after culture with MDM. Pelleted BAL fluid exosomes (30 µg) were incubated with MDM for 24 hours. Exosome concentration in different media after the experiment was determined with anti-CD9 beads based flow cytometry assay and represented as mean fluorescence (MFL) of CD9. **p<0.01, *** p<0.001, n.s. not significant, one way ANOVA, Tukey's multiple comparison tests; (B) exosomes were stained with Q-tracker (red) before the incubation with MDM for 24 hours. After the incubation, cells were rinsed with PBS before the image was taken. Exosomes (arrowed) were observed within a macrophage and near the nucleus, scale bar = 50 µm.

As shown above, the mean of the exosome levels (CD9 MFL) in the culture medium after 24 hours culture of MDM [cells(+)/exosomes(-)] was significantly increased when compared to the control medium [cells(-)/exosomes(-)] (6.29 ± 0.86 vs 2.55 ± 0.18, $p<0.01$). The change was 2.46 fold which suggested that culture of MDM released a significant amount of exosomes into the medium.

Exosomes were pelleted from BAL fluid and the resuspended BAL fluid exosomes [cells(-) / exosomes(+)] had the highest concentration among all the conditions. The incubation with MDM had significantly decreased the exosome level (14.13 ± 0.18 vs 7.53 ± 0.55, $p<0.001$). After incubation, the exosome level dropped to a level equivalent to the MDM culture medium (7.53 ± 0.55 vs 6.29 ± 0.86, $p>0.05$). The decrease of exosomes in the presence of MDM indicated that exosomes were engulfed by the macrophages after the 24 hours of incubation.

Stained exosomes were observed within some macrophages after the incubation with MDM. Exosomes were located near to the cell nucleus which was a typical location of internalised exosomes.

To test whether the external exosomes had activated the autophagy pathway, cell lysates from the above experiment were prepared for western blot and probed for LC3 expression.

7.4.12 BAL fluid exosomes increased LC3-II expression in MDM

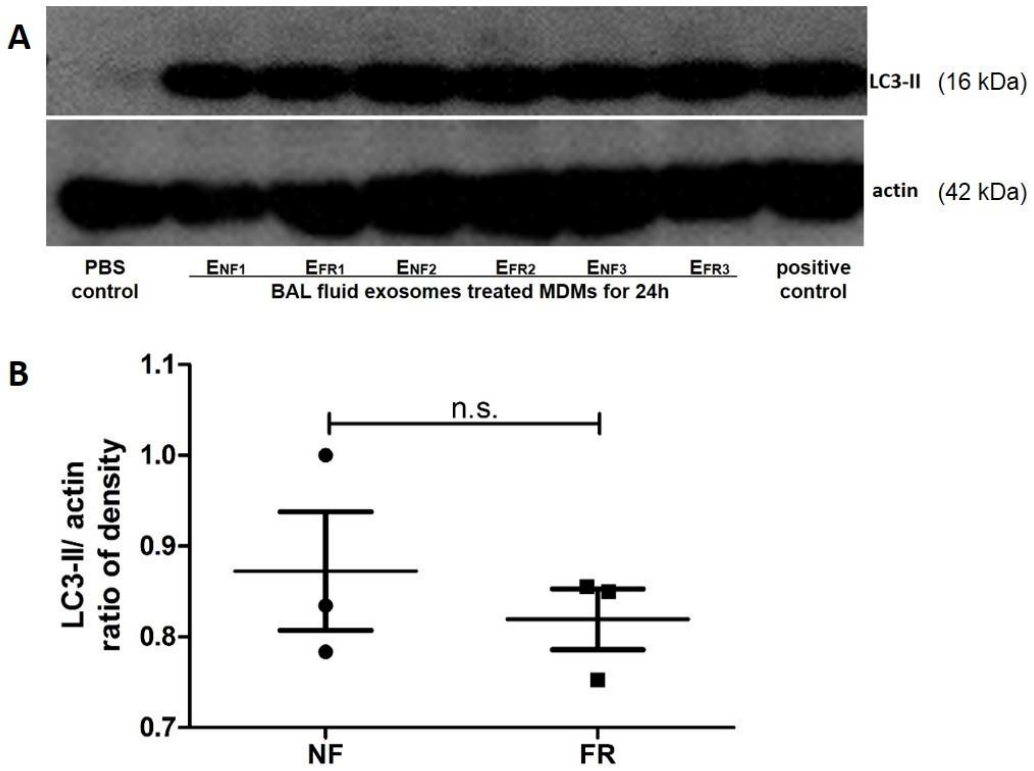

Figure 7-12 BAL fluid exosomes increased LC3-II expression in MDM.

(A) Western blotting probing for LC3-II expression. E_{NF}: pelleted BAL fluid exosomes from non-fibrotic ILD; E_{FR}: pelleted BAL fluid exosomes from fibrotic ILD; positive control: bafilomycin A1 (50 nM) treatment for 4 hours; (B) densitometry analysis of LC3-II expression. NF, non-fibrotic; FR, fibrotic. Student t-test, n.s. not significant.

7.5 Summary and Discussion

Autophagy and exosome formation are closely related processes in the maintenance of cell homoeostasis. The present study has demonstrated the interaction between the autophagy-lysosome pathway and the exosome machinery in lung fibrosis.

7.5.1 Low exosome levels are associated with fibrotic ILD

ILD is an entity that covers more than 100 different diseases [146]. One strategy to categorise ILD is based on the degree of inflammation and fibrosis of the condition [79]. It is well recognised that in fibrotic lungs, particularly in UIP, there is only mild inflammation presented [80, 81]. Interestingly, studies have shown that inflammation generally increased exosome secretion. In a mouse model of hepatitis, inflammation increased the number of circulating exosomes [526]. In sarcoidosis, an active immune disease that mainly affects the lungs, a link between active inflammation and increased exosomes activity had been reported [391]. Thus, the finding that exosomes have decreased in number in the fibrotic lungs compared to non-fibrotic ILD as presented in this study is not unexpected.

It is not known whether the lack of inflammation in IPF contributes to the low level of exosomes or less exosomes result in little inflammation in the fibrotic lungs. However, a loop of "low exosomes and little inflammation" may aggravate the condition in lung fibrosis.

As shown in this study, low exosome levels in the BAL fluid were determined in the fibrotic lungs (Fig 7.6). Furthermore, low level of exosomes in IPF patients may be associated with disease progression (Fig 7.7). Recently, a study showed an inverse relationship between the exosomes level in plasma and the stage of lung cancer, i.e., the more advanced cancer, the lower the concentration of exosomes [423]. In lung fibrosis, the deficiency of alveolar exosomes and their content suggested that they might be a potential indicator for the status of the diseases and may be a candidate for a treatment strategy.

Though there is little inflammation in IPF lungs as determined at the histological level at the point of diagnosis, inflammation may indeed be a critical factor in the development of the disease [527]. The types of cells and their status change dramatically

during lung inflammation and wound healing [528]. The continuous inflammation due to chronic lung epithelium injury may alter the exosome pool in the alveolar space dynamically. Thus, exosomes might serve as a good candidate of monitoring lung fibrosis as proposed in other lung diseases [317]. Besides the number of exosomes, their cargo protein and especially microRNA cargos are more likely to be distinct at different stages of lung fibrosis similar to other lung conditions [317]. In the later stage of established lung fibrosis, excessive ECM in the interstitial space provides cells with a unique micro-environment which might interrupt and compromise cellular communication.

7.5.2 The origin of alveolar exosomes in IPF

Besides the commonly expressed proteins, EVs may also carry membrane protein of their parent cells [331]. In the present study, the anti-CD9 beads based flow cytometry assay showed that alveolar exosomes do not express the monocyte/ macrophage lineage surface proteins that included monocyte markers (CD14 or CD16), alveolar macrophage markers (HLA-DR, Mac-2, and 25F9) or CD206 (alternatively activated macrophages). However, this does exclude macrophages contributing to the exosomal pool in the IPF lungs and in theory, they should be one of the dominant cell populations in the alveolar space. In fact, the exosomes released by human MDM on day-7 or human AM in tissue culture did not express the panel of markers tested (data not shown). The understanding of macrophage-derived exosomes in resting or stimulated status need to be further studied.

Besides macrophages, there are more than 40 types of different cells in the lungs [529]. All of them may contribute to the alveolar exosome pool. Thus, I also tested the expression of cell surface markers of other cell types included CD45 (leucocyte), CD3 and CD75 (lymphocyte), CD11b and CD11c (myeloid origin cells), CD42a (platelets) and Ep-CAM (epithelium cells) and none of these were expressed on BAL fluid exosomes (data not shown).

Microvesicles reflect the surface proteins of the membrane composition of the parent cell more closely than exosomes [323]. A mouse model of LPS induced acute lung injury (ALI) suggested that the mouse AM-derived EVs (F4/80 and CD11c as markers)

were the major population in the early phase of ALI and contributed the most to the inflammatory process [401]. The NTA data showed that in ILD BAL fluid samples, the sizes of the majority vesicles were below 200 nm and microvesicles in ILD were in very small numbers. Thus, the absence of cell surface marker supported the notion that exosomes are the major EVs in the ILD lungs.

Macrophage-derived exosomes have been shown to be functional vesicles [402-404]. Inflammation and infection can change the profile and function of macrophage-derived exosomes [396, 402]. In fact, different phenotypes of macrophages release specific exosomes with distinct properties [396]. My data showed that fibrotic AM released less exosomes *ex vivo* which suggested that the deficiency of macrophage exosomes might be an important mechanism that is associated with lung fibrosis. Characterisation of the exosomal protein and RNA profiles that are specific to unique cell types, and exosomal function, could offer new insights and tools for the clinical management of IPF patients in the future.

7.5.3 The relationship between autophagy and exosome release

Constitutive autophagy promotes cell viability and enhances homoeostasis and it is closely associated with the endocytic-exosome pathway [348, 349]. As shown in my study and by others, the modulation of autophagy can change the number of exosomes and also affect the cargos and surface protein components in exosomes [327].

In this study, I showed that fibrotic AM, which have impaired autophagy (chapter 6) released less exosomes than non-fibrotic AM which have normal functional autophagy, *ex vivo*. Modulating autophagy by treating MDM pharmacologically for a period of 4 hours resulted in no change in exosome secretion with bafilomycin, increased exosome secretion with rapamycin, and a further increase in exosome release with rapamycin and bafilomycin. (Fig 7.10). These data suggested a relationship between autophagy activity and exosome release in macrophages. Furthermore, the results of *in vitro* experiments are consistent with the clinical observation of exosomes in BAL fluid from fibrotic and non-fibrotic patients. Firstly, these data explained the effect of impaired autophagy on exosome secretion of AM as presented here (Fig 7.4). Non-fibrotic AM had functional autophagy, similar to MDM treated with rapamycin which correspondingly showed

increased exosomes *ex vivo*. In contrast, fibrotic AM had blocked autophagy, similar to MDM treated with bafilomycin, and correspondingly released less exosomes than non-fibrotic (or rapamycin-treated) cells. Secondly, these data support the clinical data of fresh BAL fluid samples which showed that the exosome levels were higher in non-fibrotic ILD (more inflammation and active autophagy) and lower in the fibrotic ILD (little inflammation and blocked autophagy) (Fig 7.6). Finally, the data presented here may suggest that the exosome machinery in AM might have been damaged during the development of lung fibrosis. There might be a stage when AM actively release exosomes when lysosomes are dysfunctional but with activated autophagy (similar to rapamycin and bafilomycin treatment). As the disease progresses, further damage may occur to the exosome machinery that leads to the final status as presented here that is similar to bafilomycin treated cells.

In theory, the induction of autophagy should limit exosome secretion and the blockage of lysosomal function should enhance it. In K562 cells, it was shown that autophagy induction promoted the fusion of MVBs with autophagosomes and therefore decreased the secretion of exosomes [353]. On the other hand, blockage of lysosome function by bafilomycin A1 increased the secretion of exosomes in a couple of studies [354-356]. It might be possible that different cell types respond differently to autophagy manipulation. The precise interaction between autophagy and exosome biogenesis in MDM needs to be further clarified. The exact mechanism by which autophagy blockage may impair exosome release in AM needs to be further studied.

7.5.4 Autophagy and exosomes as potential targets for intervention in lung fibrosis

Further studies, particularly the functional nature of exosomes in lung fibrosis are required, but the autophagy pathway an exosome release may be an attractive target for therapeutic intervention. Others have speculated that in established disease, intervention through the autophagy pathway might not be effective in the treatment of IPF [530]. In this study, I have shown that the autophagy-lysosome pathway is blocked in AM. Thus, the treatments targeting the autophagy pathway should probably start at an earlier stage of the disease, in order to gain clinical benefits for the patients.

There are on-going efforts to further test the effectiveness of modulating autophagy as a target for the treatment of IPF [531]. As mentioned earlier, animal models consistently showed that the promotion of autophagy pathway is beneficial and disruption is harmful [297, 298, 301] but the precise mechanism for inducing benefit or harm is not clear. Gui and colleagues showed chloroquine, a blocker of lysosome function, did not rescue bleomycin-mediated mouse death and when rapamycin was combined with chloroquine, mice had a higher mortality than rapamycin alone [298]. If autophagy is regarded as a therapeutic target of IPF treatment, exosomes may be the downstream mediators that exert the biological effect. Exosome levels could be used as a tool to identify the fibrotic conditions and to determine and predict disease progression (e.g., low exosomes levels and distinct proteins or RNAs) and to determine the effectiveness of treatment. It would be prudent to better define the exact role and utility of exosomes and their relation to autophagy using for example animal model of lung fibrosis before other applications.

Chapter 8 Final discussion

In this thesis, I investigated the autophagy pathway in AMs in interstitial lung disease and the effect of ECM on macrophage autophagy. Furthermore, I studied the exosome profile in the BAL fluid and linked this to the impaired autophagy in IPF lungs.

8.1 ECM regulates autophagy pathway and exosome secretion in macrophage in IPF lung

Macrophages orchestrate the major events in the alveolar space including having an essential role in normal wound healing.

As shown in Fig. 8-1, upon epithelial injury, macrophages mediated the normal wound healing process and are responsible for the removal of dead cells and the resolution of inflammation. Newly derived type 1 epithelial cells eventually replace dead or apoptotic ones and bring the alveolar epithelial lining back to the normal condition. In this setting, if macrophage function is impaired in the first place, their ability to maintain cellular and tissue homoeostasis is compromised. As shown in the right panel in Fig 8-1, basal autophagy is upregulated under continuous cellular stress which results in increased number of autophagosomes in macrophages (stage-I). This consistent up-regulation of basal autophagy is believed to be a mechanism that leads to pathological consequences [532]. Aberrant wound healing may occur due to physiological, such as ageing and gene mutation/modification, or pathophysiological factors, such as smoking, air pollution and unknown reasons (stage-II of Fig 8-1). The failure of inflammation resolution exaggerates the response to tissue repair and leads to the proliferation and activation of lung fibroblasts, differentiation of myofibroblasts, excessive deposition of ECM and the formation of pathological structures such as fibroblastic foci (stage-III of Fig 8-1).

Macrophage autophagy, a key mechanism for maintaining cellular homoeostasis, may operate at different levels through these stages. The initial internal and external cellular stress results in the continuous low-level autophagy which attempts to remove cellular waste but may not do so efficiently (stage-I of Fig 8-1). If the autophagy pathway is further damaged, through pathological factors (local inflammatory mediators, ageing, smoking, genetic mutations etc.), this results in yet further impairment to the autophagy pathway and, as a consequence, dysfunctional autophagosomes are accumulated in

macrophages (stage-II of Fig 8-1). In this thesis, I have demonstrated that the autophagosome degradation is blocked in AMs from patients with lung fibrosis, and showed the presence of dysfunctional autophagosomes accumulated in these cells. If autophagy is induced continuously in a setting of blocked autophagosome degradation, this further exacerbates cellular dysfunction. The accumulated autophagosomes are regarded as newly formed cellular waste which will initiate the formation of the isolation membrane and the formation of autophagosomes to remove the un-degraded waste; however, the newly formed autophagosome would not be degraded and thus a cycle of continuous formation of dysfunctional autophagosomes is initiated which is detrimental to the cell. This un-resolving situation eventually leads to the loss of normal homeostatic function of the alveolar macrophage and the development of disease (stage-III of Fig 8-1).

ECM in the lung is dramatically altered during the development of IPF. I have demonstrated that autophagy is more active when cells are in contact with ECM and fibrotic ECM induces autophagy. Thus ECM assists in the formation and degradation of autophagosomes. ECM is a bioactive material. Collagen-I, the most abundant component in the ECM in IPF, also upregulated basal autophagy in macrophages *in vitro*. When the epithelial barrier is compromised, bioactive ECM peptides and debris come into contact with AMs and may modulate autophagy in AMs (stage-II). As the condition progressed, the enhanced production of ECM caused excessive deposition and the feature of IPF is then established (stage-III). With the existing blockage of autophagosome degradation in alveolar macrophages, the accumulation of autophagosomes may aggravate the situation in IPF lungs.

During the development of chronic lung fibrosis, the structures and cellular composition in the alveolar space are also changed. All these factors affect the profile of lung exosomes. In this study, I showed that in IPF, the overall exosome level was decreased. I have also demonstrated that AMs from the fibrotic lungs, in which the autophagosome degradation is blocked, released fewer exosomes to the culture media *ex vivo*. The precise mechanistic link between autophagy and exosome release needs further study. Other studies have shown that when normal autophagosome degradation is blocked, the release of exosomes is increased. The clinical studies in this thesis involved patients

with already established IPF and other ILDs (stage 2 or stage 3 of Fig 8-1), and mostly the samples were from a single time points. Thus, during the development of fibrosis, there may be stages where AMs actively release exosomes or when autophagosome degradation is still functional.

The functional status of autophagy and the level of exosome at different stages in IPF need to be further investigated and to be better characterised. In this study, participants in the fibrotic group were mainly diagnosed with IPF which unfortunately was in the late stage of lung fibrosis when diagnosed. Thus, the stages of disease are unlikely to change the findings presented in this theses as in fact, the stages of the diseases were the same. However, as a group of complicated diseases, ILD including IPF, the status of autophagy and the level of exosomes might actively change during the development of the disease as discussed. In future studies, these questions need to be answered with the premise of the established methodology for early diagnosis and categorising the stages in IPF.

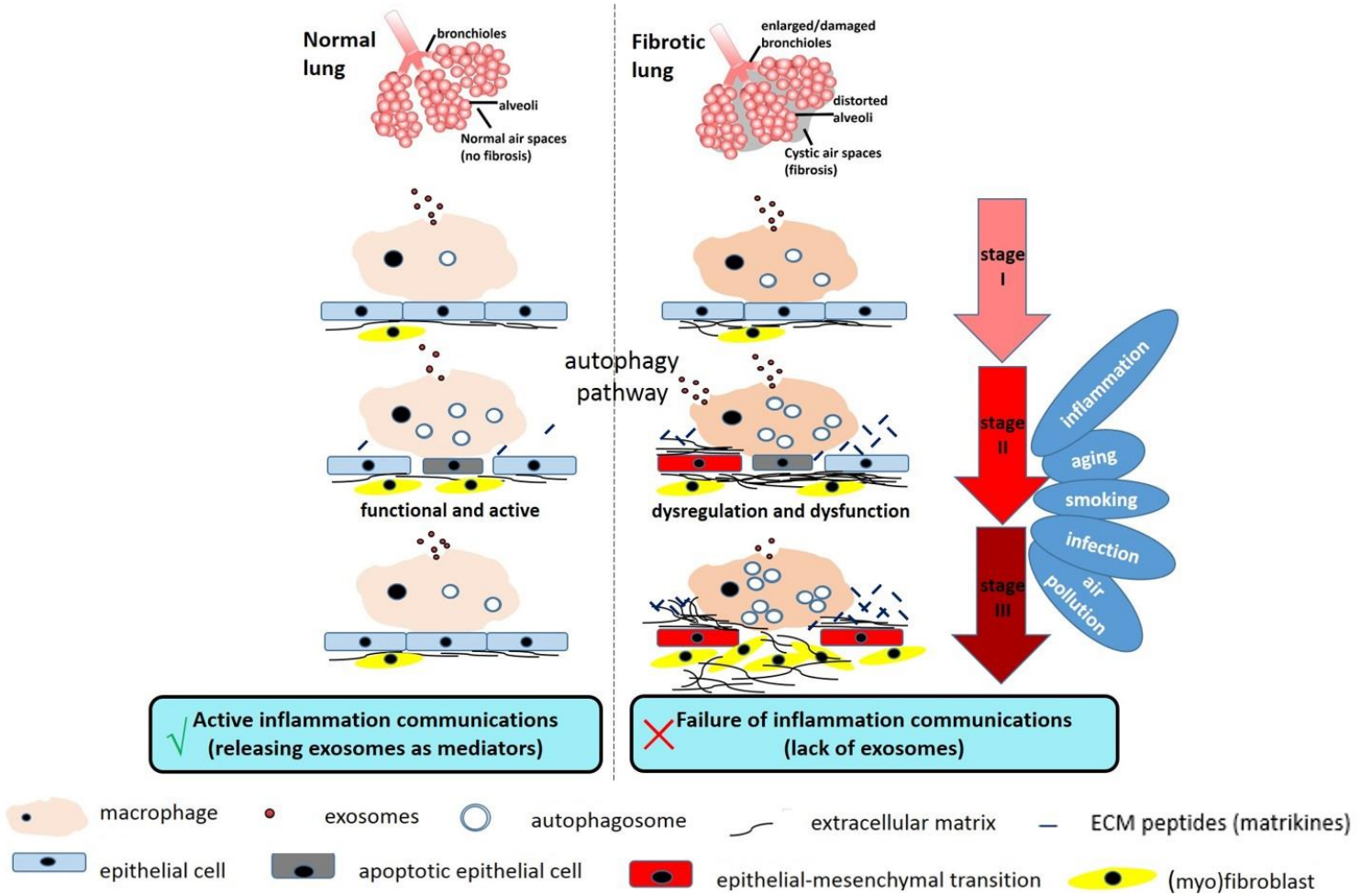

Figure 8-1 Extracellular matrix regulates the autophagy pathway and exosomes secretion in macrophages in the IPF lung.

Left panel, tissue repair, exosome release and autophagy in normal conditions; right panel, other factors such as inflammation, ageing, smoking, air pollution that contribute to the aberrant tissue repair and lung fibrosis.

8.2 The association between exosomes and inflammatory and fibrotic ILD

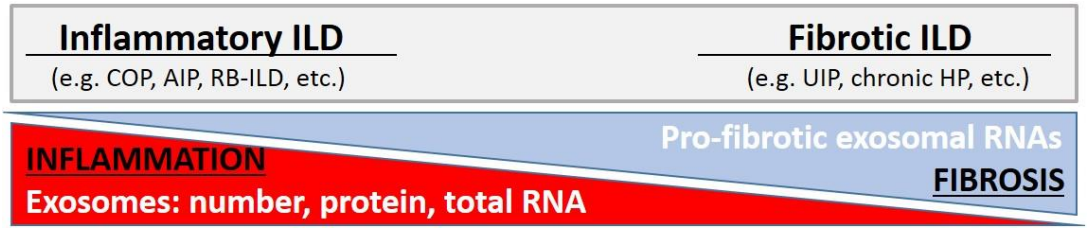

Figure 8-2 Inflammatory ILD has increased level of exosomes and total exosomal proteins and RNAs compared to fibrotic ILD.

The RNA and protein profile of fibrotic and non-fibrotic exosomes may also differ but has not been studied. For example, exosomes from different disease states may have different inflammatory, fibrotic or tissue repair properties mediated by microRNA or proteins.

According to the pathological patterns, ILD can be generally categorised into two groups depending on their status of inflammation and fibrosis [79]. UIP/IPF is characterised by lung fibrosis but little inflammation. The disease progression if IPF is thought to be a consequence of abnormal wound healing. Other ILD conditions are characterised as inflammatory-driven with limited fibrosis because wound healing is not impaired.

In my study, I showed that in IPF lungs there was significantly decreased the number of exosomes compared to other non-fibrotic ILD. Furthermore, the total exosomal protein and total RNA from the IPF lungs were significantly lower than those from non-fibrotic ILD. Most studies associate exosomes with active inflammation and suggest that exosomes are mediators of the inflammatory response. This may be the case in ILD that in fibrotic lungs, such as UIP and chronic HP that decreased level of exosomes may result in the lack of inflammation. On the contrary, in inflammatory ILD, there is a higher concentration of exosomes and increased contents mediating intercellular communication that contributes to active inflammation. Therefore reduced exosomes may be the reason that fibrotic ILD, such as IPF/UIP, exhibits little inflammation. My data also suggested that in patients with progressive IPF, the baseline level of exosomes is lower than in patients whose disease remained relatively stable over 12 months (‘non-

progressive'), which suggested that low exosome level in the lung may be a risk factor or predictor for disease progression.

Furthermore, in a larger scope, exosomes may be served as a candidate marker for inflammatory lung disease. To validate the observation of lower exosome-level in fibrotic ILD comparing to non-fibrotic ILD, other controls should be considered in future studies, such as age and sex-matched healthy volunteers and other types of lung conditions with active lung inflammation, e.g., COPD, ALI, lung cancer and pneumonia. As discussed in the first section (8.1) in detail, the exosome level might be actively changing at different stages IPF which need to be further characterised.

The specific protein and RNA profiles of fibrotic versus non-fibrotic exosomes have not been studied. For the disease-relevant proteins, it is necessary to compare the surface proteins that may mediate pro-inflammatory and anti-inflammatory pathways More interestingly, exosomal RNA in the fibrotic lungs may offer a disease marker for IPF/UIP and pro-fibrotic RNA may be present in these exosomes and might be implicated in lung fibrosis.

An alternative function for exosomes is that they mediate tissue repair. In collaboration with Prof. Donna Davies and Dr. Franco Conforti, we showed that depletion of exosomes from the BAL fluid may delay wound repair compared with original BAL fluid with exosomes in an *in vitro* epithelial wound assay (data not shown). The aberrant wound healing in IPF may be due to low levels of exosomes which carry proteins and RNA that mediate the epithelial healing. For example, exosomes exhibit heparin-binding epidermal growth factor-like growth factor (HB-EGF) and amphiregulin which are ligands for mammalian EGF receptor [533]. HB-EGF and amphiregulin can promote epithelial cell growth and are involved in epithelial wound healing. Thus, the function of BAL fluid exosomes needs to be fully explored.

8.3 Restore normal autophagy in alveolar macrophages as a strategy to treat IPF

The lysosome is the common destination for both the autophagosome and MVBs. The status of lysosomes is therefore critical in both pathways. IPF is associated with an aged population. Ageing can modulate the function of lysosomes and in aged cells,

lysosomes become less competent in dealing with cellular waste. As shown in my study, in fibrotic AMs the presence and accumulation of membranous cytoplasmic bodies (MCBs) suggested lysosomal dysfunction. The fusion of autophagosomes and lysosomes was likely not affected based on the co-localisation of autophagosomes and lysosomes. However, with other tools and assays dissecting the lysosome key proteins, enzymes, RNAs and the pH changes (acidity) may help understand this important type of organelles in both exosome and autophagy pathways in macrophages [534, 535]. Based on current evidence, restoration of the normal autophagy-lysosome pathway in the fibrotic AMs should be targeted at promoting the production and function of lysosomes [536]. Induction of lysosomal biogenesis by genetic or pharmacological activation of lysosomal transcription factor EB restored lysosomal levels [537]. Promotion of lysosome was tested in the animal model of brain diseases and effectively restored brain function and memory [538-540].

My study showed that ECM increased autophagy in macrophages, but if the autophagosome degradation is blocked, the enhancement of autophagy by ECM will aggravate cellular dysfunction and lead to the further accumulation of dysfunctional autophagosomes. In theory, promoting functional lysosomal degradation is a strategy that can be used in the presence of fibrotic ECM.

Promoting lung homeostasis by targeting the key regulatory cell, i.e. alveolar macrophage, could be a strategy that benefits the prognosis of IPF. At different stages of IPF, the induction of autophagy should be cautious but the promotion of lysosome function may be more beneficial. Besides the promotion of lysosomal function in macrophages in advanced IPF, the strategy could be aimed at early stages of fibrosis before the "permanent" damage to the autophagy-lysosome pathway. Targeting the earlier window for intervention by enhancing the cellular communication via exosomes is a promising way for the management of IPF than in the advanced IPF.

8.4 Exosomes, a cell-free approach for IPF treatment

In my study, I have shown that the level of BAL fluid exosomes was significantly decreased in fibrotic ILD and progressive IPF. Fibrotic AMs, in which autophagy is blocked, also released fewer exosomes in the culture media *ex vivo*. Restoring the

intercellular communication via normal exosomes could possibly promote normal wound healing in the early stages and resolution of fibrosis.

Mesenchymal stem cell (MSCs) derived extracellular vesicles have successfully alleviated liver fibrosis [473], peritoneal fibrosis [541], kidney injury and fibrosis [542, 543] and bleomycin-induced lung fibrosis [544-546]. This suggested that exosomes alone could be used as a strategy to manage IPF in which exosome levels were decreased as shown here. Furthermore, exosomes are able to travel through ECM and be internalised into cells *in vitro*. Thus, the excessive ECM may not limit the communication through exosomes. In established fibrosis, exosomes can be used as messengers that move across the ECM barrier and targeting other relevant cells in the lung interstitium. This would be an effective means to deal with other cells under the epithelial lining such as fibroblasts and myofibroblasts. Exosomes can reprogram the cells towards fibrosis resolution other than pro-fibrosis.

Modulation of autophagy regulates the exosome biogenesis *in vitro* and restoring the normal autophagy pathway by the strategies described above may rescue exosome biogenesis. On the other hand, exosomes also affect the autophagy pathway. In this study, I also showed that BAL fluid exosomes can be internalised into MDMs *in vitro* and increased the LC3-II expression in macrophages. Thus, exogenous exosomes also modulate the autophagy pathway. This could be a physiological positive feedback loop that enhances cellular homeostasis and re-programmes the fibrosis process to normal wound healing. Restoring exosomes in fibrotic lungs with a specific population, such as macrophage-derived exosomes, may be beneficial for the resolution of normal tissue repair.

Another strategy to enhance functional exosome secretion in the fibrotic lung, rather than the autophagy pathway, is to deliver exogenous exosomes to the lung. Administration of mesenchymal stem cell-derived exosomes can rescue fibrosis in the bleomycin model. The systemic administration of exosomes intravenous improved the functional recovery of mice in models of stroke, brain tumour and brain damage [547-549].

8.5 Future work

For the future studies, there are still many questions that need to be addressed and to be better understood, such as the dissection of autophagy and exosome pathways in macrophages at different stages of fibrosis, targeting autophagy and exosomes as means of IPF management and the role of ECM in the development of IPF.

The blockage of autophagosome degradation has been identified in AMs in the fibrotic lungs, but the precise nature and the location of the blockage in AMs need to be defined. The present evidence suggests that the damage to the autophagy pathway is in the latter stages of the pathway, most likely dysfunctional lysosomes. The factors that contribute to this blockage might be many, such as ageing, genetic susceptibility, oxidative stress, ER stress, and smoking. It is valuable to exam the lysosome-related proteins in different groups of IPF such as familial and sporadic or divided by risk factors such as smoking history, biological age, and immunological age. The proteins and signalling mechanism relating to the fusion of lysosomes with autophagosomes also need to be studied. The ATP-dependent proton pump V-ATPase is essential for the maintenance of low pH within lysosomes, the subunits of V-ATPase might be impaired. There is also V-ATPase independent mechanisms for lysosome-autophagosome fusion [490]. These results can help to design the proper strategy for intervention. Enhancement of lysosomal production and function has shown benefits in neurodegenerative diseases, however, pharmaceutical compounds are not yet available.

As discussed, the role of macrophage autophagy during lung fibrosis may change at different stages of the process. The role of macrophage autophagy in lung fibrosis needs to be further studied with animal models. Firstly, a better understanding is needed of the changes in autophagy in lung fibrosis models, such as the bleomycin model. Furthermore targeting the autophagy pathway in conditional lung macrophage knockout mice, such as Atg knockout macrophages may reveal the function of macrophage autophagy in response to fibrosis stimuli.

The dynamic changes of the lung during the initiation, progression, and resolution of lung fibrosis in the bleomycin model of lung fibrosis could give insights on the human IPF. With the modern tools, using genetically modified mice, such as the macrophage-

specific lysosome gene knockout mice, will extend the understanding of current hypothesis. The course and outcome of fibrosis in the bleomycin model of these genetically modified mice would gain more knowledge towards the stages of intervention and the possibilities to reverse the progression with the promotion of lysosome function.

The exosome machinery is impaired in IPF but the mechanism and exact molecules need to be studied. As it is a pathway closely related to the autophagy pathway, it is interesting to further explore the interactions between the two pathways. The precise mechanistic link between autophagy and exosome release in the fibrotic AM needs to be further defined.

Exosomal surface proteins study did not reveal common surface markers for specific cells in the lung. However, specific RNA contents might give more information about the contribution of different cells to the exosome pool in IPF lungs. For example, it has been shown that M1 and M2 macrophages express exosomes with different RNA profiles [413]. Fully exploring the protein and in particular, the total and microRNA profile of fibrotic and non-fibrotic AM-derived exosomes will help understand the function of these exosomes. *In vitro* epithelial wounding models and co-culture 3D models of lung fibrosis would help to understand the potential pro-fibrotic or pro-resolution properties of the AM-derived exosomes.

ILDs are heterogeneous diseases, and the classification of the disease should be optimised for treatment and research. Low concentration of exosomes may be a candidate indicator for lung fibrosis and disease progression in fibrotic ILD. For the validation of low exosome concentrations as a potential indicator for lung fibrosis, it needs to be studied with a larger population in a separate (validation) cohort. The proteins and genetic cargos in exosomes also need to be further studied, in order to gain a better understanding of their functions. With proteomic and gene array assays, there is a chance to identify the disease-relevant proteins and RNAs in exosomes.

The role of bioactive ECM should also be further investigated. Targeting the cell surface integrins, lysosome motility, and position, and soluble ECM may be relevant to

understanding the cross-talk between ECM and autophagy-lysosome pathway [215, 291].

In summary, both impaired macrophage autophagy and decreased exosome secretion may serve as targets for therapeutic purposes for IPF. Restoring functional autophagy and normalising the intercellular communication through exogenous exosomes may slow the disease progression or even reverse the fibrotic condition.

REFERENCES

1. Prasad, R., et al., *Diagnosis of idiopathic pulmonary fibrosis: Current issues.* Intractable Rare Dis Res, 2015. 4(2): p. 65-9.
2. Basset, F., et al., *Intraluminal fibrosis in interstitial lung disorders.* Am J Pathol, 1986. 122(3): p. 443-61.
3. Kuhn, C. and J.A. McDonald, *The roles of the myofibroblast in idiopathic pulmonary fibrosis. Ultrastructural and immunohistochemical features of sites of active extracellular matrix synthesis.* Am J Pathol, 1991. 138(5): p. 1257-65.
4. Nho, R.S., *Alteration of Aging-Dependent MicroRNAs in Idiopathic Pulmonary Fibrosis.* Drug Dev Res, 2015. 76(7): p. 343-53.
5. Crapo, J.D., et al., *Cell Number and Cell Characteristics of the Normal Human Lung 1–3.* American Review of Respiratory Disease, 1982. 126(2): p. 332-337.
6. Stevens, T., et al., *Lung vascular cell heterogeneity: endothelium, smooth muscle, and fibroblasts.* Proc Am Thorac Soc, 2008. 5(7): p. 783-91.
7. Ryter, S.W., S.J. Lee, and A.M. Choi, *Autophagy in cigarette smoke-induced chronic obstructive pulmonary disease.* Expert Rev Respir Med, 2010. 4(5): p. 573-84.
8. Meltzer, E.B. and P.W. Noble, *Idiopathic pulmonary fibrosis.* Orphanet J Rare Dis, 2008. 3(1): p. 8.
9. Nalysnyk, L., et al., *Incidence and prevalence of idiopathic pulmonary fibrosis: review of the literature.* Eur Respir Rev, 2012. 21(126): p. 355-61.
10. Raghu, G., et al., *High prevalence of abnormal acid gastro-oesophageal reflux in idiopathic pulmonary fibrosis.* Eur Respir J, 2006. 27(1): p. 136-42.
11. Hutchinson, J., et al., *Global incidence and mortality of idiopathic pulmonary fibrosis: a systematic review.* Eur Respir J, 2015. 46(3): p. 795-806.
12. Navaratnam, V., et al., *The rising incidence of idiopathic pulmonary fibrosis in the UK.* Thorax, 2011. 66(6): p. 462-467.
13. Raghu, G., et al., *An official ATS/ERS/JRS/ALAT statement: idiopathic pulmonary fibrosis: evidence-based guidelines for diagnosis and management.* Am J Respir Crit Care Med, 2011. 183(6): p. 788-824.
14. Ley, B., H.R. Collard, and T.E. King, Jr., *Clinical course and prediction of survival in idiopathic pulmonary fibrosis.* Am J Respir Crit Care Med, 2011. 183(4): p. 431-40.
15. Chambers, R., *Abnormal wound healing responses in pulmonary fibrosis: focus on coagulation signalling.* European Respiratory Review, 2008. 17(109): p. 130-137.
16. Wilson, M.S. and T.A. Wynn, *Pulmonary fibrosis: pathogenesis, etiology and regulation.* Mucosal Immunol, 2009. 2(2): p. 103-21.
17. Ryter, S.W. and A.M. Choi, *Autophagy in the lung.* Proc Am Thorac Soc, 2010. 7(1): p. 13-21.
18. Taskar, V.S. and D.B. Coultas, *Is idiopathic pulmonary fibrosis an environmental disease?* Proceedings of the American Thoracic Society, 2006. 3(4): p. 293-298.
19. Steele, M.P., et al., *Clinical and pathologic features of familial interstitial pneumonia.* Am J Respir Crit Care Med, 2005. 172(9): p. 1146-52.
20. Baumgartner, K.B., et al., *Cigarette smoking: a risk factor for idiopathic pulmonary fibrosis.* Am J Respir Crit Care Med, 1997. 155(1): p. 242-8.
21. Selman, M., et al., *Accelerated variant of idiopathic pulmonary fibrosis: clinical behavior and gene expression pattern.* PLoS One, 2007. 2(5): p. e482.
22. Baumgartner, K.B., et al., *Occupational and environmental risk factors for idiopathic pulmonary fibrosis: a multicenter case-control study. Collaborating Centers.* Am J Epidemiol, 2000. 152(4): p. 307-15.
23. Hubbard, R., et al., *Risk of cryptogenic fibrosing alveolitis in metal workers.* Lancet, 2000. 355(9202): p. 466-7.
24. Pinheiro, G.A., et al., *Occupational risks for idiopathic pulmonary fibrosis mortality in the United States.* Int J Occup Environ Health, 2008. 14(2): p. 117-23.
25. Hubbard, R., et al., *Occupational exposure to metal or wood dust and aetiology of cryptogenic fibrosing alveolitis.* Lancet, 1996. 347(8997): p. 284-9.
26. Scott, J., I. Johnston, and J. Britton, *What causes cryptogenic fibrosing alveolitis? A case-control study of environmental exposure to dust.* Bmj, 1990. 301(6759): p. 1015-1017.

27. Tang, Y.W., et al., *Herpesvirus DNA is consistently detected in lungs of patients with idiopathic pulmonary fibrosis.* J Clin Microbiol, 2003. 41(6): p. 2633-2640.
28. Arase, Y., et al., *Hepatitis C virus enhances incidence of idiopathic pulmonary fibrosis.* World J Gastroenterol, 2008. 14(38): p. 5880-6.
29. el-Serag, H.B. and A. Sonnenberg, *Comorbid occurrence of laryngeal or pulmonary disease with esophagitis in United States military veterans.* Gastroenterology, 1997. 113(3): p. 755-60.
30. Tobin, R.W., et al., *Increased prevalence of gastroesophageal reflux in patients with idiopathic pulmonary fibrosis.* Am J Respir Crit Care Med, 1998. 158(6): p. 1804-8.
31. Lee, J.S., et al., *Does chronic microaspiration cause idiopathic pulmonary fibrosis?* The American journal of medicine, 2010. 123(4): p. 304-311.
32. Marshall, R.P., et al., *Adult familial cryptogenic fibrosing alveolitis in the United Kingdom.* Thorax, 2000. 55(2): p. 143-6.
33. Hodgson, U., T. Laitinen, and P. Tukiainen, *Nationwide prevalence of sporadic and familial idiopathic pulmonary fibrosis: evidence of founder effect among multiplex families in Finland.* Thorax, 2002. 57(4): p. 338-342.
34. García-Sancho, C., et al., *Familial pulmonary fibrosis is the strongest risk factor for idiopathic pulmonary fibrosis.* Respiratory medicine, 2011. 105(12): p. 1902-1907.
35. Fernandez, B.A., et al., *A Newfoundland cohort of familial and sporadic idiopathic pulmonary fibrosis patients: clinical and genetic features.* Respir Res, 2012. 13(1): p. 64.
36. Thomas, A.Q., et al., *Heterozygosity for a surfactant protein C gene mutation associated with usual interstitial pneumonitis and cellular nonspecific interstitial pneumonitis in one kindred.* Am J Respir Crit Care Med, 2002. 165(9): p. 1322-8.
37. van Moorsel, C.H., et al., *Surfactant protein C mutations are the basis of a significant portion of adult familial pulmonary fibrosis in a dutch cohort.* Am J Respir Crit Care Med, 2010. 182(11): p. 1419-25.
38. Wang, Y., et al., *Genetic defects in surfactant protein A2 are associated with pulmonary fibrosis and lung cancer.* Am J Hum Genet, 2009. 84(1): p. 52-9.
39. Kropski, J.A., et al., *A Novel Dyskerin (DKC1) Mutation Is Associated With Familial Interstitial Pneumonia.* Chest, 2014. 146(1): p. E1-E7.
40. Armanios, M.Y., et al., *Telomerase mutations in families with idiopathic pulmonary fibrosis.* N Engl J Med, 2007. 356(13): p. 1317-26.
41. Tsakiri, K.D., et al., *Adult-onset pulmonary fibrosis caused by mutations in telomerase.* Proc Natl Acad Sci U S A, 2007. 104(18): p. 7552-7.
42. Seibold, M.A., et al., *A common MUC5B promoter polymorphism and pulmonary fibrosis.* N Engl J Med, 2011. 364(16): p. 1503-12.
43. Zhang, Y., et al., *A variant in the promoter of MUC5B and idiopathic pulmonary fibrosis.* N Engl J Med, 2011. 364(16): p. 1576-7.
44. Fingerlin, T.E., et al., *Genome-wide association study identifies multiple susceptibility loci for pulmonary fibrosis.* Nat Genet, 2013. 45(6): p. 613-20.
45. Peljto, A.L., et al., *The pulmonary fibrosis-associated MUC5B promoter polymorphism does not influence the development of interstitial pneumonia in systemic sclerosis.* CHEST Journal, 2012. 142(6): p. 1584-1588.
46. O'Dwyer, D.N., et al., *The Toll-like receptor 3 L412F polymorphism and disease progression in idiopathic pulmonary fibrosis.* Am J Respir Crit Care Med, 2013. 188(12): p. 1442-50.
47. Noth, I., et al., *Genetic variants associated with idiopathic pulmonary fibrosis susceptibility and mortality: a genome-wide association study.* Lancet Respir Med, 2013. 1(4): p. 309-317.
48. Meyer, K.C., et al., *An official American Thoracic Society clinical practice guideline: the clinical utility of bronchoalveolar lavage cellular analysis in interstitial lung disease.* Am J Respir Crit Care Med, 2012. 185(9): p. 1004-14.
49. du Bois, R.M., *An earlier and more confident diagnosis of idiopathic pulmonary fibrosis.* Eur Respir Rev, 2012. 21(124): p. 141-6.
50. Ohshimo, S., et al., *Significance of bronchoalveolar lavage for the diagnosis of idiopathic pulmonary fibrosis.* Am J Respir Crit Care Med, 2009. 179(11): p. 1043-7.
51. Wells, A. and N. Hirani, *Interstitial lung disease guideline.* Thorax, 2008. 63(Suppl 5): p. v1-v58.
52. Khadawardi, H. and M. Mura, *A simple dyspnoea scale as part of the assessment to predict outcome across chronic interstitial lung disease.* Respirology, 2017. 22(3): p. 501-507.

53. Wallis, A. and K. Spinks, *The diagnosis and management of interstitial lung diseases.* BMJ, 2015. 350: p. h2072.
54. Raghu, G., et al., *An Official ATS/ERS/JRS/ALAT Clinical Practice Guideline: Treatment of Idiopathic Pulmonary Fibrosis. An Update of the 2011 Clinical Practice Guideline.* Am J Respir Crit Care Med, 2015. 192(2): p. e3-19.
55. Nagai, S., et al. *Bronchoalveolar lavage in idiopathic interstitial lung diseases*. in *Seminars in respiratory and critical care medicine*. 2007. © Thieme Medical Publishers.
56. Stitt, H., *Bronchial aspiration and irrigation with a hypertonic saline solution.* J Med, 1927. 5: p. 112-117.
57. RAMIREZ-R, J., R.B. SCHULTZ, and R.E. DUTTON, *Pulmonary alveolar proteinosis: a new technique and rationale for treatment.* Archives of Internal Medicine, 1963. 112(3): p. 419-431.
58. Kylstra, J.A., et al., *Volume-Controlled Lung Lavage in the Treatment of Asthma, Bronchiectasis, and Mucoviscidosis 1–3.* American Review of Respiratory Disease, 1971. 103(5): p. 651-665.
59. Reynolds, H.Y. and H.H. Newball, *Analysis of Proteins and Respiratory Cells Obtained from Human Lungs by Bronchial Lavage.* Journal of Laboratory and Clinical Medicine, 1974. 84(4): p. 559-573.
60. Klech, H. and W. Pohl, *Technical Recommendations and Guidelines for Bronchoalveolar Lavage (Bal).* European Respiratory Journal, 1989. 2(6): p. 561-585.
61. Haslam, P.L. and R.P. Baughman, *Report of ERS Task Force: guidelines for measurement of acellular components and standardization of BAL.* Eur Respir J, 1999. 14(2): p. 245-8.
62. BAL Cooperative Group Steering Committee, *Bronchoalveolar lavage constituents in healthy individuals, idiopathic pulmonary fibrosis, and selected comparison groups.* Am Rev Respir Dis, 1990. 141: p. s169-s202.
63. Pope-Harman, A.L., et al., *Acute eosinophilic pneumonia. A summary of 15 cases and review of the literature.* Medicine (Baltimore), 1996. 75(6): p. 334-42.
64. Allen, J.N. and W.B. Davis, *Eosinophilic lung diseases.* Am J Respir Crit Care Med, 1994. 150(5 Pt 1): p. 1423-38.
65. Nicol, L., et al., *Identification of alveolar macrophage phenotypes predictive of disease progression in idiopathic pulmonary fibrosis.* QJM, 2016. 109(suppl 1): p. S2-S2.
66. Haslam, P., et al., *Bronchoalveolar lavage fluid cell counts in cryptogenic fibrosing alveolitis and their relation to therapy.* Thorax, 1980. 35(5): p. 328-339.
67. Turner-Warwick, M. and P.L. Haslam, *The Value of Serial Bronchoalveolar Lavages in Assessing the Clinical Progress of Patients with Cryptogenic Fibrosing Alveolitis 1–3.* American Review of Respiratory Disease, 1987. 135(1): p. 26-34.
68. Watters, L.C., et al., *Idiopathic Pulmonary Fibrosis: Pretreatment Bronchoalveolar Lavage Cellular Constituents and Their Relationships with Lung Histopathology and Clinical Response to Therapy 1–4.* American Review of Respiratory Disease, 1987. 135(3): p. 696-704.
69. Peterson, M.W., M. Monick, and G.W. Hunninghake, *Prognostic role of eosinophils in pulmonary fibrosis.* Chest, 1987. 92(1): p. 51-6.
70. Foster, M.W., et al., *Quantitative proteomics of bronchoalveolar lavage fluid in idiopathic pulmonary fibrosis.* J Proteome Res, 2015. 14(2): p. 1238-49.
71. Bargagli, E., et al., *Macrophage-derived biomarkers of idiopathic pulmonary fibrosis.* Pulm Med, 2011. 2011: p. 717130.
72. King Jr, T.E., et al., *A phase 3 trial of pirfenidone in patients with idiopathic pulmonary fibrosis.* N Engl J Med, 2014. 2014(370): p. 2083-2092.
73. Hamman, L. and A. Rich, *Acute diffuse interstitial fibrosis of the lungs.* Bull Johns Hopkins Hospital, 1944. 74: p. 177–212.
74. Liebow, A. and C. Carrington, *The interstitial pneumonias.* Frontiers of pulmonary radiology, 1st edition. New York: Grune & Stratton, 1969: p. 102-141.
75. Scadding, J.G., *Fibrosing Alveolitis.* Br Med J, 1964. 2(5410): p. 686.
76. Katzenstein, A.L. and J.L. Myers, *Idiopathic pulmonary fibrosis: clinical relevance of pathologic classification.* Am J Respir Crit Care Med, 1998. 157(4 Pt 1): p. 1301-15.
77. American Thoracic, S. and S. European Respiratory, *American Thoracic Society/European Respiratory Society International Multidisciplinary Consensus Classification of the Idiopathic Interstitial Pneumonias. .* Am J Respir Crit Care Med, 2002. 165(2): p. 277-304.

78. Travis, W.D., et al., *An official American Thoracic Society/European Respiratory Society statement: Update of the international multidisciplinary classification of the idiopathic interstitial pneumonias.* Am J Respir Crit Care Med, 2013. 188(6): p. 733-48.
79. Thannickal, V.J., et al., *Mechanisms of pulmonary fibrosis.* Annu Rev Med, 2004. 55: p. 395-417.
80. Selman, M. and A. Pardo, *Idiopathic pulmonary fibrosis: an epithelial/fibroblastic cross-talk disorder.* Respir Res, 2001. 3(1): p. 3.
81. Kumar, R.K., *Idiopathic pulmonary fibrosis: an epithelial/fibroblastic cross-talk disorder.* Respiratory Research, 2002. 3(1): p. 29.
82. Ryerson, C.J., et al., *Prevalence and prognosis of unclassifiable interstitial lung disease.* Eur Respir J, 2013. 42(3): p. 750-7.
83. Latsi, P.I., et al., *Fibrotic idiopathic interstitial pneumonia: the prognostic value of longitudinal functional trends.* Am J Respir Crit Care Med, 2003. 168(5): p. 531-7.
84. Troy, L., et al., *Prevalence and prognosis of unclassifiable interstitial lung disease.* Eur Respir J, 2014. 43(5): p. 1529-30.
85. National Institute for Health and Care Excellence, *Pirfenidone for treating idiopathic pulmonary fibrosis. In NICE Technology Appraisal Guidance (TA282).* 2013: Manchester,UK.
86. National Institute for Health and Care Excellence, *Nintedanib for treating idiopathic pulmonary fibrosis. In NICE Technology Appraisal Guidance (TA379).* 2016: Manchester, UK.
87. Hughes, G., et al., *Real World Experiences: Pirfenidone and Nintedanib are Effective and Well Tolerated Treatments for Idiopathic Pulmonary Fibrosis.* J Clin Med, 2016. 5(9): p. 78.
88. Woodcock, H.V. and T.M. Maher, *The treatment of idiopathic pulmonary fibrosis.* F1000Prime Rep, 2014. 6(16): p. 12703.
89. Network, I.P.F.C.R., *Prednisone, azathioprine, and N-acetylcysteine for pulmonary fibrosis.* N Engl J Med, 2012. 2012(366): p. 1968-1977.
90. Network, I.P.F.C.R., *Randomized trial of acetylcysteine in idiopathic pulmonary fibrosis.* N Engl J Med, 2014. 2014(370): p. 2093-2101.
91. Oldham, J.M., et al., *TOLLIP, MUC5B, and the Response to N-Acetylcysteine among Individuals with Idiopathic Pulmonary Fibrosis.* Am J Resp Crit Care, 2015. 192(12): p. 1475-1482.
92. Kistler, K.D., et al., *Lung transplantation in idiopathic pulmonary fibrosis: a systematic review of the literature.* BMC Pulm Med, 2014. 14(1): p. 139.
93. Yusen, R.D., et al., *The Registry of the International Society for Heart and Lung Transplantation: Thirtieth Adult Lung and Heart-Lung Transplant Report--2013; focus theme: age.* J Heart Lung Transplant, 2013. 32(10): p. 965-78.
94. Orens, J.B., et al., *International guidelines for the selection of lung transplant candidates: 2006 update--a consensus report from the Pulmonary Scientific Council of the International Society for Heart and Lung Transplantation.* J Heart Lung Transplant, 2006. 25(7): p. 745-55.
95. Valapour, M., et al., *OPTN/SRTR 2011 Annual Data Report: lung.* Am J Transplant, 2013. 13 Suppl 1(s1): p. 149-77.
96. Daccord, C. and T.M. Maher, *Recent advances in understanding idiopathic pulmonary fibrosis.* F1000Res, 2016. 5: p. 1046.
97. Cottin, V., et al., *Adherence to guidelines in idiopathic pulmonary fibrosis: a follow-up national survey.* ERJ Open Res, 2015. 1(2): p. 00032.
98. Lamas, D.J., et al., *Delayed access and survival in idiopathic pulmonary fibrosis: a cohort study.* Am J Respir Crit Care Med, 2011. 184(7): p. 842-7.
99. Homer, R.J., et al., *Modern concepts on the role of inflammation in pulmonary fibrosis.* Arch Pathol Lab Med, 2011. 135(6): p. 780-8.
100. Sakai, N. and A.M. Tager, *Fibrosis of two: Epithelial cell-fibroblast interactions in pulmonary fibrosis.* Biochim Biophys Acta, 2013. 1832(7): p. 911-21.
101. Selman, M., T.E. King, and A. Pardo, *Idiopathic pulmonary fibrosis: Prevailing and evolving hypotheses about its pathogenesis and implications for therapy.* Annals of Internal Medicine, 2001. 134(2): p. 136-151.
102. Gross, T.J. and G.W. Hunninghake, *Idiopathic pulmonary fibrosis.* N Engl J Med, 2001. 345(7): p. 517-25.
103. Wolters, P.J., H.R. Collard, and K.D. Jones, *Pathogenesis of idiopathic pulmonary fibrosis.* Annu Rev Pathol, 2014. 9: p. 157-79.

104. Katzenstein, A.L., et al., *Bronchiolitis obliterans and usual interstitial pneumonia. A comparative clinicopathologic study.* Am J Surg Pathol, 1986. 10(6): p. 373-81.
105. Kuhn III, C., et al., *An immunohistochemical study of architectural remodeling and connective tissue synthesis in pulmonary fibrosis.* American Review of Respiratory Disease, 1989. 140(6): p. 1693-1703.
106. Myers, J.L. and A.L. Katzenstein, *Epithelial necrosis and alveolar collapse in the pathogenesis of usual interstitial pneumonia.* Chest, 1988. 94(6): p. 1309-11.
107. Takemura, T., et al., *Pathological differentiation of chronic hypersensitivity pneumonitis from idiopathic pulmonary fibrosis/usual interstitial pneumonia.* Histopathology, 2012. 61(6): p. 1026-35.
108. Walsh, S.L., et al., *Relationship between fibroblastic foci profusion and high resolution CT morphology in fibrotic lung disease.* BMC medicine, 2015. 13(1): p. 241.
109. Song, J.W., et al., *Pathologic and radiologic differences between idiopathic and collagen vascular disease-related usual interstitial pneumonia.* Chest, 2009. 136(1): p. 23-30.
110. Nicholson, A.G., et al., *The relationship between individual histologic features and disease progression in idiopathic pulmonary fibrosis.* American Journal of Respiratory and Critical Care Medicine, 2002. 166(2): p. 173-177.
111. King, T.E., A. Pardo, and M. Selman, *Idiopathic pulmonary fibrosis.* The Lancet, 2011. 378(9807): p. 1949-1961.
112. Jones, M.G., et al., *Three-dimensional characterization of fibroblast foci in idiopathic pulmonary fibrosis.* JCI Insight, 2016. 1(5): p. e86375.
113. Fukuda, Y., et al., *Significance of early intra-alveolar fibrotic lesions and integrin expression in lung biopsy specimens from patients with idiopathic pulmonary fibrosis.* Hum Pathol, 1995. 26(1): p. 53-61.
114. Tomos, I.P., et al., *Extracellular matrix remodeling in idiopathic pulmonary fibrosis. It is the 'bed'that counts and not 'the sleepers'.* Expert review of respiratory medicine, 2017. 11(4): p. 299-309.
115. Kaarteenaho-Wiik, R., et al., *Localization of precursor proteins and mRNA of type I and III collagens in usual interstitial pneumonia and sarcoidosis.* J Mol Histol, 2005. 36(6-7): p. 437-46.
116. Kaarteenaho-Wiik, R., et al., *Tenascin immunoreactivity as a prognostic marker in usual interstitial pneumonia.* American journal of respiratory and critical care medicine, 1996. 154(2): p. 511-518.
117. Paakko, P., et al., *Tenascin mRNA expression at the foci of recent injury in usual interstitial pneumonia* Am J Resp Crit Care 2000. 161(3): p. 967-972.
118. Bensadoun, E.S., et al., *Proteoglycan deposition in pulmonary fibrosis.* Am J Respir Crit Care Med, 1996. 154(6 Pt 1): p. 1819-28.
119. White, E.S., M.H. Lazar, and V.J. Thannickal, *Pathogenetic mechanisms in usual interstitial pneumonia/idiopathic pulmonary fibrosis.* J Pathol, 2003. 201(3): p. 343-54.
120. Larsson, O., et al., *Fibrotic myofibroblasts manifest genome-wide derangements of translational control.* PLoS One, 2008. 3(9): p. e3220.
121. Yamashita, M., et al., *The definition of fibrogenic processes in fibroblastic foci of idiopathic pulmonary fibrosis based on morphometric quantification of extracellular matrices.* Hum Pathol, 2009. 40(9): p. 1278-87.
122. KING JR, T.E., et al., *Idiopathic pulmonary fibrosis: relationship between histopathologic features and mortality.* American journal of respiratory and critical care medicine, 2001. 164(6): p. 1025-1032.
123. Flaherty, K.R., et al., *Fibroblastic foci in usual interstitial pneumonia: idiopathic versus collagen vascular disease.* Am J Respir Crit Care Med, 2003. 167(10): p. 1410-5.
124. Hanak, V., et al., *Profusion of fibroblast foci in patients with idiopathic pulmonary fibrosis does not predict outcome.* Respiratory medicine, 2008. 102(6): p. 852-856.
125. Kinnula, V.L., et al., *Oxidative stress in pulmonary fibrosis: a possible role for redox modulatory therapy.* Am J Respir Crit Care Med, 2005. 172(4): p. 417-22.
126. Zhang, L., et al., *Endoplasmic reticulum stress, a new wrestler, in the pathogenesis of idiopathic pulmonary fibrosis.* Am J Transl Res, 2017. 9(2): p. 722-735.
127. Sakuma, Y., *Epithelial-to-mesenchymal transition and its role in EGFR-mutant lung adenocarcinoma and idiopathic pulmonary fibrosis.* Pathol Int, 2017. 67(8): p. 379-388.

128. Kim, K.K., et al., *Alveolar epithelial cell mesenchymal transition develops in vivo during pulmonary fibrosis and is regulated by the extracellular matrix.* Proceedings of the National Academy of Sciences, 2006. 103(35): p. 13180-13185.
129. Kage, H. and Z. Borok, *EMT and interstitial lung disease: a mysterious relationship.* Curr Opin Pulm Med, 2012. 18(5): p. 517-23.
130. Strieter, R.M., et al., *The role of circulating mesenchymal progenitor cells (fibrocytes) in the pathogenesis of pulmonary fibrosis.* J Leukoc Biol, 2009. 86(5): p. 1111-8.
131. Maharaj, S.S., et al., *Fibrocytes in chronic lung disease--facts and controversies.* Pulm Pharmacol Ther, 2012. 25(4): p. 263-7.
132. Wynn, T.A. and T.R. Ramalingam, *Mechanisms of fibrosis: therapeutic translation for fibrotic disease.* Nat Med, 2012. 18(7): p. 1028-40.
133. Reynolds, H.Y., *Lung inflammation and fibrosis: an alveolar macrophage-centered perspective from the 1970s to 1980s.* Am J Respir Crit Care Med, 2005. 171(2): p. 98-102.
134. Kinder, B.W., et al., *Baseline BAL neutrophilia predicts early mortality in idiopathic pulmonary fibrosis.* Chest, 2008. 133(1): p. 226-32.
135. Werner, S. and R. Grose, *Regulation of wound healing by growth factors and cytokines.* Physiol Rev, 2003. 83(3): p. 835-70.
136. Betensley, A., R. Sharif, and D. Karamichos, *A Systematic Review of the Role of Dysfunctional Wound Healing in the Pathogenesis and Treatment of Idiopathic Pulmonary Fibrosis.* J Clin Med, 2016. 6(1): p. 2.
137. Wynn, T.A. and L. Barron, *Macrophages: master regulators of inflammation and fibrosis.* Semin Liver Dis, 2010. 30(3): p. 245-57.
138. Leibovich, S.J. and R. Ross, *The role of the macrophage in wound repair. A study with hydrocortisone and antimacrophage serum.* Am J Pathol, 1975. 78(1): p. 71-100.
139. Mirza, R., L.A. DiPietro, and T.J. Koh, *Selective and Specific Macrophage Ablation Is Detrimental to Wound Healing in Mice.* American Journal of Pathology, 2009. 175(6): p. 2454-2462.
140. Goren, I., et al., *A transgenic mouse model of inducible macrophage depletion: effects of diphtheria toxin-driven lysozyme M-specific cell lineage ablation on wound inflammatory, angiogenic, and contractive processes.* Am J Pathol, 2009. 175(1): p. 132-47.
141. Murray, L.A., et al., *TGF-beta driven lung fibrosis is macrophage dependent and blocked by Serum amyloid P.* International Journal of Biochemistry & Cell Biology, 2011. 43(1): p. 154-162.
142. Iredale, J.P., *Models of liver fibrosis: exploring the dynamic nature of inflammation and repair in a solid organ.* J Clin Invest, 2007. 117(3): p. 539-48.
143. Duffield, J.S., et al., *Selective depletion of macrophages reveals distinct, opposing roles during liver injury and repair.* J Clin Invest, 2005. 115(1): p. 56-65.
144. Lucas, T., et al., *Differential roles of macrophages in diverse phases of skin repair.* J Immunol, 2010. 184(7): p. 3964-77.
145. Byrne, A.J., et al., *Pulmonary macrophages: key players in the innate defence of the airways.* Thorax, 2015. 70(12): p. 1189-96.
146. Byrne, A.J., T.M. Maher, and C.M. Lloyd, *Pulmonary Macrophages: A New Therapeutic Pathway in Fibrosing Lung Disease?* Trends Mol Med, 2016. 22(4): p. 303-16.
147. Reynolds, H.Y., *Bronchoalveolar lavage.* Am Rev Respir Dis, 1987. 135(1): p. 250-63.
148. Fels, A.O. and Z.A. Cohn, *The alveolar macrophage.* J Appl Physiol (1985), 1986. 60(2): p. 353-69.
149. Lohmann-Matthes, M.L., C. Steinmuller, and G. Franke-Ullmann, *Pulmonary macrophages.* Eur Respir J, 1994. 7(9): p. 1678-89.
150. Baran, C.P., et al., *Important roles for macrophage colony-stimulating factor, CC chemokine ligand 2, and mononuclear phagocytes in the pathogenesis of pulmonary fibrosis.* Am J Respir Crit Care Med, 2007. 176(1): p. 78-89.
151. Prasse, A., et al., *A vicious circle of alveolar macrophages and fibroblasts perpetuates pulmonary fibrosis via CCL18.* Am J Respir Crit Care Med, 2006. 173(7): p. 781-92.
152. Park, S.W., et al., *Interleukin-13 and its receptors in idiopathic interstitial pneumonia: clinical implications for lung function.* J Korean Med Sci, 2009. 24(4): p. 614-20.
153. Hussell, T. and T.J. Bell, *Alveolar macrophages: plasticity in a tissue-specific context.* Nat Rev Immunol, 2014. 14(2): p. 81-93.

154. Watson, W.H., J.D. Ritzenthaler, and J. Roman, *Lung extracellular matrix and redox regulation.* Redox Biol, 2016. 8: p. 305-15.
155. Parker, M.W., et al., *Fibrotic extracellular matrix activates a profibrotic positive feedback loop.* J Clin Invest, 2014. 124(4): p. 1622-35.
156. Sorokin, L., *The impact of the extracellular matrix on inflammation.* Nat Rev Immunol, 2010. 10(10): p. 712-23.
157. Pechkovsky, D.V., et al., *Alternatively activated alveolar macrophages in pulmonary fibrosis-mediator production and intracellular signal transduction.* Clin Immunol, 2010. 137(1): p. 89-101.
158. Song, E., et al., *Influence of alternatively and classically activated macrophages on fibrogenic activities of human fibroblasts.* Cell Immunol, 2000. 204(1): p. 19-28.
159. Hancock, A., et al., *Production of interleukin 13 by alveolar macrophages from normal and fibrotic lung.* Am J Respir Cell Mol Biol, 1998. 18(1): p. 60-5.
160. Zhang, Y., et al., *Enhanced IL-1 beta and tumor necrosis factor-alpha release and messenger RNA expression in macrophages from idiopathic pulmonary fibrosis or after asbestos exposure.* J Immunol, 1993. 150(9): p. 4188-96.
161. Atabai, K., et al., *Mfge8 diminishes the severity of tissue fibrosis in mice by binding and targeting collagen for uptake by macrophages.* J Clin Invest, 2009. 119(12): p. 3713-22.
162. Gordon, S. and P.R. Taylor, *Monocyte and macrophage heterogeneity.* Nat Rev Immunol, 2005. 5(12): p. 953-64.
163. Sica, A. and A. Mantovani, *Macrophage plasticity and polarization: in vivo veritas.* J Clin Invest, 2012. 122(3): p. 787-95.
164. Mills, C.D., *Anatomy of a discovery: m1 and m2 macrophages.* Front Immunol, 2015. 6: p. 212.
165. Rhee, I., *Diverse macrophages polarization in tumor microenvironment.* Arch Pharm Res, 2016. 39(11): p. 1588-1596.
166. Gharib, S.A., et al., *MMP28 promotes macrophage polarization toward M2 cells and augments pulmonary fibrosis.* J Leukoc Biol, 2014. 95(1): p. 9-18.
167. Wynn, T.A., A. Chawla, and J.W. Pollard, *Macrophage biology in development, homeostasis and disease.* Nature, 2013. 496(7446): p. 445-55.
168. Tao, B., et al., *Myeloid-specific disruption of tyrosine phosphatase Shp2 promotes alternative activation of macrophages and predisposes mice to pulmonary fibrosis.* J Immunol, 2014. 193(6): p. 2801-11.
169. Varin, A. and S. Gordon, *Alternative activation of macrophages: immune function and cellular biology.* Immunobiology, 2009. 214(7): p. 630-41.
170. Martinez, F.O., L. Helming, and S. Gordon, *Alternative activation of macrophages: an immunologic functional perspective.* Annu Rev Immunol, 2009. 27: p. 451-83.
171. Brombacher, F., et al., *Analyzing classical and alternative macrophage activation in macrophage/neutrophil-specific IL-4 receptor-alpha-deficient mice.* Methods Mol Biol, 2009. 531: p. 225-52.
172. Lawrence, T. and G. Natoli, *Transcriptional regulation of macrophage polarization: enabling diversity with identity.* Nat Rev Immunol, 2011. 11(11): p. 750-61.
173. Thannickal, V.J., et al., *Matrix biology of idiopathic pulmonary fibrosis: a workshop report of the national heart, lung, and blood institute.* Am J Pathol, 2014. 184(6): p. 1643-51.
174. Frantz, C., K.M. Stewart, and V.M. Weaver, *The extracellular matrix at a glance.* J Cell Sci, 2010. 123(24): p. 4195-4200.
175. Cox, T.R. and J.T. Erler, *Remodeling and homeostasis of the extracellular matrix: implications for fibrotic diseases and cancer.* Dis Model Mech, 2011. 4(2): p. 165-78.
176. Todd, N.W., I.G. Luzina, and S.P. Atamas, *Molecular and cellular mechanisms of pulmonary fibrosis.* Fibrogenesis Tissue Repair, 2012. 5(1): p. 11.
177. Rock, J.R., et al., *Multiple stromal populations contribute to pulmonary fibrosis without evidence for epithelial to mesenchymal transition.* P Natl Acad Sci USA, 2011. 108(52): p. E1475-E1483.
178. McKleroy, W., T.H. Lee, and K. Atabai, *Always cleave up your mess: targeting collagen degradation to treat tissue fibrosis.* American Journal of Physiology-Lung Cellular and Molecular Physiology, 2013. 304(11): p. L709-L721.
179. Nimni, M.E., *Collagen: structure, function, and metabolism in normal and fibrotic tissues.* Seminars in arthritis and rheumatism, 1983. 13(1): p. 1-86.

180. Orgel, J.P., et al., *Microfibrillar structure of type I collagen in situ.* Proc Natl Acad Sci U S A, 2006. 103(24): p. 9001-5.
181. Smith, C., et al., *Mapping the collagen-binding site in the I domain of the glycoprotein Ia/IIa (integrin α2β1).* Journal of Biological Chemistry, 2000. 275(6): p. 4205-4209.
182. Song, F., et al., *Matrix metalloproteinase dependent and independent collagen degradation.* Front Biosci, 2006. 11: p. 3100-20.
183. Dzamba, B.J., et al., *Fibronectin binding site in type I collagen regulates fibronectin fibril formation.* J Cell Biol, 1993. 121(5): p. 1165-72.
184. San Antonio, J.D., et al., *Mapping the heparin-binding sites on type I collagen monomers and fibrils.* J Cell Biol, 1994. 125(5): p. 1179-88.
185. Romijn, R.A., et al., *Identification of the collagen-binding site of the von Willebrand factor A3-domain.* J Biol Chem, 2001. 276(13): p. 9985-91.
186. Sweeney, S.M., et al., *Candidate cell and matrix interaction domains on the collagen fibril, the predominant protein of vertebrates.* J Biol Chem, 2008. 283(30): p. 21187-97.
187. Orgel, J.P., J.D. San Antonio, and O. Antipova, *Molecular and structural mapping of collagen fibril interactions.* Connect Tissue Res, 2011. 52(1): p. 2-17.
188. Buhling, F., et al., *Pivotal role of cathepsin K in lung fibrosis.* Am J Pathol, 2004. 164(6): p. 2203-16.
189. Klein, T. and R. Bischoff, *Physiology and pathophysiology of matrix metalloproteases.* Amino Acids, 2011. 41(2): p. 271-90.
190. Hartung, H.P. and B.C. Kieseier, *The role of matrix metalloproteinases in autoimmune damage to the central and peripheral nervous system.* J Neuroimmunol, 2000. 107(2): p. 140-7.
191. Shapiro, S.D. and R.M. Senior, *Matrix metalloproteinases. Matrix degradation and more.* Am J Respir Cell Mol Biol, 1999. 20(6): p. 1100-2.
192. Everts, V., et al., *Phagocytosis and intracellular digestion of collagen, its role in turnover and remodelling.* Histochem J, 1996. 28(4): p. 229-45.
193. Lucattelli, M., et al., *Collagen phagocytosis by lung alveolar macrophages in animal models of emphysema.* Eur Respir J, 2003. 22(5): p. 728-34.
194. Lee, W., J. Sodek, and C.A. McCulloch, *Role of integrins in regulation of collagen phagocytosis by human fibroblasts.* J Cell Physiol, 1996. 168(3): p. 695-704.
195. East, L., et al., *A targeted deletion in the endocytic receptor gene Endo180 results in a defect in collagen uptake.* EMBO Rep, 2003. 4(7): p. 710-6.
196. Martinez-Pomares, L., et al., *Carbohydrate-independent recognition of collagens by the macrophage mannose receptor.* Eur J Immunol, 2006. 36(5): p. 1074-82.
197. von Delwig, A., et al., *Inhibition of macropinocytosis blocks antigen presentation of type II collagen in vitro and in vivo in HLA-DR1 transgenic mice.* Arthritis Res Ther, 2006. 8(4): p. R93.
198. van der Zee, E., et al., *Cytokines modulate phagocytosis and intracellular digestion of collagen fibrils by fibroblasts in rabbit periosteal explants. Inverse effects on procollagenase production and collagen phagocytosis.* J Cell Sci, 1995. 108(10): p. 3307-15.
199. Siwik, D.A., D.L.-F. Chang, and W.S. Colucci, *Interleukin-1β and tumor necrosis factor-α decrease collagen synthesis and increase matrix metalloproteinase activity in cardiac fibroblasts in vitro.* Circulation research, 2000. 86(12): p. 1259-1265.
200. Selman, M., et al., *Changes of collagen content in fibrotic lung disease.* Arch Invest Med (Mex), 1982. 13(2): p. 93-100.
201. Fulmer, J.D., et al., *Collagen Concentration and Rates of Synthesis in Idiopathic Pulmonary Fibrosis 1–2.* American Review of Respiratory Disease, 1980. 122(2): p. 289-301.
202. Rozin, G.F., et al., *Collagen and elastic system in the remodelling process of major types of idiopathic interstitial pneumonias (IIP).* Histopathology, 2005. 46(4): p. 413-21.
203. Specks, U., et al., *Increased expression of type VI collagen in lung fibrosis.* Am J Respir Crit Care Med, 1995. 151(6): p. 1956-64.
204. Estany, S., et al. *Lung extracellular matrix profile of patients with idiopathic pulmonary fibrosis*. in *ATS 2011*. 2011. Am Thoracic Soc.
205. Bateman, E.D., M. Turner-Warwick, and B.C. Adelmann-Grill, *Immunohistochemical study of collagen types in human foetal lung and fibrotic lung disease.* Thorax, 1981. 36(9): p. 645-53.
206. Fukuda, Y., et al., *The role of intraalveolar fibrosis in the process of pulmonary structural remodeling in patients with diffuse alveolar damage.* Am J Pathol, 1987. 126(1): p. 171-82.

207. Gay, S.E., et al., *Idiopathic pulmonary fibrosis: predicting response to therapy and survival.* Am J Respir Crit Care Med, 1998. 157(4 Pt 1): p. 1063-72.
208. White, E.S., *Lung extracellular matrix and fibroblast function.* Ann Am Thorac Soc, 2015. 12 Suppl 1(Supplement 1): p. S30-3.
209. Clarke, D.L., et al., *Matrix regulation of idiopathic pulmonary fibrosis: the role of enzymes.* Fibrogenesis Tissue Repair, 2013. 6(1): p. 20.
210. Rocco, P.R., et al., *Lung tissue mechanics and extracellular matrix remodeling in acute lung injury.* Am J Respir Crit Care Med, 2001. 164(6): p. 1067-71.
211. Suki, B. and J.H. Bates, *Extracellular matrix mechanics in lung parenchymal diseases.* Respir Physiol Neurobiol, 2008. 163(1-3): p. 33-43.
212. van Zuijlen, P.P., et al., *Collagen morphology in human skin and scar tissue: no adaptations in response to mechanical loading at joints.* Burns, 2003. 29(5): p. 423-431.
213. Maki, J.M., *Lysyl oxidases in mammalian development and certain pathological conditions.* Histol Histopathol, 2009. 24(5): p. 651-60.
214. Newman, S.L. and M.A. Tucci, *Regulation of human monocyte/macrophage function by extracellular matrix. Adherence of monocytes to collagen matrices enhances phagocytosis of opsonized bacteria by activation of complement receptors and enhancement of Fc receptor function.* J Clin Invest, 1990. 86(3): p. 703-14.
215. Neill, T., L. Schaefer, and R.V. Iozzo, *Instructive roles of extracellular matrix on autophagy.* Am J Pathol, 2014. 184(8): p. 2146-53.
216. Tuloup-Minguez, V., et al., *Regulation of autophagy by extracellular matrix glycoproteins in HeLa cells.* Autophagy, 2011. 7(1): p. 27-39.
217. Avivar-Valderas, A., et al., *Regulation of autophagy during ECM detachment is linked to a selective inhibition of mTORC1 by PERK.* Oncogene, 2013. 32(41): p. 4932-4940.
218. Horiguchi, M., M. Ota, and D.B. Rifkin, *Matrix control of transforming growth factor-beta function.* J Biochem, 2012. 152(4): p. 321-9.
219. Lipson, K.E., et al., *CTGF is a central mediator of tissue remodeling and fibrosis and its inhibition can reverse the process of fibrosis.* Fibrogenesis & tissue repair, 2012. 5(1): p. S24.
220. Leask, A. and D.J. Abraham, *The role of connective tissue growth factor, a multifunctional matricellular protein, in fibroblast biology.* Biochem Cell Biol, 2003. 81(6): p. 355-63.
221. Sonnylal, S., et al., *Connective tissue growth factor causes EMT-like cell fate changes in vivo and in vitro.* J Cell Sci, 2013. 126(10): p. 2164-75.
222. Bonnans, C., J. Chou, and Z. Werb, *Remodelling the extracellular matrix in development and disease.* Nature reviews Molecular cell biology, 2014. 15(12): p. 786-801.
223. Levine, B. and G. Kroemer, *Autophagy in the pathogenesis of disease.* Cell, 2008. 132(1): p. 27-42.
224. Kaur, J. and J. Debnath, *Autophagy at the crossroads of catabolism and anabolism.* Nature Reviews Molecular Cell Biology, 2015. 16(8): p. 461-472.
225. De Duve, C., ed. *The lysosome concept*. Ciba Foundation Symposium-Lysosomes. 1963, Wiley Online Library. 1-35.
226. Ohsumi, Y., *Historical landmarks of autophagy research.* Cell Res, 2014. 24(1): p. 9-23.
227. Tooze, S.A. and I. Dikic, *Autophagy Captures the Nobel Prize.* Cell, 2016. 167(6): p. 1433-1435.
228. Levine, B. and D.J. Klionsky, *Autophagy wins the 2016 Nobel Prize in Physiology or Medicine: Breakthroughs in baker's yeast fuel advances in biomedical research.* Proc Natl Acad Sci U S A, 2017. 114(2): p. 201-205.
229. Jiang, P. and N. Mizushima, *Autophagy and human diseases.* Cell Res, 2014. 24(1): p. 69-79.
230. Mizushima, N., T. Yoshimori, and B. Levine, *Methods in mammalian autophagy research.* Cell, 2010. 140(3): p. 313-26.
231. Shibutani, S.T. and T. Yoshimori, *A current perspective of autophagosome biogenesis.* Cell Res, 2014. 24(1): p. 58-68.
232. Gutierrez, M.G., et al., *Rab7 is required for the normal progression of the autophagic pathway in mammalian cells.* Journal of cell science, 2004. 117(13): p. 2687-2697.
233. Jager, S., et al., *Role for Rab7 in maturation of late autophagic vacuoles.* J Cell Sci, 2004. 117(Pt 20): p. 4837-48.
234. Ganley, I.G., *Autophagosome maturation and lysosomal fusion.* Essays Biochem, 2013. 55: p. 65-78.

235. Kinchen, J.M. and K.S. Ravichandran, *Phagosome maturation: going through the acid test.* Nature Reviews Molecular Cell Biology, 2008. 9(10): p. 781-795.
236. Mizushima, N. and M. Komatsu, *Autophagy: renovation of cells and tissues.* Cell, 2011. 147(4): p. 728-41.
237. Kabeya, Y., et al., *LC3, a mammalian homologue of yeast Apg8p, is localized in autophagosome membranes after processing.* Embo Journal, 2000. 19(21): p. 5720-5728.
238. Tanida, I., et al., *The human homolog of Saccharomyces cerevisiae Apg7p is a protein-activating enzyme for multiple substrates including human Apg12p, GATE-16, GABARAP, and MAP-LC3.* J Biol Chem, 2001. 276(3): p. 1701-1706.
239. Tanida, I., et al., *Human Apg3p/Aut1p homologue is an authentic E2 enzyme for multiple substrates, GATE-16, GABARAP, and MAP-LC3, and facilitates the conjugation of hApg12p to hApg5p.* Journal of Biological Chemistry, 2002. 277(16): p. 13739-13744.
240. Kabeya, Y., et al., *LC3, GABARAP and GATE16 localize to autophagosomal membrane depending on form-II formation.* J Cell Sci, 2004. 117(13): p. 2805-12.
241. Yang, Z. and D.J. Klionsky, *Mammalian autophagy: core molecular machinery and signaling regulation.* Curr Opin Cell Biol, 2010. 22(2): p. 124-31.
242. Chang, Y.Y. and T.P. Neufeld, *An Atg1/Atg13 complex with multiple roles in TOR-mediated autophagy regulation.* Mol Biol Cell, 2009. 20(7): p. 2004-14.
243. Hosokawa, N., et al., *Atg101, a novel mammalian autophagy protein interacting with Atg13.* Autophagy, 2009. 5(7): p. 973-9.
244. Itakura, E., et al., *Beclin 1 forms two distinct phosphatidylinositol 3-kinase complexes with mammalian Atg14 and UVRAG.* Mol Biol Cell, 2008. 19(12): p. 5360-72.
245. Matsunaga, K., et al., *Two Beclin 1-binding proteins, Atg14L and Rubicon, reciprocally regulate autophagy at different stages.* Nature Cell Biology, 2009. 11(4): p. 385-U69.
246. Wei, Y., et al., *JNK1-mediated phosphorylation of Bcl-2 regulates starvation-induced autophagy.* Mol Cell, 2008. 30(6): p. 678-88.
247. Zhong, Y., et al., *Distinct regulation of autophagic activity by Atg14L and Rubicon associated with Beclin 1-phosphatidylinositol-3-kinase complex.* Nat Cell Biol, 2009. 11(4): p. 468-76.
248. Harris, J., et al., *Th1-Th2 polarisation and autophagy in the control of intracellular mycobacteria by macrophages.* Vet Immunol Immunopathol, 2009. 128(1): p. 37-43.
249. Delgado, M., et al., *Autophagy and pattern recognition receptors in innate immunity.* Immunol Rev, 2009. 227(1): p. 189-202.
250. Xu, Y., et al., *Toll-like receptor 4 is a sensor for autophagy associated with innate immunity.* Immunity, 2007. 27(1): p. 135-144.
251. Huang, J., et al., *Activation of antibacterial autophagy by NADPH oxidases.* Proc Natl Acad Sci U S A, 2009. 106(15): p. 6226-31.
252. Mizushima, N., et al., *Dissection of autophagosome formation using Apg5-deficient mouse embryonic stem cells.* Journal of Cell Biology, 2001. 152(4): p. 657-668.
253. Geng, J., et al., *Quantitative analysis of autophagy-related protein stoichiometry by fluorescence microscopy.* J Cell Biol, 2008. 182(1): p. 129-40.
254. Fujita, N., et al., *An Atg4B mutant hampers the lipidation of LC3 paralogues and causes defects in autophagosome closure.* Mol Biol Cell, 2008. 19(11): p. 4651-9.
255. Murrow, L. and J. Debnath, *Autophagy as a stress-response and quality-control mechanism: implications for cell injury and human disease.* Annual Review of Pathology: Mechanisms of Disease, 2013. 8: p. 105-137.
256. Jung, C.H., et al., *mTOR regulation of autophagy.* FEBS Lett, 2010. 584(7): p. 1287-95.
257. Pfeifer, U., *Inhibition by insulin of the formation of autophagic vacuoles in rat liver. A morphometric approach to the kinetics of intracellular degradation by autophagy.* J Cell Biol, 1978. 78(1): p. 152-67.
258. Klemes, Y., J.D. Etlinger, and A.L. Goldberg, *Properties of abnormal proteins degraded rapidly in reticulocytes. Intracellular aggregation of the globin molecules prior to hydrolysis.* J Biol Chem, 1981. 256(16): p. 8436-44.
259. Aparicio, I., et al., *Autophagy-related proteins are functionally active in human spermatozoa and may be involved in the regulation of cell survival and motility.* Scientific reports, 2016. 6.
260. Schworer, C.M., K.A. Shiffer, and G.E. Mortimore, *Quantitative relationship between autophagy and proteolysis during graded amino acid deprivation in perfused rat liver.* Journal of Biological Chemistry, 1981. 256(14): p. 7652-7658.

261. Fimia, G.M., G. Kroemer, and M. Piacentini, *Molecular mechanisms of selective autophagy.* Cell Death Differ, 2013. 20(1): p. 1-2.
262. Stolz, A., A. Ernst, and I. Dikic, *Cargo recognition and trafficking in selective autophagy.* Nat Cell Biol, 2014. 16(6): p. 495-501.
263. Mizushima, N., *Methods for monitoring autophagy.* Int J Biochem Cell Biol, 2004. 36(12): p. 2491-502.
264. Klionsky, D.J., A.M. Cuervo, and P.O. Seglen, *Methods for monitoring autophagy from yeast to human.* Autophagy, 2007. 3(3): p. 181-206.
265. Biederbick, A., H. Kern, and H. Elsässer, *Monodansylcadaverine (MDC) is a specific in vivo marker for autophagic vacuoles.* European journal of cell biology, 1995. 66(1): p. 3-14.
266. Bampton, E.T., et al., *The dynamics of autophagy visualised in live cells: from autophagosome formation to fusion with endo/lysosomes.* Autophagy, 2005. 1(1): p. 23-36.
267. Vazquez, C.L. and M.I. Colombo, *Assays to Assess Autophagy Induction and Fusion of Autophagic Vacuoles with a Degradative Compartment, Using Monodansylcadaverine (MDC) and DQ‐BSA.* Methods in enzymology, 2009. 452: p. 85-95.
268. Chan, L.L., et al., *A novel image-based cytometry method for autophagy detection in living cells.* Autophagy, 2012. 8(9): p. 1371-82.
269. Pankiv, S., et al., *p62/SQSTM1 binds directly to Atg8/LC3 to facilitate degradation of ubiquitinated protein aggregates by autophagy.* J Biol Chem, 2007. 282(33): p. 24131-45.
270. Komatsu, M., et al., *Homeostatic levels of p62 control cytoplasmic inclusion body formation in autophagy-deficient mice.* Cell, 2007. 131(6): p. 1149-63.
271. Zatloukal, K., et al., *p62 is a common component of cytoplasmic inclusions in protein aggregation diseases.* Am J Pathol, 2002. 160(1): p. 255-263.
272. Kuusisto, E., A. Salminen, and I. Alafuzoff, *Ubiquitin-binding protein p62 is present in neuronal and glial inclusions in human tauopathies and synucleinopathies.* Neuroreport, 2001. 12(10): p. 2085-2090.
273. Nagaoka, U., et al., *Increased expression of p62 in expanded polyglutamine-expressing cells and its association with polyglutamine inclusions.* J Neurochem, 2004. 91(1): p. 57-68.
274. Inami, Y., et al., *Persistent activation of Nrf2 through p62 in hepatocellular carcinoma cells.* Journal of Cell Biology, 2011. 193(2): p. 275-284.
275. Watson, R.O., P.S. Manzanillo, and J.S. Cox, *Extracellular M. tuberculosis DNA targets bacteria for autophagy by activating the host DNA-sensing pathway.* Cell, 2012. 150(4): p. 803-15.
276. Ponpuak, M., et al., *Delivery of cytosolic components by autophagic adaptor protein p62 endows autophagosomes with unique antimicrobial properties.* Immunity, 2010. 32(3): p. 329-41.
277. Kruse, K.B., J.L. Brodsky, and A.A. McCracken, *Autophagy: an ER protein quality control process.* Autophagy, 2006. 2(2): p. 135-7.
278. Jorgensen, E., et al., *Cigarette smoke induces endoplasmic reticulum stress and the unfolded protein response in normal and malignant human lung cells.* BMC Cancer, 2008. 8(1): p. 229.
279. Zhang, H.F., et al., *Mitochondrial autophagy is an HIF-1-dependent adaptive metabolic response to hypoxia.* J Biol Chem, 2008. 283(16): p. 10892-10903.
280. Endo, M., et al., *The ER stress pathway involving CHOP is activated in the lungs of LPS-treated mice.* Journal of biochemistry, 2005. 138(4): p. 501-507.
281. Oh, S.H. and S.C. Lim, *Endoplasmic Reticulum Stress-Mediated Autophagy/Apoptosis Induced by Capsaicin (8-Methyl-N-vanillyl-6-nonenamide) and Dihydrocapsaicin is Regulated by the Extent of c-Jun NH2-Terminal Kinase/Extracellular Signal-Regulated Kinase Activation in WI38 Lung Epithelial Fibroblast Cells.* J Pharmacol Exp Ther, 2009. 329(1): p. 112-122.
282. Pagano, A. and C. Barazzone-Argiroffo, *Alveolar cell death in hyperoxia-induced lung injury.* Ann N Y Acad Sci, 2003. 1010(1): p. 405-16.
283. Kiffin, R., U. Bandyopadhyay, and A.M. Cuervo, *Oxidative stress and autophagy.* Antioxid Redox Signal, 2006. 8(1-2): p. 152-62.
284. MacNee, W., *Oxidative stress and lung inflammation in airways disease.* Eur J Pharmacol, 2001. 429(1-3): p. 195-207.
285. Kim, H.P., et al., *Autophagic proteins regulate cigarette smoke-induced apoptosis: protective role of heme oxygenase-1.* Autophagy, 2008. 4(7): p. 887-95.
286. Scherz-Shouval, R., et al., *Reactive oxygen species are essential for autophagy and specifically regulate the activity of Atg4.* EMBO J, 2007. 26(7): p. 1749-60.

287. Chen, Y., M. Azad, and S. Gibson, *Superoxide is the major reactive oxygen species regulating autophagy.* Cell Death & Differentiation, 2009. 16(7): p. 1040-1052.
288. Chen, J.-L., et al., *Novel roles for protein kinase Cδ-dependent signaling pathways in acute hypoxic stress-induced autophagy.* Journal of Biological Chemistry, 2008. 283(49): p. 34432-34444.
289. Virgin, H.W. and B. Levine, *Autophagy genes in immunity.* Nat Immunol, 2009. 10(5): p. 461-70.
290. Delgado, M.A., et al., *Toll-like receptors control autophagy.* EMBO J, 2008. 27(7): p. 1110-21.
291. Lock, R. and J. Debnath, *Extracellular matrix regulation of autophagy.* Curr Opin Cell Biol, 2008. 20(5): p. 583-8.
292. Cinque, L., et al., *FGF signalling regulates bone growth through autophagy.* Nature, 2015. 528(7581): p. 272-88.
293. Kim, S.I., et al., *Autophagy promotes intracellular degradation of type I collagen induced by transforming growth factor (TGF)-β1.* Journal of Biological Chemistry, 2012. 287(15): p. 11677-11688.
294. Rangarajan, S., et al., *Novel mechanisms for the antifibrotic action of nintedanib.* Am J Respir Cell Mol Biol, 2016. 54(1): p. 51-9.
295. Li, L., et al., *New autophagy reporter mice reveal dynamics of proximal tubular autophagy.* J Am Soc Nephrol, 2014. 25(2): p. 305-15.
296. Mi, S., et al., *Blocking IL-17A promotes the resolution of pulmonary inflammation and fibrosis via TGF-β1–dependent and–independent mechanisms.* The Journal of Immunology, 2011. 187(6): p. 3003-3014.
297. Patel, A.S., et al., *Autophagy in idiopathic pulmonary fibrosis.* PLoS One, 2012. 7(7): p. e41394.
298. Gui, Y.S., et al., *mTOR Overactivation and Compromised Autophagy in the Pathogenesis of Pulmonary Fibrosis.* PLoS One, 2015. 10(9): p. e0138625.
299. Mao, Y.Q. and X.M. Fan, *Autophagy: A new therapeutic target for liver fibrosis.* World J Hepatol, 2015. 7(16): p. 1982-6.
300. Li, Z.Y., et al., *Autophagy as a double-edged sword in pulmonary epithelial injury: a review and perspective.* Am J Physiol Lung Cell Mol Physiol, 2017. 313(2): p. L207-L217.
301. Araya, J., et al., *Insufficient autophagy in idiopathic pulmonary fibrosis.* Am J Physiol Lung Cell Mol Physiol, 2013. 304(1): p. L56-69.
302. Hynes, R.O., *The extracellular matrix: not just pretty fibrils.* Science, 2009. 326(5957): p. 1216-1219.
303. Gan, B., Y. Yoo, and J.L. Guan, *Association of focal adhesion kinase with tuberous sclerosis complex 2 in the regulation of s6 kinase activation and cell growth.* J Biol Chem, 2006. 281(49): p. 37321-9.
304. Petrovski, G., et al., *Clearance of dying autophagic cells of different origin by professional and non-professional phagocytes.* Cell Death Differ, 2007. 14(6): p. 1117-28.
305. Fung, C., et al., *Induction of autophagy during extracellular matrix detachment promotes cell survival.* Mol Biol Cell, 2008. 19(3): p. 797-806.
306. Pu, J., et al., *Mechanisms and functions of lysosome positioning.* J Cell Sci, 2016. 129(23): p. 4329-4339.
307. Lakkaraju, A. and E. Rodriguez-Boulan, *Itinerant exosomes: emerging roles in cell and tissue polarity.* Trends Cell Biol, 2008. 18(5): p. 199-209.
308. Johnstone, R.M., et al., *Exosome Formation during Maturation of Mammalian and Avian Reticulocytes - Evidence That Exosome Release Is a Major Route for Externalization of Obsolete Membrane-Proteins.* Journal of Cellular Physiology, 1991. 147(1): p. 27-36.
309. Yang, J.M. and S.J. Gould, *The cis-acting signals that target proteins to exosomes and microvesicles.* Biochemical Society Transactions, 2013. 41: p. 277-282.
310. Chargaff, E. and R. West, *The biological significance of the thromboplastic protein of Wood.* Journal of Biological Chemistry, 1946. 166: p. 189-197.
311. Harding, C., J. Heuser, and P. Stahl, *Endocytosis and intracellular processing of transferrin and colloidal gold-transferrin in rat reticulocytes: demonstration of a pathway for receptor shedding.* Eur J Cell Biol, 1984. 35(2): p. 256-63.
312. Pan, B.-T. and R.M. Johnstone, *Fate of the transferrin receptor during maturation of sheep reticulocytes in vitro: selective externalization of the receptor.* Cell, 1983. 33(3): p. 967-978.
313. Raposo, G., et al., *B lymphocytes secrete antigen-presenting vesicles.* J Exp Med, 1996. 183(3): p. 1161-72.

314. Valadi, H., et al., *Exosome-mediated transfer of mRNAs and microRNAs is a novel mechanism of genetic exchange between cells.* Nature Cell Biology, 2007. 9(6): p. 654-9.
315. Cocucci, E., G. Racchetti, and J. Meldolesi, *Shedding microvesicles: artefacts no more.* Trends in cell biology, 2009. 19(2): p. 43-51.
316. Gyorgy, B., et al., *Membrane vesicles, current state-of-the-art: emerging role of extracellular vesicles.* Cell Mol Life Sci, 2011. 68(16): p. 2667-88.
317. Alipoor, S.D., et al., *Exosomes and Exosomal miRNA in Respiratory Diseases.* Mediators Inflamm, 2016. 2016: p. 5628404.
318. Sato, K., et al., *Exosomes in liver pathology.* Journal of hepatology, 2016. 65(1): p. 213-221.
319. Milbank, E., M.C. Martinez, and R. Andriantsitohaina, *Extracellular vesicles: Pharmacological modulators of the peripheral and central signals governing obesity.* Pharmacol Ther, 2016. 157: p. 65-83.
320. H. Rashed, M., et al., *Exosomes: From Garbage Bins to Promising Therapeutic Targets.* Int J Mol Sci, 2017. 18(3): p. 538.
321. Pan, B.T., et al., *Electron microscopic evidence for externalization of the transferrin receptor in vesicular form in sheep reticulocytes.* J Cell Biol, 1985. 101(3): p. 942-8.
322. Pant, S., H. Hilton, and M.E. Burczynski, *The multifaceted exosome: biogenesis, role in normal and aberrant cellular function, and frontiers for pharmacological and biomarker opportunities.* Biochem Pharmacol, 2012. 83(11): p. 1484-94.
323. Andaloussi, S.E., et al., *Extracellular vesicles: biology and emerging therapeutic opportunities.* Nature reviews Drug discovery, 2013. 12(5): p. 347-357.
324. Raposo, G. and W. Stoorvogel, *Extracellular vesicles: exosomes, microvesicles, and friends.* J Cell Biol, 2013. 200(4): p. 373-83.
325. Witwer, K.W., et al., *Standardization of sample collection, isolation and analysis methods in extracellular vesicle research.* J Extracell Vesicles, 2013. 2(1): p. 20360.
326. Zaborowski, M.P., et al., *Extracellular vesicles: Composition, biological relevance, and methods of study.* Bioscience, 2015. 65(8): p. 783-797.
327. Eitan, E., et al., *Impact of lysosome status on extracellular vesicle content and release.* Ageing Res Rev, 2016. 32: p. 65-74.
328. Atkin-Smith, G.K., et al., *A novel mechanism of generating extracellular vesicles during apoptosis via a beads-on-a-string membrane structure.* Nat Commun, 2015. 6: p. 7439.
329. Jin, Y., et al., *DNA in serum extracellular vesicles is stable under different storage conditions.* BMC cancer, 2016. 16(1): p. 753.
330. Yanez-Mo, M., et al., *Biological properties of extracellular vesicles and their physiological functions.* J Extracell Vesicles, 2015. 4(1): p. 27066.
331. Hanson, P.I. and A. Cashikar, *Multivesicular body morphogenesis.* Annu Rev Cell Dev Biol, 2012. 28: p. 337-62.
332. Yoon, Y.J., O.Y. Kim, and Y.S. Gho, *Extracellular vesicles as emerging intercellular communicasomes.* Bmb Reports, 2014. 47(10): p. 531-539.
333. Thery, C., et al., *Isolation and characterization of exosomes from cell culture supernatants and biological fluids.* Curr Protoc Cell Biol, 2006. Chapter 3: p. Unit 3 22.
334. Musante, L., et al., *A simplified method to recover urinary vesicles for clinical applications, and sample banking.* Sci Rep, 2014. 4: p. 7532.
335. Filipe, V., A. Hawe, and W. Jiskoot, *Critical evaluation of Nanoparticle Tracking Analysis (NTA) by NanoSight for the measurement of nanoparticles and protein aggregates.* Pharm Res, 2010. 27(5): p. 796-810.
336. Gardiner, C., et al., *Extracellular vesicle sizing and enumeration by nanoparticle tracking analysis.* J Extracell Vesicles, 2013. 2(1): p. 19671.
337. Szatanek, R., et al., *Isolation of extracellular vesicles: Determining the correct approach (Review).* Int J Mol Med, 2015. 36(1): p. 11-7.
338. Raiborg, C. and H. Stenmark, *The ESCRT machinery in endosomal sorting of ubiquitylated membrane proteins.* Nature, 2009. 458(7237): p. 445-52.
339. Trajkovic, K., et al., *Ceramide triggers budding of exosome vesicles into multivesicular endosomes.* Science, 2008. 319(5867): p. 1244-7.
340. Stuffers, S., et al., *Multivesicular endosome biogenesis in the absence of ESCRTs.* Traffic, 2009. 10(7): p. 925-37.

341. Theos, A.C., et al., *A lumenal domain-dependent pathway for sorting to intralumenal vesicles of multivesicular endosomes involved in organelle morphogenesis.* Dev Cell, 2006. 10(3): p. 343-54.
342. van Niel, G., et al., *The tetraspanin CD63 regulates ESCRT-independent and -dependent endosomal sorting during melanogenesis.* Dev Cell, 2011. 21(4): p. 708-21.
343. Mobius, W., et al., *Immunoelectron microscopic localization of cholesterol using biotinylated and non-cytolytic perfringolysin O.* Journal of Histochemistry & Cytochemistry, 2002. 50(1): p. 43-55.
344. Savina, A., M. Vidal, and M.I. Colombo, *The exosome pathway in K562 cells is regulated by Rab11.* Journal of Cell Science, 2002. 115(12): p. 2505-2515.
345. Ostrowski, M., et al., *Rab27a and Rab27b control different steps of the exosome secretion pathway.* Nat Cell Biol, 2010. 12(1): p. 19-30; sup pp 1-13.
346. Hsu, C., et al., *Regulation of exosome secretion by Rab35 and its GTPase-activating proteins TBC1D10A-C.* J Cell Biol, 2010. 189(2): p. 223-32.
347. Géminard, C., et al., *Degradation of AP2 during reticulocyte maturation enhances binding of hsc70 and Alix to a common site on TFR for sorting into exosomes.* Traffic, 2004. 5(3): p. 181-193.
348. Fader, C.M. and M.I. Colombo, *Autophagy and multivesicular bodies: two closely related partners.* Cell Death Differ, 2009. 16(1): p. 70-8.
349. Baixauli, F., C. Lopez-Otin, and M. Mittelbrunn, *Exosomes and autophagy: coordinated mechanisms for the maintenance of cellular fitness.* Front Immunol, 2014. 5: p. 403.
350. Berg, T.O., et al., *Isolation and characterization of rat liver amphisomes. Evidence for fusion of autophagosomes with both early and late endosomes.* Journal of Biological Chemistry, 1998. 273(34): p. 21883-92.
351. Hyttinen, J.M., et al., *Maturation of autophagosomes and endosomes: a key role for Rab7.* Biochim Biophys Acta, 2013. 1833(3): p. 503-10.
352. Szatmari, Z., et al., *Rab11 facilitates cross-talk between autophagy and endosomal pathway through regulation of Hook localization.* Mol Biol Cell, 2014. 25(4): p. 522-531.
353. Fader, C.M., et al., *Induction of autophagy promotes fusion of multivesicular bodies with autophagic vacuoles in k562 cells.* Traffic, 2008. 9(2): p. 230-50.
354. Alvarez-Erviti, L., et al., *Lysosomal dysfunction increases exosome-mediated alpha-synuclein release and transmission.* Neurobiol Dis, 2011. 42(3): p. 360-7.
355. Miao, Y.X., et al., *A TRP Channel Senses Lysosome Neutralization by Pathogens to Trigger Their Expulsion.* Cell, 2015. 161(6): p. 1306-1319.
356. Poehler, A.M., et al., *Autophagy modulates SNCA/alpha-synuclein release, thereby generating a hostile microenvironment.* Autophagy, 2014. 10(12): p. 2171-92.
357. Murrow, L., R. Malhotra, and J. Debnath, *ATG12–ATG3 interacts with Alix to promote basal autophagic flux and late endosome function.* Nat Cell Biol, 2015. 17(3): p. 300-310.
358. Simon, D., et al., *Proteostasis of tau. Tau overexpression results in its secretion via membrane vesicles.* FEBS Lett, 2012. 586(1): p. 47-54.
359. Hasegawa, T., et al., *The AAA-ATPase VPS4 regulates extracellular secretion and lysosomal targeting of alpha-synuclein.* PLoS One, 2011. 6(12): p. e29460.
360. Rusten, T.E. and A. Simonsen, *ESCRT functions in autophagy and associated disease.* Cell Cycle, 2008. 7(9): p. 1166-72.
361. Colombo, M., G. Raposo, and C. Thery, *Biogenesis, secretion, and intercellular interactions of exosomes and other extracellular vesicles.* Annu Rev Cell Dev Biol, 2014. 30: p. 255-89.
362. Kajimoto, T., et al., *Ongoing activation of sphingosine 1-phosphate receptors mediates maturation of exosomal multivesicular endosomes.* Nat Commun, 2013. 4: p. 2712.
363. Huang, L.S., et al., *Sphingosine-1-phosphate lyase is an endogenous suppressor of pulmonary fibrosis: role of S1P signalling and autophagy.* Thorax, 2015. 70(12): p. 1138-1148.
364. Kalani, A., A. Tyagi, and N. Tyagi, *Exosomes: mediators of neurodegeneration, neuroprotection and therapeutics.* Mol Neurobiol, 2014. 49(1): p. 590-600.
365. Robbins, P.D. and A.E. Morelli, *Regulation of immune responses by extracellular vesicles.* Nat Rev Immunol, 2014. 14(3): p. 195-208.
366. Fruhbeis, C., D. Frohlich, and E.M. Kramer-Albers, *Emerging roles of exosomes in neuron-glia communication.* Front Physiol, 2012. 3: p. 119.
367. Lai, R.C., R.W. Yeo, and S.K. Lim, *Mesenchymal stem cell exosomes.* Semin Cell Dev Biol, 2015. 40: p. 82-8.

368. Record, M., et al., *Exosomes as new vesicular lipid transporters involved in cell-cell communication and various pathophysiologies.* Biochimica Et Biophysica Acta-Molecular and Cell Biology of Lipids, 2014. 1841(1): p. 108-120.
369. Llorente, A., B. van Deurs, and K. Sandvig, *Cholesterol regulates prostasome release from secretory lysosomes in PC-3 human prostate cancer cells.* Eur J Cell Biol, 2007. 86(7): p. 405-15.
370. Subra, C., et al., *Exosome lipidomics unravels lipid sorting at the level of multivesicular bodies.* Biochimie, 2007. 89(2): p. 205-212.
371. Subra, C., et al., *Exosomes account for vesicle-mediated transcellular transport of activatable phospholipases and prostaglandins.* J Lipid Res, 2010. 51(8): p. 2105-20.
372. Beloribi, S., et al., *Exosomal lipids impact notch signaling and induce death of human pancreatic tumoral SOJ-6 cells.* PLoS One, 2012. 7(10): p. e47480.
373. Kim, C.W., et al., *Extracellular membrane vesicles from tumor cells promote angiogenesis via sphingomyelin.* Cancer Res, 2002. 62(21): p. 6312-7.
374. Sullivan, R. and F. Saez, *Epididymosomes, prostasomes, and liposomes: their roles in mammalian male reproductive physiology.* Reproduction, 2013. 146(1): p. R21-R35.
375. Bellingham, S.A., B. Guo, and A.F. Hill, *The secret life of extracellular vesicles in metal homeostasis and neurodegeneration.* Biol Cell, 2015. 107(11): p. 389-418.
376. Guo, J.L. and V.M. Lee, *Cell-to-cell transmission of pathogenic proteins in neurodegenerative diseases.* Nat Med, 2014. 20(2): p. 130-8.
377. Rajendran, L., et al., *Alzheimer's disease beta-amyloid peptides are released in association with exosomes.* Proc Natl Acad Sci U S A, 2006. 103(30): p. 11172-7.
378. Squadrito, M.L., et al., *Endogenous RNAs modulate microRNA sorting to exosomes and transfer to acceptor cells.* Cell Rep, 2014. 8(5): p. 1432-46.
379. Milane, L., et al., *Exosome mediated communication within the tumor microenvironment.* Journal of Controlled Release, 2015. 219: p. 278-294.
380. Van Giau, V. and S.S.A. An, *Emergence of exosomal miRNAs as a diagnostic biomarker for Alzheimer's disease.* Journal of the neurological sciences, 2016. 360: p. 141-152.
381. Skog, J., et al., *Glioblastoma microvesicles transport RNA and proteins that promote tumour growth and provide diagnostic biomarkers.* Nature Cell Biology, 2008. 10(12): p. 1470-U209.
382. Mittelbrunn, M., et al., *Unidirectional transfer of microRNA-loaded exosomes from T cells to antigen-presenting cells.* Nat Commun, 2011. 2: p. 282.
383. Brinton, L.T., et al., *Formation and role of exosomes in cancer.* Cell Mol Life Sci, 2015. 72(4): p. 659-71.
384. Hoshino, A., et al., *Tumour exosome integrins determine organotropic metastasis.* Nature, 2015. 527(7578): p. 329-35.
385. Thakur, B.K., et al., *Double-stranded DNA in exosomes: a novel biomarker in cancer detection.* Cell Res, 2014. 24(6): p. 766-9.
386. Lazaro-Ibanez, E., et al., *Different gDNA content in the subpopulations of prostate cancer extracellular vesicles: apoptotic bodies, microvesicles, and exosomes.* Prostate, 2014. 74(14): p. 1379-90.
387. Azmi, A.S., B. Bao, and F.H. Sarkar, *Exosomes in cancer development, metastasis, and drug resistance: a comprehensive review.* Cancer Metastasis Rev, 2013. 32(3-4): p. 623-42.
388. Bellingham, S.A., et al., *Exosomes: vehicles for the transfer of toxic proteins associated with neurodegenerative diseases?* Front Physiol, 2012. 3: p. 124.
389. Pisitkun, T., R.F. Shen, and M.A. Knepper, *Identification and proteomic profiling of exosomes in human urine.* Proc Natl Acad Sci U S A, 2004. 101(36): p. 13368-73.
390. Ramachandra, L., et al., *Mycobacterium tuberculosis synergizes with ATP to induce release of microvesicles and exosomes containing major histocompatibility complex class II molecules capable of antigen presentation.* Infect Immun, 2010. 78(12): p. 5116-25.
391. Qazi, K.R., et al., *Proinflammatory exosomes in bronchoalveolar lavage fluid of patients with sarcoidosis.* Thorax, 2010. 65(11): p. 1016-24.
392. Lener, T., et al., *Applying extracellular vesicles based therapeutics in clinical trials - an ISEV position paper.* J Extracell Vesicles, 2015. 4: p. 30087.
393. Admyre, C., et al., *Exosomes with major histocompatibility complex class II and co-stimulatory molecules are present in human BAL fluid.* Eur Respir J, 2003. 22(4): p. 578-83.
394. Torregrosa Paredes, P., et al., *Bronchoalveolar lavage fluid exosomes contribute to cytokine and leukotriene production in allergic asthma.* Allergy, 2012. 67(7): p. 911-9.

395. Levanen, B., et al., *Altered microRNA profiles in bronchoalveolar lavage fluid exosomes in asthmatic patients.* J Allergy Clin Immunol, 2013. 131(3): p. 894-903.
396. Bhatnagar, S., et al., *Exosomes released from macrophages infected with intracellular pathogens stimulate a proinflammatory response in vitro and in vivo.* Blood, 2007. 110(9): p. 3234-44.
397. Zhu, M., et al., *Exosomes as extrapulmonary signaling conveyors for nanoparticle‐induced systemic immune activation.* Small, 2012. 8(3): p. 404-412.
398. Almqvist, N., et al., *Serum-derived exosomes from antigen-fed mice prevent allergic sensitization in a model of allergic asthma.* Immunology, 2008. 125(1): p. 21-7.
399. Kulshreshtha, A., et al., *Proinflammatory role of epithelial cell-derived exosomes in allergic airway inflammation.* J Allergy Clin Immunol, 2013. 131(4): p. 1194-203.
400. Villalba, M., R. Rodriguez, and E. Batanero, *The spectrum of olive pollen allergens. From structures to diagnosis and treatment.* Methods, 2014. 66(1): p. 44-54.
401. Soni, S., et al., *Alveolar macrophage-derived microvesicles mediate acute lung injury.* Thorax, 2016. 71(11): p. 1020-1029.
402. McDonald, M.K., et al., *Functional significance of macrophage-derived exosomes in inflammation and pain.* Pain, 2014. 155(8): p. 1527-39.
403. Holder, B., et al., *Macrophage Exosomes Induce Placental Inflammatory Cytokines: A Novel Mode of Maternal-Placental Messaging.* Traffic, 2016. 17(2): p. 168-78.
404. Huber, H.J. and P. Holvoet, *Exosomes: emerging roles in communication between blood cells and vascular tissues during atherosclerosis.* Current Opinion in Lipidology, 2015. 26(5): p. 412-419.
405. Esser, J., et al., *Exosomes from human macrophages and dendritic cells contain enzymes for leukotriene biosynthesis and promote granulocyte migration.* J Allergy Clin Immunol, 2010. 126(5): p. 1032-40.
406. Qu, Y., et al., *P2X7 receptor-stimulated secretion of MHC class II-containing exosomes requires the ASC/NLRP3 inflammasome but is independent of caspase-1.* Journal of Immunology, 2009. 182(8): p. 5052-5062.
407. Ismail, N., et al., *Macrophage microvesicles induce macrophage differentiation and miR-223 transfer.* Blood, 2013. 121(6): p. 984-95.
408. Sarkar, A., et al., *Monocyte derived microvesicles deliver a cell death message via encapsulated caspase-1.* PLoS One, 2009. 4(9): p. e7140.
409. O'Neill, H.C. and B.J. Quah, *Exosomes secreted by bacterially infected macrophages are proinflammatory.* Sci Signal, 2008. 1(6): p. pe8.
410. Singh, P.P., et al., *Exosomes isolated from mycobacteria-infected mice or cultured macrophages can recruit and activate immune cells in vitro and in vivo.* Journal of Immunology, 2012. 189(2): p. 777-785.
411. Walters, S.B., et al., *Microparticles from mycobacteria-infected macrophages promote inflammation and cellular migration.* J Immunol, 2013. 190(2): p. 669-77.
412. Cestari, I., et al., *Trypanosoma cruzi immune evasion mediated by host cell-derived microvesicles.* J Immunol, 2012. 188(4): p. 1942-52.
413. Garzetti, L., et al., *Activated macrophages release microvesicles containing polarized M1 or M2 mRNAs.* J Leukoc Biol, 2014. 95(5): p. 817-825.
414. Sandfeld-Paulsen, B., et al., *Exosomal proteins as prognostic biomarkers in non-small cell lung cancer.* Mol Oncol, 2016. 10(10): p. 1595-1602.
415. Takahashi, T. and H. Kubo, *The role of microparticles in chronic obstructive pulmonary disease.* Int J Chron Obstruct Pulmon Dis, 2014. 9: p. 303-14.
416. Moon, H.G., et al., *CCN1 secretion and cleavage regulate the lung epithelial cell functions after cigarette smoke.* Am J Physiol Lung Cell Mol Physiol, 2014. 307(4): p. L326-37.
417. Letsiou, E., et al., *Pathologic mechanical stress and endotoxin exposure increases lung endothelial microparticle shedding.* Am J Respir Cell Mol Biol, 2015. 52(2): p. 193-204.
418. MacNee, W., *ABC of chronic obstructive pulmonary disease - Pathology, pathogenesis, and pathophysiology.* British Medical Journal, 2006. 332(7551): p. 1202-1204.
419. Donaldson, A., et al., *Increased skeletal muscle-specific microRNA in the blood of patients with COPD.* Thorax, 2013. 68(12): p. 1140-9.
420. Burke, H., et al., *Role of exosomal microRNA in driving skeletal muscle wasting in COPD*. 2015, Eur Respiratory Soc. p. OA2930.

421. Jakobsen, K.R., et al., *Exosomal proteins as potential diagnostic markers in advanced non-small cell lung carcinoma.* Journal of Extracellular Vesicles, 2015. 4(1): p. 26659.
422. Minnis, P., et al., *Serum exosomes from IPF patients display a fibrotic miRNA profile that correlates to clinical measures of disease severity.* European Respiratory Journal, 2015. 46(suppl 59): p. PA3845.
423. Dimtrakopoulos, F.-I.D., et al., *Correlation of exosome concentrations in the plasma of lung cancer patients with disease stage.* Journal of Clinical Oncology, 2016. 34(15 (suppl)): p. e23016.
424. Krause, M., A. Samoylenko, and S.J. Vainio, *Exosomes as renal inductive signals in health and disease, and their application as diagnostic markers and therapeutic agents.* Frontiers in cell and developmental biology, 2015. 3: p. 65.
425. Borges, F.T., et al., *TGF-β1–containing exosomes from injured epithelial cells activate fibroblasts to initiate tissue regenerative responses and fibrosis.* Journal of the American Society of Nephrology, 2013. 24(3): p. 385-92.
426. Vella, L.J., *The emerging role of exosomes in epithelial-mesenchymal-transition in cancer.* Front Oncol, 2014. 4: p. 361.
427. Murray, P.J. and T.A. Wynn, *Protective and pathogenic functions of macrophage subsets.* Nat Rev Immunol, 2011. 11(11): p. 723-37.
428. Varol, C., A. Mildner, and S. Jung, *Macrophages: development and tissue specialization.* Annu Rev Immunol, 2015. 33: p. 643-75.
429. Ivanova, E.A. and A.N. Orekhov, *Monocyte Activation in Immunopathology: Cellular Test for Development of Diagnostics and Therapy.* J Immunol Res, 2016. 2016: p. 4789279.
430. Viken, K.E. and J. Lamvik, *Structural and functional properties of blood monocytes cultured in vitro.* APMIS, 1974. 82(2): p. 223-234.
431. de Mulder, P.H., et al., *Characterization of monocyte maturation in adherent and suspension cultures and its application to study monocyte differentiation in Hodgkin's disease.* Clin Exp Immunol, 1983. 54(3): p. 681-8.
432. van der Meer, J.W., et al., *Characteristics of human monocytes cultured in the Teflon culture bag.* Immunology, 1982. 47(4): p. 617-25.
433. Kaplan, G. and G. Gaudernack, *In vitro differentiation of human monocytes. Differences in monocyte phenotypes induced by cultivation on glass or on collagen.* J Exp Med, 1982. 156(4): p. 1101-14.
434. Musson, R.A., *Human serum induces maturation of human monocytes in vitro. Changes in cytolytic activity, intracellular lysosomal enzymes, and nonspecific esterase activity.* Am J Pathol, 1983. 111(3): p. 331-40.
435. Czuprynski, C.J. and H. Hamilton, *The effects of serum on the in vitro adherence and maturation of bovine monocytes.* Vet Immunol Immunopathol, 1985. 9(2): p. 189-93.
436. Rey-Giraud, F., M. Hafner, and C.H. Ries, *In vitro generation of monocyte-derived macrophages under serum-free conditions improves their tumor promoting functions.* Plos One, 2012. 7(8): p. e42656.
437. Murray, P.J., et al., *Macrophage activation and polarization: nomenclature and experimental guidelines.* Immunity, 2014. 41(1): p. 14-20.
438. Joshi, S., et al., *Rac2 controls tumor growth, metastasis and M1-M2 macrophage differentiation in vivo.* PLoS One, 2014. 9(4): p. e95893.
439. Fleetwood, A.J., et al., *GM-CSF- and M-CSF-dependent macrophage phenotypes display differential dependence on type I interferon signaling.* J Leukoc Biol, 2009. 86(2): p. 411-21.
440. van der Meer, J.W., et al., *Culture of mononuclear phagocytes on a teflon surface to prevent adherence.* J Exp Med, 1978. 147(1): p. 271-6.
441. Moore, J.K., et al., *Phenotypic and functional characterization of macrophages with therapeutic potential generated from human cirrhotic monocytes in a cohort study.* Cytotherapy, 2015. 17(11): p. 1604-16.
442. Shen, M. and T.A. Horbett, *The effects of surface chemistry and adsorbed proteins on monocyte/macrophage adhesion to chemically modified polystyrene surfaces.* J Biomed Mater Res, 2001. 57(3): p. 336-45.
443. Xiao, F., et al., *In vitro cyto-biocompatibility and cell detachment of temperature-sensitive dextran hydrogel.* Colloids Surf B Biointerfaces, 2009. 71(1): p. 13-8.
444. Rossi, A.G., et al., *Regulation of macrophage phagocytosis of apoptotic cells by cAMP.* J Immunol, 1998. 160(7): p. 3562-8.

445. Kawanishi, N., et al., *Exercise training inhibits inflammation in adipose tissue via both suppression of macrophage infiltration and acceleration of phenotypic switching from M1 to M2 macrophages in high-fat-diet-induced obese mice.* Exerc Immunol Rev, 2010. 16(16): p. 105-118.
446. Mylonas, K.J., et al., *Alternatively Activated Macrophages Elicited by Helminth Infection Can Be Reprogrammed to Enable Microbial Killing.* Journal of Immunology, 2009. 182(5): p. 3084-3094.
447. Stout, R.D., et al., *Macrophages sequentially change their functional phenotype in response to changes in microenvironmental influences.* Journal of Immunology, 2005. 175(1): p. 342-349.
448. Stout, R.D. and J. Suttles, *Functional plasticity of macrophages: reversible adaptation to changing microenvironments.* J Leukoc Biol, 2004. 76(3): p. 509-13.
449. Arnold, L., et al., *Inflammatory monocytes recruited after skeletal muscle injury switch into antiinflammatory macrophages to support myogenesis.* Journal of Experimental Medicine, 2007. 204(5): p. 1057-1069.
450. Ramprasad, M.P., et al., *Cell surface expression of mouse macrosialin and human CD68 and their role as macrophage receptors for oxidized low density lipoprotein.* P Natl Acad Sci USA, 1996. 93(25): p. 14833-14838.
451. Roszer, T., *Understanding the mysterious M2 macrophage through activation markers and effector mechanisms.* Mediat Inflamm, 2015. 2015: p. 816460.
452. Chen, S., et al., *Impact of Detachment Methods on M2 Macrophage Phenotype and Function.* J Immunol Methods, 2015. 426: p. 56-61.
453. Ulrich, F., *Effects of trypsin on protein synthesis in macrophages.* Exp Cell Res, 1976. 101(2): p. 267-77.
454. Komatsu, H., et al., *Trypsin inhibits lipopolysaccharide signaling in macrophages via toll-like receptor 4 accessory molecules.* Life Sci, 2012. 91(3-4): p. 143-50.
455. Prieto, J., A. Eklund, and M. Patarroyo, *Regulated expression of integrins and other adhesion molecules during differentiation of monocytes into macrophages.* Cell Immunol, 1994. 156(1): p. 191-211.
456. Chambers, T.J., *Multinucleate giant cells.* J Pathol, 1978. 126(3): p. 125-48.
457. Kreipe, H., et al., *Multinucleated giant cells generated in vitro. Terminally differentiated macrophages with down-regulated c-fms expression.* Am J Pathol, 1988. 130(2): p. 232-43.
458. Johnson, W.D., Jr., B. Mei, and Z.A. Cohn, *The separation, long-term cultivation, and maturation of the human monocyte.* J Exp Med, 1977. 146(6): p. 1613-26.
459. Zuckerman, S.H., S.K. Ackerman, and S.D. Douglas, *Long-term human peripheral blood monocyte cultures: establishment, metabolism and morphology of primary human monocyte-macrophage cell cultures.* Immunology, 1979. 38(2): p. 401-11.
460. Meyer, K.C. and G. Raghu, *Bronchoalveolar lavage for the evaluation of interstitial lung disease: is it clinically useful?* European Respiratory Journal, 2011. 38(4): p. 761-769.
461. Clayton, A., et al., *Analysis of antigen presenting cell derived exosomes, based on immuno-magnetic isolation and flow cytometry.* J Immunol Methods, 2001. 247(1-2): p. 163-74.
462. Rupp, A.K., et al., *Loss of EpCAM expression in breast cancer derived serum exosomes: role of proteolytic cleavage.* Gynecol Oncol, 2011. 122(2): p. 437-46.
463. Kowal, J., et al., *Proteomic comparison defines novel markers to characterize heterogeneous populations of extracellular vesicle subtypes.* Proc Natl Acad Sci U S A, 2016. 113(8): p. E968-77.
464. Boismenu, R., et al., *A role for CD81 in early T cell development.* Science, 1996. 271(5246): p. 198-200.
465. Maecker, H.T. and S. Levy, *Normal lymphocyte development but delayed humoral immune response in CD81-null mice.* J Exp Med, 1997. 185(8): p. 1505-10.
466. Levy, S., S.C. Todd, and H.T. Maecker, *CD81 (TAPA-1): a molecule involved in signal transduction and cell adhesion in the immune system.* Annu Rev Immunol, 1998. 16(1): p. 89-109.
467. Charrin, S., et al., *The major CD9 and CD81 molecular partner. Identification and characterization of the complexes.* J Biol Chem, 2001. 276(17): p. 14329-37.
468. Takeda, Y., et al., *Tetraspanins CD9 and CD81 function to prevent the fusion of mononuclear phagocytes.* J Cell Biol, 2003. 161(5): p. 945-56.
469. Brazzoli, M., et al., *CD81 is a central regulator of cellular events required for hepatitis C virus infection of human hepatocytes.* Journal of virology, 2008. 82(17): p. 8316-29.

470. Rubinstein, E., et al., *Reduced fertility of female mice lacking CD81.* Dev Biol, 2006. 290(2): p. 351-8.
471. Tippett, E., et al., *Characterization of tetraspanins CD9, CD53, CD63, and CD81 in monocytes and macrophages in HIV-1 infection.* J Leukoc Biol, 2013. 93(6): p. 913-20.
472. Jacquel, A., et al., *Autophagy is required for CSF-1-induced macrophagic differentiation and acquisition of phagocytic functions.* Blood, 2012. 119(19): p. 4527-31.
473. Li, T., et al., *Exosomes derived from human umbilical cord mesenchymal stem cells alleviate liver fibrosis.* Stem Cells Dev, 2013. 22(6): p. 845-54.
474. Crotzer, V.L. and J.S. Blum, *Autophagy and its role in MHC-mediated antigen presentation.* J Immunol, 2009. 182(6): p. 3335-41.
475. Tey, S.K. and R. Khanna, *Autophagy mediates transporter associated with antigen processing-independent presentation of viral epitopes through MHC class I pathway.* Blood, 2012. 120(5): p. 994-1004.
476. Harris, J., et al., *T helper 2 cytokines inhibit autophagic control of intracellular Mycobacterium tuberculosis.* Immunity, 2007. 27(3): p. 505-17.
477. Roca, H., et al., *CCL2 and interleukin-6 promote survival of human CD11b+ peripheral blood mononuclear cells and induce M2-type macrophage polarization.* J Biol Chem, 2009. 284(49): p. 34342-54.
478. Monick, M.M., et al., *Identification of an autophagy defect in smokers' alveolar macrophages.* J Immunol, 2010. 185(9): p. 5425-35.
479. Simler, N.R., et al., *The rapamycin analogue SDZ RAD attenuates bleomycin-induced pulmonary fibrosis in rats.* Eur Respir J, 2002. 19(6): p. 1124-7.
480. Mizushima, N., Y. Ohsumi, and T. Yoshimori, *Autophagosome formation in mammalian cells.* Cell Struct Funct, 2002. 27(6): p. 421-9.
481. Mehrpour, M., et al., *Overview of macroautophagy regulation in mammalian cells.* Cell Res, 2010. 20(7): p. 748-62.
482. Bjorkoy, G., et al., *Monitoring autophagic degradation of p62/SQSTM1.* Methods Enzymol, 2009. 452: p. 181-97.
483. Jiang, P.D. and N. Mizushima, *LC3-and p62-based biochemical methods for the analysis of autophagy progression in mammalian cells.* Methods, 2015. 75: p. 13-18.
484. Mizushima, N. and T. Yoshimori, *How to interpret LC3 immunoblotting.* Autophagy, 2007. 3(6): p. 542-545.
485. Nyfeler, B., et al., *Relieving autophagy and 4EBP1 from rapamycin resistance.* Mol Cell Biol, 2011. 31(14): p. 2867-76.
486. Cheng, P.H., et al., *Combination of autophagy inducer rapamycin and oncolytic adenovirus improves antitumor effect in cancer cells.* Virol J, 2013. 10(1): p. 293.
487. Proikas-Cezanne, T., et al., *Human WIPI-1 puncta-formation: a novel assay to assess mammalian autophagy.* FEBS Lett, 2007. 581(18): p. 3396-404.
488. Foster, D.A. and A. Toschi, *Targeting mTOR with rapamycin: one dose does not fit all.* Cell Cycle, 2009. 8(7): p. 1026-1029.
489. Zullo, A.J., K.L. Jurcic Smith, and S. Lee, *Mammalian target of Rapamycin inhibition and mycobacterial survival are uncoupled in murine macrophages.* BMC Biochem, 2014. 15(1): p. 4.
490. Mauvezin, C., et al., *Autophagosome-lysosome fusion is independent of V-ATPase-mediated acidification.* Nat Commun, 2015. 6: p. 7007.
491. Cohn, Z.A. and E. Wiener, *The Particulate Hydrolases of Macrophages. I. Comparative Enzymology, Isolation, and Properties.* J Exp Med, 1963. 118(6): p. 991-1008.
492. Piao, S. and R.K. Amaravadi, *Targeting the lysosome in cancer.* Ann N Y Acad Sci, 2016. 1371(1): p. 45-54.
493. Behura, A., *Effect of PMA on Autophagy in Human Monocyte Cell-Line, THP-1*. 2015.
494. Xu, Y., et al., *Silver nanoparticles impede phorbol myristate acetate-induced monocyte-macrophage differentiation and autophagy.* Nanoscale, 2015. 7(38): p. 16100-9.
495. Remijsen, Q., et al., *Neutrophil extracellular trap cell death requires both autophagy and superoxide generation.* Cell Research, 2011. 21(2): p. 290-304.
496. Gray, R.D., et al., *Activation of conventional protein kinase C (PKC) is critical in the generation of human neutrophil extracellular traps.* Journal of Inflammation-London, 2013. 10(1): p. 12.
497. Jiang, H., et al., *Protein kinase C inhibits autophagy and phosphorylates LC3.* Biochem Biophys Res Commun, 2010. 395(4): p. 471-6.

498. Yuk, J.M., et al., *Vitamin D3 induces autophagy in human monocytes/macrophages via cathelicidin.* Cell Host Microbe, 2009. 6(3): p. 231-43.
499. Zhang, Y., et al., *Induction of autophagy is essential for monocyte-macrophage differentiation.* Blood, 2012. 119(12): p. 2895-2905.
500. Codogno, P. and A. Meijer, *Autophagy and signaling: their role in cell survival and cell death.* Cell Death & Differentiation, 2005. 12(suppl 2): p. 1509-1518.
501. Miranti, C.K. and J.S. Brugge, *Sensing the environment: a historical perspective on integrin signal transduction.* Nature Cell Biology, 2002. 4(4): p. E83-E90.
502. Luo, B.H., C.V. Carman, and T.A. Springer, *Structural basis of integrin regulation and signaling.* Annu Rev Immunol, 2007. 25: p. 619-47.
503. Mitra, S.K., D.A. Hanson, and D.D. Schlaepfer, *Focal adhesion kinase: in command and control of cell motility.* Nat Rev Mol Cell Biol, 2005. 6(1): p. 56-68.
504. Werb, Z., M.J. Banda, and P.A. Jones, *Degradation of connective tissue matrices by macrophages.* J Exp Med, 1980. 152: p. 1340-1357.
505. Ye, Q.S., et al., *Endo180 and MT1-MMP are involved in the phagocytosis of collagen scaffolds by macrophages and is regulated by interferon-gamma.* Eur Cell Mater, 2010. 20: p. 197-209.
506. Lu, P., et al., *Extracellular matrix degradation and remodeling in development and disease.* Cold Spring Harb Perspect Biol, 2011. 3(12): p. a005058.
507. Maquart, F.X., et al., *An introduction to matrikines: extracellular matrix-derived peptides which regulate cell activity - Implication in tumor invasion.* Critical Reviews in Oncology Hematology, 2004. 49(3): p. 199-202.
508. Monboisse, J.C., et al., *Activation of human neutrophils by type I collagen. Requirement of two different sequences.* Biochem J, 1990. 270(2): p. 459-62.
509. Parkinson-Lawrence, E.J., et al., *Lysosomal storage disease: revealing lysosomal function and physiology.* Physiology, 2010. 25(2): p. 102-15.
510. Dvorak, A.M., et al., *Ultrastructural immunogold localization of prostaglandin endoperoxide synthase (cyclooxygenase) to non-membrane-bound cytoplasmic lipid bodies in human lung mast cells, alveolar macrophages, type II pneumocytes, and neutrophils.* J Histochem Cytochem, 1992. 40(6): p. 759-69.
511. Bozza, P.T., K.G. Magalhaes, and P.F. Weller, *Leukocyte lipid bodies - Biogenesis and functions in inflammation.* Biochim Biophys Acta, 2009. 1791(6): p. 540-51.
512. Nairz, M., et al., *"Pumping iron"-how macrophages handle iron at the systemic, microenvironmental, and cellular levels.* Pflugers Archiv-European Journal of Physiology, 2017. 469(3-4): p. 397-418.
513. Porto, G. and M. De Sousa, *Iron overload and immunity.* World J Gastroenterol, 2007. 13(35): p. 4707-15.
514. Cherayil, B.J., *Iron and immunity: immunological consequences of iron deficiency and overload.* Arch Immunol Ther Exp (Warsz), 2010. 58(6): p. 407-15.
515. Kao, J.-K., et al., *Chronic Iron Overload Results in Impaired Bacterial Killing of THP-1 Derived Macrophage through the Inhibition of Lysosomal Acidification.* PloS one, 2016. 11(5): p. e0156713.
516. Korolnek, T. and I. Hamza, *Macrophages and iron trafficking at the birth and death of red cells.* Blood, 2015. 125(19): p. 2893-2897.
517. Boven, L.A., et al., *Gaucher cells demonstrate a distinct macrophage phenotype and resemble alternatively activated macrophages.* Am J Clin Pathol, 2004. 122(3): p. 359-69.
518. Aflaki, E., et al., *Lysosomal storage and impaired autophagy lead to inflammasome activation in Gaucher macrophages.* Aging Cell, 2016. 15(1): p. 77-88.
519. Borger, D.K., et al., *Impaired autophagy leads to inflammasome activation and a heightened inflammatory profile of macrophages in Gaucher disease.* Molecular Genetics and Metabolism, 2015. 114(2): p. S24.
520. Weber, K. and J.D. Schilling, *Distinct lysosome phenotypes influence inflammatory function in peritoneal and bone marrow-derived macrophages.* Int J Inflam, 2014. 2014: p. 154936.
521. Liu, K., et al., *Impaired macrophage autophagy increases the immune response in obese mice by promoting proinflammatory macrophage polarization.* Autophagy, 2015. 11(2): p. 271-84.
522. Kiselyov, K., et al., *Autophagy, mitochondria and cell death in lysosomal storage diseases.* Autophagy, 2007. 3(3): p. 259-62.
523. Santamaria, F., et al., *Respiratory manifestations in patients with inherited metabolic diseases.* Eur Respir Rev, 2013. 22(130): p. 437-53.

524. Zaffagnini, G. and S. Martens, *Mechanisms of Selective Autophagy.* J Mol Biol, 2016. 428(9 Pt A): p. 1714-24.
525. Scherzer, M.T., et al., *Fibroblast-derived extracellular matrices: an alternative cell culture system that increases metastatic cellular properties.* Plos One, 2015. 10(9): p. e0138065.
526. Momen-Heravi, F., et al., *Increased number of circulating exosomes and their microRNA cargos are potential novel biomarkers in alcoholic hepatitis.* J Transl Med, 2015. 13(1): p. 261.
527. Bringardner, B.D., et al., *The role of inflammation in the pathogenesis of idiopathic pulmonary fibrosis.* Antioxid Redox Signal, 2008. 10(2): p. 287-301.
528. Hough, K.P., et al., *Exosomes in immunoregulation of chronic lung diseases.* Allergy, 2017. 72(4): p. 534-544.
529. Kováčiková, Z. and E. Tatrai, *Significance of alveolar macrophages, pneumocyte type II and Clara cells in lung toxicology.* Biologia, 1997. 52(3): p. 425-429.
530. Malouf, M.A., et al., *An investigator-driven study of everolimus in surgical lung biopsy confirmed idiopathic pulmonary fibrosis.* Respirology, 2011. 16(5): p. 776-83.
531. Mercer, P.F., et al., *Exploration of a potent PI3 kinase/mTOR inhibitor as a novel anti-fibrotic agent in IPF.* Thorax, 2016. 71(8): p. 701-711.
532. Cuervo, A.M., *Autophagy and aging: keeping that old broom working.* Trends in Genetics, 2008. 24(12): p. 604-612.
533. Higginbotham, J.N., et al., *Amphiregulin exosomes increase cancer cell invasion.* Curr Biol, 2011. 21(9): p. 779-86.
534. Pryor, P.R., *Analyzing lysosomes in live cells.* Methods Enzymol, 2012. 505: p. 145-57.
535. Guha, S., et al., *Approaches for detecting lysosomal alkalinization and impaired degradation in fresh and cultured RPE cells: evidence for a role in retinal degenerations.* Exp Eye Res, 2014. 126: p. 68-76.
536. Galluzzi, L., et al., *Pharmacological modulation of autophagy: therapeutic potential and persisting obstacles.* Nat Rev Drug Discov, 2017. 16(7): p. 487-511.
537. Dehay, B., et al., *Pathogenic lysosomal depletion in Parkinson's disease.* J Neurosci, 2010. 30(37): p. 12535-44.
538. Yang, D.-S., et al., *Reversal of autophagy dysfunction in the TgCRND8 mouse model of Alzheimer's disease ameliorates amyloid pathologies and memory deficits.* Brain, 2010. 134(1): p. 258-277.
539. Parr, C., et al., *Glycogen synthase kinase 3 inhibition promotes lysosomal biogenesis and autophagic degradation of the amyloid-beta precursor protein.* Mol Cell Biol, 2012. 32(21): p. 4410-8.
540. Li, Y., et al., *Protein kinase C controls lysosome biogenesis independently of mTORC1.* Nat Cell Biol, 2016. 18(10): p. 1065-77.
541. Ueno, T., et al., *Mesenchymal stem cells ameliorate experimental peritoneal fibrosis by suppressing inflammation and inhibiting TGF-β1 signaling.* Kidney international, 2013. 84(2): p. 297-307.
542. Grange, C., et al., *Biodistribution of mesenchymal stem cell-derived extracellular vesicles in a model of acute kidney injury monitored by optical imaging.* Int J Mol Med, 2014. 33(5): p. 1055-63.
543. Wang, B., et al., *Mesenchymal Stem Cells Deliver Exogenous MicroRNA-let7c via Exosomes to Attenuate Renal Fibrosis.* Mol Ther, 2016. 24(7): p. 1290-301.
544. Jun, D., et al., *The Pathology of Bleomycin‐Induced Fibrosis Is Associated with Loss of Resident Lung Mesenchymal Stem Cells That Regulate Effector T‐cell Proliferation.* Stem cells, 2011. 29(4): p. 725-735.
545. Monsel, A., et al., *Mesenchymal stem cell derived secretome and extracellular vesicles for acute lung injury and other inflammatory lung diseases.* Expert Opin Biol Ther, 2016. 16(7): p. 859-71.
546. Elliot, S.J., et al., *Therapeutic Benefits Of Exosomes Derived From Mesenchymal Stromal Cells In Bleomycin-Induced Pulmonary Fibrosis In Aged Mice.* Am J Resp Crit Care, 2017. 195: p. A1213.
547. Xiong, Y., A. Mahmood, and M. Chopp, *Emerging potential of exosomes for treatment of traumatic brain injury.* Neural Regen Res, 2017. 12(1): p. 19-22.
548. Katakowski, M. and M. Chopp, *Exosomes as Tools to Suppress Primary Brain Tumor.* Cellular and Molecular Neurobiology, 2016. 36(3): p. 343-352.

549. Zhang, Z.G. and M. Chopp, *Exosomes in stroke pathogenesis and therapy.* J Clin Invest, 2016. 126(4): p. 1190-7.

APPENDIX

Appendix A: Additional results

Normally, autophagy can be induced with relatively low concentrations of rapamycin with a longer period (e.g., 24 hours) incubation. In RAW264.7 mouse macrophages, autophagy induced with low concentrations of rapamycin was not reproducible. The pattern observed on western blotting with low concentrations of rapamycin was similar to the pattern of the starvation-induced autophagy as presented in Figure 5-1.

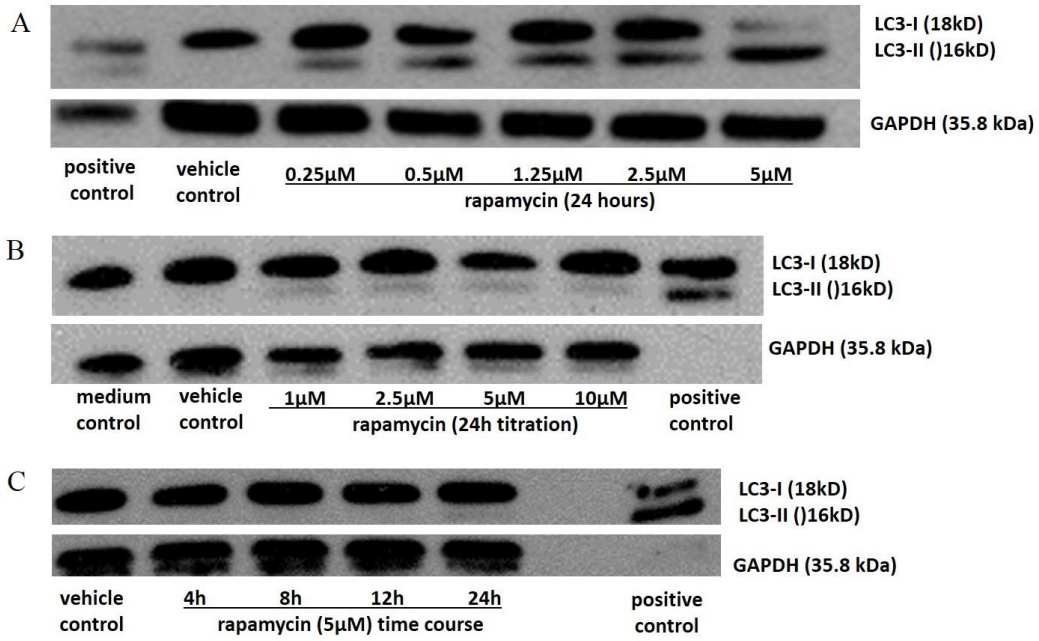

Figure A-1 Autophagy induction with low concentrations of rapamycin was not reproducible in RAW264.7 mouse macrophages.

RAW264.7 cells (1×10^6) were seeded in a six-well plate the day before treatment. On the next day, cells were treated as indicated. (A) Succesful autophagy induction, i.e. decrease of LC3-I and increase of LC3-II expression, was observed with low concentrations of rapamycin with 24 hour incubation (n=1); (B) the autophagy induction with low concentrations of rapamycin was not reproducible, representative blot of experiments performed 4 times on different occasions (n=4); (C) time-course experiment with low concentrations of rapamycin did not show different LC3-II expression at different time points within 24 hours (n=1). Cells were treated as indicated before the cell lysates were prepared for western blotting. Positive control: Neuro 2A cell lysate; vehicle control: DMSO diluted in complete DMEM medium (as highest rapamycin); medium control: DMEM with 10% FBS. Representative blots are shown for A and C (performed once) and for B (performed 4 times on separate occasions).

Appendix B: Patient information

Table 1 Patients information for Figure 6-3, the Cyto-ID staining for autophagic vacuoles.

Patient ID	Diagnosis	Gender (M=1, F=0)	AGE (years) at time of BAL	Smoking category
1118	IPF	0	64	1
0853	IPF	1	66	1
0395	IPF	1	77	3
0947	IPF	0	74	2
1134	IIP (no fibrosis)	0	58	1
1123	IIP (no fibrosis)	0	66	2
0983	IIP (no fibrosis)	0	70	4
0951	IIP (no fibrosis)	1	78	4
0948	IIP (no fibrosis)	1	78	1
1155	IIP (no-fibrosis)	0	56	2

Smoking category: 1=Never; 2= Ex-smokers (Ex) <20pyr; 3=Ex 20-40pyr; 4= Ex >40pyr; 5=current smoker<20pyr; 6= current smoker 20-40pyr; 7= current smoker >40pyr. Pyr= pack year history, 1 pack year = 20 cigarettes a day for 1 year.

Table 2 Patients information for Figure 6-4, western blotting data LC3 and p62 expression.

Position On WB	Group	Patient ID	Diagnosis	Gender (M=1, F=0)	Age(years) at time of BAL	Smoking category
Lane-1	NF	1035	IIP	0	71	2
Lane-2	NF	1043	IIP	1	53	4
Lane-3	**FR**	**0823**	**IPF**	**1**	**75**	**1**
Lane-4	**FR**	**1044**	**IPF**	**1**	**74**	**3**
Lane-5	**FR**	**1045**	**Asbestosis**	**1**	**70**	**3**
Lane-6	**FR**	**0996**	**IPF**	**1**	**71**	**1**
Lane-7	NF	1035	IIP	0	71	2
Lane-8	**FR**	**0849**	**IPF**	**1**	**69**	**1**
Lane-9	**FR**	**1033**	**IPF**	**0**	**54**	**3**
Lane-10	NF	1056	Sarcoidosis	0	64	1
Lane-11	NF	1051	IIP	1	79	1
Lane-12	NF	0564	IIP)	1	71	5
Lane-13	**FR**	**0579**	**IPF**	**1**	**78**	**2**
Lane-14	NF	1023	IIP	0	57	5

Smoking category : 1=Never; 2= Ex-smokers (Ex)<20pyr; 3=Ex 20-40pyr; 4= Ex >40pyr; 5=current smoker<20pky; 6= current smoker 20-40pky; 7= current smoker >40pky. Fibrotic group is highlighted in bold. Nearly half were never smokers Cat-1 (n-3), one patient was ex-smoker Cat-2 (n=1) and the other three patients were ex-smoker Cat-3 (n=3). Pyr= pack year history, 1 pack year = 20 cigarettes a day for 1 year.

The level of smoking and years of age of participants between the fibrotic and non-fibrotic groups at the time of recruitment were compared and no difference was found.

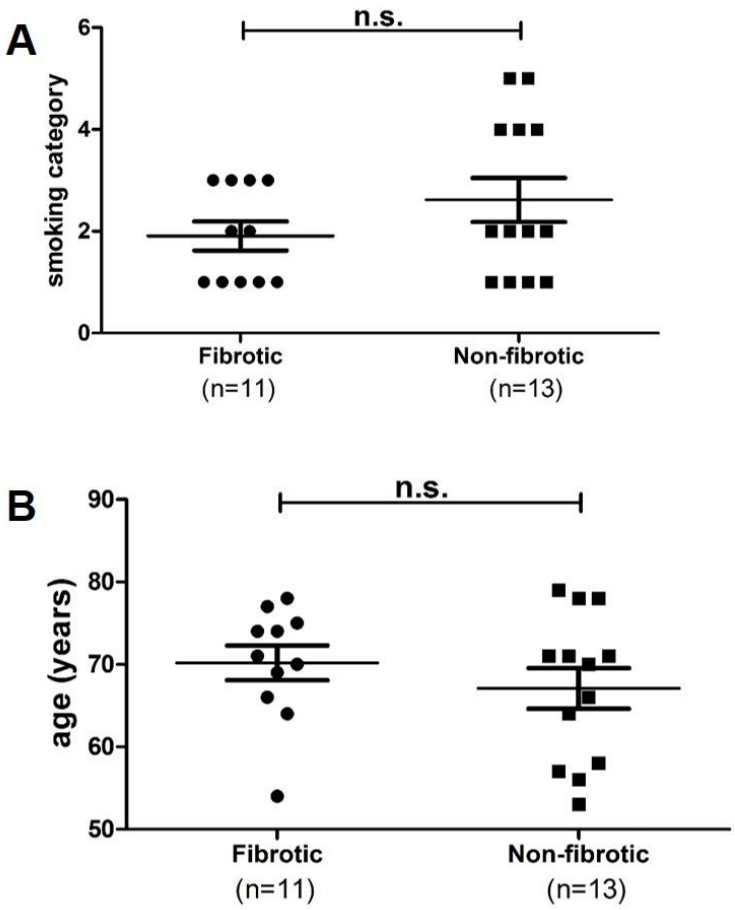

Figure A-2 No difference was found in smoking or age of the participants between fibrotic and non-fibrotic groups in this study.

The smoking history and age of participants as listed in the above table were grouped and compared. (A) No difference was found in smoking history in the two groups, fibrotic vs non-fibrotic = 1.91 ± 0.28 vs 2.62 ± 0.43; (B) No difference was found in age of the two groups, fibrotic vs non-fibrotic = 70.18 ± 2.09 vs 67.08 ± 2.47, student's t-test. n.s., not significant.

Appendix C: Publications and poster presentation

Publications

F. Li, A. Zhang, E. Ryan, P. Coelho, J. Marwick, A. Rossi, N. Hirani. An easy-detach method to differentiate human monocytes into macrophages. (Manuscript in preparation)

F. Li, A. Zhang, R. Wang, R. Mills, A. MacKinnon, I. Drainsfield, J. Pound, C. Gregory, A. Rossi, N. Hirani. An anti-CD9 bead-based flow cytometry assay for exosome study in BAL fluid from ILD lungs. (Manuscript in preparation)

F. Li, A. Zhang, R. Wang, J. Marwick, R. Mills, J. Pound, A. MacKinnon, I. Drainsfield, C. Gregory, S. Howie, W. MacNee, A. Rossi, N. Hirani. Extracellular matrix increased autophagy in macrophages and aggravate the impairment of autophagosome degradation in alveolar macrophages in IPF. (Manuscript in preparation)

Poster presentation

F. Li, A. Zhang, R. Mills, J. Pound, J. Marwick, L. Nicol, A. MacKinnon, I. Drainsfield, S. Howie, W. MacNee, A. Rossi, C. Gregory, N. Hirani. Exosomes levels are decreased in Bronchoalveolar Lavage fluid from patients with fibrotic interstitial lung diseases due to blockage of the autophagy pathway. 19th International Colloquium on Lung and Airway Fibrosis (ICLAF), Dublin, September 2016.